CHARACTERIZATION OF A

CONSTITUTIVE HETEROCHROMATIN ABNORMALITY

IN ROBERTS SYNDROME

by

Karen Judith Harrison, B.Sc., M.Sc.

A Thesis

Submitted to the School of Graduate Studies

in Partial Fulfilment of the Requirements

for the Degree

Doctor of Philosophy

October, 1991

CHARACTERIZATION OF A CONSTITUTIVE HETEROCHROMATIN ABNORMALITY IN ROBERTS SYNDROME

DOCTOR OF PHILOSOPHY (1992) McMASTER UNIVERSITY

(Medical Sciences) Hamilton, Ontario

TITLE: Characterization of a Constitutive Heterochromatin
Abnormality in Roberts syndrome

AUTHOR: Karen Judith Harrison B.Sc. (U. of Guelph)

M.Sc. (Brock University)

SUPERVISOR: Dr. D.J. Tomkins

NUMBER OF PAGES: xxiii, 338

ABSTRACT

Roberts syndrome (RS) is a rare autosomal recessive developmental disorder that is characterized by severe pre- and post-natal growth retardation, tetraphocomelia and various craniofacial abnormalities. In some patients with Roberts syndrome (RS+) but not others (RS-), RS is associated with a cytogenetic abnormality which presents as an unusual "puffing" of the constitutive heterochromatin and nucleolar organizing regions. The decondensed appearance of the constitutive heterochromatin suggests an alteration in chromatin structure in RS+. Two main questions were addressed in this study; 1) are altered levels of DNA methylation associated with the constitutive heterochromatin abnormality of RS+ chromosomes and 2) is the timing of DNA replication of constitutive heterochromatin, relative to the rest of the genome, altered in RS+ lymphoblast cells? Levels of methylated cytosine residues of RS+ and RS- heterochromatin DNA, assessed using MspI and HpaII isoschizomer restriction enzyme digestion and Southern blot hybridization with a repetitive probe (D15Z1) to the heterochromatin DNA, were found to be significantly lower (p=0.048) in RS+ fibroblast cell strains compared to control and RS- cell strains. In addition to this, D15Z1 DNA methylation levels differed significantly (p≤0.05) at early and late passage in fibroblast cell strains of all three

groups, suggesting that decreased levels of DNA methylation were associated with an _in vitro_ aging effect. The chromosome replication patterns of the constitutive heterochromatin regions of chromosomes 1, 9, 16 and Y were investigated using terminal 5-bromodeoxyuridine labelling and an S phase subclassification system. A significant delay ($p < 0.001$ for male cell lines; $p < 0.05$ for female cell lines) was observed in the timing of RS+ constitutive heterochromatin. These results suggest that the cytogenetic abnormality of the constitutive heterochromatin of RS+ cells is associated with alterations in DNA conformation and synthesis.

ACKNOWLEDGEMENTS

TABLE OF CONTENTS

x

LIST OF TABLES

LIST OF FIGURES

LIST OF FIGURES (continued)

LIST OF ABBREVIATIONS

α-MEM	alpha minimal essential medium
5-azaC	5-azacytidine
ANOVA	analysis of variance
bp	basepair
BrdUrd	5-bromodeoxyuridine
DMSO	dimethyl sulfoxide
DNase I	pancreatic deoxyribonuclease
D-PBS	Dulbeccos' phosphate buffered saline
EDTA	ethylenediaminetetraacetic acid
FBS	fetal bovine serum
G-banding	Giemsa banding
GLIM	Generalized Linear Model
GLM	General Linear Model
kb	kilobase
LMP	low melting point
m	mean
m^5cyt	5-methylcytosine
MMC	mitomycin C
MN	micrococcal nuclease
OD	optical density
P	passage
PAGE	polyacrylamide gel electrophoresis
R-banding	Reverse banding
RNase	ribonuclease

LIST OF ABBREVIATIONS (continued)

RS	Roberts syndrome
RS+	Roberts syndrome with constitutive heterochromatin abnormality
RS-	Roberts syndrome without constitutive heterochromatin abnormality
s	standard deviation
SDS	sodium dodecyl sulphate
TdR	thymidine

1. INTRODUCTION

1.1. ROBERTS SYNDROME

1.1.1 CLINICAL PRESENTATION OF ROBERTS SYNDROME

Roberts syndrome (RS) is a rare, autosomal recessive, developmental disorder in humans that was first reported by Dr. J.B. Roberts in 1919. The clinical features of this syndrome include tetraphocomelia with ectrodactyly and syndactyly, cleft lip or palate with protrusion of the intermaxillary portion of the upper jaw, ocular hypertelorism, prominance of the phallus, cryptorchidism in males, and severe pre- and post-natal growth retardation (Freeman et al., 1974; Herrmann and Opitz, 1977). It has been postulated that all of the abnormalities associated with RS could be the result of a disturbance in normal development that occurred before the seventh week of gestation (Freeman et al., 1974).

Roberts syndrome was first recognized as a genetic syndrome by Appelt et al. (1966). The mode of inheritance is considered to be autosomal recessive as pedigree analysis indicates that both sexes are affected, the parents are phenotypically normal and affected siblings have been reported. However, there was much controversy early in the

1

literature concerning the defining nosologic features of the syndrome. Herrmann et al. (1969) defined four cases that were affected with RS as "pseudothalidomide syndrome" because of their phenotypic similarities to the drug-induced phenotype of thalidomide. The authors argued the cases did not represent RS as the phenotypic presentation of their patients was more heterogenous and less severe than those previously defined as being affected with RS. Herrmann and Opitz (1977) later defined the syndrome as "SC-phocomelia", named after the initials of the families studied. Consequently, there was much debate as to whether RS represented a distinct syndrome with variable presentation of its clinical features or several syndromes with similar clinical features. In 1977, Herrmann and Opitz concluded that pseudothalidomide, SC-phocomelia and Roberts syndrome were caused by the same gene and the heterogeneity of its phenotype was the result of variable expression. This hypothesis also received support from Grosse et al. (1975), Fryns et al. (1980) and Zergollen and Hitrec (1982).

1.1.2. CYTOGENETIC ABNORMALITY OF THE CONSTITUTIVE HETEROCHROMATIN

Approximately one half of the patients affected with RS also possess a cytogenetic abnormality that has been described as an unusual "puffing" of the constitutive heterochromatin around the centromere and nucleolar

organizing regions of chromosomes 15, 9, 22, 1, 21, 16, 6, 13 and 7 and on the long arm of the Y, listed in order of occurring frequency (Judge, 1973; Tomkins, 1978; Tomkins et al., 1979).   In addition to the unusual puffing of the constitutive heterochromatin, Tomkins et al. (ibid) and German (1979) also described the chromosomes of some RS cells to have a "railroad track" appearance, whereby the chromatids are not joined at the centromere. The phenomenon has also been referred to as premature centromere separation or centromere splitting (German, 1979).   Both cytogenetic manifestations of the constitutive heterochromatin abnormality are collectively defined by the term "RS effect". Roberts syndrome patients with the RS effect are referred to here as RS+ while those without the cytogenetic abnormality are RS-. However the presence or absence of the cytogenetic abnormality does not distinguish two groups of RS patients on the basis of phenotype.

The RS effect is generally not expressed in the parents of an individual affected with RS, although Paulson et al. (1989) recently reported a parent expressing a mild form of the RS effect.   The RS+ cytogenetic abnormality can be corrected by somatic cell hybridization of RS+ with control cells, which is consistent with a recessive trait. This was demonstrated by Gunby et al. (1987) using human fibroblast cell strains.   Krassikoff et al. (1986) also

observed correction of the RS effect in RS+ fibroblasts fused with Chinese Hamster Ovary (CHO) cells. Preliminary studies by Knoll and Ray (1986) and Allingham and Tomkins (1990) using other human cells confirm these studies. The results suggest that the normal genome of the hybrid cell was able to provide a product that corrected the cytogenetic abnormality of the constitutive heterochromatin and that the product necessary for normal constitutive heterochromatin structure is missing or defective in RS+ cells.

The importance of the decondensed appearance of the constitutive heterochromatin of some RS patients is not known. German (1979) hypothesized that the RS effect was the result of premature separation of sister chromatids. The distribution of chromosomes affected in RS+ is the opposite of what has been reported to be the normal distribution of centromere separation in colcemid treated cells (Vig, 1981). In RS+, the centromeres of chromosomes that generally separate last appear to separate first and those that generally separate first, do so last. This has led to the hypothesis that constitutive heterochromatin may play a role in normal centromere function in mitosis.

1.1.3. IN VITRO GROWTH CHARACTERISTICS

In vitro growth studies of RS+ cells grown in culture have revealed the existence of many cellular abnormalities

(Tomkins and Siskens, 1984). RS+ cells have an altered cell morphology from that of normal cells, possess a severely reduced capacity to grow and are plagued by long and variable cell cycles. Many abnormalities are specifically related to mitosis as the mitotic cell cycle is also long and variable. Many cells fail to complete metaphase, possibly due to a delay in the onset of chromosome movement. Cytokinetic abnormalities involving inappropriate cleavage furrow formation have also been observed. Subsequently, many RS+ cells fail to survive and senesce at an earlier passage _in vitro_. Tomkins and Sisken (ibid) postulated that the developmental abnormalities of RS could be the result of growth deficiencies of cells in developing anlagen.

1.1.4. MUTAGEN SENSITIVITY ASSOCIATED WITH ABNORMAL CONSTITUTIVE HETEROCHROMATIN STRUCTURE

An X-linked temperature-sensitive, lethal mitotic mutant, mus-101$^{ts\iota}$, has been described in _Drosophila melanogaster_ identifying a gene controlling heterochromatin condensation during mitosis (Gatti et al., 1983). This mutation also confers hypersensitivity to mutagens and defective postreplication repair. Gatti et al. (ibid) postulated that the mutagen sensitivity and defective repair processes of the mus-101$^{ts\iota}$ mutation were due to abnormal heterochromatin structure, resulting in the chromatin being more susceptible to mutagen damage or less accessible for DNA

repair.

Burns and Tomkins (1989) demonstrated that RS+ fibroblast cell strains were hypersensitive to cell-killing by the DNA cross-linking agent mitomycin C (MMC) compared to control cell strains. The RS- cells, on the other hand, were not hypersensitive to MMC, suggesting an association between the heterochromatin abnormality and the mutagen sensitivity. RS+ cell strains have also been found to be hypersensitive to other cross-linking agents, cisplatin, bleomycin, methyl methane sulphonate, N-methyl-nitrosurea and 8-methoxypsoralen (Gentner et al. 1985; 1986). Sensitivity to acute gamma radiation and high linear energy transfer ionizing radiation was much less marked, suggesting that RS+ cells may be defective in specific DNA repair processes (Gentner et al., 1985; 1986).

Correction of both the cytogenetic abnormality and hypersensitivity to MMC was demonstrated in lymphoblast/ lymphoblast somatic cell hybrids between RS+ and control cell lines by Allingham and Tomkins (1990). This supports the idea that the cytogenetic abnormality and the mutagen sensitivity are associated in RS+ cells. However, it is not clear if one is the cause or effect of the other or if they are both secondary effects of a primary defect.

1.1.5. ROBERTS SYNDROME HYPOTHESIS-GENETIC HETEROGENEITY

It has been proposed that a single gene defect is affecting heterochromatin structure and function in RS (Tomkins et al., 1979). Cytogenetic studies have clearly shown that constitutive heterochromatin is affected in RS+ patients rather than the centromere alone (Tomkins et al., 1979; Louie and German, 1981). The abnormal appearance of the constitutive heterochromatin suggests that a structural abnormality is involved in RS heterochromatin which could subsequently affect its function.

There has been much speculation concerning the nature of the genetic defect of RS and the mechanism by which this defect presents itself. Tomkins and Sisken (1984) suggested that it was the lack of normal gene product that affected cell growth rates, cell division and chromosome behavior in RS. Dev and Wertelecki (1984) alternatively proposed that the RS effect was the result of an abnormal gene product, implicating an autosomal dominant mode of inheritance. The recent work involving the somatic cell hybridization studies previously described suggests that a normal gene product is missing in RS+ cells (Gunby et al. 1987; Knoll and Ray, 1986; Krassikoff et al. 1986; Allingham and Tomkins, 1990).

The RS effect is not seen in all RS patients but is consistent within a family, suggesting that genetic heterogeneity is associated with the syndrome. There are

several genetic models that can be used to explain RS+ and RS- phenotypes. The first model states that RS+ and RS- are the result of the same allele of the same gene (RBS), as defined by the genotype aa. The second model states that there are two mutant alleles at the RBS gene locus. Thus RS+ genotype would be represented by aa and the RS- genotype by a'a or a'a'. If the genotype of RS- is defined as a heterozygote (a'a), it is predicted that the homozygous a'a' genotype could represent a closely related syndrome such as Fanconi's anemia. The last model considers RS+ and RS- to be the result of two different genes. The RS+ genotype would be represented by aaB_ and the RS- genotype by A_bb. This model suggests that both genes affect the same biochemical pathway and therefore present with the same clinical phenotype.

1.2. CHARACTERISTICS OF CONSTITUTIVE HETEROCHROMATIN STRUCTURE AND FUNCTION

1.2.1. DEFINING CONSTITUTIVE HETEROCHROMATIN

The term heterochromatin was initially introduced by Heitz in 1928 to define chromosomes or chromosome regions that remained permanently condensed throughout the cell cycle (reviewed by John, 1988). In contrast, euchromatin was decondensed during interphase and only became condensed as visible chromosome structures during mitosis. Heitz observed that heterochromatin formed condensed regions within

interphase nuclei called chromocenters. This type of heterochromatin is now defined as constitutive heterochromatin as it has since been determined that different heterochromatin types also exist in the form of tissue-specific condensed euchromatin, facultative and intercalary heterochromatin.

In humans, constitutive heterochromatin represents a distinct class of chromatin that is localized to specific regions of metaphase chromosomes and to chromocenters of interphase nuclei. These regions can be demonstrated by a cytological staining technique called C-banding that stains constitutive heterochromatin differentially from euchromatin, facultative heterochromatin and intercalary heterochromatin (Arrighi and Hsu, 1971; Sumner, 1972). In humans, constitutive heterochromatin is localized to the centromeric region of all chromosomes and to the distal long arm of the Y chromosomes. Chromosome 1, 9 and 16 usually have large blocks of paracentromeric constitutive heterochromatin. The location, but not the amount, of constitutive heterochromatin is the same for all homologous chromosomes in all cell types, providing that aberrant structural rearrangements of chromosomes have not taken place.

In addition to Heitz's structural definition, constitutive heterochromatin has several distinct properties by which it can be characterized. Its DNA composition

generally consists of large amounts of chromosome-specific repetitive DNA sequences, some of which have been identified as satellite DNA (Singer, 1982). For the most part it is considered to be transcriptionally inactive by virtue of its condensed chromatin state (John, 1988). However there are some exceptions to this generalization; for example, a number of genes have been localized to the constitutive heterochromatin regions of _Drosophila_ _melanogaster_ chromosomes (Hilliker and Appels, 1980). Mammalian constitutive heterochromatin sequences are also highly methylated in the form of 5-methyl-cytosine compared to other genomic sequences (Miller _et_ _al_. 1974; Harbers _et_ _al_. 1975). It is generally considered to be late replicating (Schmid and Leppert, 1969). In the past this has been used as a criterion for its definition, although this may not be always hold true for all constitutive heterochromatin in all species (John, 1988). The amount of constitutive heterochromatin within a genome can vary between individuals of the same species and between different species, although differences in DNA content between species generally reflect differences in their amount of heterochromatin (Ris and Korenberg, 1979).

1.2.2. CONDENSATION OF CONSTITUTIVE HETEROCHROMATIN THROUGHOUT THE CELL CYCLE

Constitutive heterochromatin differs in structure from euchromatin throughout the cell cycle except during mitosis

when interphase chromatin is organized into metaphase chromosomes. The difference in chromatin condensation of euchromatin and heterochromatin during interphase is believed to be the result of differences in the level of their chromatin organization.

Chromatin structure can be classified into three major levels of organization, revealing a complex ultrastructure that is still not well defined (reviewed by Rattner and Lin, 1988). The three levels of organization can be categorized as 1) a basic 10 nm nucleosome fiber, 2) a 30 nm fiber and 3) a 200-300 nm fiber. Each level is subsequently organized to form a more compacted chromatin conformation. Heterochromatin and euchromatin appear to differ in chromatin structure most importantly at interphase with euchromatin being less compacted (Rattner and Lin, 1988).

Electron microscopy studies have shown that the lowest level of chromatin organization consists of a basic 10 nm-fiber made up of nucleosomes. A nucleosome consists of a core particle containing an octamer of histones H4, H3, H2A, H2B and approximately 146 basepairs (bp) of DNA in the B form wrapped around it in two left-handed superhelical turns (Reeves, 1984; Igo-Kemenes et al. 1982; Weisbrod, 1982; Mathis et al. 1980). Confirmed by X-ray diffraction analysis, neutron scattering, chemical cross-linkage studies and electron microscopy image reconstruction techniques, the

nucleosome has been described as a wedge-shaped disc that is approximately 11 nm in diameter and 5.7 nm in height (Reeves, 1984). The nucleosomes are arranged in a repeating array with intermittent linker or spacer DNA that can be 0-80 bp in length. This organization has often been described as "beads on a string" (Olins and Olins, 1979). This beaded appearance of the 10 nm chromatin fiber has been observed with heterochromatin as well as euchromatin, suggesting that it is a common level of organization of all chromatin types (Rattner and Lin, 1988).

The next level of chromatin ultrastructure is defined by the 30 nm fiber. The way in which the 30 nm fiber is organized is not clear and several models have been proposed to explain its organization (reviewed by Rattner and Lin, 1988). McGhee and Felsenfeld (1980) proposed that the 10 nm fiber is compacted by the formation of a supercoiled solenoid that consists of histone H1 complexed nucleosomes stacked in a helical manner so that a radial arrangement of approximately 6 nucleosomes per turn is achieved. The second model, known as the superbead model, proposes that the nucleosomes are aggregated into a "superbead" structure that can contain a number of nucleosomes, with 8-48 having been reported (cited in Rattner and Lin, 1988). The twisted ribbon model predicts that the nucleosome fiber is folded into a zigzag ribbon which is then wound in a helical manner

to produce the 30 nm fiber.

The packing ratio of the 30 nm fiber is in the interval of 40-50:1, and is thought to represent the bulk of the interphase chromatin that exists _in vivo_ (Olins and Olins, 1979). The 30 nm fiber appears to be stabilized by histone H1 and H5, with histone H1 being less tightly bound (Allan _et al_. 1981). One could then predict that the removal of histone H1 would result in the unwinding of the 30 nm fiber back to the 10 nm fiber. A number of studies have shown that chromatin regions containing actively transcribed genes appear to be depleted of histone H1 proteins compared to inactive bulk chromatin (Weintraub and Groudine, 1976; Burkholder and Weaver, 1977). Non-histone proteins have also been associated with inactive chromatin fractions. Burkholder and Weaver (_ibid_) observed that chromatin contained both histone and non-histone proteins but that the non-histone proteins were more tightly associated with the DNA in the condensed chromatin fraction than in the dispersed chromatin fraction. There is some evidence suggesting that the histone protein needs to be phosphorylated for this organization to occur and it has been postulated that the H1 modification may influence the compact nature of heterochromatin (Rattner and Lin, 1988).

The 30 nm fiber is subsequently compacted to the level of chromatin condensation (200-300 nm) observed in metaphase

chromosomes or chromocenters of interphase nuclei. Again, several models exist, describing the way in which the 30 nm fiber can be further condensed (reviewed by Reeves, 1984; Rattner and Lin, 1988). DuPraw (1965) initially introduced the "folded fiber" model which hypothesized that the 30 nm fiber was randomly folded back on itself along the chromatid arm. The "radial loop" model dictates that the 30 nm fiber is organized as a series of loops that originate from the chromatid axis. The loops or domains are thought to consist of supercoiled stretches of DNA of 35-100 bp that are attached to a central axis (chromosome scaffold) by specific non-histone proteins. Compaction of chromosomal loops at this level of chromatin organization is well documented but the existence and structure of a chromosome scaffold is still somewhat controversial. The additional folding of the chromatin fibers in metaphase chromosomes would condense the 30 nm fiber to such a degree that the compaction factor of 400-800 or more would be achieved (Lewis and Laemmli, 1982).

Rattner and Lin (1988) described an additional level of chromatin condensation that differentiated euchromatin and centromeric heterochromatin of mouse metaphase chromosomes. Non-centromeric chromatin of metaphase chromosomes appeared to undergo an additional helical packing of the 200-300 nm fiber as helical coils and radial loops. The centromeric regions did not appear to be helically compacted to the same

extent as the rest of the chromosome, retaining a chromatin fiber diameter of 200-300 nm. It was concluded that this difference in organization was responsible for the constricted appearance of the centromeric region of metaphase chromosomes.

The structure of euchromatin and heterochromatin appears to differ the most at interphase. At this stage, euchromatin is considered to be organized as radial loops of the 30 nm fiber to give a final fiber of 200-300 nm. Heterochromatin, which would include constitutive heterochromatin as well, is thought to be organized at the level observed in metaphase chromosomes. Constitutive heterochromatin may also be differentially organized in metaphase chromosomes, as it was initially identified as a secondary constriction and can be distinguished by a cytological staining technique that is dependent upon chromatin structure.

1.2.3. SEQUENCE COMPOSITION OF CONSTITUTIVE HETEROCHROMATIN

Heterochromatin DNA is highly repetitive in nature, consisting of simple and complex arrangements of families of satellite sequences, satellite-related sequences and non-satellite sequences. Satellite DNA sequences have been categorized into two broad subclasses defined as "classical" and alphoid- (α-) satellite DNA (Singer, 1982). The former

was isolated from total genomic DNA using cesium chloride (CsCl) or Cs_2SO_4/CsCl density gradient separation based upon differing buoyant densitities, resulting in the identification of four main satellite fractions in human genomic DNA, originally designated fractions I-IV (Corneo et al. 1968; 1970; 1971; 1972). These sequences were found to be highly repetitive and localized to heterochromatin DNA of chromatin fractions (Corneo et al. 1971). Collectively, they represent approximately 2 to 5% of the total eukaryotic genome (Singer, 1982). Additional minor satellite DNA fractions have also been identified using heavy metal treatment before isopycnic centrifugation (Manuelidas, 1978a). These minor satellite DNA fractions have been referred to as satellite DNA fractions A, B, C and D and as alphoid satellite DNA sequences (Babu and Verma, 1988; Singer, 1982).

Alphoid satellite DNA sequences were first detected in the African Green-monkey. They were subsequently discovered in other primates including humans based upon a consensus sequence that has been conserved among species (Singer, ibid). These sequences are highly repetitive and comprise a 170 bp core repeat that is tandemly arrayed. Restriction enzyme digestion of alphoid DNA yields a ladder of DNA fragments that are multiples of the 170 bp core repeat. Manuelidas (1978a) identified a human alphoid-related

satellite sequence that consisted of a 340 bp monomer using EcoRI digestion. This fragment was localized to the centromeric regions of almost all of the chromosomes of the human complement (Manuelidas, 1978b).

Gosden et al. (1975a) determined the chromosomal location of human satellite DNA I-IV using in situ hybridization studies. The four satellite DNA's were isolated from condensed and dispersed chromatin fractions using density gradient centrifugation. The purified DNA was then transcribed in vitro to produce radioactively labelled complementary RNA (cRNA) that was subsequently hybridized to fixed metaphase chromosomes. The satellite DNA isolated from the condensed chromatin fraction hybridized to the constitutive heterochromatin regions of chromosomes 1, 9 and Y and to the centromeric regions of chromosomes 13, 14, 15, 20, 21 and 22. Gosden et al. (ibid) described the distribution of labelling identical to that obtained with G-11 banding, a modified C-banding procedure that labels the constitutive heterochromatin regions of chromosomes 1, 3, 5, 7, 9, 10, 13, 14, 15, 20, 21, 22 and Y. Hybridization of the cRNA transcribed from the DNA of the dispersed chromatin fraction was more widely distributed over all of the chromosome arms, although some labelling of the constitutive heterochromatin regions of chromosome 9 and Y and the acrocentric chromosomes was also observed. This implied that

there was some similarity in the sequences extracted from both chromatin fractions. The results of this study indirectly suggest that satellite DNA sequences of condensed chromatin fraction, representative of heterochromatin, are localized to the constitutive heterochromatin regions of specific chromosomes.

The specific chromosomal location of each individual satellite DNA fraction was determined in a subsequent study by Gosden et al. (1975b), using a similar experimental approach. Complementary RNA sequences were transcribed from each satellite DNA fraction and then hybridized in situ to human metaphase chromosomes to see if a specific satellite fraction hybridized to a specific chromosome region. The hybridization pattern observed overall was similar for all four satellite cRNA probes. The C-band region of chromosome 9, Y and the centromeric regions of chromosome 15, 21 and 22 were generally labelled, although some differences were observed between the four satellite groups. Only satellite II cRNA hybridized to the constitutive heterochromatin region of chromosome 16 and it was the only satellite fraction that did not hybridize to chromosome 13. The satellite fractions also differed in their amount of hybridization to specific chromosomes, with some chromosome regions being more heavily labelled than others. The major hybridization sites of satellite I cRNA were to chromosome 9 and Y, while satellite

II hybridized to the Y chromosome and to 1 and 16. Satellites III and IV both hybridized to chromosomes 9, Y and 15. The results of this study suggest that satellite DNA I-IV sequences are mainly localized to the constitutive heterochromatin regions and that a single chromosome region can have large amounts of more than one satellite DNA type. This interpretation would only be correct, however, if each of the four fractions isolated were pure fractions and no significant cross-reactivity occurred between the fractions.

Mitchell et al. (1979) were the first to characterize the distinguishing features of the four major satellite DNA fractions in a comprehensive study involving buoyant density measurements, molecular reassociation kinetics and restriction enzyme analysis. Buoyant density values suggested that satellite DNA fractions I-III were more A-T rich than satellite IV DNA or main band DNA but this was contradicted by thermal denaturation studies which showed only satellite I DNA to more A-T rich. Sequence homologies between the four satellite DNA fractions were assessed using reassociation and cross-hybridization annealing experiments whereby denatured ^{32}P-labelled satellite DNA fractions were annealed with excess denatured, cold strands of homologous or heterologous satellite DNA from various fractions.

Cross-hybridization kinetics indicated that satellite III and IV DNA were indistinguishable while 40% of the

satellite III DNA sequences cross-reacted with 10% of the sequences of satellite I and II. No detectable cross-hybridization was observed between satellite I and II. Sequence homologies between the four satellite DNA fractions were also determined using Southern blot analysis of EcoRI- and HaeIII- digested satellite DNA hybridized with radioactively labelled probes from each satellite DNA fraction. Again, cross-hybridization was observed between satellite I and III but not between satellite I and II. The results of this study also gave more credibility to the earlier in situ hybridization studies that showed that various satellite DNA fractions hybridized to the same constitutive heterochromatin region of specific chromosomes.

Recent studies have focused on the characterization of satellite DNA sequences at the molecular level using restriction enzyme analysis to gain some insight to their sequence organization and complexity. The work of Frommer et al. (1982) and Prosser et al. (1986) demonstrated that the four classes of satellite DNA could be differentiated by their HinfI and TaqI restriction fragment products. Sequence analysis of their respective restriction fragment products revealed that each satellite fraction was characterized by a specific consensus sequence.

Frommer et al. (1982) demonstrated that TaqI and HinfI digestion differentiated satellite DNA I, II and III by

different fragment products. Satellite I DNA could not be digested by TaqI but Hinf I digestion produced three fragments that were 770, 850 and 950 bp in size as well as a very high molecular weight band that represented undigested DNA. Satellite II DNA could be completely digested by HinfI producing a large number of fragments that were 80 bp in size or less. Digestion with TaqI also gave a series of fragments that were 35 to 190 bp in size. Satellite III DNA could be completely digested with HinfI, producing a ladder of fragments of 5 bp increments that varied from 15 to 250 bp. This DNA fraction was more resistant to TaqI digestion than satellite II DNA, as a faint ladder of 5 bp increment similar to that obtained for HinfI digestion could only be detected after prolonged autoradiographic exposure.

Sequence analysis of HinfI and TaqI restriction fragments of the four classes of satellite DNA performed by Frommer et al. (1982) and Prosser et al. (1986) revealed that all four satellite DNA fractions were characterized by a basic repeat consensus sequence of 5'TTCCA'3 that was tandemly arrayed. However, this common consensus sequence seems to have diverged in some subsets of sequences, resulting in a more complex arrangement in the different satellite DNA fractions. For example, the 5 bp consensus sequence of satellite II DNA has undergone extensive sequence variation and is subsequently organized into higher order

repeats that contain frequent but irregularly spaced HinfI and Taq I sites. Frommer et al. (1982) proposed that this divergent subset of satellite II DNA be called satellite 2. Similarly, satellite III DNA was found to have a major family of simple sequence repeats of the consensus sequence, 5'(ATTCC)$_n$ATTGGGTTG'3, that appear to have diverged from the 5 bp consensus sequence. Prosser et al. (1986) defined this subfamily as satellite 3. Satellite III DNA also appears to have a set of sequences that are similar to α-satellite DNA sequences and may comprise yet another subset of the major fraction. Satellite I DNA appears to have a more complex tandem arrangement consisting of two amplified segments of sequences that are alternately arrayed into large segments. Satellite I DNA was described as having a simple sequence component, satellite 1, that was very different from satellite 2 and 3 DNA. There did not appear to be any similarities in the sequences of satellite 1 with satellite 2 and 3.

From the studies reviewed so far, it is obvious that heterochromatin DNA is made up of many simple and complex repeats of satellite DNA sequences. It has been estimated, however, that satellite DNA represents approximately 20% of the heterochromatin DNA sequences, implying that heterochromatin DNA is composed of other repetitive sequences that may or may not be related to satellite DNA (John, 1988).

Many satellite-related DNA sequences have been detected using methods other than gradient centrifugation. These sequences have generally been identified by their restriction digest pattern, revealing a tandem array of a set of DNA fragments of a repeating unit length.

Simmons et al. (1984) isolated an amplified 1.8 kb fragment from a human melanoma cell line, MeWo, using KpnI or Sau3A restriction digests of genomic DNA. The repetitive DNA sequence was specifically obtained from a homogeneously staining region (HSR) on an X chromosome and a derivative chromosome 15. The HSR regions on both chromosomes were stained by G- and C-banding, suggesting that they were composed of centromeric heterochromatin. The derivative chromosome 15 also fluoresced very brightly with distamycin A-DAPI staining, a fluorochrome that specifically stains the heterochromatin of chromosomes 1, 9, 15p, 16 and Y.

Digestion of DNA with Sau3A or KpnI produced very strong 1.8 kb and 3.6 kb bands that were seen with ethidium bromide staining after gel electrophoresis. These bands were estimated to represent 1.1-1.2% of the total DNA extracted from the MeWo cell line. The bands were extracted from the gel and cloned into plasmid DNA. A 1.8 kb clone, identified as D15Z1, was characterized using a variety of restriction enzymes and was found to contain many TaqI and HinfI sites, suggesting that it could be related to satellite II DNA.

Hybridization of the clone to KpnI-digested MeWo and control placental DNA detected a ladder of fragments that were 1.8, 3.6 and 5.4 kb in size, suggesting a tandem array of the 1.8 kb monomer. Sequence analysis revealed a 5 bp consensus sequence of 5'AATGG'3, that showed a sequence variation of the second nucleotide when compared to the general consensus sequence of satellite DNA. Restriction enzyme and sequence analysis revealed D15Z1 to be repetitive and a member of the KpnI family of moderately repetitive sequences.

The chromosomal location of D15Z1 was determined by Higgins et al. (1985) using in situ hybridization. At low stringency conditions, D15Z1 strongly hybridized to the paracentromeric heterochromatin regions of chromosomes 15p and 9 and with less intensity to the centromeric regions of chromosomes 1, 16, the distal long arm of the Y and to the short arms of the acrocentric chromosomes, 13, 14, 21 and 22. With higher stringency, D15Z1 seemed to specifically hybridize to chromosome 15 and, to a lesser extent, chromosome 9.

The chromosomal localization of D15Z1 showed a great deal of similarity to that of satellite III DNA. The consensus sequence of D15Z1 was compared to the consensus sequence of two known satellite III DNA sequences and three putative satellite III sequences. Similarities were observed between the sequences of D15Z1 and the HinfI ladder

previously described by Frommer et al. (1982) as well as an EcoRI Y-specific sequence and a HaeIII 170 bp fragment that is specific for chromosome 1 (Cooke and Hindley, 1979). The similarity of the consensus sequence of D15Z1 to two known satellite III DNA family sequences suggested that the 1.8 kb sequence may be related to satellite III but the large number of TaqI and HinfI sites suggested that it could be related to satellite II. When D15Z1 sequences were fractionated using Ag+-Cs$_2$SO$_4$ gradient centrifugation, they were localized to the satellite III DNA band. Subsequent digestion with HinfI produced a ladder of fragments identical to tha. .eported by Frommer et al. (1982), suggesting that D15Z1 is found as a subset of the HinfI ladder fragments of satellite III or possibly IV.

More recently, Fowler et al. (1987; 1988) demonstrated that specific domains of satellite III DNA are deficient in TaqI sites while other domains are not. The TaqI sites appear to have arisen from a single C-G point mutation in the 5 bp consensus sequence repeat, 5'TTCCA'3, so that a TaqI restriction site (TCGA) is created. The TaqI-enriched domains, called "K domains", were previously described by Burk et al. (1985) to be represented by 1.8 and 3.6 kb KpnI tandem repeats that were localized to chromosome 15. The "K domains" have also been localized to the heterochromatin region of the Y chromosome. This would strongly suggest that

D15Z1 is a satellite III-related sequence belonging to a "K domain".

Moyzis et al. (1987) were able to isolate two repetitive sequences as clones from a human repetitive DNA library that was constructed from sheared human placental DNA. Nucleotide sequencing revealed one clone, pHuR 98, to be related to satellite 3 DNA, consisting of a 10 bp repeat sequence, 5'CAACCGAGT'3 and a 5 bp repeat, 5'GGAAT'3. This sequence contained only restriction recognition sites for HinfI and TaqI. In situ hybridization localized pHuR98 to the constitutive heterochromatin region of chromosome 9 under moderate hybridization stringency that required 75 to 80% sequence homology. The second clone, pHuR195, was determined by nucleotide sequencing to be related to satellite II DNA. This 1.2 kb fragment also had recognition sites for HinfI and TaqI only. In situ hybridization studies showed that this sequence specifically hybridized to the constitutive heterochromatin region of chromosome 16.

The authors indicated that this is apparently the first report of the identification of specific repetitive DNA sequences that demonstrate a high specificity for a single chromosome. Usually the satellite DNA sequences reported in earlier studies hybridized to several chromosome regions. Moyzis et al. (ibid) concluded that the clusters of sequences homologous to pHuR9S and pHuR195 are specifically localized

to the constitutive heterochromatin regions of chromosomes 9 and 16, respectively. This study provides further evidence that subfamilies of satellite DNA sequences exist and that other sequences specific for constitutive heterochromatin on other chromosomes could be isolated using this approach.

From the studies reviewed so far, it is apparent that constitutive heterochromatin DNA consists mainly of highly repetitive sequences that are tandemly arranged in their organization. Characterization of the sequence composition of constitutive heterochromatin has largely been confined to the study of satellite DNA sequences and their related subfamilies. It is estimated that the constitutive heterochromatin recognized by C-banding comprises approximately 13% of the human genome while satellite DNA sequences represent about 4% of the total DNA content (John, 1988). It is quite obvious that constitutive heterochromatin DNA is made up of repetitive sequences other than satellite DNA. The results of Moyzis et al. (1987) suggest that the remaining repetitive sequences may be more difficult to isolate than satellite DNA because of an unusual lack of restriction enzyme recognition sites. The fact that constitutive heterochromatin DNA shows sequence homology between chromosomes within a species and between species suggests that their presence and characteristic organization may reflect some property of structure and function.

Knowledge of the molecular organization and distribution of these sequences within the genome may provide a better understanding of such properties.

1.2.4. METHYLATION STATUS OF CONSTITUTIVE HETEROCHROMATIN DNA SEQUENCES

Methylation of mammalian DNA is found in the ubiquitous form of 5-methylcytosine (m^5cyt) (Razin and Riggs, 1980). A post-replication DNA modification process, DNA methylation involves the enzymatic transfer of a methyl group from 5-adenosyl methionine to the cytosine residue of a CpG dinucleotide. Approximately 50-70% of all CpG dinucleotides are methylated in various vertebrate species (Wigler, 1981).

Both biochemical and cytological studies have shown that constitutive heterochromatin DNA is highly methylated. Miller et al. (1974) showed that m^5cyt antibodies preferentially bound to the centromeric regions of mouse chromosomes and to the C-band regions of human chromosomes using immunofluorescence. Specifically, the antibodies recognized the constitutive heterochromatin regions of human chromosomes 1, 9, 16, Y and the centromere and short arm of chromosome 15. The centromeric C-bands of chromosomes 10, 17, 22 and Y were sometimes labelled as well. Similar results were reported using an indirect immunoperoxidase labelling method by Lubit et al. (1976).

Harbers et al. (1975) showed that mouse satellite DNA,

localized to the C-banded centromeric regions of murine chromosomes, was highly methylated compared to the rest of the genome. Mouse L-cells were grown in the presence of [^{3}H-methyl]-L-methionine, resulting in the radioactive labelling of m^{5}cyt. By fractionating satellite DNA from the main band DNA using cesium chloride gradient analysis, it was determined that satellite DNA contained 3.5 to 4.6% of m^{5}cyt, a level that was 3 times the amount found in main band DNA. Similar findings were reported by Singer et al. (1977) for satellite DNA isolated from rat hepatoma cells.

The chromatin distribution of m^{5}cyt residues was studied in mouse L cells using hybridization kinetics and deoxyribonucleases (Solage and Cedar, 1978). Nuclei were isolated from cells that were radioactively labelled with [^{3}H-methyl]-L-methionine and digested with micrococcal nuclease (MN) or pancreatic deoxyribonuclease (DNase I). A high proportion of the m^{5}cyt residues was localized to the nucleosome cores in DNA resistant to MN and DNase I digestion. Extraction of the DNA from the digested nuclei and self-hybridization kinetic studies indicated that 50% of m^{5}cyt was localized to satellite DNA sequences, 10% to intermediate repetitive sequences and the remaining 40% to unique DNA sequences. Ball et al. (1983) also demonstrated that m^{5}cyt was localized to nucleosomes containing histone H1 fractionated from mouse cell chromatin while nucleosomes

lacking histone H1 proteins were 1.6- to 2.3-fold undermethylated.

Changes in the methylation status of repetitive DNA sequences have been observed during mammalian development. Data have been obtained mainly for mouse major and minor middle repetitive satellite sequences, although some evidence is available for human repetitive sequences as well (reviewed by May-Hoopes, 1989). Sanford et al. (1984) determined that mouse centromeric major and minor satellite DNA were undermethylated in sperm and oocyte DNA using MspI and HpaII digest analysis. Undermethylation was demonstrated by the susceptibility of sperm and oocyte DNA to HpaII digestion, producing a ladder of fragments identical to that obtained with MspI digestion. It was estimated that 30 to 50% of the MspI sites of the sperm major satellite DNA sequences were recognized by HpaII. Interspersed repetitive sequences were not found to be undermethylated in the germ cells, showing similar levels of methylation to samples obtained from liver. These findings have been confirmed in a subsequent study by Chapman et al. (1984). Gama-Sosa et al. (1983) also showed in an earlier study, that the EcoRI family of alphoid tandemly repeated sequences were undermethylated 10-fold at a HhaI site in human sperm DNA compared to brain and placental DNA. These studies collectively indicate that mammalian repetitive DNA sequences are undermethylated during

gametogenesis.

The investigation of the methylation status of repetitive sequences in adult tissues has generally shown that a change in the level of methylation has occurred. The previously described study by Sanford et al. (1984) demonstrated that mouse centromeric satellite DNA was almost completely methylated in adult control tissues, suggesting that de novo methylation has occurred at some point in time after fertilization. Chapman et al. (1984) reported tissue specific methylation patterns for mouse middle repetitive sequences. Levels of DNA methylation of embryonic and extraembryonic early cell lineages and adult somatic tissues were assessed using MspI and HpaII restriction enzyme analysis. Repetitive DNA from two extraembryonic cell lineages was significantly undermethylated compared to that from the embryonic cell lineage, primitive ectoderm, of 7.5 day embryos and adult somatic tissues. These results suggest that tissue specific methylation of mouse repetitive satellite sequences had occurred very early during embryonic development.

Howlett et al. (1989) more recently examined the in vivo methylation status of the previously described mouse major and minor satellite DNA sequences from liver DNA using HPLC analysis as well as HpaII and MnlI restriction enzyme analysis to see if any age-related changes in methylation had

occurred. Comparison of MnlI digests of DNA isolated from the livers of 2-, 8-, 10- and 31-month old mice showed similar extent of digestion, although a 2-fold difference in the ratio of unit monomers compared to unit monomers and dimers was observed between 2 and 10 months. Comparison of digests from 10-month and 31-month samples showed very little difference in the proportion of unit monomer to monomer and dimers, although densitometry scans of the autoradiograph of a Southern blot hybridized with the major satellite probe showed a 2.7-fold increase in band densities of the ladder of fragments of multiples of unit size. It was concluded that the greatest change in methylation was observed between 2 and 10 months. After this stage, the MnlI site did not appear to undergo extensive demethylation.

The methylation status of the minor satellite DNA sequences was also assessed using MspI and HpaII restriction enzyme analysis. Southern blot hybridization indicated that these sequences remained fully methylated with increasing age. On the other hand, HPLC analysis of the m^5cyt content of the sequences isolated by cesium chloride/Hoechst dye gradients revealed that the repetitive sequences isolated from the livers of very young mice were almost completely methylated while sequences of middle-aged and old liver donors showed a decrease in methylation levels that parallelled that seen in main band DNA. It was concluded

that overall decreases in DNA methylation of satellite sequences may be observed with increasing adult age. May-Hoopes (1989), in reviewing this study, speculated that differences detected in liver samples from young and old mice by HPLC analysis may not have been detectable at the same level using methylation-sensitive restriction enzyme analysis.

The _in vitro_ methylation status of three classes of highly repetitive DNA isolated from three human diploid fibroblast cells strains was assessed at the molecular level using methylation-sensitive restriction enzyme analysis (Shmookler-Reis and Goldstein, 1982a). Digestion of genomic DNA with _MspI_, when radioactively end-labelled, electrophoresed and autoradiographed, produced fragments that were 45, 110 and 175 bp in size. It was estimated that these fragments are present as 10^5 copies per genome. Digestion with the methylation-sensitive isoschizomer restriction enzyme, _HpaII_, did not result in the production of the same bands, suggesting that the repeats were extensively methylated. Quantification of the autoradiographic exposures indicated that 70-80% of the cytosine sites analyzed were methylated consistently, both at early and late passage. Although no significant changes in the levels of DNA methylation were observed for repetitive sequences, decreases in the amount of repetitive DNA, presumably due to deletions,

were detected in aging diploid fibroblast cultures.

The relatively stable level of methylation observed for repetitive sequences contrasts with the changes that have been reported for unique sequences and total DNA. Generally, decreases in total DNA methylation and variations in the methylation patterns of specific genes have been observed in aging diploid human and rodent fibroblast cultures (Shmookler-Reis and Goldstein, 1982a,b; Wilson and Jones, 1983). Shmookler-Reis and Goldstein (1982a,b) attributed the heterogeneity of DNA methylation of certain genes to de novo demethylation within specific clones of a culture.

The recent analysis of in vivo methylation levels of mouse satellite repetitive DNA by Howlett et al. (1989) suggests that age-related demethylation occurs within these sequences paralleling that seen for total DNA. However, it cannot be as readily detected using methylation-sensitive restriction enzyme analysis as by HPLC. One could also speculate that the level of mouse satellite repetitive DNA methylation differs in vivo compared to in vitro or that the differences observed in vivo during aging are much more subtle than those changes observed for the same sequences early in development.

1.2.5. POSSIBLE EFFECT OF DNA MODIFICATION BY METHYLATION ON CHROMATIN STRUCTURE

Chromatin studies have shown that repetitive DNA

sequences containing m^{5}cyt are localized within nucleosome core particles that are complexed with histone H1 proteins (Ball et al., 1983). Histone H1-complexed nucleosomes are generally found in transcriptionally inactive chromatin fractions that are also resistant to endonuclease digestion (Gottesfeld et al., 1974; Egan and Levy-Wilson, 1981). These studies collectively suggest that highly methylated repetitive DNA sequences are non-randomly organized within a defined subclass of chromatin of a particular conformation.

DNA modification by methylation is thought to play a role in a variety of cellular processes including transcription repression, chromatin structure formation and the stabilization of chromosome condensation for cell division. The effect of DNA methylation on chromatin conformation and its relationship to gene activity was investigated by Keshet et al. (1986) using transfected exogenous DNA. The chromatin configurations of methylated and unmethylated DNA sequences were determined in vivo by transfecting different gene constructs into mouse L cells by DNA-mediated gene transfer.

Three gene constructs consisting of the chloramphenicol acetyl transferase gene, pBR322 and SV40 sequences, the 2.0 kb PvuII Herpes simplex virus thymidine kinase gene and the 4.4 kb PstI fragment of the human β-globin gene were inserted into the M13 vector. The

methylated constructs were synthesized _in_ _vitro_ by complementary strand synthesis in the presence of 2-deoxy-5-methylcytidine triphosphate while the unmethylated constructs incorporated deoxycytidine triphosphate. The chromatin structure of the transfected methylated and unmethylated gene constructs was assessed using MN and DNase I digestion analysis of nuclei.

The methylation status of the constructs after transfection was determined by MspI and HpaII restriction enzyme analysis. It was predicted that if methylated sequences were localized to inactive chromatin domains, these regions would be more resistant to endonuclease digestion than active chromatin configurations. The methylated constructs maintained their methylation levels upon transfection into mouse L cells, they were localized to chromatin domains that were resistant to MN and DNase I digestion, and they demonstrated very little gene activity compared to the unmethylated constructs. More specifically, the methylated gene constructs were found to be localized in supranucleosomal particles that are known to reside in inactive chromatin domains. DNA methylation did not seem to have any effect on nucleosome structure and spacing as MN digestion produced a normal nucleosome ladder. The results suggest that DNA methylation influences local chromatin structure in the regions of the modified sequences.

It was postulated that methylated DNA sequences influence DNA-protein interactions so that the surrounding chromatin assumes an inactive configuration. This could be achieved by influencing the interaction of the methylated sequences with structural nuclea_ proteins such as histones, high mobility group (HMG) or matrix proteins, playing an important role in the organization of a specific chromatin state within a defined region. DNA methylation could also influence the transcriptional potential of these sequences by modifying interactions with transcription factors. Keshet et al. (ibid) also suggested that DNA methylation could ensure that a stable chromatin structure is reproduced following DNA replication and cell division, as methylation of DNA occurs shortly after replication and before the formation of active chromatin configurations and the placement of histone proteins.

Razin et al. (1985) presented a "nucleosome locking model" to explain the role of DNA methylation in the clonal inheritance of chromatin structure. This model is based upon the observed findings that hypomethylation of total genomic DNA occurs in vitro in differentiating cell populations, m^5cyt is non-randomly distributed in nucleosomes, and site-specific methylation is correlated with a defined chromatin configuration and gene activity (reviewed in Razin et al. (ibid). It was proposed that transient demethylation of DNA

sequences during differentiation would allow the movement of nucleosomes along the DNA. During this period of movement, specific proteins, called determinators, would be able to access particular regulatory sites and stabilize a new nucleosome structure that is subsequently "locked" into place by de novo methylation. Methylation could only occur in sequences that were not protected by the determinator proteins. The chromatin structure would be maintained by maintenance methyltransferases that have an affinity for hemimethylated sites. Such a process would ensure the stable inheritance of a particular chromatin structure without the repeated need for determinator proteins.

Considering the broad specificity of known methyltransferases, the model could account for the observed regions of site-specific methylation and its correlation with chromatin structure and gene activity. However, this model also implies that methylation of DNA would be the primary regulator of chromatin structure and would require the correlation of undermethylation of gene sequences, active chromatin configurations and gene activity to be absolute. Not all actively transcribed gene sequences are undermethylated nor does undermethylation of genes result in their subsequent transcription. This model would also predict that the global demethylation of genomic DNA associated with aging would result in the dedifferentiation

of normal aging tissue, a phenomenon that has not generally been observed except in cancers. This suggests that other regulatory processes in addition to DNA methylation are involved in gene expression and the formation of chromatin structure.

Evidence that DNA methylation may influence chromosome structure has been demonstrated in mitotic chromosomes that have incorporated a m^5cyt nucleoside analogue, 5-azacytidine (5-azaC). This nucleoside, when incorporated into DNA, cannot be methylated in vivo as it presumably inhibits DNA methyltransferase activity by covalent binding, resulting in subsequent hypomethylation (Reeves, 1984). At very high concentrations, 5-azaC also inhibits DNA, RNA and protein synthesis (Cihak et al., 1974).

Viegas-Pequignot and Dutrillaux (1976) initially demonstrated the effect of 5-azaC on human chromosome structure. Lymphocyte cultures were treated with 5-azaC, inducing a delay or lack of condensation of certain chromosome regions that corresponded to G-bands, giving a segmentation pattern that was similar to R-banding. Decondensation of the secondary constrictions of chromosomes 1, 9 and 16, the short arms of the acrocentric chromosomes and occasionally paracentromeric regions was also particularly evident. Simultaneous tritiated thymidine labelling for 1-3 hours with 5-azaC resulted in the labelling

of the segmented regions. Because 5-azaC has been shown to alter or inhibit protein synthesis in <u>Escherichia</u> <u>coli</u>, Viegas-Pequignot and Dutrillaux <u>(ibid)</u> postulated that the mechanism of chromosome segmentation may have been caused by the direct incorporation of the cytidine analogue itself or by a disturbance in protein synthesis that subsequently affected the formation of chromosome structure.

Schmid <u>et</u> <u>al</u>. (1984) demonstrated that 5-azaC treatment of human peripheral blood cultures inhibited the condensation of specific chromosome regions. Different doses and treatment times of 5-azaC resulted in the appearance of three different segmentation patterns that could be classified into three types of metaphases. Very high concentrations of 5-azaC produced chromosomes that were undercondensed at so many regions that they were described as appearing pulverized. Treatment of lymphocytes with 10^{-4}-$5X10^{-7}$ mol/L 5-azaC for 7 hours resulted in segmented chromosomes that appeared R-banded, indicating that the G-bands were undercondensed while the R-bands remained normally condensed. Treatment with low doses of 5-azaC ($2X10^{-6}$-10^{-7} mol/L) for 7 hours produced undercondensation of the constitutive heterochromatin regions of chromosomes 1, 9, 15, 16 and Y in about 80% of metaphases. Usually the undercondensation effect was more pronounced in the constitutive heterochromatin regions of chromosomes 1 and Y

compared to 9 and 16. The phenomenon of undercondensation of metaphase chromosomes by 5-azaC treatment was observed to be a tissue-specific response, being more pronounced in lymphocytes than in fibroblast cells.

The results of Viegas-Pequignot and Dutrillaux (1976) and Schmid et al. (1984) collectively demonstrated that treatment of cells during S phase with 5-azaC, a known modifier of DNA methylation, resulted in the modification of chromosome structure localized to G-bands and constitutive heterochromatin regions. The pronounced effect of 5-azaC on the constitutive heterochromatin regions of chromosomes 1, 9, 15, 16 and Y compared to other regions suggested to Schmid et al. (ibid) that these regions comprised a distinct class of heterochromatin that was characterized by a sensitivity to the cytosine analogue. It is difficult to prove that the change in chromosome structure observed with 5-azaC treatment was the direct result of the inhibition of DNA methylation and not protein synthesis, although it is thought that low doses of 5-azaC do not interfere with protein synthesis (May-Hoopes, 1989).

The studies just described suggest that levels of DNA methylation affect chromatin structure. Methylated DNA sequences could conceivably influence DNA-protein interactions so that the surrounding chromatin assumes an inactive configuration. In addition to this, DNA methylation

could ensure that a stable chromatin structure is reproduced following DNA replication and cell division. However the correlation of undermethylation of DNA sequences, active chromatin configurations and gene activity is not absolute, suggesting that DNA methylation is not the primary regulator of chromatin structure. Changes in DNA methylation have largely been associated with differentiation and development (Sanford et al. 1984; Chapman et al. 1984), chromatin structure (Keshet et al. 1986) and aging (Shmookler-Reis and Goldstein, 1982a,b; Howlett et al. 1989).

1.2.6. REPLICATION BEHAVIOR OF CONSTITUTIVE HETEROCHROMATIN

Constitutive heterochromatin is generally considered to replicate late during the S phase of the cell cycle. In an early study using tritiated thymidine (TdR) pulse-labelling in two cultured rodent cell strains, Schmid and Leppert (1969) demonstrated that different types of chromatin replicated at various times during S phase in a reproducible manner. It was observed that euchromatin replicated early during S phase, followed by the replication of the active X chromosome, and ending with facultative (inactive X chromosome) and constitutive heterochromatin replication. In addition to this, differences in the rate of DNA synthesis were observed between euchromatin and constitutive heterochromatin. This was determined by the

cumulative frequency of labelling patterns observed for each chromatin type at hourly intervals over a period of 10 hours. The median duration of DNA synthesis was estimated from the 50% value of the labelling curve and was approximated to be 2 hours for constitutive heterochromatin while euchromatin replicated over a period of 4-5 hours in both rodent cell strains. This suggested that the rate of constitutive heterochromatin replication was approximately twice as fast as that of euchromatin.

With the development of specialized pulse-labelling techniques using a thymidine analogue, 5- bromodeoxyuridine (BrdUrd), the replication order of different types of chromatin has been determined with greater resolution. Incorporation of BrdUrd during DNA synthesis can be visualized as a differential chromosome banding pattern in human metaphase chromosomes (Latt, 1973; Wolf and Perry, 1974). Depending on the time of the BrdUrd pulse within S phase, chromosome banding patterns similar to reverse- (R-banding) or Giemsa- (G-banding) banding can be obtained (Grzeschik et al., 1975). Reverse-bands are representative of early replicating regions of chromosomes, while G-bands are late replicating (Holmquist, 1987).

Because the chromosomal location of constitutive heterochromatin is well defined for both banding types, their replication pattern can be followed during S phase using

BrdUrd pulse labelling. In metaphase chromosomes of unsynchronized cultured human peripheral lymphocytes, Grzeschik et al. (1975) observed late replication patterns that coincided with the position of G-bands. Using continuous BrdUrd for nearly one cell cycle followed by a short 4-5 hour pulse with dTR, it was established that the constitutive heterochromatin regions on chromosomes 1, 9 and 16 replicated at the end of S phase. A similar observation was made for chromosomes from human fibroblast and amniotic fluid cells by Epplen et al. (1975).

The use of synchronized cultures has helped to further define at what position in S phase a cell may be when pulsed with BrdUrd or TdR. Schmidt (1980) also demonstrated the existence of early and late replicating phases in human lymphocyte cultures synchronized at the G_1 - S transition stage of the cell cycle using BrdUrd pulse labelling at various time intervals. DNA synthesis occurred in R-bands during the first three hours of S phase followed by G-band replication in the remaining 7-8 hours of S phase. The results of this study suggest that the late replicating phase was two to three times longer than the early replicating phase. Although cell synchronization may have resulted in the shortening of the early replicating phase, Schmidt still concluded that the late replication period was more variable and several times longer than the early replicating phase.

This was based upon the concept that the late replication period was not affected by the synchronizaton process. More recent evidence suggests that synchronization of the cell cycle using DNA synthesis inhibitors may only be partial and that some cells still progress through S phase before the release of the block (Camargo and Cervenka, 1980). This could give the illusion that replication in the early phase of S phase proceeds at a faster rate than in late S phase.

A subsequent study by Camargo and Cervenka (1982), using high resolution chromosome banding and terminal BrdUrd labelling to determine the replication behaviour of different types of chromatin, again revealed a biphasic replication programme. Euchromatin, localized to R-bands of chromosomes replicated early in S phase while constitutive, facultative and intercalary heterochromatin replicated later in S phase only after early replication was complete. By subdividing S phase into five substages, Camargo and Cervenka (ibid) observed that constitutive heterochromatin replicated during the last two substages at a very fast rate with the constitutive heterochromatin region of the Y chromosome being one of the last regions of the genome to replicate.

A number of studies have suggested that S phase consists of an early replicating phase that is divided from the late replicating stage by a gap known as the "3C pause" (reviewed by Holmquist, 1987). Holmquist et al. (1982)

demonstrated the existence of a bimodal S phase in V79-8 Chinese hamster lung fibroblast cultures that were synchronized by mitotic shakeoff harvests. Labelling with BrdUrd revealed that Giemsa-light bands, equivalent to R-bands, replicated during the first half of S phase and that Giemsa-dark bands replicated during the second half. Labelling curves of synchronized fibroblast cells that were pulsed with tritiated thymidine for 30 minutes, showed that the early and late replicating phases were separated by a pause in DNA synthesis, as evidenced by very little thymidine incorporation. Since this reduction in DNA synthesis occurred when half of the genome had replicated and the cells had a 3C DNA content, this stage was defined as the 3C pause. Holmquist et al. (ibid) postulated that the 3C pause allowed for the transition of replication events from early replicating regions to late replicating regions.

Although it is well documented that constitutive heterochromatin replicates late in S phase, it has been very difficult to establish a consistent chronological pattern of replication for the large constitutive heterochromatin regions found on chromosomes 1, 9, 16 and Y. A review of a number of studies showed that a 4-5 hour terminal pulse with BrdUrd or TdR distinguished constitutive heterochromatin replication late in S phase (Ganner and Evans, 1971; Knight and Luzzatti, 1973; Calderon and Schnedl, 1973; Epplen et

al., 1975; Grzeschik et al., 1975; Kondra and Ray, 1978;
Schemp et al., 1978; Schmidt, 1980; Camargo and Cervenka,
1980, 1982). Epplen et al. (1975) attempted to establish the
sequence of late replication patterns in human fibroblast and
several amniotic fluid cell types by charting the time
sequence of the disappearance of bands from individual
chromosomes. The constitutive heterochromatin regions of
chromosomes 1, 2, 3, 13, 14, 15, 16, 18, 20 and 22 (C-group
chromosomes were excluded from this study) were the last
bands to disappear for each chromosome with the exception of
chromosomes 5, 17 and 21 where other bands were found to be
later replicating. The constitutive heterochromatin region
of chromosome 1 was reported as being the last band of all
the chromosomes studied to disappear, suggesting that it may
be the latest replicating band of the genome. The
constitutive heterochromatin region of chromosome 16
replicated earlier than that of chromosome 1.

Grzeschik et al. (1975) presented a similar outline of
late S phase replication patterns of chromosomes from human
peripheral blood lymphocytes. The replication patterns were
defined into four successive stages that were determined by
BrdUrd labelling followed by a 4, 4.5 and 5 hour TdR
treatment at the end of S phase. The constitutive
heterochromatin regions of chromosomes 1, 9, 16 and Y all
showed complete replication with the 5 hour thymidine

treatment but a variable replication pattern was observed with the shorter treatments. Contrary to the results of Epplen et al. (1975), the constitutive heterochromatin of chromosome 1, localized to band 1q1-2, was not the last band to replicate on this chromosome nor was it the latest replicating region of the genome. Comparing the replication pattern of the constitutive heterochromatin of chromosomes 1, 9, 16 and Y, the schematic presentation of Grzeschik et al. (ibid) suggested that band 1q1-2 replicated earlier than the constitutive heterochromatin localized to band 9q1-2 or 16q1. Similarly the constitutive heterochromatin regions of chromosomes 9 and 16 were not the last bands to replicate for each chromosome either. The constitutive heterochromatin region of the Y chromosome showed partial replication with the 4 hour TdR labelling and complete replication with the 4.5 and 5 hour labelling time, suggesting that it may replicate later than the other constitutive heterochromatin regions. This would be in agreement with the results reported by Camargo and Cervenka (1982).

The replication map of human fibroblast chromosomes presented by Kondra and Ray (1978), determined by similar labelling techniques, also revealed that the constitutive heterochromatin regions of chromosomes 1, 9 and 16 were the latest replicating regions of each chromosome and that they replicated very late in S phase. Although it can be

concluded that the constitutive heterochromatin regions of chromosomes 1, 9, 16 and Y replicated very late in S phase, it is very difficult to establish a consistent chronological order of replication. Kondra and Ray (ibid) have suggested that the variability observed in the replication patterns of human chromosomes may be explained by differences due to tissue specificity, experimental approaches and individual subject variation.

1.2.7. POSSIBLE FUNCTIONS OF CONSTITUTIVE HETEROCHROMATIN

The function of constitutive heterochromatin is still very much undefined although it appears to have an effect on a number of cellular events (John, 1988). Many of the described effects and speculated functions of constitutive heterochromatin have been structural in nature. The proximal location of constitutive heterochromatin to the centromeres of all chromosomes suggests that it may play a role in centromere stability. John (ibid) disputed this hypothesis by contending that there is no real evidence to support such a functional role. Yamato and Miklos (1977) investigated this functional aspect of constitutive heterochromatin in Drosophila melanogaster by comparing the centromere activity and chromosome segregation pattern of X chromosomes that had deletions of variable amounts of centric heterochromatin. There did not appear to be any difference in the function of

centromeres that had less heterochromatin associated with them than those that had more. In addition to this, the polymorphic variations in heterochromatin content observed between individuals of the same species and between species also suggests that centromere function is not greatly influenced by the amount of adjacent constitutive heterochromatin.

Constitutive heterochromatin has also been implicated in determining the three dimensional structure of interphase nuclei (John, 1988). Heitz (1928) originally observed that chromocenters were formed by the association of specific chromosome regions that remained condensed after mitosis (cited in John, 1988). Evidence that individual chromosomes are spatially arranged in interphase nuclei has accumulated from in situ hybridization studies using chromosome-specific DNA probes (Manuelidis, 1985; Bourgeois et al., 1985; Rappold et al., 1984). Similar chromosome-specific domains have also been detected in interphase nuclei using in situ endonuclease digestion and distamycin A-DAPI staining (Verma et al., 1986). It has been postulated that the heterochromatic regions of chromosomes are closely associated with the nuclear membrane, forming a structure by which chromosome specific domains can be attached (Hancock and Boulikas, 1982). In addition to this, it has been suggested that the chromosomal domains are attached to the nuclear membrane only

when gene sequences are being transcribed, providing a controlling mechanism for genetic activity (Reeves, 1984). John (1988) maintains that the major question that needs to be asked is whether constitutive heterochromatin is located at a specific site because of associated function or is it localized within a specific region by another mechanism. As more information becomes available regarding the spatial organization of constitutive heterochromatin of individual chromosomes within the interphase nucleus, its functional role may be better understood.

Heterochromatin does, however, appear to have an effect on meiotic recombination in germ cells (John, 1988). During diplotene of meiosis, chiasmata formation appears to be confined to the euchromatic regions of chromosomes. This lack of chiasmata formation between homologous heterochromatin regions includes intercalary as well as constitutive heterochromatin. Decreased chiasmata formation between homologous regions of heterochromatin appears to affect the frequency of their formation between adjacent homologous euchromatic regions and is also associated with a decrease in intrachromosomal recombination. Very little recombination appears to take place in the euchromatic regions adjacent to centric heterochromatin, leading to the hypothesis that constitutive heterochromatin may protect the ribosomal genes, located to the satellites of acrocentric

chromosomes in humans, from mutation and crossing over (Yunis and Yasmineh, 1971).

In some species, constitutive heterochromatin appears to promote homologous and non-homologous pairing during the first meiotic prophase (John, 1988). In the case of homologous pairing, this has led to the hypothesis that centromeric heterochromatin may play an important role in synapsis formation of the centromere regions (Macgregor and Kezer, 1971; cited in John, 1988). This hypothesis does not seem to be supported by the evidence presented in D. melanogaster by Yamamoto (1977) that suggested that pairing was dependent upon euchromatin homology rather than heterochromatin homology.

It is obvious that despite all that is known about constitutive heterochromatin and its distinct characteristics, very little is known about its function. Speculation concerning its functional role has mainly focused on structural roles, correlating its defined position within the chromosome complement with centromere activity. The variation of heterochromatin content within individuals of a species and between species has often weakened much of the evidence presented for some organisms regarding its possible function(s) and effect, as consistency between species is not always evident. However, it is difficult to accept the possibility that such a distinct class of chromatin is purely

redundant in nature.

1.3. APPROACHES TO THE CHARACTERIZATION OF CONSTITUTIVE HETEROCHROMATIN

1.3.1. USE OF METHYLATION SENSITIVE ISOSCHIZOMER RESTRICTION ENZYMES TO CHARACTERIZE DNA METHYLATION LEVELS OF CONSTITUTIVE HETEROCHROMATIN

A variety of techniques have been used to identify and quantify levels of m^5cyt in DNA. Earlier studies used radioactive labelling and two-dimensional thin layer chromatography to measure m^5cyt content (Harbers et al., 1975; Singer et al., 1977; Solage and Cedar, 1978). Other methods such as gas chromatography and high resolution mass spectrometry have also been reported (Razin and Riggs, 1980). Methylated regions of intact chromosomes have been detected using antibodies to m^5cyt that were visualized by indirect immunofluorescence or immunoperoxidase labelling methods (Miller et al., 1974; Lubit et al., 1976). These techniques have provided important information about the m^5cyt content of genomic DNA but gave limited insight as to any possible functions.

Methylated cytosine residues can be detected by restriction enzymes that recognize the CpG dinucleotide as part of their recognition sequence. Some of these restriction endonucleases such as XhoI, HhaI, SalI and HpaII are defined as methylation sensitive, being unable to the cut the DNA if the CpG site within their recognition sequence is

methylated (Weissbach et al. 1989). The isoschizomer restriction enzymes MspI and HpaII are probably the most commonly used enzymes for the detection of methylated sequences. Both restriction enzymes recognize the same sequence, CCGG, but HpaII will not cleave the sequence C^mCGG if the internal cytosine is methylated. MspI is able to cleave both methylated and unmethylated CCGG sequences if it is the internal cytosine that is methylated.

Bird and Southern (1978) introduced a now commonly used technique to detect methylated cytosine residues. The molecular approach of Southern blot analysis involves cutting total genomic DNA with MspI or HpaII, separating the digested fragments by agarose gel electrophoresis, blotting the separated fragments onto a nitrocellulose or nylon membrane and hybridizing with radioactively labelled DNA or RNA probes. Levels of DNA methylation are then assessed by comparing the fragments produced by MspI and HpaII digestion. If the sequences of interest are methylated, HpaII digestion would result in fewer or larger sized restriction fragments than those obtained with MspI. This method would allow one to investigate DNA methylation of specific genes or regulatory regions of the genome.

Waalwijk and Flavell (1978) were one of the first groups to show the existence of tissue specific differences in DNA methylation using this technique by investigating the

methylation status of the rabbit ß-globin gene. The first correlation of gene expression and site-specific DNA methylation was reported for the chicken ß-globin gene by McGhee and Ginder (1979) using this method. This molecular approach has subsequently provided many examples correlating different levels of DNA methylation with gene expression and chromatin configuration. Actively transcribing gene sequences are often undermethylated and associated with chromatin domains that are sensitive to endonuclease digestion. DNA methylation has also been implicated in genomic imprinting and in the inheritance of epigenetic defects in the form of epimutations and functional hemizygosity (Weissbach et al., 1989).

One of the disadvantages of restriction enzyme analysis of DNA methylation levels is that this method detects only 5-15% of the CpG sites and does not distinguish hemimethylated and fully methylated DNA (Weissbach et al., 1989). An alternative follow-up approach to detecting the remaining CpG dinucleotides would be to sequence the region of DNA being investigated. This method, although more time consuming and labour intensive without automation, would not only detect all CpG sequences but could also determine the methylation status of these sites.

1.3.2. CHARACTERIZATION OF REPLICATION BEHAVIOR OF CONSTITUTIVE HETEROCHROMATIN

1.3.2.1. IDENTIFICATION OF REPLICATION EVENTS OF MITOTIC CHROMOSOMES

DNA replication events in S phase were initially studied using an autoradiographic technique of labelling chromosomes with tritiated thymidine (^{3}H-TdR). This method was first described by Taylor et al. (1957) with Vicia fabia chromosomes. Schmid (1963) applied the technique to human chromosomes by labelling fibroblast and peripheral blood lymphocytes with ^{3}H-TdR during the last 2 hours of S phase. The DNA labelling pattern visualized by autoradiography was described as "step-wise patterns of completion of DNA replication in specific chromosomes" that were defined as early, intermediate and late stages of S phase. The constitutive heterochromatin regions of chromosomes 1, 16 and Y were specifically labelled with silver grains during the late S phase stage. Comparable results were also reported by Sasaki and Makino (1963) and Saksela and Moorhead (1962) using similar labelling techniques.

The relationship between DNA replication patterns and structural chromosome banding patterns was investigated by Ganner and Evans (1971) using Q-bands by fluorescence using quinacrine (QFQ). Human peripheral blood lymphocyte cultures were labelled for 5 hours with ^{3}H-TdR before harvesting, QFQ-banded and then processed for autoradiography. The

fluorescent QFQ-banding pattern was then compared to the DNA replication pattern produced by autoradiography. Late replicating DNA was generally found localized to the brightly fluorescent bands with the exception of the constitutive heterochromatin regions of chromosomes 1, 9 and 16 which were characterized by dull fluorescence with QFQ-banding. The early replicating DNA labelling patterns were localized to dull fluorescent QFQ-bands. Similar results using QFQ-banding were also reported by Calderon and Schnedl (1973). These studies showed that a definite relationship existed between the DNA replication patterns observed with ^{3}H-TdR labelling and the structural chromosome bands produced by cytochemical staining techniques. Autoradiographic studies, however, are very labour intensive and time consuming and the labelling pattern produced by this method is not very distinct, making analysis somewhat difficult.

The introduction of various cytochemical staining methods to detect the incorporation of BrdUrd into cellular DNA has greatly improved the DNA replication patterns seen in metaphase chromosomes. Latt (1973) introduced a staining technique that differentiated BrdUrd incorporation using the fluorescent dye, Hoechst 33258. Differential staining was the result of reduced fluorescence observed by the Hoechst dye when bound to DNA which had incorporated BrdUrd. Latt (ibid) postulated that differential fluorescence was caused

by the uncoiling of the chromosome regions containing BrdUrd-substituted DNA or by altered DNA-protein interactions affecting the accessibility of the dye to the DNA.

Alterations in chromosome structure due to BrdUrd incorporation have been observed in late replicating regions (Zakharov and Egolina, 1972, Zakharov et al., 1974). Zakharov et al. (ibid) referred to the stretching or extension of these chromosome regions as "delayed spiralization", a phenomenon that was observed in 70-80% of the cells. The late replicating heterochromatic regions of chromosomes 4, 5, 6, 9, 13, 16, X and Y were the most frequently involved with chromosomes 17, 18, 19, 20, 21 and 22 being somewhat affected. It was postulated that incorporation of BrdUrd into late replicating DNA regions may produce changes in secondary DNA structure and/or may be associated with changes in protein-DNA interactions.

Wolf and Perry (1974) described another cytochemical staining procedure that has subsequently undergone modification and is now referred to as the fluorescence-plus-Giemsa (FPG) technique. This procedure detects BrdUrd-incorporated DNA by Hoechst 33258 staining followed by ultraviolet (UV) light treatment and Giemsa staining. With this method, it is believed that BrdUrd-substituted DNA undergoes photolysis when exposed to UV light that is enhanced by the photosensitivity of the Hoechst dye.

Acridine orange has also been used as a fluorescent dye to differentiate BrdUrd-substituted DNA (Verma and Babu, 1989). The dye exhibits green fluorescence when bound to unaltered double stranded DNA and red fluorescence when bound to the single stranded DNA that results from photolysis due of the BrdUrd-substituted DNA.

Drouin et al. (1989) have proposed a model explaining how DNA replication banding patterns are differentiated using this technique. They have postulated that BrdUrd-incorporated DNA is clustered within a defined chromosome region. Degradation of BrdUrd-DNA by photolysis would result in its subsequent loss from the chromosome region and be visualized as a pale-staining band. Alternatively, DNA that has thymidine incorporated in its strand during replication would not be degraded by photolysis and would stain darkly with Giemsa.

Other mechanisms have been implicated in the differentiation process using the FPG staining technique. It has been suggested that UV-photolysis of BrdUrd-substituted DNA results in debromination of the DNA and also causes alterations in DNA-protein interactions (Mezzanotte et al., 1989). The DNA-protein alterations that have been described include UV-induced protein-protein cross-linking and breakage of disulphide bonds (Bianchi et al., 1985, Buys and Stienstra, 1980). Using monoclonal antibodies to single

stranded and double stranded DNA, Mezzanotte et al. (1989) demonstrated that UV treatment of BrdUrd-substituted DNA resulted in the loss of DNA from the chromosome but that this was not the only effect of photolysis. Differences in staining differentiation were observed in chromosomes depending on whether the template strand contained TdR or BrdUrd, suggesting that UV light has a different effect on BrdUrd-DNA-protein interactions. If TdR was incorporated into the template strand of a chromosome region, this region does not stain as palely as the region with BrdUrd incorporated into the template strand.

1.3.2.2. REPLICATION PROFILES OF HUMAN METAPHASE CHROMOSOMES

Replication events occurring at different stages of S phase can be followed by labelling DNA with BrdUrd for various lengths of time. Pulse labelling with BrdUrd at regular time intervals over the course of S phase, termed discontinuous labelling, has proven to be useful for studying early replication events (Camargo and Cervenka, 1980; Vogel et al., 1985). Very long BrdUrd labelling periods have also been used to monitor early replication events (Epplen et al., 1975; Kondra and Ray, 1978; Schmidt, 1980). Continuous labelling with BrdUrd for 2-5 hours at the end of S phase has been used to investigate late replicating events (Latt, 1973; Wolf and Perry, 1974; Grzeschik et al., 1975; Epplen et al.,

1975). With both continuous and discontinuous labelling procedures, DNA that has replicated in the presence of BrdUrd will be pale staining using the staining procedures described in the previous section. Late replication events have also been followed by labelling cells for nearly one cell cycle in the presence of BrdUrd and then pulsing with TdR for the last 4-5 hours before harvesting (Epplen et al., 1975; Grzeschik et al., 1975; Kondra and Ray 1978). With this approach, all early replicating chromosome regions will be pale staining because of BrdUrd incorporation while late replicating regions, having incorporated TdR, would be dark staining.

As previously described, a general relationship between DNA replication banding and structural chromosome banding patterns has been established. Schmidt (1980) demonstrated using discontinuous BrdUrd pulse labelling that early replicating DNA was localized to R-bands. Ganner and Evans (1971) observed that late replicating bands were localized to the brightly fluorescent bands produced by QFQ-banding with the exception of the constitutive heterochromatin regions of chromosomes 1, 9 and 16. Grzeschik et al. (1975) established that late replication bands were localized to the dark G-bands. These studies collectively indicate that late replicating DNA, with the exception of certain regions of constitutive heterochromatin, is localized to brightly fluorescent Q-bands or dark G-bands.

The constitutive heterochromatin regions of chromosomes 1 and 16 were localized to dull Q-bands and dark G-bands. The constitutive heterochromatin of chromosome 9 is also dully fluorescent but is localized to a light G-band. The constitutive heterochromatin found on the Y chromosome is brightly fluorescent with QFQ-banding but is variably stained with G-banding.

A model demonstrating the possible relationship between the appearance of a particular DNA replication banding pattern and structural chromosomal banding patterns has been presented by Holmquist et al. (1982). This model predicts that clusters of replication units, defined as replicons, reside within a chromosome band region. These clusters initiate DNA synthesis at different times during S phase, with early replicons residing in R-bands and late-initiating replicons in G-bands. The chromatin structure of actively replicating regions during S phase would be decondensed and diffuse compared to the condensed chromatin state of nonreplicating regions. The replication activity of constitutive heterochromatin which is localized to both light and dark staining G-bands, may be determined by its condensed state.

1.3.2.3. SUBCLASSIFICATION OF METAPHASE CELLS IN S PHASE

Most studies have simply classified BrdUrd-labelled

mitotic cells as early or late replicating, depending on the presence of replicated R- or G-bands. Camargo and Cervenka (1982) presented a descriptive model of replication chronology that subdivided S phase into five substages, I-V, according to the replication banding patterns as well as replication of the X chromosomes and of constitutive heterochromatin localized to C-band regions of chromosomes. Stage I generally corresponded to cells that had undergone one round of replication in the presence of BrdUrd and therefore would stain completely pale without any banding pattern. Stages II and III mitotic cells were characterized by incomplete and complete R-banding patterns, respectively, representative of early replicating regions. During the third substage, the early X chromosome would appear R-banded while the late replicating X would generally be pale staining. Stage IV was said to be characterized by a transition from early replicating R-bands to late replicating G-bands. Constitutive heterochromatin regions, localized to C-bands, would also begin replication during this substage. By the last substage, the constitutive heterochromatin regions and a few major G-band regions would have completed their replication.

Savage et al. (1984) developed a subclassification system for replication banded chromosomes that used "artificial keys" to place a cell within a certain substage

of S phase.   Two artificial keys used for chronological S phase subclassification are outlined in Figures 1 and 2. Key 1, shown in Figure 1,   uses chromosomes 2 and 5 to classify cells   within   five   subphases,   designated   Sk1-5. Subclassification depends on the presence or absence of a particular replication band for each chromosome. Key 4 uses chromosomes 3 and 4 for S subphase classification resulting in four stages, SkI-IV, as outlined in Figure 2.

Asynchronous human fibroblast and lymphocyte cultures were labelled with BrdUrd varying from 2-16 hours in duration and were sequentially harvested at 2 hour intervals using a 2 hour colcemid treatment. Short BrdUrd labelling periods of 4-6 hours resulted in a greater proportion of cells in the fourth and fifth subphase while longer labelling periods of 8-12 hours gave a greater distribution of cells in the earlier subphases. Cells were also classified as pre-S phase or G_1 by staining completely pale without any dark bands or as G_2 by staining uniformly dark without any pale bands.

Comparison   of   the   relative   subphase   frequency distribution showed that the order of the subphases were the same for each of the cultures, regardless of cell type, although differences in the duration of subphases, relative to each other, were observed. The mean S phase duration was also shorter in lymphocyte cultures compared to fibroblast cultures. The advantage of such a system is that it provides

65

Figure 1.   Artificial key (λ) used fcr the chronological subclassification of human cells in S phase (modified from Savage et al. 1984).

Key 1: Based on criteria from chromosomes 2 and 5
and results in five subphases, Sk1-5.

α   At least one 2q devoid of replication bands   Sk1
    Obvious bands on both 2q

β   2p with distinct mid-gap region (region 14-16)   γ
    2p with mid-gap absent (or poorly demarcated)   δ

γ   5q with distinct terminal gap (34)   Sk2
    5q without terminal gap   Sk3

δ   5p with distinct mid-gap (14)   Sk4
    5p solid, without distinct gap   Sk5

2   S
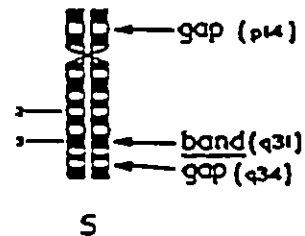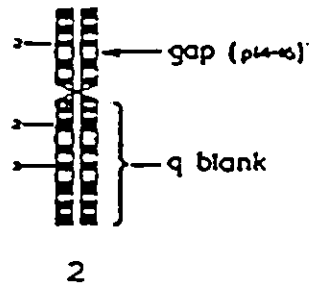
Figure 2. Artificial key (4) used for the chronological subclassification of human cells in S phase (modified from Savage et al. 1984).

Key 4: Based on criteria from chromosomes 3 and 4
and results on four subphases, SkI-IV.

3p with clear proximal gap (11-12)   α
3p without clear proximal gap   .   β

α   4q with band (21) absent from both chromosomes SkI
     4q (21) present on one or both homologues   SkII

β   4q with clear proximal gap (13) on both   SkIII
     chromosomes

     4q without obvious proximal gap (13) on one   SkIV
     or both chromosomes

3

4
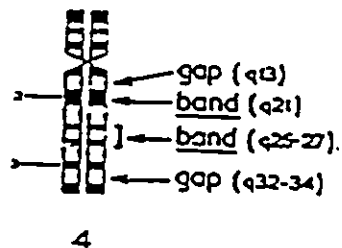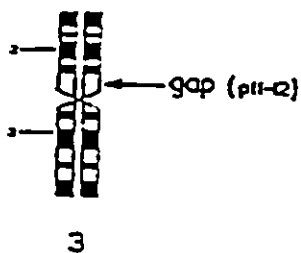
quantitative information about the replication process of different cell populations based upon relative subphase order and duration without synchronization or identical experimental conditions. In addition to this, it is possible to quantitatively determine when other bands replicate during S phase by subphase classification.

1.4. CHARACTERIZATION OF ROBERTS SYNDROME CONSTITUTIVE HETEROCHROMATIN: QUESTIONS ADDRESSED IN THIS STUDY

The structure and function of heterochromatin is still not well defined. It is highly condensed in structure, for the most part genetically inactive, its DNA is highly methylated, repetitive in nature and late replicating The striking chromosome abnormality exhibited by approximately half of the RS patients involving the constitutive heterochromatin regions of most chromosomes suggests that the organization of the heterochromatin may be structurally altered. The major focus of this research project has been to characterize RS constitutive heterochromatin and its DNA with respect to levels of DNA methylation and replication. It was hoped that characterization of heterochromatin DNA conformation and replication programme may provide more insight into the nature of the RS defect.

1.4.1. CHARACTERIZATION OF RS HETEROCHROMATIN DNA METHYLATION

The centromeric heterochromatin regions of many

mitotic chromosomes are considered to be highly methylated. The high levels of methylation of the centromeric DNA sequences may influence the structure of the chromatin by specific DNA-protein interactions. The methylation of DNA sequences has been strongly implicated in the formation of inactive chromatin configurations. Changes in DNA methylation have been associated with development and differentiation, aging, changes in chromatin structure and processes of DNA repair. The structurally abnormal appearance of RS heterochromatin DNA prompts one to ask whether altered levels of DNA methylation are associated with its decondensed state. A similar puffing phenomenon has been reported in the chromosomes of megaloblastic anemia patients with abnormal folate metabolism, a system which is responsible for the synthesis of the methyl donor, S-adenosyl methionine (Lawler et al. 1971). The heterochromatin abnormality in these patients was corrected by vitamin B_{12} and folate treatment.

The effect of short term manipulation of nucleotide pools or methylation on the RS heterochromatin abnormality has been investigated in vitro (Gunby, M.Sc. thesis, 1986). Attempts were made to reproduce the cytogenetic abnormality of RS in normal human lymphocyte and fibroblast chromosomes by treating the cells in culture with 5-azacytidine or cytosine arabinoside, agents which both cause demethylation

of DNA (Jones and Taylor, 1980; Evans and Mengel, 1964). Decondensation and stretching were observed in normal cells but the characteristic RS puffing was not reproduced. Alternatively, correction of the RS effect was not achieved when RS cells were treated with vitamin B_{12} or deoxycytidine.

In the present study, levels of methylated cytosine residues of RS heterochromatin DNA extracted from fibroblast cell strains were assessed using restriction endonuclease analysis with the isoschizomer enzymes, MspI and HpaII, Southern blot analysis and hybridization with a heterochromatin repetitive DNA sequence probe, D15Z1. The DNA methylation levels of the heterochromatin sequences of Roberts syndrome cell strains with and without the cytogenetic abnormality were compared controls using quantitative analysis to determine whether these levels correlated with the presence or absence of the RS effect.

1.4.2. REPLICATION STUDIES OF RS CONSTITUTIVE HETEROCHROMATIN

Constitutive heterochromatin is considered to be later replicating than euchromatin. There is a direct correlation between the degree of chromatin condensation and the time of DNA replication during S phase. One could postulate that should the RS effect be due to decondensed chromatin structure, the timing of its DNA replication may be altered. There is some indication that the timing of DNA synthesis in

RS is impaired. The rate of DNA synthesis of RS+ fibroblast cultures was compared to controls using BrdUrd incorporation (Gani et al., 1984). The DNA of the RS+ fibroblast strains incorporated less BrdUrd, suggesting that some of the characteristics of RS could be due to a defect in the pathways leading to DNA synthesis. The consequences of such an event could be important because it is well established that different regions of each chromosome replicate in a reproducible order during S phase and that the timing of the replication patterns are specific (Stubblefield, 1975).

In the present study, the DNA replication pattern of constitutive heterochromatin regions have been investigated by terminally labelling RS+ and control lymphoblast cells in S phase with BrdUrd. Metaphases were classified as having replicated during a particular substage of S phase using a subclassification system for replication banded chromosomes (Savage, personal communication). Subclassification involved the use of an artificial key that placed a cell within one of four successive substages of S phase, depending on the presence or absence of particular replication bands on chromosomes 3 and 4 (see Figure 2). The replication pattern of the constitutive heterochromatin of RS+ and control metaphases was determined by analysing the proportion of cells within each subphase that had BrdUrd incorporated within the constitutive heterochromatin regions of

chromosomes 1, 9, 16 and Y. In addition to this, the DNA replication pattern of the inactive X chromosome, a reliable indicator of a late replicating chromosome, was also assessed in female RS and control cell lines.

2. MATERIALS AND METHODS

2.1. CELL STRAINS AND LINES

The fibroblast cell strains were established from dermal skin biopsies in the laboratory of Dr. D.J. Tomkins, except for those controls purchased from the ATCC Cell Repository, Rockville, Maryland, U.S.A. Lymphoblast cell lines were established in the laboratory of Dr. Tomkins by transformation of peripheral blood lymphocytes with Epstein Barr virus (Neitzel, 1986). Roberts syndrome cell strains or lines were matched according to sex and age of the subject at the time of biopsy (Table 1).

2.2. TISSUE CULTURE

2.2.1. FIBROBLAST CELL STRAINS

Fibroblast cultures of all Roberts syndrome and control cell strains used were grown in 100 mm polystyrene tissue culture dishes (Corning 25020) with complete alpha minimal essential medium (α-MEM) containing ribo- and deoxyribonucleotides (Gibco 320-2571) and supplemented with 15% fetal bovine serum (FBS, Gibco 200-6140). The cultures were incubated at 37°C and 5% CO_2 with medium changes every 3-4 days until confluent. Confluent cultures were expanded by removing the culture medium, rinsing the monolayer with

Table 1.   Roberts syndrome and control fibroblast cell strains and lymphoblast cell lines used.

ROBERTS SYNDROME	CONTROL

A.   Fibroblast cell strains

R22 6 year-old male, RS+	GM3349 10 year-old, male
S6012 12 year-old female, RS+	GM0969B 2 year-old, female
S6008 neonate male, RS-	S6007 neonate, male
S6006 4 year-old female, RS-	GM0969B 2 year-old, female

B.   Lymphoblast cell lines

R20 equivalent to R22	DM 25 year-old, male
LB1 25 year-old female, RS+	JaKr 30 year-old, female

2 mL of Dulbecco's phosphate buffered saline (D-PBS, Gibco 310-4190) and then trypsinizing the cells for 3-5 minutes with 2 mL of trypsin-EDTA (1X, Gibco 610-5300). Trypsinization was inactivated by the addition of 2 mL of α-MEM with 15% FBS. The cell strains were usually subcultured at a 1:2 or 1:3 ratio.

The passage (P) of the fibroblast cell strains was defined according to the subculture used. The passage was increased by 1 when a confluent 100 mm dish was subcultured 1:2. If cultures were subcultured 1:3, the passage number was increased by 1 for every other subculture and then increased by 2 for each alternate subculture. With this method, the passage number increased by 1.5 with each 1:3 split. Cultures of fibroblast cell strains were defined as early passage if the passage number was less than one-third of their replicative lifespan and late passage when at two-thirds of their replicative lifespan. The replicative lifespan is defined as the total number of passages achieved by a cell strain up to senescence.

Freezing of fibroblast cell strains involved growing the cultures to confluency in 100 mm polystyrene tissue culture dishes with complete α-MEM medium and 15% FBS. The cells were removed from the culture dishes by trypsinization as previously described, transferred to a 15 mL polystyrene conical centrifuge tube (Falcon 2099) and pelleted by

centrifuging at 180xg for 10 minutes in an IEC Centra-7 centrifuge. The supernatant was removed and the pellet was gently resuspended in 1.0 mL freezing medium consisting of complete α-MEM and 10% dimethyl sulfoxide (DMSO, BDH). Two confluent dishes of Roberts syndrome cell strains (approximately 1.5×10^6 cells) were frozen in 1.0 mL of freezing solution while one confluent dish was used for the control cell strains (approximately 3.0×10^6 cells). The cell suspension was transferred to a 1.5 mL cryogenic vial (Evergreen, Diamed) and frozen at -70°C overnight before transferring to liquid nitrogen for long term storage.

Fibroblast cell strains were thawed rapidly by warming the cell suspension in a 37°C waterbath. The thawed cell suspension was then transferred to a 100 mm polystyrene tissue culture dish containing 14 mL of prewarmed (37°C) complete α-MEM medium and 15% FBS. The cells were allowed to attach overnight before changing the medium the next day.

2.2.2. LYMPHOBLASTOID CELL LINES

Lymphoblast cell lines were grown as cell suspensions in 25 cm^2 (Falcon 3013) or 75 cm^2 (Corning 25110-75) tissue culture flasks with RPMI 1640 medium containing 25 mmol/L Hepes buffer and L-glutamine (Gibco 380-2400) and supplemented with 15% FBS. Subculturing involved collecting the cultures in a sterile 50 mL polypropylene tube (Falcon)

and centrifuging the cell suspension at 180xg with a IEC Centra-7 centrifuge for 10 minutes. The supernatant was removed and a fresh aliquot of RPMI 1640 with 15% FBS of known volume was added to the cell pellet. Viable cell counts were determined with 0.4% trypan blue stain (Gibco 630-5250) and a hemacytometer using a microscope and 25X objective (250X magnification). Roberts syndrome cell lines were reseeded at a density of 5.0 X 10^5 cells/mL and control cell lines at 2.5 X 10^5 cells/mL.

Lymphoblast cell lines were frozen as 1.0 X 10^7 cells in 1.0 mL of RPMI, 15% FBS and 10% DMSO in a cryogenic vial and then frozen as previously described for fibroblast cell strains. Frozen lymphoblast cell lines were thawed in a 37°C waterbath and transferred to a 50 mL polypropylene centrifuge tube containing 10 mL of complete RPMI with 15% FBS. The cells were centrifuged for 10 minutes at 180xg in a IEC Centra-7 centrifuge. The supernatant was removed and the pellet was gently resuspended in 2 or 3 mL of fresh medium. Viable cell counts were determined with 0.4% trypan blue stain and a hemacytomer using a microscope and 25X objective (250X magnification). Suspension cultures were initiated at the seeding densities described above for Roberts syndrome and control cell lines using viable cell counts.

2.3. ANALYSIS OF METHYLATION LEVELS OF CONSTITUTIVE HETEROCHROMATIN DNA

2.3.1. EXTRACTION OF GENOMIC DNA FROM FIBROBLAST CELLS

High molecular weight genomic DNA was extracted from fibroblast cultures of RS and control cell strains using a modification of the method described by Shmookler-Reis and Goldstein (1980). Fibroblast cultures were grown to and maintained at confluency for 5 to 7 days to ensure that a state of quiescence was achieved. The monolayer cultures were rinsed twice with 5 mL of D-PBS (Gibco) and lysed by adding 0.5 mL of 0.5% sodium dodecyl sulphate (SDS, Biorad) in 60 mmol/L Tris-HCl pH 8.4 and 20 mmol/L ethylenediaminetetraacetic acid (EDTA, Sigma) to each 100 mm tissue culture dish for 15 minutes. The lysed cells were collected with a sterile rubber policeman into a 50 mL polypropylene centrifuge tube (Falcon). The cell suspension was then treated with 50 μg/mL of proteinase K (BRL) in 0.01 mol/L Tris-HCl pH 7.8, 0.005 mol/L EDTA and incubated overnight at 37°C, as recommended by Maniatis et al. (1982). The proteinase K treatment was repeated the following morning using a fresh aliquot and incubated for an additional two hours at 37°C. The DNA solution was then extracted twice, for five minutes each, with 1:1 volume of salt saturated phenol (BRL) and chloroform:isoamyl alcohol (24:1 v/v, Caledon Laboratories). The DNA-containing aqueous phase was separated from the solvent phase by centrifugation at 180xg

for 5 minutes using an IRC Centra-7 tabletop centrifuge. If any protein was still present at the aqueous solvent interface after the initial two extractions with phenol:chloroform:isoamyl alcohol, additional extractions were performed until there was no visible appearance of contaminating protein. The aqueous solution was subsequently extracted two times with chloroform:isoamyl alcohol for 5 minutes each. The DNA solution was precipitated by adding 3 mol/L sodium acetate (BDH) to a final concentration of 0.3 mol/L followed by 2.5 volumes of cold 100% ethanol, resulting in a final concentration of 70%. The samples were allowed to precipitate on ice for 30-60 minutes or overnight at 4°C.

The precipiated DNA samples were pelleted by transferring the ethanol solution to a 50 mL Oakridge centrifuge tube (Nalgene) and centrifuged in a Sorval centrifuge at 12000xg for 20 minutes at 4°C using a SS34 rotor. The supernatant was immediately poured off and the DNA pellet was allowed to air dry. The dried DNA sample was subsequently dissolved in 1-2 mL of 10 mmol/L Tris-HCl pH 7.4 and 1 mmol/L ethylenediaminetetraacetic acid (EDTA) (TE buffer) and stored at 4°C until fully dissolved.

Contaminating RNA was removed from the dissolved DNA samples by incubating with 50 μg/mL RNase (Sigma or Pharmacia) for one hour at 37°C. At this point the proteinase K treatment was repeated as previously described

followed by ethanol precipitation and the DNA pellet was redissolved in 1-2 mL of TE buffer. The DNA samples were then dialysed against the 1-2 litres of TE buffer at 4°C with constant stirring. The buffer was changed every two hours for a total of four buffer changes with the third buffer change dialysing the samples overnight. The dialysates were collected and precipitated with 70% ethanol as previously described. The precipitated DNA samples were pelleted as previously described, washed twice with cold 70% ethanol before being allowed to air dry and then redissolved in TE buffer.

The concentrations of the DNA samples were quantitated using the ethidium bromide fluorescence method described by Morgan et al. (1979). A total of 0.5 μg in 5 μL of uncut high molecular weight lambda DNA (BRL) was used to standardize a Sequoia-Turner fluorometer (filters NB 520 and SC585) to give a reading of 100. Five microlitres of each DNA sample and the standard was added to 2.0 mL of buffer pH 11.8 containing 0.5 μg/mL ethidium bromide (Schwarz Mann), 20 mmol/L K_3PO_4 (BDH) and 0.5 mmol/L EDTA in a glass tube (Canlab Dispo culture tube 12mm X 75mm). The DNA concentration was determined by converting the fluorometry reading (20 units equalled 0.1 μg) to micrograms of DNA in 5μL.

2.3.2. RESTRICTION ENZYME DIGESTION OF GENOMIC DNA

High molecular weight genomic DNA was digested overnight at 37°C with 10 or 20 times excess (10 or 20 units per μg of DNA) MspI or HpaII (BRL) with the appropriate React buffer supplied by the manufacturer. The following day, the extent of digestion was checked by electrophoresis of 0.1-0.2 μg of digested DNA on a 0.7% agarose (Schwarz-Mann) horizontal gel (IBI horizontal gel apparatus, model MPH) containing 0.5 μg/mL ethidium bromide for 1-2 hours in Tris-borate buffer (0.089 mol/L Tris-borate, 0.089 mol/L boric acid, 0.002 mol/L EDTA, 1XTBE) at 50 milliamps using a Pharmacia EPS 500/400 electrophoresis power supply. After electrophoresis, the DNA samples were visualized using a long wave ultraviolet transilluminator (Chromato-vue Transilluminator Model C-60, Ultra-Violet Products, Inc.) and photographed with a Polaroid MP-3 Land camera using Polaroid T57 film. If digestion was not complete, determined by the amount of undigested high molecular weight DNA remaining, an additional 5 units of restriction enzyme was added and digestion was allowed to proceed for an additional 2-5 hours. As a control for restriction enzyme activity in some experiments, an additional reaction was set up whereby 5 units of restriction enzyme was added to 1 μg of uncut lambda DNA.

Double digestion of genomic DNA with MspI/EcoRI and

HpaII/EcoRI involved initially digesting the samples for four hours with 10 times excess MspI or HpaII with the React buffers recommended by the manufacturer under the conditions previously described. The extent of digestion was checked using gel electrophoresis as described above and if complete, the reaction buffer was then adjusted to that required for EcoRI digestion. The samples were digested with 10 times excess EcoRI enzyme overnight at 37°C. The concentration of single and double digested samples were re-estimated after digestion using the ethidium bromide fluorometry assay previously described.

2.3.3. ISOLATION AND RADIOACTIVE LABELLING OF DNA PROBES
2.3.3.1. ISOLATION OF PLASMID DNA

The plasmid, pD15Z1, was received as a gift from Dr. J. Holden, Queens University. A restriction digest map of the plasmid is illustrated in Figure 3. Plasmid pMT-hmyc, schematically presented in Figure 4., was a gift from Dr. C. Harley. The plasmid, pMT-hmyc, is 7.5 kb in size and contains the promoter of the human metallothionein (MT) gene IIA and two exons of the human c-myc gene. The promoter region of the MT IIA gene was used as an internal control for analysing DNA methylation levels in RS and control fibroblast cell strains.

The stock plasmids were subsequently transfected into

Figure 3.   Schematic illustration of the restriction map of
pD15Z1 (from Higgins <u>et</u> <u>al</u>. 1985)
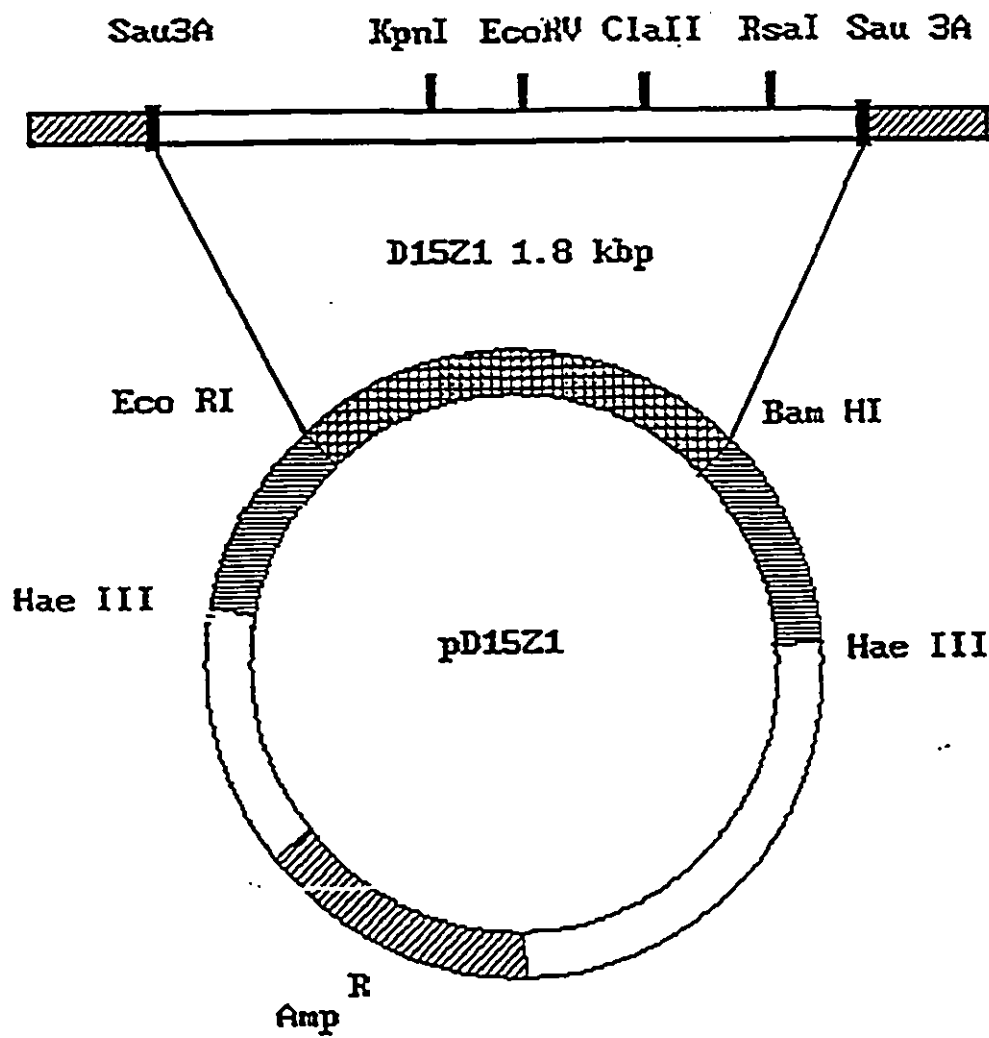
Figure 4. Schematic illustration of the plasmid pMT-hmyc
(from Tyers, Ph.D. thesis. 1988)
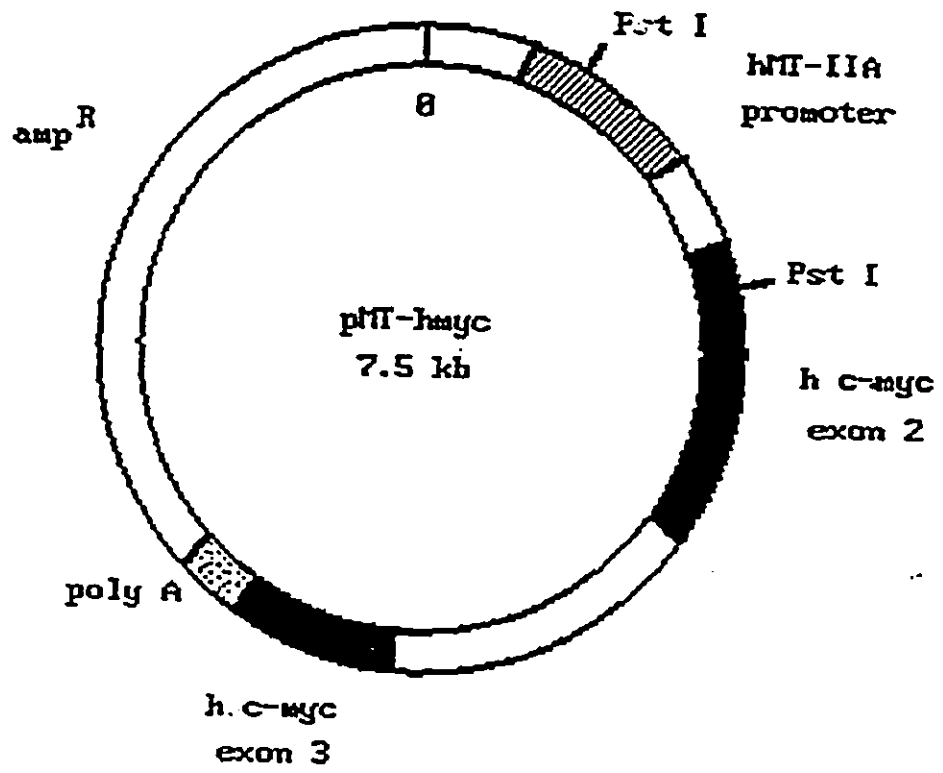
E. coli LE294 using the calcium chloride transformation procedure described by Maniatis et al. (1982) or the transfection procedure for BRL DH5α competent cells as described by the supplier. The plasmids were isolated from the ampicillin-resistant bacterial cells using a large scale plasmid preparation. A 5 mL culture of Luria broth containing 30 μg/mL of ampicillin (Sigma) was inoculated with the bacterial strain containing the desired plasmid and allowed to grow overnight in a shaking incubator (Orbit) at 37°C. The starter culture was then used to inoculate a 500 mL culture of Luria broth containing 30 μg/mL ampicillin and allowed to grow for an additional 4 hours in a shaking incubator at 37°C. Some plasmid cultures were further amplified with 240 μg/mL of chloramphenicol by incubation overnight using the growing conditions just described.

Isolation of the plasmid from the bacteria involved centrifuging the 500 mL bacterial culture in two 350 mL Sorvall centrifuge tubes for 20 minutes at 8000xg in a Sorvall centrifuge using a SS34 rotor. The bacterial pellet was then resuspended in 10 mL of solution A, containing 50 mmol/L glucose, 25 mmol/L Tris-HCl, pH 8.0 and 10 mmol/L EDTA, and treated with 5 mg/mL lysozyme (Boehringer Mannheim) for 5 minutes at room temperature. Twenty millilitres of solution B containing 0.2 N NaOH and 1% SDS was added to the cultures, mixed by inversion and incubated on ice for 10

minutes. Fifteen mL of ice-cold solution C (3 mol/L potassium acetate, 11.5% v/v glacial acetic acid) was then added, mixed well and incubated on ice for an additional 10 minutes. The suspension was then transferred to 50 mL Oakridge centrifuge tubes and centrifuged at 47000xg for 20 minutes at 4°C using a Beckman L8-80 Ultracentrifuge and 70.1Ti rotor. The supernatant was recovered and precipitated with 0.6 volume of 100% isopropanol for 20 minutes at room temperature. The precipitated plasmid solution was pelleted by centrifugation at 12000xg for 30 minutes at room temperature using a Sorvall centrifuge and SS34 rotor. The crude plasmid DNA pellet was washed once with cold 70% ethanol and allowed to air dry before being dissolved in 2.0 mL of TE buffer.

Contaminating RNA was removed from the plasmid preparation by incubating the sample with 50 μg/mL of DNase-free RNase (Sigma or Pharmacia) at 37°C for 60 minutes. The sample was then extracted once for five minutes with an equal volume of phenol:chloroform/isoamyl alcohol (1:1 v/v), recovered as the aqueous phase, to which a final concentration of 2 mol/L ammonium acetate was added before precipitating with two volumes of 100% ethanol. The sample was stored at -20°C for a minimum of 2 hours. The precipitated plasmid was recovered by centrifugation at 12000xg for 30 minutes at room temperature using a Sorvall

centrifuge with SS34 rotor. After removing the supernatant, the DNA pellet was washed with cold 70% ethanol, air dried and resuspended in 1.8 mL of solution D pH 8.0 containing 10 mmol/L Tris-HCl, 1 mmol/L EDTA and 1 mol/L NaCl.

The plasmid preparation was subsequently isolated in a circular, uncut form using pZ523 columns (5 Prime→3 Prime Inc.) as described by the manufacturers with slight modifications. The pZ523 columns were prepared by draining the equilibration buffer and centrifuging the column tube assembly for 1 minute at 1100xg using an IEC Centra-7 centrifuge. After discarding the effluent from the column after centrifugation, 1.8 mL of the plasmid sample was carefully applied to the resin bed of the tube assembly. The column containing the plasmid sample was again centrifuged at 1100xg for 24 minutes. The purified plasmid sample was collected as the effluent from the column after centrifugation and precipitated using 0.6 volumes of 100% isopropanol at room temperature for 20 minutes. The plasmid preparation was pelleted by centrifugation at 12000xg for 30 minutes at room temperature using a Sorvall centrifuge as previously described. The plasmid pellet was again washed with cold, 70% ethanol, air dried and resuspended in 0.5-1.0 mL of TE buffer.

2.3.3.2. OLIGONUCLEOTIDE LABELLING OF PLASMID DNA SEQUENCES

Plasmid pD15Z1 was linearized by EcoRI digestion (5 units/μg DNA, BRL) with the appropriate React buffer for a minimum of 4 hours at 37°C. The digested plasmid was extracted twice, for five minutes each, with an equal volume of salt saturated phenol:chloroform/isoamyl alcohol(1:1 v/v), ethanol precipated and pelleted by centrifugation in a 1.5 mL microtube (Diamed) for 20 minutes at room temperature using an Eppendorf microcentrifuge (Model 5415). The plasmid pellet was allowed to air dry and resuspended in TE buffer to a final concentration of 25 μg/mL.

Plasmid pMT-hmyc (10-20 μg) was digested with PstI (5 units/μg DNA, BRL) to isolate the 1.1 kb MT insert. The digested plasmid sample was then extracted with phenol:CIA and ethanol precipitated as described for D15Z1. The air dried plasmid DNA sample was resuspended in 20 μL of TE. The 1.1 kb PstI MT insert was then isolated using polyacrylamide gel electrophoresis (PAGE) as described by Maniatis et al. (1982) or low melting temperature agarose gel electrophoresis as described in Current Protocols in Molecular Biology (1989).

PAGE involved electrophoresis of the digested plasmid using a 3.5% polyacrylamide gel (DNA grade, Biorad) in 1XTBE running buffer for 3 hours at 50 volts using a Biorad Mini-Protein II Electrophoresis cell. After

electrophoresis, the gel was stained with 1.5 μg/mL ethidium bromide for 45 minutes, visualized using a long wave ultraviolet transilluminator and photographed with Polaroid MP-3 Land camera using Polaroid T57 film. The 1.1 kb PstI-MT insert band was then excised from the polyacrylamide gel, cut into small pieces and transferred to a sterile 1.5 mL microcentrifuge tube. The sample was centrifuged briefly with a microcentrifuge to settle the contents of the tube and to estimate its approximate volume. To this, 1.5 volumes of elution buffer was added, consisting of 0.5 mol/L ammonium acetate and 1 mmol/L EDTA pH 8.0. The plasmid sample was eluted by overnight incubation in a 37°C shaker bath. The next day, the fragment was recovered by passing the sample through a 0.2 micron filter (Millipore) using two washes of 0.5 volume of elution buffer. The eluted plasmid insert was then precipated with 70% ethanol as previously described and finally dissolved in TE. The amount of insert recovered was determined using the ethidium bromide fluorometry assay previously described.

The PstI-MT insert was also isolated by a simpler and quicker method that involved electrophoresis of 10-20 μg of digested sample using a 0.7% Low Melting Point (LMP) agarose (BRL Ultrapure) gel in 1XTBE buffer at 60 milliamps for 1-2 hours using an IBI Multipurpose horizontal gel apparatus and Pharmacia electrophoresis power supply. The gel was stained

with 2 µg/mL ethidium bromide for 30 minutes and the plasmid DNA was visualized by ultraviolet light as previously described. The 1.1 kb PstI-MT fragment was excised from the LMP agarose gel and transferred to a 1.5 mL microtube. The insert was subsequently purified from the LMP agarose using a Elutip-D column (Schleicher and Schuell) as outlined in Ausubel et al. (1987). The gel slice was melted at 65°C and 10 volumes of prewarmed low salt solution (0.4 mol/L NaCl in TE) was added to the sample. The Elutip column was prepared according to the manufacturer's protocol and the fragment eluted according to the modified protocol outlined in Ausubel et al. (ibid). The sample was finally precipitated with 70% ethanol and stored overnight at -20°C. The dried pellet with the fragment was dissolved in the volume of TE buffer necessary to achieve a final concentration of 25 µg/ml.

All DNA probes were labelled with α-[^{32}P]-dCTP (NEN) using the oligonucleotide labelling kit manufactured by Pharmacia. Fifty nanograms of linearized pD15Z1 or 1.1 kb PstI-MT plasmid DNA was prepared in 34 µl of TE buffer in a microcentrifuge tube (Safe-Lok, Eppendorf) and denatured by boiling (95-100°C) for 10 minutes. The sample was placed on ice for two minutes, centrifuged briefly (20-30 seconds) using an Eppendorf microcentrifuge. Ten microlitres of Reagent Mix (containing 1.25 mol/L Tris-HCl, 0.125 mol/L MgCl$_2$, 2 mol/L Hepes buffer; deoxyribonucleotides dATP, dGTP,

dTTP and random hexadeoxyribonucleotides), provided with the labelling kit, was added to the denatured DNA sample before adding 50 μCi of ^{32}[P]-dCTP (NEN). Finally, 10 units of Klenow fragment, also provided with the labelling kit, was added to the reaction mixture, mixed well and incubated at 37°C for 2-3 hours. Unincorporated radioactively-labelled nucleotides were removed from the DNA sample using a Pharmacia Nick column before determining the specific activity of labelling.

2.3.4. SOUTHERN BLOT ANALYSIS OF RESTRICTION ENZYME DIGESTED GENOMIC DNA AND HYBRIDIZATION

After requantification of digested genomic DNA sample concentrations using fluorometry, equal amounts of DNA from each cell strain was applied to a 1% agarose (Schwartz Mann or Pharmacia) gel (10X14 cm) along with dye buffer type II [0.25% bromophenol blue (BP), 0.25% xylene cyanol (XC) and 15% Ficoll type 400] or type III (0.25% BP, 0.25% XC and 30% glycerol). Electrophoresis was carried out in 1XTBE running buffer at 25 volts (V) overnight using an IBI Multipurpose horizontal gel apparatus and Pharmacia electrophoresis power supply. The gel was subsequently stained with 2 μg/mL ethidium bromide for 1 hour and the electrophoresed DNA samples were visualized using a long wave ultraviolet transilluminator and photographed with Polaroid MP-3 Land camera using Polaroid T57 film.

The gel was subsequently treated with two washes of 0.25 N HCl for 10 minutes each, to ensure depurination of the digested DNA samples. After rinsing with sterile distilled water (dH$_2$0), the gel was rinsed twice with 0.4 N NaOH for 10 minutes each. The nylon membrane (Gene Screen Plus, Dupont) was prepared by first rinsing with sterile dH$_2$0 until completely wetted and then treated with 10XSSC for 15 minutes. The Southern bloc assembly used was essentially that described by the manufacturer of the nylon membrane. A sponge was wetted and placed in a plastic container with approximately 500 mL of 10XSSC. Three 10 cm X 14 cm filter papers (Whatman 3MM) were also wetted in 10XSSC and placed on top of the wet sponge. When gel alkalinization was completed, the gel was placed, face down, on top of the filter papers. The wetted nylon membrane was also placed, charged side down, on top of the gel. Five more 10 cm X 14 cm pieces of filter paper were placed on top of the nylon membrane followed by a 7-10 cm layer of paper towelling, also cut to size. The Southern blot was weighed down with a glass plate and a 500 gram weight. The transfer was allowed to proceed overnight with frequent changing of paper towelling and the addition of 10XSSC as needed. The following morning, the blot was taken apart and the nylon membrane was immersed in approximately 150 mL of 0.4 N NaOH for 30 seconds to denature the bound DNA and then neutralized by rinsing with

excess buffer consisting of 0.2 mol/L Tris-HCl, pH 7.5 and 2XSSC. The nylon membrane was blotted on a 10 cm X 14 cm filter paper, covered with a plastic wrap and the transferred DNA cross-linked to the membrane by exposing it to long wave ultraviolet light for 2-3 minutes using a Chromato-vue transilluminator.

The nylon membrane was prepared for hybridization by wetting the blot with 15 mL of hybridization mixture that consisted of 50% deionized formamide (BRL), 1 mol/L NaCl and 1% SDS. The membrane was sealed in a Scotch Pak sealable plastic bag with the hybridization mixture and incubated at 42°C for 15-30 minutes. A total of 1 X 10^7 cpm (1.0 X 10^6 cpm/mL of hybridization mixture) of radioactively labelled EcoRI-D1521 or PstI-MT probe and 150 μg/mL of sonicated carrier DNA (salmon sperm DNA, Sigma) were prepared in an equal volume of hybridization mixture and denatured by boiling (95-100°C) for 10 minutes. The denatured solution was then added to the nylon membrane contained within the heat sealable plastic bag, which was resealed and the hybridization mixture was spread around to ensure even distribution of the DNA probe. Hybridization was allowed to proceed overnight at 42°C before being subjected to two 30 minute low stringency washes (2XSSC, 1% SDS) at 65°C and two 30 minute high stringency washes (0.1XSSC, 0.1% SDS) at the same temperature. The washed nylon membrane was blotted onto

a 3MM Whatman paper filter cut to the same size to remove excess moisture before being wrapped in plastic wrap. The hybridized membrane was then placed within an X-ray film cassette and exposed to 20 cm X 25 cm X-ray film (X-Omat AR, Kodak) for an initial 24 hour period without an intensifying screen at -70°C. The membrane was then exposed to additional films for the appropriate time needed. The film was developed using an automatic developer.

After the completion of the Southern blot analysis using EcoRI-D15Z1, the bound probe was removed by washing the nylon membrane 3-5 times with 0.1XSSC/1% SDS at 95°C for 20-30 minutes each wash. The nylon membrane was then exposed to X-ray film for 2-4 days to check for residual binding of the repetitive probe. Once the EcoRI-D15Z1 plasmid was sufficiently removed so that no radioactive signal could be detected below the 3.5 kb HindIII molecular weight marker, the membrane was rehybridized with PstI-MT at 42°C overnight using a hybridization solution containing 50% deionized formamide, 1 mol/L NaCl, 50% dextran sulfate (Pharmacia) and 1% SDS. The next morning the membrane was washed twice for 15 minutes each with 2XSSC/0.1% SDS at room temperature, followed by two 15 minutes washes with 0.1XSSC/0.1% SDS at 48°C. The nylon membrane was subsequently exposed to X-ray film without an intensifying screen for an initial 24 hour period followed by a minimum exposure of six days using the

conditions as previously described. If the autoradiograph exposed for 24 hours had too much nonspecific background, the nylon membrane was rewashed using the lower stringency wash conditions and reexposed for 6 days.

2.3.5. QUANTIFICATION OF DNA METHYLATION LEVELS OF CONSTITUTIVE HETEROCHROMATIN DNA SEQUENCES USING VIDEO DENSITOMETRY

2.3.5.1. AUTORADIOGRAPHS OF SOUTHERN BLOTS USING MSPI AND HPAII DIGESTION

Levels of constitutive heterochromatin DNA methylation levels were quantified by scanning Southern blots with a Biorad Video Densitometer. The area optical density (OD) of the 3.5, 4.0 and 6.0 kb bands recognized by the EcoRI-D15Z1 plasmid after MspI and HpaII digestion were compared. The area OD was analysed using 1-D Analyst Data Analysis software (Biorad). The scan parameters for each lane were altered so that the background of the autoradiograph was subtracted, a point-to-point baseline for each peak was identified above the background level and a minimal smoothing factor of 4 was applied. With these alterations, the area OD was used to represent the signal of the band above background.

The relationship of the area OD of the 3.5 kb band, recognized by D15Z1, to increasing amounts of MspI digested genomic DNA was obtained from six experiments, using three fibroblast control cell strains, GM0969B, GM3349 and S6007.

The amount of DNA used for Experiments 1-5 were 1.5, 2.5, 3.5 and 5.0 μg and for Experiment 6, 0.5, 1.0, 2.0 and 3.0 μg.

Eight Southern blots were used to determine levels of constitutive heterochromatin DNA methylation in RS+, RS- and control fibroblast genomic DNA digested with MspI or HpaII. The RS and control cell strains used for each experiment are outlined in Table 2.

The level of D15Z1 DNA methylation was mathematically represented by the ratio of the area OD of the MspI 3.5 kb band (A) to the area OD of the HpaII 3.5 kb band (B), for each cell strain. If the HpaII 3.5 kb band was absent or too faint to determine the area OD by the video densitometer, a "maximum minimum" value was assigned by using the minimum area OD value estimated for the HpaII 3.5 kb band from another cell strain on the same autoradiograph. This would slightly overestimate the area OD of the HpaII band in these cases and, therefore underestimate the A/B ratio. If either the MspI or HpaII 3.5 kb band of any of the DNA samples was affected by a "whiteout", identified as an unusually pale region localized to an area on the autoradiograph, its area OD values was excluded from the final statistical analysis. The ratios, A/B for each cell strain, were categorized as controls, RS+ or RS-, according to passage (early or late).

Table 2. Summary of fibroblast cell strains used in Southern
blot experiments quantified by video densitometry.

Experiment	Fibroblast Cell Strain		
	Control	RS+	RS-
7	GM0969B P23	S6012 P10	
	GM3349 P32	R22 P26	
8	GM0969B P23	S6012 P12	
	GM0969B P35	S6012 P32	
9	GM0969B P19*	S6012 P12	
	GM0969B P23	S6012 P36	
10	GM3349 P18	R22 P16	
	GM3349 P30*	R22 P27	
11	GM3349 P20	R22 P12	
	GM0969B P23		S6006 P20
12	GM0969B P19		S6006 P20
	GM0969B P23		S6006 P30
13	S6007 P15		S6008 P15
	S6007 P31		S6008 P28
14	S6007 P15		S6008 P15
	S6007 P34		S6008 P31

* Area OD A/B value for 3.5 kb band excluded from statistical
analysis due to autoradiograph whiteouts
P = passage.

2.3.5.2. AUTORADIOGRAPHS OF SOUTHERN BLOTS USING MSPI/ECORI AND HPAII/ECORI DIGESTION

Levels of constitutive heterochromatin DNA methylation were quantified by scanning autoradiographs of Southern blots containing MspI/EcoRI and HpaII/EcoRI digested DNA samples with a Biorad Video Densitometer as described in the previous section. The level of D15Z1 DNA methylation was mathematically represented by the "adjusted" ratio of the area OD of the MspI/EcoRI 2.5 kb band to the HpaII/EcoRI 2.5 kb band (C/D). To standardize the area OD value obtained for the 2.5 kb band with respect to the amount of DNA present in each lane, the area OD values obtained for the MspI/EcoRI and HpaII/EcoRI band were adjusted by dividing each value by the area OD value estimated for the 1.6 kb band of the same lane. The 1.6 kb band was considered to be a suitable reference band to control for unequal intensities that may be due to unequal amounts of DNA present in each lane as it was the product of EcoRI digestion only and so not dependent on methylation status.

2.4. CHARACTERIZATION OF THE REPLICATION PROGRAM OF CONSTITUTIVE HETEROCHROMATIN OF METAPHASE CHROMOSOMES

2.4.1. CONTINUOUS LABELLING OF LYMPHOBLAST CULTURES WITH BrdUrd

Four 10 mL cultures of each RS+ lymphoblast cell line, R20 and LB1, and each control lymphoblast cell line, DM and JaKr, were seeded at 2.5 X 10^5 cells per mL using the medium

and growing conditions previously described. The cultures were allowed to grow for 36-48 hours before 0.1 mL of BrdUrd solution was added, resulting in a final concentration of 10^{-2} mol/L BrdUrd (Sigma), 4 X 10^{-5} mol/L fluorodeoxyuridine (FUdR, Sigma) and 6 X 10^{-4} mol/L uridine (a gift from Dr. Blajchman) (Verma and Babu, 1989). One 10 mL culture from each of the four cell lines was continuously labelled with BrdUrd for 4, 5, 6 or 7 hours before being treated with 0.075 µg/mL Colcemid for an additional two hours in the presence of BrdUrd. There were two replicates of the experiment.

2.4.2. CHROMOSOME HARVESTING PROCEDURE

Lymphoblast cultures that were treated with Colcemid were collected into 15 mL conical polystyrene centrifuge tubes and pelleted by centrifugation at 180xg for 10 minutes in an IEC Centra-7 centrifuge. All but 0.5 mL of the supernatant containing Colcemid was removed and 8-10 mL of prewarmed (37°C) hypotonic solution, 0.07 mol/L potassium chloride (KCl), was added to each tube. The tubes were incubated at 37°C for 12-15 minutes before being centrifuged again using the previously described conditions. The cells were then fixed with cold, freshly prepared methanol/glacial acetic acid (3:1) by adding the first millilitre of fixative slowly in a dropwise manner, with vigorous mixing in between.

All fixed cell suspensions were stored at 4°C overnight and were given a fixative change the following morning and stored at 4°C for at least 30 minutes before making slides.

2.4.3. SLIDE MAKING PROCEDURE FOR METAPHASE CHROMOSOMES

Metaphases harvested from all cell types were made by layering or dropping single drops of cell suspension on cold, precleaned, water-covered slides (double frosted, Propper) and then blown or flamed to further disperse individual cells. The slides were allowed to dry on a slidewarmer at 40-60°C.

2.4.4. DIFFERENTIAL STAINING OF BrdUrd-LABELLED CHROMOSOMES BY GIEMSA

Slides, aged for 1-7 days, were stained in 0.5 μg/mL bisbenzimidazole (Hoescht 33258, Canadian Hoechst Ltd.) aqueous solution for 30-60 minutes at room temperature and subsequently rinsed with PBS, pH 6.8 (Fisher). The slides were then mounted with PBS using a 20 mm X 50 mm coverslip (No. 1, Corning), placed on a hotplate set at 55-60°C and exposed to black light using a Black Light Lamp (BLB, Sankyo Denki) at a distance of 2.5-5.0 cm for 3 minutes. After rinsing again with PBS pH 6.8, the slides were stained for 30-150 seconds with a 5% Giemsa staining solution (Gurr Giemsa) made with Gurr buffer, pH 6.8.

2.4.5. S PHASE SUBCLASSIFICATION OF METAPHASE CHROMOSOMES

Suitably spread metaphases, free of cytoplasm, with minimal overlap of chromosomes and identifiable chromosomes 3 and 4 were chosen for S phase subclassification using Key 4 (as previously outlined in Figure 2, page 70).   If possible, both homologues of chromosomes 3 and 4 were analysed. Cells were classified as SkI if band 3p13 appeared pale staining and the dark staining band, 4q21, was absent. Cells were considered to belong to subphase SkII if band 3p13 was pale staining and band 4q21 was present. A cell was classified as SkIII if band 3p13 was not pale staining or a dark staining band was present within this band and band 4q13 was pale staining or as SkIV if band 4q13 was absent on one or both homologues. Fifty metaphases were analysed from each culture.

Once a cell was classified within a subphase, the constitutive heterochromatin regions of chromosomes 1, 9, 16, and in male cell lines, the Y chromosome, were analysed separately as being pale or darkly stained. The staining pattern of the X chromosome was also analysed in female cell lines. Only X chromosomes that were completely pale staining or almost all pale with just the tip of the p arm dark staining were scored. Metaphases were photographed using a Leitz Laborlux 12 photomicroscope at 1000X magnification (100X oil immersion objective) and Kodak Tri-pan X film 2415,

ASA 100. The film was developed and photographs were printed as described in Section 2.5.

2.5. PHOTOGRAPHY

BrdUrd-incorporated metaphases were photographed using a Leitz Laborlux 12 photomicroscope at 1000X magnification (100X oil immersion objective) and Kodak Tri-pan X film 2415, ASA 100. The film was developed using Kodak HC-110 developer, dilution B (1:7) for 6 minutes at 20°C and fixed with Kodak Fixer for 4 minutes. All pictures were printed on Ilford Ilfospeed 2.1M or 4.1M photographic paper and developed using an Ilford Ilfospeed automatic developer (model 2001).

Southern blot autoradiographs were photographed by the Audio Visual Department of McMaster University. Prints were made from 85 cm X 130 cm negatives using Ilford Ilfospeed 2.1M photographic paper and developed as previously described.

2.6. STATISTICAL METHODS

2.6.1. QUANTIFICATION OF PATTERN OF HYBRIDIZATION TO DEFINED AMOUNTS OF MSPI AND HPAII GENOMIC DNA

The relationship of D15Z1 binding to specified amounts of digested genomic DNA was determined by comparing the ratio of the area OD of MspI 3.5 kb band signal obtained for each specified amount of DNA used in Experiments 1-6. To

mathematically describe the response that was observed for each experiment, the area OD of the <u>Msp</u>I 3.5 kb band for each amount of DNA was modelled using General Linear Modelling (GLM) using the computer software program, Minitab v.7.2. The model for Experiments 1-6 was defined as $y=r+d+r*d$, where the factor 'r' represented the effect due to experiment, factor 'd' the amount of DNA (μg) applied in each lane, and the effect due to interaction of the two factors, 'r*d'. The results of Experiments 1-5 were modelled separately from the results of Experiment 6 because of the different amounts of DNA used. Experiments 1-5 were then pooled by entering the results of each experiment as a repeated measure and were modelled using $y=d$, as the effect of factor 'r' was not significant and therefore was not required.

2.6.2. STATISTICAL ANALYSIS OF D15Z1 HETEROCHROMATIN DNA METHYLATION LEVELS IN ROBERTS SYNDROME

The level of D15Z1 DNA methylation was mathematically represented by the ratio of the area OD of the <u>Msp</u>I 3.5 kb band (A) to the area OD of the <u>Hpa</u>II 3.5 kb band (b) for each cell strain. Thus a higher A/B ratio would indicate a higher methylation level and a lower A/B ratio would indicate a lower methylation level. The ratios A/B for each cell strain were categorized as controls, RS+ or RS- according to passage (early or late). The data were analysed using GLM and Analysis of Variance (ANOVA) using Minitab v.7.2. Various

GLM models were fitted to the data and ANOVA was used to test three main hypotheses. The factors of the GLM models represented the effect due to passage (EvsL), experiment (Exps) and cell strain [RS+ (R+), RS- (R-) and controls (C)]. The first null hypothesis stated that there were no differences in the level of D15Z1 DNA methylation between experiments. The second null hypothesis stated that there were no differences in the level of D15Z1 DNA methylation between cells at early and late passage. The third null hypothesis that was tested stated that there were no differences in the level of D15Z1 DNA methylation, represented by the 3.5 kb band area OD ratio (A/B), between RS+, RS- and control fibroblast cell strains. These hypotheses were tested using four different GLM models involving various comparisons of the three cell strain groups. Because of unequal sample size, the mean O.D ratio of each group was compared using an unmatched ANOVA.

2.6.3. STATISTICAL ANALYSIS OF S SUBPHASE DISTRIBUTIONS USING GENERALIZED LINEAR MODELLING

The data were analysed using a Generalized Linear Model (GLIM) and probit transformation (GLIM version 3.77, Royal Statistical Society, 1985, on the SSC VAX at McMaster University). A linear predictor model, based upon the general linear predictor equation βx, was used to fit the results. Here β is the vector of unknown parameters and x is

case specific set of levels of the factors being considered in the model. A binomial error distribution and a probit link was used to connect the linear predictor model to the binomial error. The predicted values determined by the fitted GLM model were estimated for each case and predicted back to estimate the counts and proportions.

The appropriate GLIM predicted linear formula was determined by looking at the effect of certain design variables, namely r and t, and the effect of interaction between the two variables. The coding used was r=1 (Controls) or r=2 (RS+), t=4, 5, 6 and 7 hours BrdUrd, y=number of metaphases scored in a subphase, n=total number of metaphases scored (50). Then a1=estimate of intercept of model equation (r=1) a2=estimate of intercept of model equation (r=2), b1=estimate of slope of model equation (r=1), b2=estimate of slope of model equation (r=2); these four estimates constitute the β vector. This involved including the predictor variable(s) in the GLIM model and determining their statistical effects. From this analysis, it was determined that the best linear predictor formula was essentially y=t+r+rt, as BrdUrd treatment time, differences between cell lines and the interaction of the latter two variables were found to have a significant effect on the model at the 5% level of significance.

Differences in the subphase distribution between RS+

and control cell lines involved estimating the slopes of the lines formed by plotting the predicted values determined by the model against BrdUrd treatment time. Slopes and intercepts of the linear predictor line were also estimated using GLIM. This involved estimating the slope of the line for each cell line (b1, b2) and then fitting a model with a common slope for both linear predictor equation for each subphase. The scaled difference in deviance values represents a Chi-square (X^2) value. The change in degrees of freedom (df) of the scaled deviances represents the df associated with the X^2 value.

Significant differences in the slopes of the linear predictor models for RS+ and control cell lines were determined by looking at the change in the scaled deviance produced when the model was changed from y=a1+b1t+a2+b2t (representing individual estimates of slopes and intercepts) to y=a1+a2+bt, resulting in the estimation a common slope for both models. If the X^2 square value obtained by the change in the scaled deviance of the two models was significant ($\alpha=0.05$), then the slopes of the linear predictor models of RS+ and controls were determined to be significantly different. Significant differences in the estimated slopes were then interpreted to represent significant differences in the subphase distribution with respect to BrdUrd treatment time between RS+ and control lymphoblastoid cell lines.

A comparison of the intercepts of the model equation of RS+ and control cell strains was also used to evaluate differences in subphase frequencies. If the slopes of the RS+ and control fitted lines were not significantly different, the data were fitted using a common slope, represented by the model y=a1+a2+bt, as previously described. A significant difference between the intercepts a1 and a2 was determined by fitting a common intercept to both lines (model y=a+bt) and the value of the X^2 obtained from the difference in the deviance of this model and the previous model. If the intercepts estimated for the RS+ and control fitted lines were found to be significantly different (α=0.05), then the two lines were said to be parallel with a significant vertical distance between the lines. This would represent a significant difference in the subphase frequency of RS+ and control lymphoblastoid cell lines at a particular time during S phase.

2.6.4. STATISTICAL ANALYSIS OF CONSTITUTIVE HETEROCHROMATIN REPLICATION USING GENERALIZED LINEAR MODELLING

The data were analysed using GLIM and probit transformation using GLIM 3.77. The methodology used to define the appropriate model to fit the observed results was similar to that described for the S subphase distributions except that the linear predictor formula was defined to be y=r+t, using the same abbreviations described in the previous

section. The predicted values were calculated from the linear predictor equation, y=r+t. With this statistical approach, differences in constitutive heterochromatin replication were determined for subphases SkII, III and IV by estimating the slopes of the line obtained by plotting the predicted proportions against BrdUrd treatment time.

Additional comparisons of constitutive heterochromatin replication of RS+ and control lymphoblastoid cell lines were also made using GLM and ANOVA from Minitab. For this statistical analysis, the weighted mean number of metaphase cells with labelled constitutive heterochromatin regions observed for each suphase of RS+ and control cell lines were compared. The weighted mean was calculated as $m=\Sigma n_i Y_i / \Sigma n_i$, where n represents the number of cells observed in each subphase and Y_i the number of cells with labelled constitutive heterochromatin. The data obtained from Experiments 1-4 were modelled using factors representing the effect of subphase (s, 3 levels), chromosome (c, 4 levels) and cell type (r, 2 levels) as well as the effect of interaction between subphase and chromosome, and cell type and chromosome. Two models were used for the ANOVA and were defined as y=s+c+r+s*c+r*s and y=c+r+s+s*c+r*s. The ANOVA's were constructed to represent a 2X3X4 design, with the number of levels of each factor previously indicated in parentheses and with replicate data as repeated measures.

3. RESULTS

3.1. MOLECULAR CHARACTERIZATION OF THE METHYLATION STATUS OF CONSTITUTIVE HETEROCHROMATIN DNA ISOLATED FROM RS AND CONTROL FIBROBLAST CELL STRAINS

3.1.1. PATTERN OF D15Z1 HYBRIDIZATION TO MSPI AND HPAII DIGESTED GENOMIC DNA

The restriction fragments recognized by Southern blot hybridization of D15Z1 to MspI and HpaII digested genomic DNA isolated from control fibroblast cell strains are shown in Figure 5. Hybridization of D15Z1 to MspI digested genomic DNA recognized four main bands that varied from 3.5 kb to a high molecular weight band that was greater than 23 kb (+23 kb) in size. The 3.5 kb and the +23 kb bands were consistently observed in each Southern blot. The other two bands were usually identified as 4.0 and 6.0 kb in size although they tended to be polymorphic in size between cell strains.

Digestion of fibroblast genomic DNA with HpaII resulted in the recognition of fewer restriction fragments. The high molecular weight band of +23 kb was always observed to be of equal or greater intensity than that observed for MspI digested genomic DNA. Both the 4.0 and 6.0 kb bands were usually present but were less intense than those bands present with MspI digested genomic DNA. However, qualitative comparison of these band intensities was made more difficult

113

Figure 5.   Southern blot autoradiograph of D15Z1 _MspI_ and _HpaII_ digested genomic DNA obtained from a control fibroblast cell strain, GM0969B, hybridized with D15Z1.   Lane 1, _MspI_ 1.5 μg DNA; lane 2, _HpaII_ 1.5 μg DNA; lane 3, _MspI_ 2.5 μg DNA; lane 4, _HpaII_ 2.5 μg DNA; lane 5, _MspI_ 3.5 μg DNA; lane 6, _HpaII_ 3.5 μg DNA; lane 7, _MspI_ 5.0 μg DNA; lane 8, _HpaII_ 5.0 μg DNA (Experiment 1).
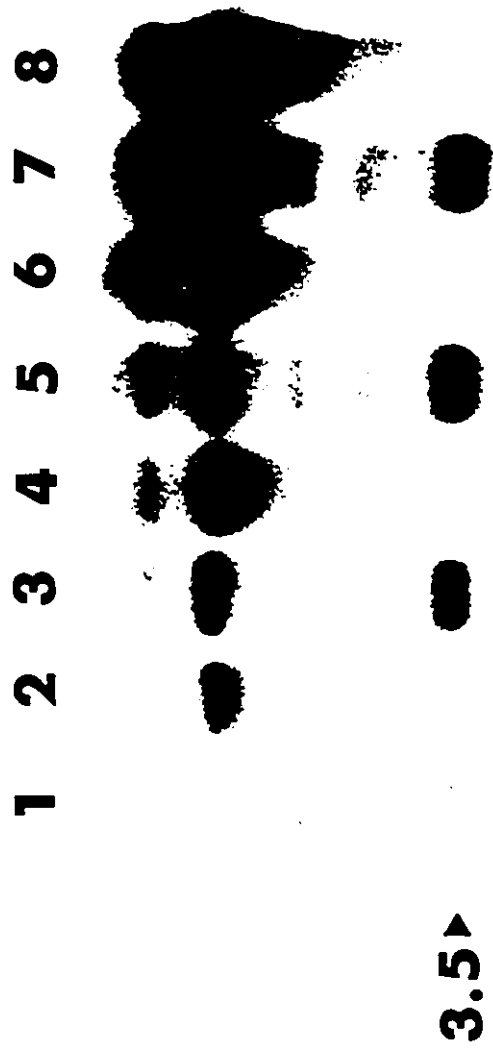
1 2 3 4 5 6 7 8

3.5▸

because of the increased background signal observed in the regions of the higher molecular weight fragments. The HpaII 3.5 kb band was determined to be methylation-sensitive as its signal could be much less intense than the MspI 3.5 kb band or not present at all.

From the pattern of restriction fragments recognized by D15Z1 with MspI and HpaII digested genomic DNA, it is clear that the 3.5 kb band was the most useful for evaluating differences in heterochromatin DNA methylation. Therefore methylation levels among different fibroblast cell strains were determined by comparing the ratio of the MspI 3.5 kb band signal to the HpaII 3.5 kb band signal obtained for each. Because the intensity of the signal could be influenced by the amount of digested DNA present in each lane, the relationship of D15Z1 binding to specified amounts of digested genomic DNA was determined by quantifying the intensity of the signal obtained for each amount.

The intensity of the MspI 3.5 kb reference band was quantified using a video densitometer and the area OD was estimated using the 1-D Analyst Data Analysis software program as described in the Materials and Methods section. The autoradiographs of six Southern Blots were analysed and the area OD values for the MspI 3.5 kb band obtained are summarized in Table 3. The area OD values for all other bands for each experiment are summarized in Tables A-1-6

Table 3. Summary of the area OD of MspI 3.5 kb obtained from six Southern blots hybridized with D15Z1

Experiment	Cell Strain (Passage)	Area OD of MspI 3.5 kb band Amount of DNA (μg)			
		1.5	2.5	3.5	5.0
1	GM0969B (P23)	1.013	3.332	5.262	5.854
2	GM0969B (P23)	6.907	8.240	8.644	7.653
3	GM3349 (P36)	1.090	4.010	5.272	2.602
4	GM3349 (P36)	1.374	1.220	2.707	3.631
5	GM3349 (P30)	0.366	1.054	2.199	3.088

		Amount of DNA (μg)			
		0.5	1.0	2.0	3.0
6	S6007 (P15)	0.827	0.787	5.635	6.794

(Appendix 1). The Southern blot autoradiograph of Experiment 1 is shown in Figure 5. Figure 6A graphically illustrates the relationship of the area OD of the 3.5 kb band to increasing amounts of MspI digested genomic DNA obtained from two fibroblast control cell strains, GM0969B and GM3349 (Experiments 1-5). The graph of Figure 6B represents the third control cell strain, S6007 (Experiment 6). For all six experiments, the area OD of the MspI 3.5 kb band increased with increasing amounts of digested DNA up to 3.5 μg. However variation in the intensity of the MspI 3.5 kb band relative to specified amounts of DNA present was observed between experiments. A summary of the estimated slopes and intercept for all experiments are presented in Table 4. The estimated slope for Experiment 6 was observed to be higher than that obtained for the other experiments. This may reflect the lower amounts of digested DNA used for Experiment 6, such that the slope was not affected by the saturation of signal intensity which appears to occur above 3 μg of DNA.

To mathematically derive the response that was observed for each experiment, the slopes of the lines were modelled and compared using GLM. The factors representing experiment (r), amount of DNA (d) and the interaction between these two factors were required for the model (y=r+d+r*d). The slope of each line was compared for Experiments 1-5 to

Figure 6. Relationship of Area O.D. of <u>Msp</u>I 3.5 kb band to
increasing amounts of digested genomic DNA.

(A) Experiments 1-5 (B) Experiment 6.

A — Area O D (A) of 3.5 kb band vs Amount of MspI digested DNA (ug); Exp.1, Exp.2, Exp.3, Exp.4, Exp.5

B — Area O D (A) of 3.5 kb band vs Amount of MspI digested DNA (ug); Exp. 6
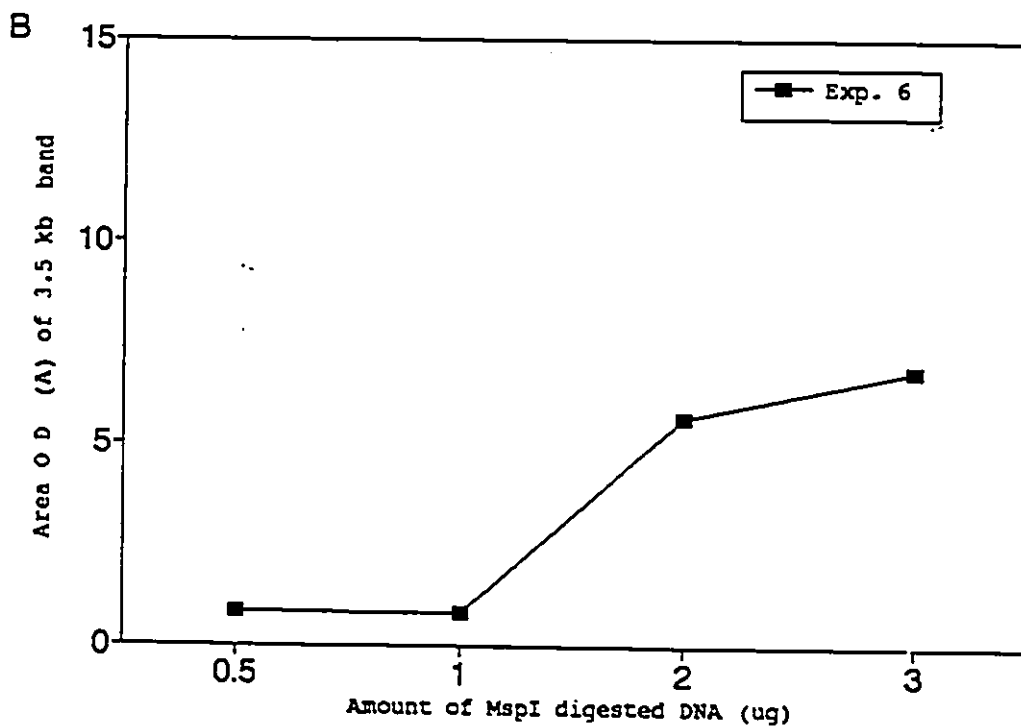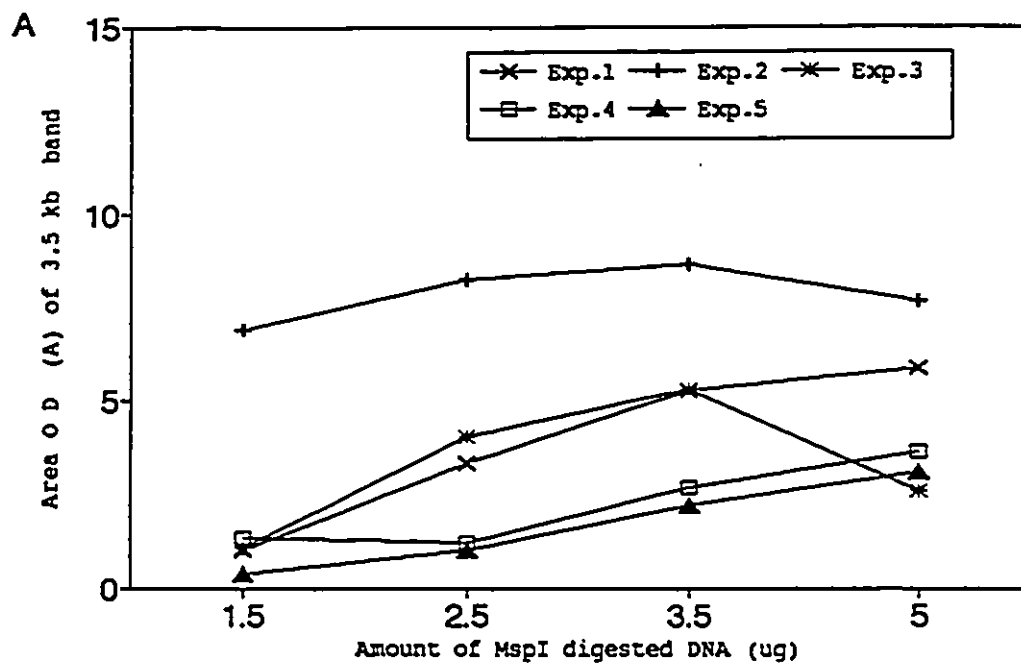
Table 4. Summary of linear equations predicted for area OD values of <u>Msp</u>I 3.5 kb band obtained Experiments 1-6 using the linear equation model, y=a+bx.

	Experiment	Predicted Linear Equation
1	GM0969B (P23)	$y=-0.44+1.38x^*$
2	GM0969B (P23)	$y= 7.29+0.18x^*$
3	GM3349 (P30)	$y= 2.04+0.39x$
4	GM3349 (P36)	$y=-0.02+0.72x$
5	GM3349 (P30)	$y=-0.83+0.80x$
6	S6007 (P15)	$y=-0.91+2.72x$

* Estimates of slopes for Experiments 1 and 2 were significantly different ($\alpha=0.05$). No other statistically significant differences among Experiments 1-5 were detected.

determine if the relationship of the intensity of the MspI 3.5 kb band relative to specified amounts of DNA was the same for each (Table 4). The slopes of all five experiments were analysed using a Student's t-test (Minitab v7.2) and were not found to be statistically different from a slope of 1 (p=0.62). Significant differences in the estimates of slopes were observed between Experiments 1 and 2 only (p<0.05).

The results of the six experiments indicated that 1.5-3.5 μg of digested DNA was sufficient for Southern blot hybridization with D15Z1. The use of 0.5-1.0 μg MspI digested DNA did not correspond to an increase in the binding of D15Z1 (Figure 6B), suggesting that a minimum amount of DNA was required for detection. A saturation in the signal intensity of the 3.5 kb band appeared to occur when more than 3.5 μg of digested genomic DNA was used. The results of Experiments 2 and 3 indicated that a saturation level in the intensity of the 3.5 kb band was achieved with 5.0 μg of DNA.

The intensity of the restriction fragments recognized by D15Z1 hybridization, as defined by the area OD of the MspI 3.5 kb. band, corresponded to an increase in amount of DNA present. Variability among experiments may have been due to differences in amounts of DNA used, to inherent variability in cultured fibroblast cells or to nonspecific binding resulting from hybridization with a repetitive probe.

Because the area OD estimated for a specific band represents the intensity of the signal above the background, with very high background signal, increased background intensity could obscure the actual area OD value of a specific band.

3.1.2. CHARACTERIZATION OF D15Z1 HETEROCHROMATIN DNA METHYLATION LEVELS IN ROBERTS SYNDROME

Eight Southern blots were used to determine the level of constitutive heterochromatin DNA methylation in RS and control fibroblast genomic DNA digested with MspI or HpaII. The D15Z1 restriction fragments of RS+, RS- and age- and sex-matched control fibroblast cell strains were compared. The effect of passage on D15Z1 DNA methylation levels was also assessed for most Southern blot hybridizations to determine whether alterations in methylation levels are associated with the age of the fibroblast cultures.

The autoradiograph presented in Figure 7 shows the MspI and HpaII restriction fragments of two RS+ fibroblast cell strains, S6012 P10 and R22 P26 and with two control cell strains, GM0969B P23 and GM3349 P32. The MspI 3.5 kb band was present for all cell strains. A faint HpaII 3.5 kb band was observed with both RS+ fibroblast cell strains (lanes 2 and 6) but not with the control cell strains. This implied that the 3.5 kb band recognized by D15Z1 was slightly undermethylated in RS+ HpaII digested genomic DNA compared to controls.

Figure 7.   Southern blot autoradiograph of MspI and HpaII
digested genomic DNA obtained from two RS+ (S6012 and R22)
and two control (GM0969B, GM3349) fibroblast cell strains,
hybridized with D15Z1. A total of 2 μg of DNA was applied to
each lane. Lane 1, S6012 P10 MspI; lane 2, S6012 P10 HpaII;
lane 3, GM0969B P23 MspI; lane 4, GM0969B P23 HpaII; lane 5,
R22 P26 MspI; lane 6, R22 P26 HpaII; lane 7, GM3349 P32 MspI;
lane 8, GM3349 P32 HpaII (Experiment 7).
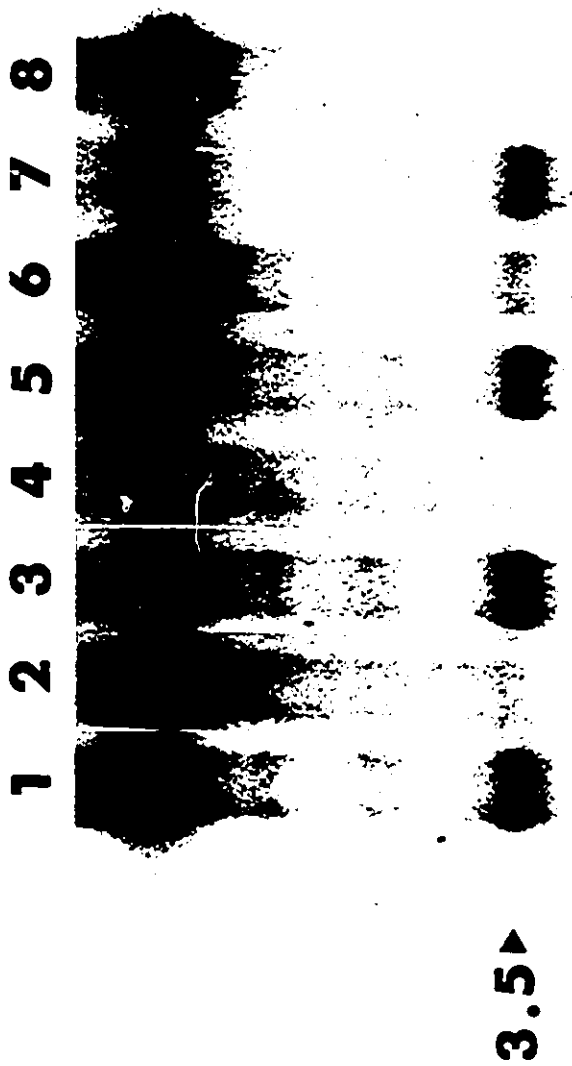
The methylation status of D15Z1 heterochromatin DNA sequences was also assessed for two other genomic DNA samples obtained from the RS+ fibroblast cell strain, S6012, at early and late passage (Figure 8). As with Figure 7, the 3.5 kb band was present for all MspI digested genomic DNA samples. The HpaII digested DNA samples of both RS+ and control also revealed the presence of a faint 3.5 kb band. The HpaII 3.5 kb band of the RS+ digested DNA samples (lanes 2 and 4) appeared to be slightly more intense than that of the control (lanes 6 and 8). This again suggested that the D15Z1 3.5 kb sequences may be less methylated in RS+ than the control fibroblast cell strain.

The MspI and HpaII restriction digest pattern of two different samples of the RS+ fibroblast cell strain, S6012, and its age- and sex-matched control cell strain, GM0969B, are shown in Figure 9. The effect of passage on D15Z1 DNA methylation levels was assessed by isolating genomic DNA from early and late passage fibroblast cultures. As with the other autoradiographs previously described, the 3.5 kb band was present for all MspI digested DNA samples. The 3.5 kb band was also present for all HpaII digested DNA samples and appeared to be slightly more intense with the RS+ samples (lanes 2 and 4). This would again imply that the sequences of the 3.5 kb band recognized by D15Z1 may be not be methylated to the same the degree in the RS+ cell strain.

126

Figure 8. Southern blot autoradiograph of <u>Msp</u>I and <u>Hpa</u>II digested genomic DNA obtained from an RS+ (S6012) and control (GM0969B) fibroblast cell strain, hybridized with D15Z1. A total of 2 μg of DNA was applied to each lane. Lane 1, <u>Msp</u>I S6012 P10; lane 2, <u>Hpa</u>II S6012 P10; lane 3, <u>Msp</u>I S6012 P32; lane 4, <u>Hpa</u>II S6012 P32; lane 5, <u>Msp</u>I GM0969B P23; lane 6, <u>Hpa</u>II GM0969B P23; lane 7, GM0969B P35; <u>Msp</u>I lane 8, <u>Hpa</u>II GM0969B P35 (Experiment 8).

128
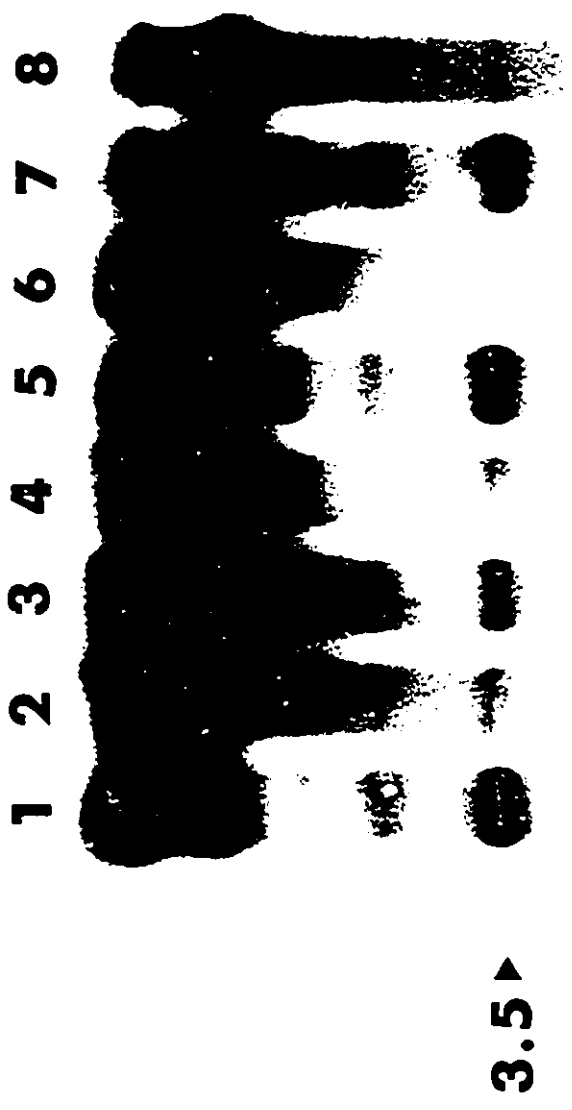
Figure 9. Southern blot autoradiograph of MspI and HpaII
digested genomic DNA obtained from an RS+ (S6012) and control
(GM0969B) fibroblast cell strain, hybridized with D15Z1. A
total of 4.0 μg of DNA was applied to each lane. Lane 1,
MspI S6012 P12; lane 2, HpaII S6012 P12; lane 3, MspI S6012
P36; lane 4, HpaII S6012 P36; lane 5, MspI GM0969B P19; lane
6, HpaII GM0969B P19; lane 7, MspI GM0969B P23; lane 8, HpaII
GM0969B P23 (Experiment 9).
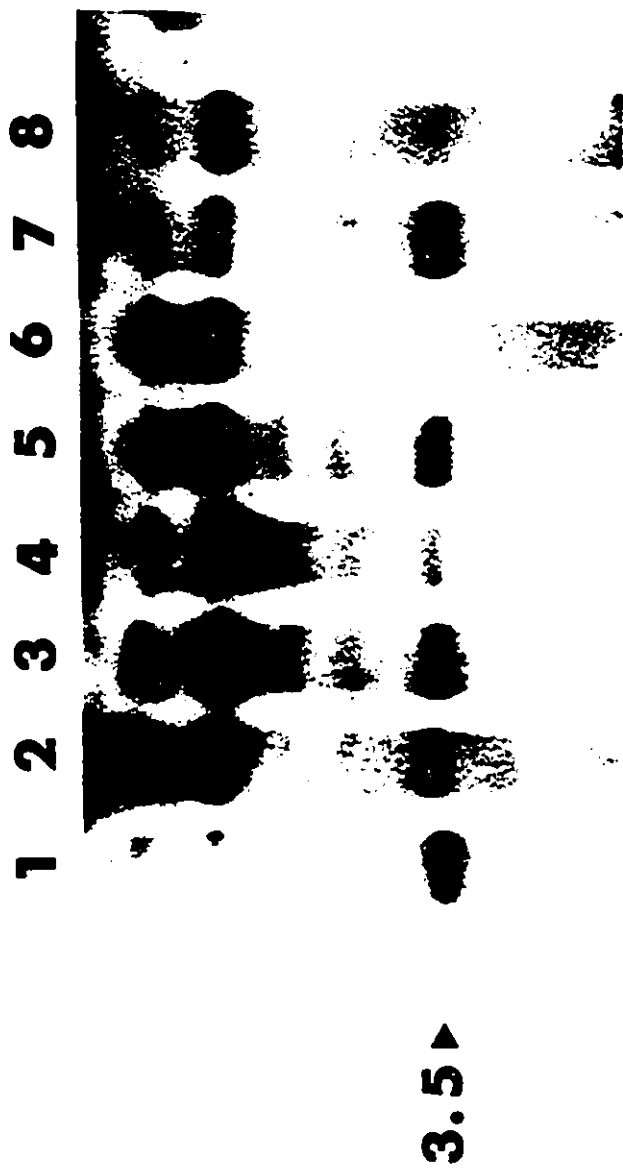
However the comparison of RS+ with control proved to be more difficult for this experiment as the intensity of the HpaII 3.5 kb band was more variable for the control DNA samples. The HpaII 3.5 kb band present in lane 6 may have been affected by a "whiteout" and the signal of the band in lane 8 was somewhat obscured by increased background.

The autoradiograph shown in Figure 10 consists of MspI and HpaII digested genomic DNA obtained from the RS+ fibroblast cell strain, R22, at early (P16) and late (P27) passage and from GM3349, a control cell strain, also at early and late passages (P18, P30). The 3.5 kb band was present for all MspI digested genomic DNA samples. The intensity of this band was more variable between lanes, with very strong signals observed in lanes 1 and 7. The HpaII digested samples of both cell strains also had the 3.5 kb band present. The intensity of the band appeared to be slightly greater for the RS+ HpaII digested genomic DNA samples at early and late passage. It was difficult to compare the intensity of the HpaII 3.5 kb band of the later passaged control cell strain with the RS+ strain because of the "whiteout" effect in lane 8. Because of this, the effect of passage on D15Z1 methylation levels for this experiment could not be clearly evaluated.

The D15Z1 hybridization pattern of genomic DNA isolated from RS+ and RS- fibroblast cell strains, R22 and

Figure 10. Southern blot autoradiograph of MspI and HpaII digested genomic DNA obtained from an RS+ (R22) and control (GM3349) fibroblast cell strain, hybridized with D15Z1. A total of 2.1 μg of DNA was applied to each lane. Lane 1, MspI R22 P16; lane 2, HpaII R22 P16; lane 3, MspI R22 P27; lane 4, HpaII R22 P27; lane 5, MspI GM3349 P18; lane 6, HpaII GM3349 P18; lane 7, MspI GM3349 P30; lane 8, HpaII GM3349 P30 (Experiment 10).

1 2 3 4 5 6 7 8
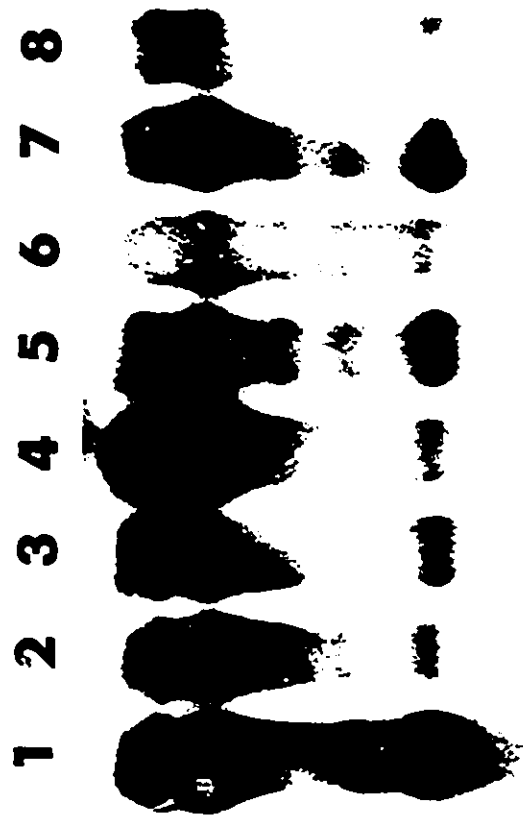
3.5▶

S6006 respectively, and two control strains, GM3349 and GM0969B, obtained at early passages, is shown in Figure 11. The presence of MspI and HpaII restriction fragments of the RS+, RS- and control DNA samples are very similar in this autoradiograph. The MspI 3.5 kb band is of strong intensity for all cell strains and a slight HpaII 3.5 kb band can be detected above the nonspecific background in lanes 4 and 6, and to a lesser extent, in lanes 2 and 8. The results of this Southern blot analysis would suggest that the D15Z1 heterochromatin DNA sequences of RS+, RS- and control genomic DNA samples analysed were similarly methylated.

Figures 12-14 are autoradiographs of Southern blots analysing the MspI and HpaII digested genomic DNA obtained from RS- fibroblast cell strains and their age- and sex-matched controls. A comparison of the restriction digest pattern of S6006 at early (P20) and late passage (P30) with GM0969B (P19, P23) is shown in Figure 12. The 3.5 kb band is present for all digested DNA samples of both cell strains and again the intensity of the MspI band signal is much stronger than the HpaII band. There is some variability in the intensity of the MspI signal between RS- and controls, as the band signal appears to be stronger for GM0969B. This could be due to the presence of more DNA in lanes 5 and 7. The faint HpaII 3.5 band signal suggests that some of the D15Z1 DNA sequences are undermethylated for both S6006 and GM0969B.

Figure 11.   Southern blot autoradiograph of MspI and HpaII
digested genomic DNA obtained from RS+ (R22), RS- (S6006) and
control (GM3349, GM0969B) fibroblast cell strains, hybridized
with D15Z1.   A total of 4.8 μg of DNA was applied to each
lane.   Lane 1, MspI R22 P12; lane 2, HpaII R22 P12; lane 3,
MspI GM3349 P20; lane 4, HpaII GM3349 P20; lane 5, MspI S6006
P20; lane 6, HpaII S6006 P20; lane 7, MspI GM0969B P23; lane
8 HpaII GM0969B P23 (Experiment 11).
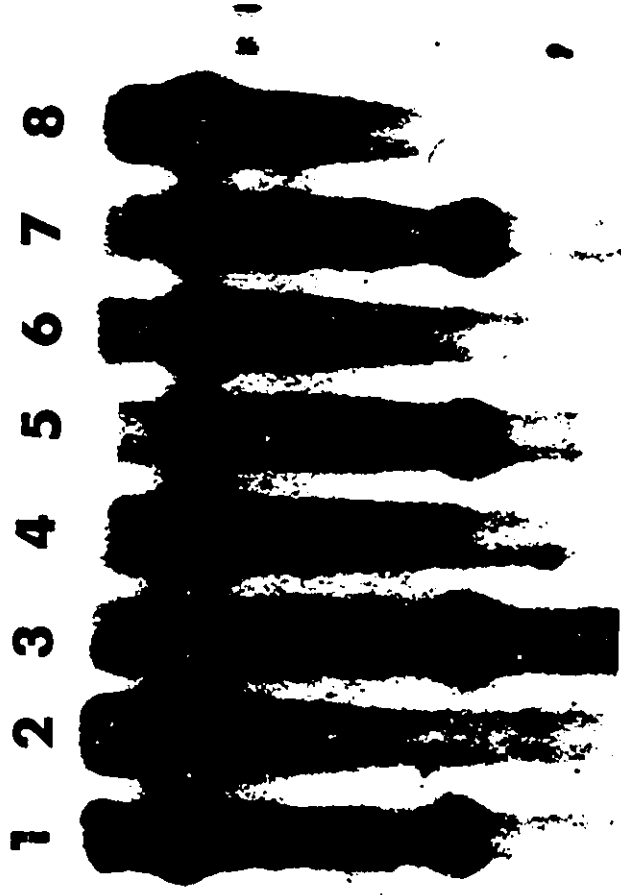
Figure 12. Southern blot autoradiograph of MspI and HpaII digested genomic DNA obtained from an RS- (S6006) and control (GM0969B) fibroblast cell strain, hybridized with D15Z1. A total of 1.7 μg of DNA was applied to each lane. Lane 1, MspI S6006 P20; lane 2, HpaII S6006 P20; lane 3, MspI S6006 P30; lane 4, HpaII S6006 P30; lane 5, MspI GM0969B P19; lane 6, HpaII GM0969B P19; lane 7, MspI GM0969B P23; lane 8, HpaII GM0969B P23 (Experiment 12)
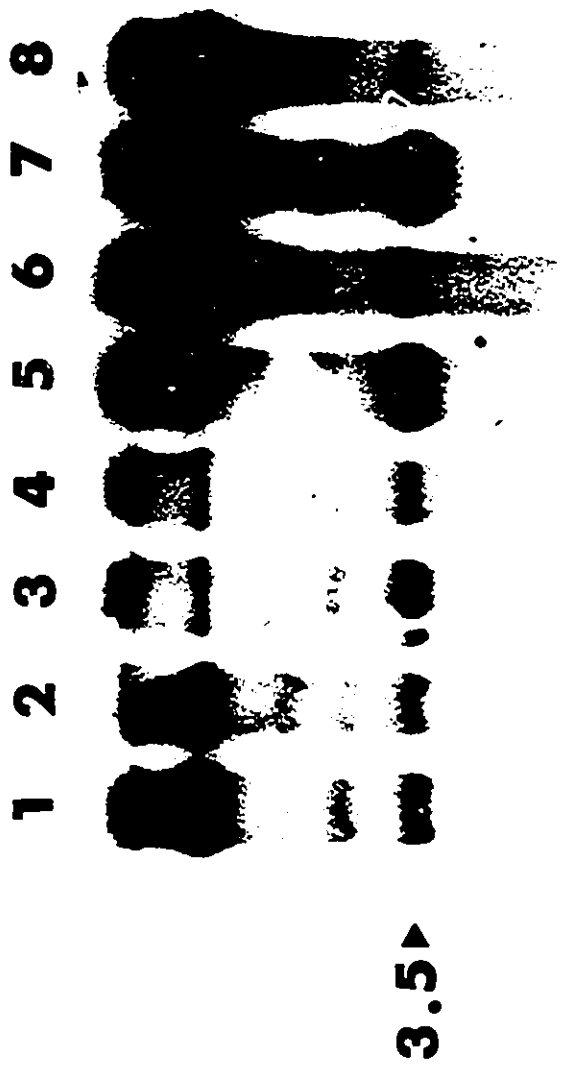
Figure 13. Southern blot autoradiograph of MspI and HpaII digested genomic DNA obtained from an RS- (S6008) and control (S6007) fibroblast cell strain, hybridized with D15Z1. A total of 3.0 μg of DNA was applied to each lane. Lane 1, MspI S6008 P15; lane 2, HpaII S6008 P15; lane 3, MspI S6008 P28; lane 4, HpaII S60C8 P28; lane 5, MspI S6007 P15; lane 6, HpaII S6007 P15; lane 7, MspI S6007 P31; lane 8, HpaII S6007 P31 (Experiment 13).

Figure 14.   Southern blot autoradiograph of MspI and HpaII
digested genomic DNA obtained from an RS- (S6008) and control
(S6007) fibroblast cell strain, hybridized with D15Z1.   A
total of 3.5 μg of DNA was applied to each lane.   Lane 1,
MspI S6007 P15; lane 2, HpaII S6007 P15; lane 3, MspI S6007
P34; lane 4, HpaII S6007 P34; lane 5, MspI S6008 P15; lane 6,
HpaII S6008 P15; lane 7, MspI S6008 P31; lane 8, HpaII S6008
P34 (Experiment 14).
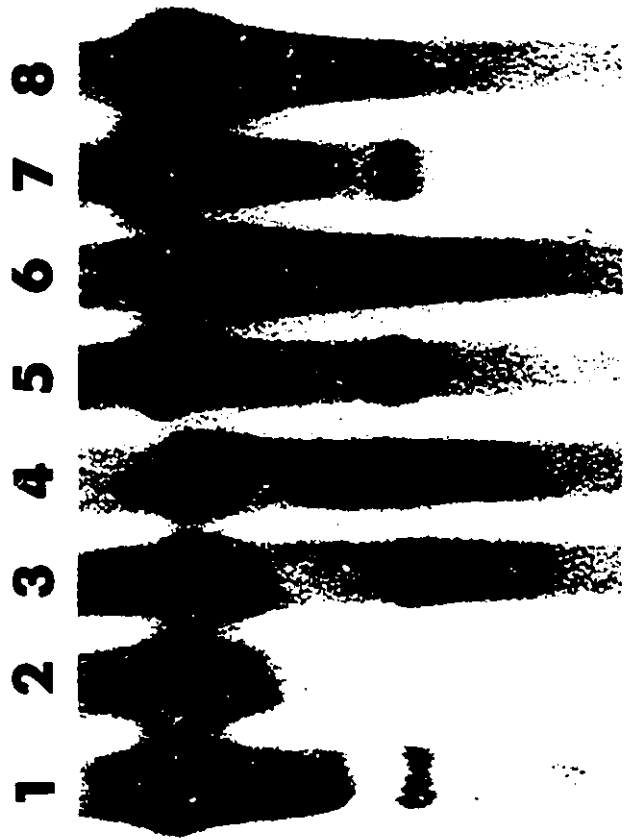
The autoradiographs of Figures 13 and 14 compare the MspI and HpaII restriction fragments of two different DNA samples obtained from the RS- fibroblast cell strain, S6008 and its control, S6007, at early and late passage. The restriction fragments recognized by D15Z1 appear to be very similar for both cell strains. Strong 3.5 kb bands of similar intensity were observed for all MspI digested DNA samples. A very faint HpaII 3.5 kb band can be detected above the background signal for lanes 6 and 8 of Figure 13 and lanes 4 and 8 of Figure 14, suggesting some digestion by HpaII.

Qualitative assessment of methylation levels of D15Z1 heterochromatin DNA sequences, dependent upon the presence or absence of the MspI and HpaII 3.5 kb band, proved to be difficult with the experiments just described. There was some suggestion, based on the results observed for the RS+ fibroblast cell strains (Figures 7-10), that the D15Z1 heterochromatin DNA sequences represented by the HpaII 3.5 kb band showed some degree of undermethylation. There was also some indication that D15Z1 sequences of genomic DNA samples obtained from later passaged RS and control fibroblast cultures were less methylated as well. The presence of a faint HpaII 3.5 kb band for some of the digested DNA samples required that a ratio of the signal intensity of the MspI 3.5 kb band to that of the HpaII 3.5 kb band be made. This was

difficult to do qualitatively as the signal intensity of the MspI 3.5 kb band had to be visually compared to the signal intensity of the HpaII 3.5 kb band. Therefore some measurement of the intensity of the signal of the 3.5 kb band was required.

Levels of constitutive heterochromatin DNA methylation levels were quantified by scanning eight autoradiographs with a video densitometer. The area OD of the bands of each lane was measured using the 1-D Analyst Data Analysis software program (Appendix 1, Tables A-7-14). The level of D15Z1 DNA methylation was mathematically represented by the ratio of the area OD of the MspI 3.5 kb band (A) to the area OD of the HpaII 3.5 kb band (B) for each cell strain. A higher A/B ratio would indicate a higher methylation level and a lower A/B ratio would indicate a lower methylation level. The ratios A/B for each cell strain, categorized as controls, RS+ and RS-, and according to passage (early and late) are summarized in Table 5.

Some of the Southern blots were rehybridized with PstI-MT-hmyc to be used as an internal control for the amount of DNA present in each lane. Hybridization of MspI and HpaII digested genomic DNA with PstI-MT-hmyc resulted in the recognition of a single fragment that was estimated to be 0.5 kb in size. The presence of HpaII 0.5 kb band that was of

Table 5. Summary of area OD ratios (A/B) of 3.5 kb band recognized by D15Z1 from fibroblast cell strains using Southern blot analysis.

Exp	Cont-E	Cont-L	RS+E	RS+L	RS-E	RS-L
7	44.340^H	22.670^H	29.420	14.566	*	*
8	12.028	15.682	11.024	3.718	*	*
9	8.718	*	2.522	4.950	*	*
9	–	*	*	*	*	*
10	11.238	–	4.056	1.803	*	*
11	40.931	*	49.172^H	*	48.700^H	*
11	57.909	*	*	*	*	*
12	4.034	*	*	*	2.008	3.971
12	13.635	*	*	*	*	*
13	16.762	14.285	*	*	17.871^H	16.826^H
14	4.931^H	2.704	*	*	13.633^H	6.899

Exp = Experiment number
Cont-E = Control fibroblast cell strains at early passages
Cont-L = Control fibroblast cell strains at late passages
RS+E = RS+ fibroblast cell strains at early passages
RS+L = RS+ fibroblast cell strains at late passages
RS-E = RS- fibroblast cell strains at early passages
RS-L = RS- fibroblast cell strains at late passages
* no cell strain included in experiment
– Area OD A/B value for 3.5 kb band excluded from statistical analysis due to autoradiograph whiteouts
H = estimated area OD value (B) for HpaII 3.5 kb band

equal intensity to the MspI 0.5 kb indicated that the MT-hmyc sequences were undermethylated in RS and control fibroblast cell strains. For this reason, it was initially thought that the PstI-MT-hmyc probe may be useful as an internal control. The use of this probe was limited by the fact that a minimum of 5 μg of DNA was required for a signal to appear with a minimum 6 day autoradiograph exposure period. Because many of the Southern blots had only 1.7-3.5 μg of DNA present in each lane, the resulting PstI-MT-hmyc signal, upon rehybridization, was too faint for densitometry quantification.

The data presented in Table 5 were modelled with GLM and analysed by ANOVA using Minitab version 7.2. The models were designed so that the mean area OD ratio (A/B) of controls, RS+ and RS- could be compared while minimizing the effect of variability due to experiments and passage effect. Four models were analysed to test three main hypotheses. The first hypothesis stated that there were no significant differences in the level of D15Z1 DNA methylation between experiments, as represented by the mean ratio of the area OD MspI 3.5 kb band to the area OD HpaII 3.5 kb band. The second null hypothesis stated that there were no significant differences in the level of D15Z1 DNA methylation between cells at early and late passage. The third hypothesis stated that there were no significant differences in the level of

D15Z1 DNA methylation, between RS+, RS- and control fibroblast cell strains. Statistical analyses were performed using ANOVA and the null hypotheses were rejected if p≤0.05 (α=0.05).

The first model included two factors that compared the area OD ratio of the 3.5 kb band of all control fibroblast cell strains with all RS+ and all RS- strains at the same time among the three cell groups but without accounting for the effect of experimental variability. The effect of passage on the area OD ratio was introduced into the model as the last factor. There were no significant differences in the mean area OD ratio of RS+, RS- and controls (Table 6). Without removing the effect of experimental variability, the p value derived from the ANOVA was 0.828. There were no significant differences in the level of D15Z1 DNA methylation observed with the comparisons made by this model. In addition to this, there was no significant effect of passage on the mean area OD ratio of control, RS+ and RS- fibroblast cell strains (p=0.100).

The second model, involving three factors, again compared the area OD ratio of all three cell groups (Table 7). The use of this model also maximized the sample size by comparing the mean ratio, A/B, of all cell strains from all experiments but minimized the effects of experimental variability and passage by entering them into the model

Table 6. Analysis of variance comparing the mean Area OD ratio of RS+, RS- and control fibroblast cell strains and the effect of passage as defined by Model i)

Source	DF	Seq SS	Adj SS	Adj MS	F	P
CvR+vR-	2	194.0	94.5	47.3	0.19	0.828
EvsL	1	721.9	721.9	721.9	2.91	0.100
Error	26	6445.4	6445.4	247.9		
Total	29	7361.3				

Unusual Observations for OD

Obs.	OD	Fit	St.dev.fit	Residual	St.resid.
7	57.9090	22.2249	4.5482	35.6841	2.37R
28	49.1720	18.0514	5.8951	31.1206	2.13R

Table 7. Analysis of variance comparing the mean Area OD ratio of RS+, RS- and control fibroblast cell strains and the effect of experiment and passage as defined by Model ii)

Source	DF	Seq SS	Adj SS	Adj MS	F	P
Exps	7	6440.02	5836.50	833.79	26.02	<0.001
CvR+vR-	2	176.74	137.41	68.70	2.14	0.145
EvsL	1	135.65	135.65	135.65	4.23	0.054
Error	19	608.87	608.87	32.05		
Total	29	7361.28				

Unusual Observations for OD

Obs.	OD	Fit	St.dev.fit	Residual	St.resid.
1	44.340	33.0214	3.3034	11.3186	2.46R

first. The differences observed in the mean area OD ratios between experiments were significant, indicating that there was a great deal of experimental variability. The effect of passage did not have a significant effect on the mean area OD ratios of the three groups. A p value of 0.145 indicated that the mean area OD ratios were not significantly different between control, RS+ and RS- fibroblast cell strains. Thus for this model, there was no statistical evidence to show that there were differences in D15Z1 DNA methylation among control, RS+ and RS- fibroblast cell strains. However, the power of the statistical test for both Models i) and ii) was estimated to be 10%, which is well below the generally accepted minimum level of 80%. Thus there was a low probability that the null hypothesis would be rejected for these models.

The third model was a four factor model that considered the effect of experiments and passage and subsequently compared the mean area OD ratio of controls to RS+ and RS- individually. Because of the unbalanced sample size of RS+ and RS-, the statistical program required that the two factors be introduced into the model as covariates. No significant differences were detected in the mean area OD ratios of controls compared to RS+ (p=0.062) or RS- (p=0.264, Table 8). However, there are certain aspects of this model that need to be taken into consideration. The

Table 8. Analysis of variance comparing the mean Area OD ratio of RS+ or RS- with control fibroblast cell strains and the effect of experiment and passage, as defined by Model iii)

Source	DF	Seq SS	Adj SS	Adj MS	F	P
RS+vC	1	191.64	126.17	126.17	3.94	0.062
RS-vC	1	2.41	42.36	42.36	1.32	0.264
Exps	7	6422.71	5836.50	8?3.79	26.02	<0.001
EvsL	1	135.65	135.65	ι ɟ5.65	4.23	0.054
Error	19	608.87	608.87	32.05		
Total	29	7361.28				

Unusual Observations for OD

Obs.	OD	Fit	St.dev.fit	Residual	St.resid.
1	44.3400	33.0214	3.3034	11.3186	2.46R

singular comparison of RS+ with controls, and RS- with controls, has resulted in a reduction of one degree of freedom with the ANOVA. The partitioning of the groups has also resulted in a reduction in sample size of the two groups which affected the power of the study, which was estimated to be 10-15%.

Unlike the first two models, the fourth model addressed the main question of whether altered heterochromatin DNA methylation levels are associated with the abnormal constitutive heterochromatin structure found in RS+ chromosomes. This model included three factors that considered the effect of experiments and passage and then compared the mean area OD ratio of RS+ fibroblast cell strains with all cell strains possessing normal constitutive heterochromatin (controls and RS-). The effect of experimental variability and passage on the mean area OD ratio was minimized by entering the two factors into the model first before a comparison was made between the two groups. By combining all cell strains with normal constitutive heterochromatin structure (RS- and controls), the sample size of this comparison was increased thereby increasing the power of the statistical test. As with the first three models, the differences observed in the mean area OD ratios between experiments were significant (Table 9). The effect of passage on the mean area OD ratio was also

Table 9. Analysis of variance comparing the mean Area OD ratio of RS+ cell strains with cell strains without the heterochromatin abnormality and the effect of experiment and passage as defined by Model iv)

Source	DF	Seq SS	Adj SS	Adj MS	F	P
Exps	7	6440.02	5854.73	836.39	27.38	<0.001
EvsL	1	174.98	133.48	133.48	4.37	0.050
CRS-vRS+	1	135.22	135.22	135.22	4.43	0.048
Error	20	611.05	611.05	30.55		
Total	29	7361.27				

Unusual Observations for OD

Obs.	OD	Fit	St.dev.fit	Residual	St.resid.
6	40.9310	50.6297	2.8486	-9.6987	-2.05R
1	44.3400	33.0158	3.2255	11.3242	2.52R

significant for RS+, RS- and control fibroblast cell strains (p=0.05). The subsequent comparison of RS+ to RS- and control fibroblast cell strains also revealed a significant difference in the mean area OD ratio of the two groups (p=0.048). This suggested that there were significant differences in the D15Z1 DNA methylation levels of RS+ fibroblast cell strains compared to cell strains with normal constitutive heterochromatin, as represented by the methylation status of the 3.5 kb band.

3.1.3. MspI/EcoRI AND HpaII/EcoRI DIGESTION

Single digestion with MspI and HpaII resulted in one band (3.5 kb) showing marked differential sensitivity to restriction. However the bulk of the DNA was not digested with MspI or HpaII, as evidenced by the very large +23 kb band. Genomic DNA isolated from RS+, RS- and control fibroblast cell strains were digested with MspI/EcoRI or HpaII/EcoRI to determine if additional methylation sensitive restriction fragments could be identified. Recognition sites that can be cleaved by EcoRI are observed more frequently than MspI or HpaII restriction sites. Genomic DNA samples obtained from a control fibroblast cell strain, S6007, were digested with MspI, HpaII, EcoRI, MspI/EcoRI or HpaII/EcoRI to determine the number and size of restriction fragments recognized by D15Z1 hybridization. Southern blot

hybridization with D15Z1 to EcoRI digested genomic DNA obtained from a control fibroblast cell strain, S6007 P15, recognized six restriction fragments defined to be 1.6, 1.8, 3.6, 5.4, 7.2 and +23 kb in size (Figure 15). This is in agreement with the findings previously reported by Higgins et al. (1985).

A number of bands of MspI/EcoRI digested DNA were recognized by D15Z1 hybridization (lane 4 of Figure 15). The size of the fragments were estimated to be 0.5, 1.6, 1.8, 2.5, 3.6, 4.1, 4.6, 5.0, 7.5 and +23 kb. Of all the bands listed, three bands were considered to be the products of single restriction enzyme digestions. The 1.6, 1.8 and 3.6 kb bands were the result of EcoRI digestion. The MspI 3.5 kb band was not present with MspI/EcoRI digestion. There were two bands, 0.5 and 2.5 kb, that were observed with MspI/EcoRI digested DNA only and were not observed with MspI or EcoRI digestion. As these bands were absent or were observed to be less intense with HpaII/EcoRI digested DNA samples, these bands were thought to represent DNA sequences that possessed methylated 5'-CCGG-3' sites. A group of bands ranging from 1.8-2.0 kb in size was observed with HpaII/EcoRI digestion only or as much less prominent with MspI/EcoRI digestion. These bands were not observed with HpaII or EcoRI digestion. There was some question of whether MspI/EcoRI and HpaII/EcoRI digestion was complete for these two DNA samples as

Figure 15.   Southern blot autoradiograph of MspI, HpaII, EcoRI, MspI/EcoRI and HpaII/EcoRI digested genomic DNA obtained from a control fibroblast cell strain, S6007 P15, hybridized with D15Z1. A total of 3 μg of DNA was applied to each lane.   Lane 1, MspI; lane 2, HpaII; lane 3, EcoRI; lane 4, MspI/EcoRI; lane 5, HpaII/EcoRI (Experiment 15).
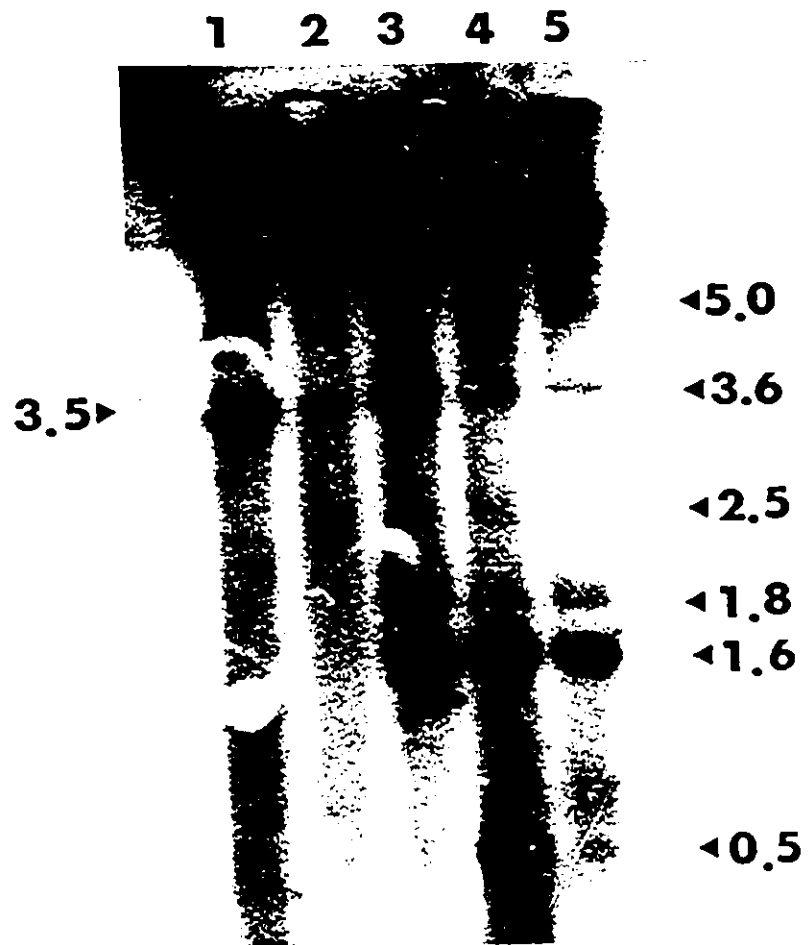
additional bands were recognized by D15Z1 in Figures 16-18.

Referring to Figures 16-18, the additional bands that resulted from MspI/EcoRI and HpaII/EcoRI digestion were often polymorphic. Some bands were observed for a particular cell strain or small differences in size were observed between cell strains. For example, a 4.0 kb band was observed for MspI/EcoRI digested DNA obtained from S6008 while a 4.1 kb band was observed for the control fibroblast cell strain, S6007 (Figure 18). Summarizing the results of Figures 16-18, the bands demonstrating polymorphisms were identified as being 2.3, 2.9, 3.0, 3.2, 3.3, 3.8, 4.0, 4.1, 4.3, 4.6, 5.0, 6.0, 6.3, 6.4, 6.6, 7.3, 7.5, and 9.5 kb in size.

Levels of constitutive heterochromatin DNA methylation were quantified by scanning the three autoradiographs shown in Figure 16-18 with a video densitometer. The area OD of the bands of each lane was analysed using the 1-D Analyst Data Analysis software program. The area OD estimated for all the bands are presented in Tables A-15-26 (Appendix 1). Because the 2.5 kb band was differentially digested with MspI/EcoRI compared to HpaII/EcoRI, this band was used to represent levels of D15Z1 DNA methylation. The 0.5 kb band was not used as it was not always detectable on all blots.

To standardize the area OD value obtained for the 2.5 kb band with respect to the amount of DNA present in each lane, the area OD values obtained for both the MspI/EcoRI and

158

Figure 16.   Southern blot autoradiograph of MspI/EcoRI and
HpaII/EcoRI digested genomic DNA obtained from an RS+ (S6012)
and control (GM0969B) fibroblast cell strain hybridized with
D15Z1.   A total of 1.4 μg of DNA was applied to each lane.
Lane 1 MspI/EcoRI S6012 P10; lane 2, HpaII/EcoRI S6102 P10;
lane 3, MspI/EcoRI S6102 P28; lane 4, HpaII/EcoRI S6012 P28;
lane 5, MspI/EcoRI GM0969B P23; lane 6, HpaII/EcoRI GM0969B
P23; lane 7, MspI/EcoRI GM0969B P32; lane 8, HpaII/EcoRI
GM0969B P32 (Experiment 16).
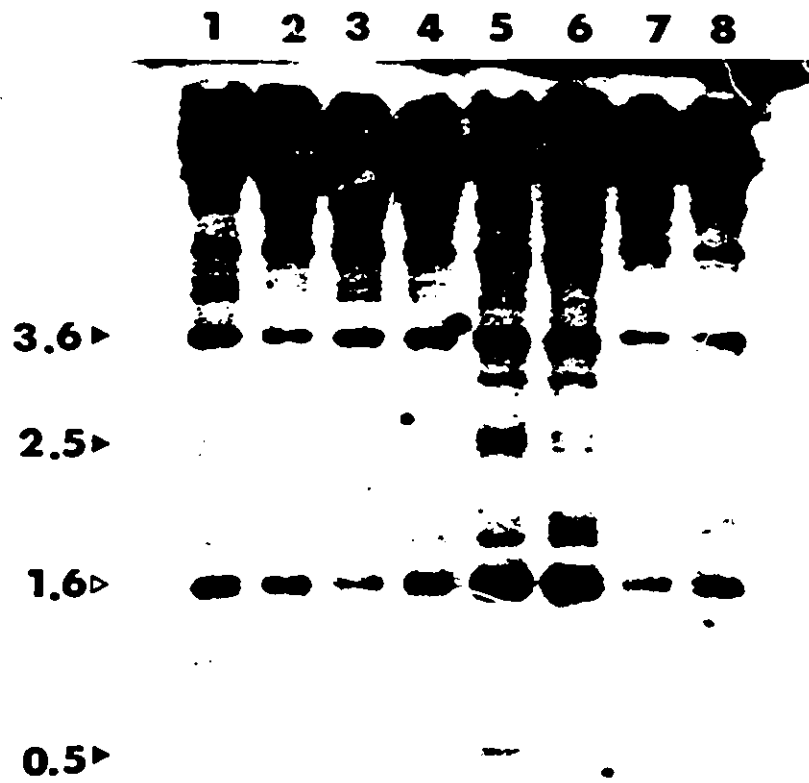
Figure 17. Southern blot autoradiograph of MspI/EcoRI and HpaII/EcoRI digested genomic DNA obtained from an RS+ (R22) and control (GM3349) fibroblast cell strain hybridized with D15Z1. A total of 2 μg of DNA was applied to each lane. Lane 1, MspI/EcoRI R22 P12; lane 2, HpaII/EcoRI R22 P12; lane 3, MspI/EcoRI R22 P26; lane 4, HpaII/EcoRI R22 P26; lane 5, MspI/EcoRI GM3349 P17; lane 6, HpaII/EcoRI GM3349 P17; lane 7, MspI/EcoRI GM3349 P32; lane 8, HpaII/EcoRI GM3349 P32 (Experiment 17)
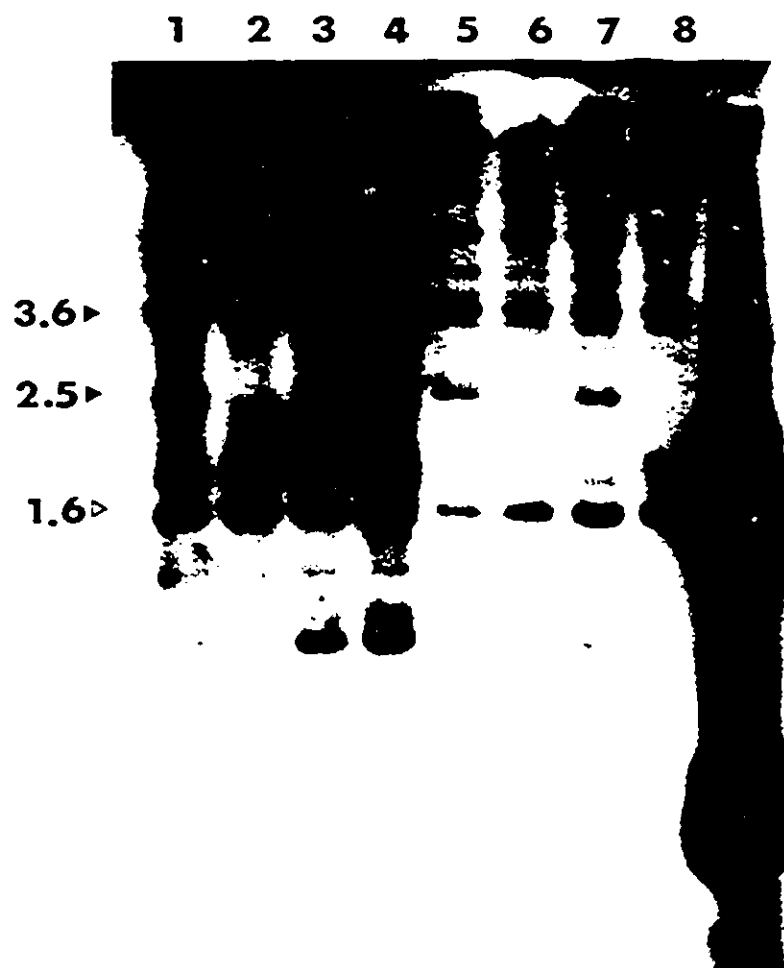
Figure 18.   Southern blot autoradiograph of MspI/EcoRI and HpaII/EcoRI digested genomic DNA obtained from an RS- (S6008) and control (S6007) fibroblast cell strain, hybridized with D15Z1.   A total of 3 μg of DNA was applied to each lane. Lane 1, MspI/EcoRI S6008 P15; lane 2, HpaII/EcoRI S6008 P15; lane 3, MspI/EcoRI S6008 P28; lane 4, HpaII/EcoRI S6008 P28; lane 5, MspI/EcoRI S6007 P15; lane 6, HpaII/EcoRI S6007 P15; lane 7, MspI/EcoRI S6007 P31; lane 8, HpaII/EcoRI S6007 P31 (Experiment 18).
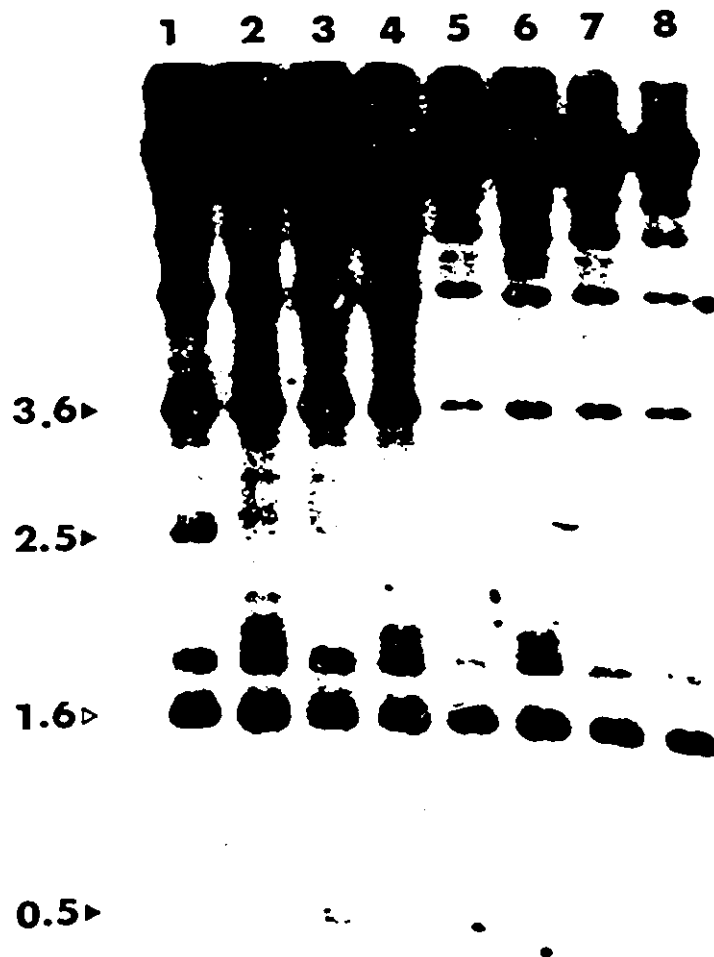
HpaII/EcoRI band were adjusted by dividing each value by the area OD value of 1.6 kb band of the same lane. The 1.6 kb band was considered to be a suitable reference band to control for unequal signal intensities that may be caused by unequal amounts of DNA present in each lane because the band was considered to be the product of EcoRI digestion, was present in every lane and was characterized by a strong signal that could be easily quantified by video densitometry.

The level of D15Z1 DNA methylation was mathematically represented by the ratio of the adjusted area OD of the MspI/EcoRI 2.5 kb band to the adjusted area OD of the HpaII/EcoRI 2.5 kb. band (C/D). If the 5'-CCGG-3' sequences of the 2.5 kb band were methylated, the sequences would only be cleaved with MspI/EcoRI and not by HpaII/EcoRI digestion. If altered levels of D15Z1 DNA methylation were associated with the abnormal constitutive heterochromatin structure of RS+ chromosomes, then the adjusted area OD ratio (C/D) of the controls and RS- would be expected to be higher than the ratio of RS+ cell strains.

The adjusted area OD ratios (C/D) of the 2.5 kb band obtained from three Southern blot autoradiographs are summarized in Table 10. For Experiment 16, the ratio of the

Table 10. Summary of the area OD ratios MspI/EcoRI and HpaII/EcoRI 2.5 kb band (C/D) obtained from an RS+, RS-fibroblast cell strains and control fibroblast cell strains, at early and late passages (Experiments 16-18).

	Area OD Ratio (C/D)	
	Early Passage	Late Passage
Experiment 16		
RS+ S6012	3.069	20.714
C GM0969B	C>D*	4.243
Experiment 17		
RS+ R22	C>D$^+$	0.238
C GM3349	C>D$^+$	C>D
Experiment 18		
RS- S6008	8.365	2.522
C S6007	8.000	12.857

* Band was visible on autoradiograph but could not be distinguished by video densitometer
+ HpaII/EcoRI 2.5 kb. band absent on autoradiograph, no estimate of area OD of band

adjusted area OD, C/D, was estimated to be 3.069 for the RS+ fibroblast cell strain, S6012, at early passage (P10) and 20.714 at late passage (P28). The ratio C/D could not be estimated for the control fibroblast cell strain, GM0969B, at early passage (P23) as the HpaII/EcoRI 2.5 kb band could not be distinguished by video densitometry scanning. For this reason, C was interpreted to be much greater than D. The ratio could be estimated for the later passage (P32) digested control DNA samples and was calculated to be 4.243.

The area OD ratios of another RS+ fibroblast cell strain at early passage, R22 (P10), and of a control cell strain, GM3349, at both early and late passages, was represented by C being much greater than D (Experiment 17). The area OD ratio of the late passage RS+ cell strain was estimated to be less than 1. Since one would not expect a C/D ratio of less than 1, this estimated ratio must be interpreted with caution. The ratio of 0.238 is most likely due to the unequal amounts of DNA present in lanes 3 and 4. The background signal of the first four lanes was unusually heavy and may have resulted in overestimation of the area OD value of the HpaII/EcoRI 2.5 kb band.

Experiment 15 compared the area OD ratios of an RS- cell strain, S6008, with a control cell strain, S6007, at early and late passages. The area OD ratio, C/D, was estimated to be 8.365 at early passage (P15) and 2.622 at

late passage (P28). The area OD ratio of the control cell strain, S6007 was 8.000 at early passage and 12.857 at late passage. Again, the ratio for the control was considered to be much greater than 1. Using this criterion, decreased levels of D15Z1 DNA methylation were not detected in the two fibroblast cell strains as represented by the 2.5 kb band.

It was difficult to draw any firm conclusion from the results of the double digest experiments. The adjusted area OD ratio, C/D, was greater than 1 for all fibroblast cell strains except the RS+ cell line, R22, at late passage. This suggested that the HpaII/EcoRI 2.5 kb fragment was not completely unmethylated, as an adjusted area OD ratio (C/D) of 1 would have been expected. Since undermethylation of the 2.5 kb band in RS+ fibroblast genomic DNA would have been represented by an adjusted area OD ratio (C/D) that was greater than 1 but less than that observed for controls, it was not possible to compare the ratio (C/D) of RS+, RS- and control cell strains. For some fibroblast cell strains, it was not possible to estimate an adjusted area OD ratio as the intensity of the HpaII/EcoRI 2.5 kb band was too faint to be quantified by video densitometry or it was absent. The variability in the adjusted area OD ratios observed within and between cell strain was problematic as it appeared to be greatly influenced by differences in the amount of digested DNA present in each lane and by increased background signal

due to the use of a repetitive DNA probe.

3.2. CHROMOSOME REPLICATION STUDIES OF ROBERTS SYNDROME
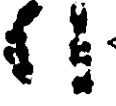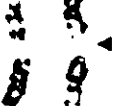
3.2.1. CHARACTERIZATION OF S SUBPHASE DISTRIBUTIONS IN ROBERTS SYNDROME

The chromosome replication patterns were investigated in RS+ (LB1 and R20) and control (JaKr and DM) lymphoblasts by terminally labelling cells in S phase with BrdUrd. Metaphases were classified as having replicated during a particular substage of S phase using the classification system of Savage (personal communication) for replication banded chromosomes, previously outlined in Figure 2. Classification involved the use of an artificial key based on Band Appearance Distribution curves that placed a cell within one of four successive substages of S phase, SkI-IV, depending on the presence or absence of particular replication bands on chromosomes 3 and 4.

An example of three partial metaphases classified as having replicated during a particular substage in S phase using chromosomes 3 and 4 is shown in Figure 19. The first cell was defined to have replicated in SkII as the band 3p1-2 is completely pale staining for both homologues and the dark staining band q21 is present on chromosome 4. The second cell was classified as SkIII as the band 3p1-2 is not completely pale staining in one homologue. A very faint dark staining band is present in the middle of band 3p1-2.

Figure 19. Subclassification of three metaphase cells in S
phase based upon the pattern of BrdUrd incorporation and the
classification system of Key 4, using chromosomes 3 and 4.
The metaphases were obtained from the female control
lymphoblastoid cell line, JaKr. (◄) Indicates band used for
classification system.   (+) Denotes that the band or gap as
defined by the subclassification system of Key 4 is present.
(-) Denotes that the band or gap is absent. (◄) Indicates a
dark staining band within band 3p1-2.

CHROMOSOME   3   4

SKII

3p1-2(+)   4q21(+)

SKIII

3p1-2(+/-)   4q13(+)

SKIV

3p1-2(-)   4q13(-)

KEY 4

However, this band can be seen more clearly when analysed directly under the microscope using 100X magnification. The 4q13 band was found to be pale staining on both homologues. The last cell was defined to have replicated during the last subphase, SkIV, as band 3p1-2 is dark staining and band 4q13 is not obviously pale staining.

The subphase distribution of metaphases from RS+ cell lines were compared to controls to determine if there were any detectable differences in S phase. Replicate experiments 1 and 2 compared the female RS+ lymphoblast cell line, LB1, with a female control, JaKr. Replicate experiments 3 and 4 compared the replication programme of a male RS+ lymphoblast cell line, R20, with a male control, DM. Each cell line was labelled with BrdUrd for 4, 5, 6 and 7 hours. Fifty metaphases were analysed from each BrdUrd treatment time. Experiments 2 and 4 were analysed blind as to donor and treatment time. The data from these four experiments are summarized in Tables 11-14. Analysis of Experiment 4 involved scoring two subsets of the experiment, A and B. The data of DM were obtained from Experiment 4A and the data of R20 from Experiment 4B. However, the comparison between DM and R20 was made only after determining that the results obtained for DM using the 4 and 7 hour BrdUrd treatment times were not significantly different for each experiment.

Table 11A. S phase subclassification of metaphases from a female control lymphoblastoid cell line, JaKr, subjected to various BrdUrd treatment times (Exp. 1)

BrdUrd Treatment Time (hours)	Cells Scored	Number of Cells in Subphase			
		SkI	SkII	SkIII	SkIV
4	50	0	17	20	13
5	≥0	0	25	18	7
6	50	0	21	8	21
7	50	1	26	6	17
Total	200	1	89	52	58

Table 11B. S phase subclassification of metaphases from a female control lymphoblastoid cell line, JaKr, subjected to various BrdUrd treatment times (Exp. 2)

BrdUrd Treatment Time (hours)	Cells Scored	Number of Cells in Subphase			
		SkI	SkII	SkIII	SkIV
4	50	0	8	31	11
5	50	0	9	34	7
6	50	0	12	33	5
7	50	0	13	30	7
Total	200	0	42	128	30

Table 12A.   S phase subclassification of metaphases from a female Roberts syndrome lymphoblastoid cell line, LB1, with various BrdUrd treatment times (Exp.1)

BrdUrd Treatment Time (hours)	Cells Scored	SkI	Number of Cells in Subphase		
			SkII	SkIII	SkIV
4	50	0	8	15	27
5	50	0	8	33	9
6	50	0	7	13	30
7	50	0	13	24	13
Total	200	0	36	85	79

Table 12B.   S phase subclassification of metaphases from a female Roberts syndrome lymphoblastoid cell line, LB1, with various BrdUrd treatment times (Exp.2)

BrdUrd Treatment Time (hours)	Cells Scored	SkI	Number of Cells in Subphase		
			SkII	SkIII	SkIV
4	50	0	12	10	28
5	50	0	4	8	38
6	50	0	2	16	32
7	50	0	10	25	15
Total	200	0	28	59	113

Table 13A.   S phase subclassification of metaphases from a male control lymphoblastoid cell line, DM, subjected to various BrdUrd treatment times (Exp. 3)

BrdUrd Treatment Time (hours)	Cells Scored	Number of Cells in Subphase			
		SkI	SkII	SkIII	SkIV
4	50	0	23	27	0
5	50	0	17	28	5
6	50	0	9	20	21
7	50	0	21	20	9
Total	200	0	70	95	35

Table 13B.   S phase subclassification of metaphases from a male control lymphoblastoid cell line, DM, subjected to various BrdUrd treatment times (Exp. 4)

BrdUrd Treatment Time (hours)	Cells Scored	Number of Cells in Subphase			
		SkI	SkII	SkIII	SkIV
4	50	0	5	27	18
5	50	0	8	26	16
6	50	0	15	21	14
7	50	0	26	18	6
Total	200	0	54	92	54

Table 14A. S phase subclassification of metaphases from a male Roberts syndrome lymphoblastoid cell line, R20, with various BrdUrd treatment times (Exp.3)

BrdUrd Treatment Time (hours)	Cells Scored	Number of Cells in Subphase			
		SkI	SkII	SkIII	SkIV
4	50	0	11	15	24
5	50	0	15	17	18
6	50	0	17	12	21
7	50	0	21	21	8
Total	200	0	64	65	71

Table 14B. S phase subclassification of metaphases from a male Roberts syndrome lymphoblastoid cell line, R20, with various BrdUrd treatment times (Exp.4)

BrdUrd Treatment Time (hours)	Cells Scored	Number of Cells in Subphase			
		SkI	SkII	SkIII	SkIV
4	50	0	6	22	22
5	50	0	4	29	17
6	50	0	11	21	18
7	50	0	12	27	11
Total	200	0	33	99	68

3.2.2. STATISTICAL ANALYSIS OF S SUBPHASE DISTRIBUTIONS USING GENERALIZED LINEAR MODELLING

The subphase classification system of Savage and Papworth (1988) is based upon the serial sampling of steady-state cell populations throughout S phase. This gave Band Appearance Distribution curves that are sigmoidal and well approximated by cumulative Normal distributions with similar standard deviations. The probit transformation is the mathematical transformation of a sigmoidal curve to a straight line (Finney, 1971). Each percentage point, in this case defined as the proportion of cells classified within a certain subphase, is transformed to its Normal Equivalent Deviant (NED). A probit (probability unit) is equal to the NED+5. The probit regression line is a graphical approximation to the regression line of the response probit on x (BrdUrd treatment time). The probits were then converted back to expected proportions as predicted by the linear predictor model. These proportions are converted to frequencies by multiplying by 50.

The data presented in Tables 11-14 were analysed using probit transformation and GLIM (GLIM version 3.77, Royal Statistical Society, 1985). The appropriate GLIM predicted linear formula was determined by looking at the effect of certain predictor variables, namely cell line (r) and BrdUrd treatment time (t), and the effect of interaction between the two variables. This involved including the predictor

variables in the GLIM model and determining their statistical effect. From this analysis, it was determined that the best linear prediction formula was y=t+r+rt, as BrdUrd treatment time, differences between cell lines and the interaction of the two latter variables were found to have a significant effect on the model.

Differences in the subphase distribution between RS+ and control cell lines involved estimating the slopes of the lines formed by plotting the predicted values determined by the model against BrdUrd treatment time. Slopes and intercepts of the linear predictor line were estimated using GLIM. Significant differences in the estimated slopes were then interpreted to represent significant differences in the subphase distribution with respect to BrdUrd treatment time between RS+ and control lymphoblastoid cell lines. It was predicted that differences in rate or timing of replication between RS+ and control cell lines could lead to alterations in the subphase distributions.

The estimates of slopes obtained for the subphase distribution of RS+ and control cell lines for the four experiments are summarized and compared in Tables 15-18. A comparison of each subphase distribution for each RS+ and control cell line was made for each experiment and are shown graphically in Figures 20-22. Each figure represents a graph of the fitted values of each subphase obtained from the

Table 15. Summary of slopes estimated from a linear predictor model
(y=t+r+rt) with probit transformation comparing the S subphase
distribution of control (JaKr and DM) lymphoblastoid cell lines.

Sub-phase	Exp	JaKr	Exp	DM	Comparison of slopes
SkII	1	$y=-0.784+0.117t$	3	$y= 0.022-0.074t$	$p>0.05$
	2	$y=-1.508+0.126t$	4	$y=-3.220+0.460t$	$p<0.025$
Comparison of slopes		$p>0.05$		$p<0.001$	
SkIII	1	$y= 1.172-0.339t$	3	$y= 0.743-0.147t$	$p>0.05$
	2	$y= 0.476-0.021t$	4	$y= 0.793-0.163t$	$p>0.05$
Comparison of slopes		$p<0.01$		$p>0.05$	
SkIV	1	$y=-1.401+0.153t$	3	$y=-3.193+0.394t$	$p>0.05$
	2	$y=-0.395-0.118t$	4	$y= 0.681-0.239t$	$p>0.05$
Comparison of slopes		$p<0.05$		$p<0.001$	

Table 16. Summary of slopes estimated from a linear predictor model (y=t+r+rt) with probit transformation comparing the S subphase distribution of RS+ (LB1 and R20) lymphoblastoid cell lines.

Sub-phase	Exp	LB1	Exp	R20	Comparison of slopes
SkII	1	y=-1.501+0.105t	3	y=-1.476+0.182t	p>0.05
	2	y=-0.714-0.067t	4	y=-2.125+0.205t	p<0.05
Comparison of slopes		p>0.05		p>0.05	
SkIII	1	y=-0.387+0.036t	3	y=-0.850+0.072t	p>0.05
	2	y=-2.301+0.315t	4	y=-0.206+0.035t	p<0.025
Comparison of slopes		p<0.02		p>0.05	
SkIV	1	y= 0.336-0.110t	3	y= 0.990-0.251t	p>0.05
	2	y= 1.431-0.230t	4	y=-0.206+0.035t	p<0.025
Comparison of slopes		p>0.05		p>0.05	

Table 17. Summary of slopes estimated from a linear predictor model $(y=t+r+rt)$ with probit transformation comparing the S subphase distribution of an RS+ (LB1) and control (JaKr) lymphoblastoid cell line.

Sub-phase	Exp	Control	RS+	Comparison of slopes
SkII	1	$y=-0.784+0.117t$	$y=-1.501+0.105t$	$p>0.05$
	2	$y=-1.508+0.126t$	$y=-0.714-0.067t$	$p>0.05$
SkIII	1	$y=1.172-0.339t$	$y=-0.387+0.036t$	$p<0.01$
	2	$y=0.476-0.021t$	$y=-2.301+0.315t$	$p<0.01$
SkIV	1	$y=-1.401+0.153t$	$y=0.336-0.110t$	$p<0.05$
	2	$y=-0.395-0.118t$	$y=1.431-0.230t$	$p>0.05$

Table 18. Summary of slopes estimated from a linear predictor model (y=t+r+rt) with probit transformation comparing the S subphase distribution of an RS+ (R20) and control (DM) lymphoblastoid cell line.

Sub-phase	Exp	Control	RS+	Comparison of slopes
SkII	3	y= 0.022-0.074t	y=-1.476+0.182t	p<0.05
	4	y=-3.220+0.460t	y=-2.125+0.205t	p>0.05
SkIII	3	y= 0.743-0.147t	y=-0.850+0.072t	p>0.05
	4	y= 0.793-0.163t	y=-0.206+0.035t	p>0.05
SkIV	3	y=-3.193+0.394t	y= 0.990-0.251t	p<0.001
	4	y= 0.681-0.239t	y= 0.556-0.178t	p>0.05

Figure 20. Comparison of the number of metaphases classified as SkII from RS+ (R) and control (C) lymphoblastoid cell lines. The data were obtained from a Generalized Linear Model using a probit transformation. Modelled data are indicated by lines and observed values are indicated by symbols. A. RS+, LB1; C, JaKr. Experiment 1 (E1); Experiment 2 (E2). B. RS+, R20; C, DM. Experiment 3 (E3); Experiment 4 (E4). A straight line was not obtained with the data modelled from the control cell line, DM, in Experiment 4.

A

SkII subphase: JaKr (C) and LB1 (RS+)
Comparison of Experiments 1 and 2

B

SkII subphase: DM (C) and R20 (RS+)
Comparison of Experiments 3 and 4
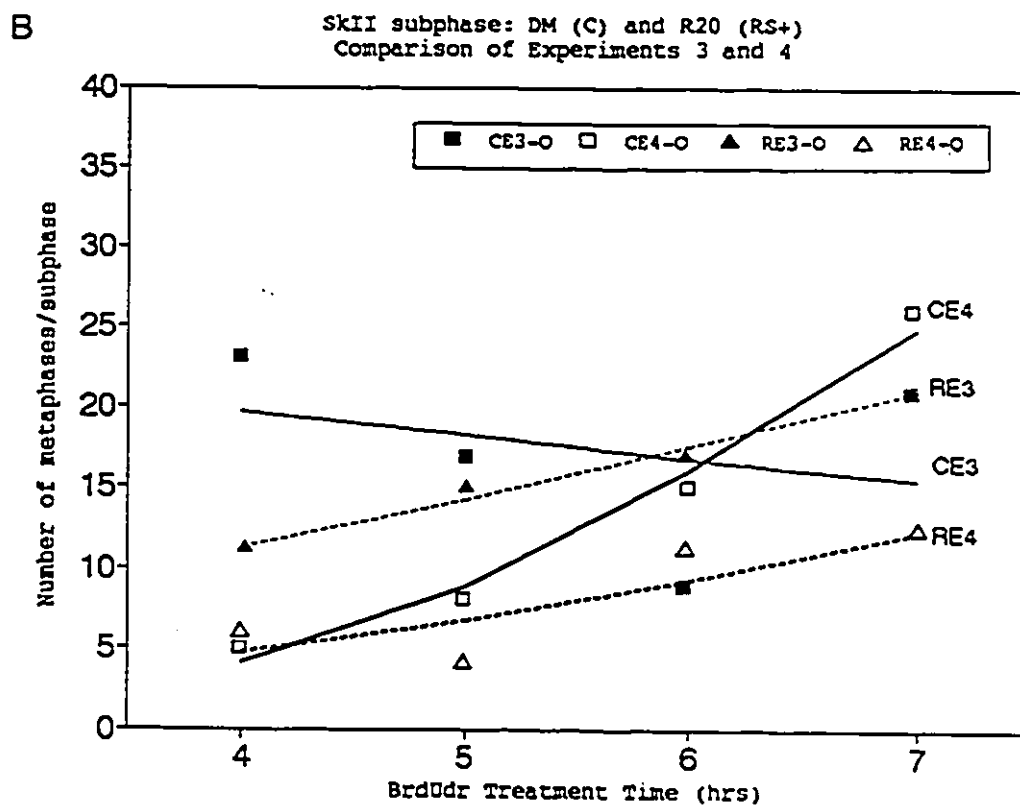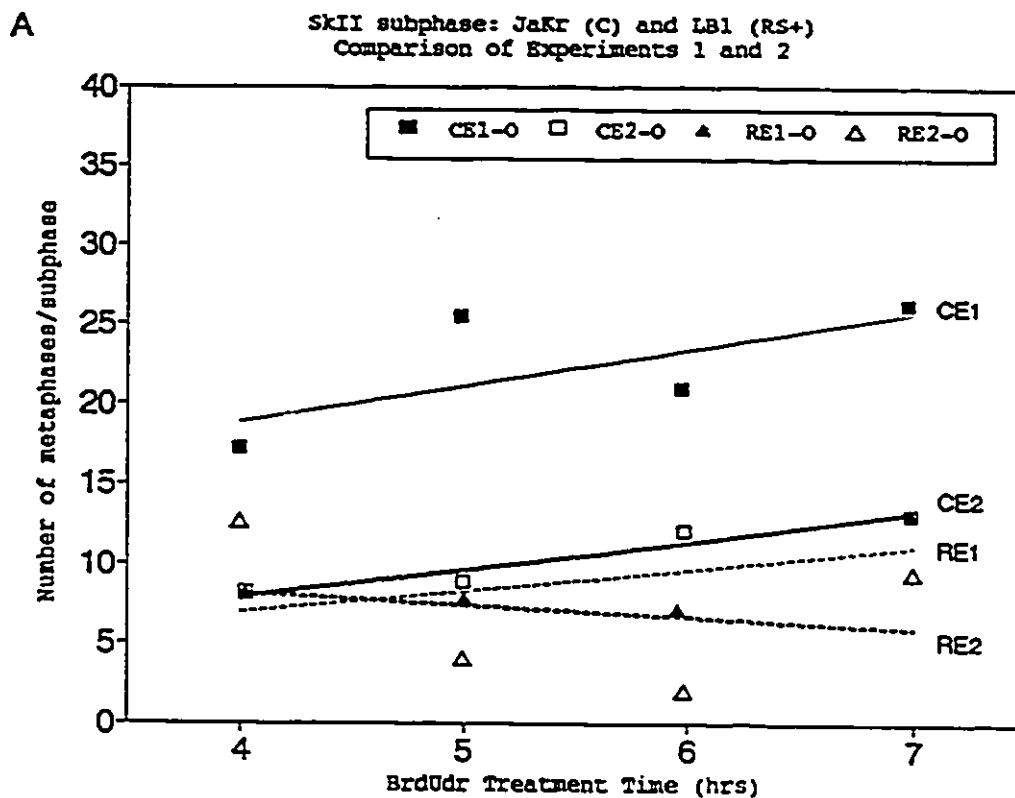
Figure 21. Comparison of the number of metaphases classified as SkIII from RS+ (R) and control (C) lymphoblastoid cell lines. The data were obtained from a Generalized Linear Model using a probit transformation. Modelled data are indicated by lines and observed values are indicated by symbols. A. RS+, LB1; C, JaKr. Experiment 1 (E1); Experiment 2 (E2). B. RS+, R20; C, DM. Experiment 3 (E3); Experiment 4 (E4). A straight line was not obtained with the data modelled from the RS+ cell line, LB1, in Experiment 2.

A

SkIII subphase distribution
Comparison of Experiments 1 and 2
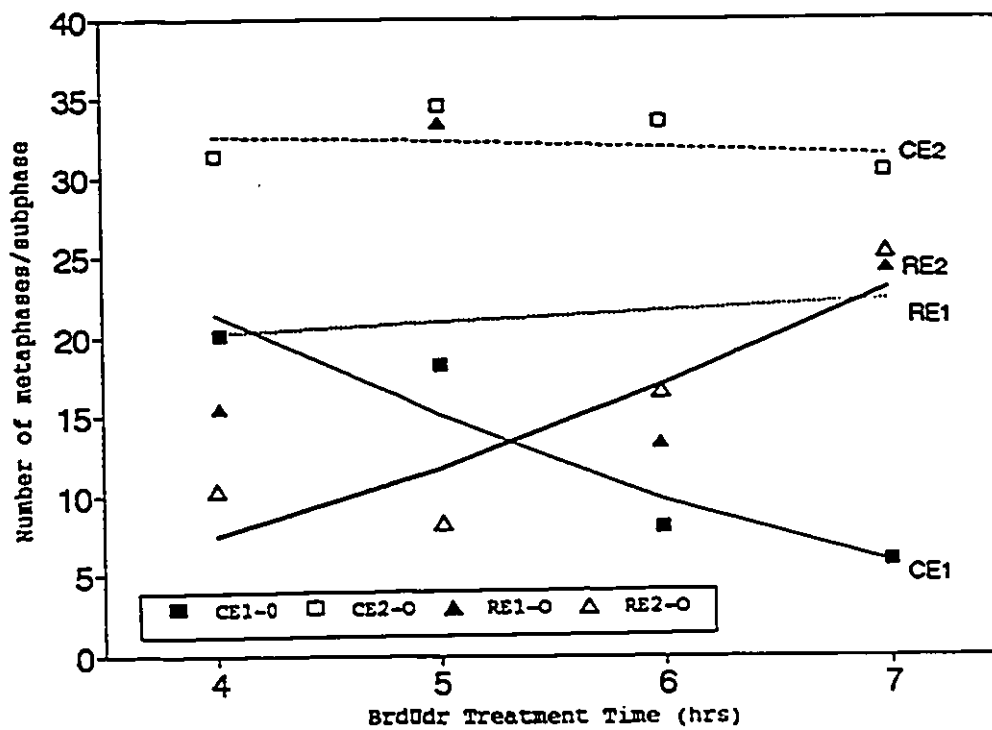
B

SkIII subphase distribution
Comparison of Experiments 3 and 4
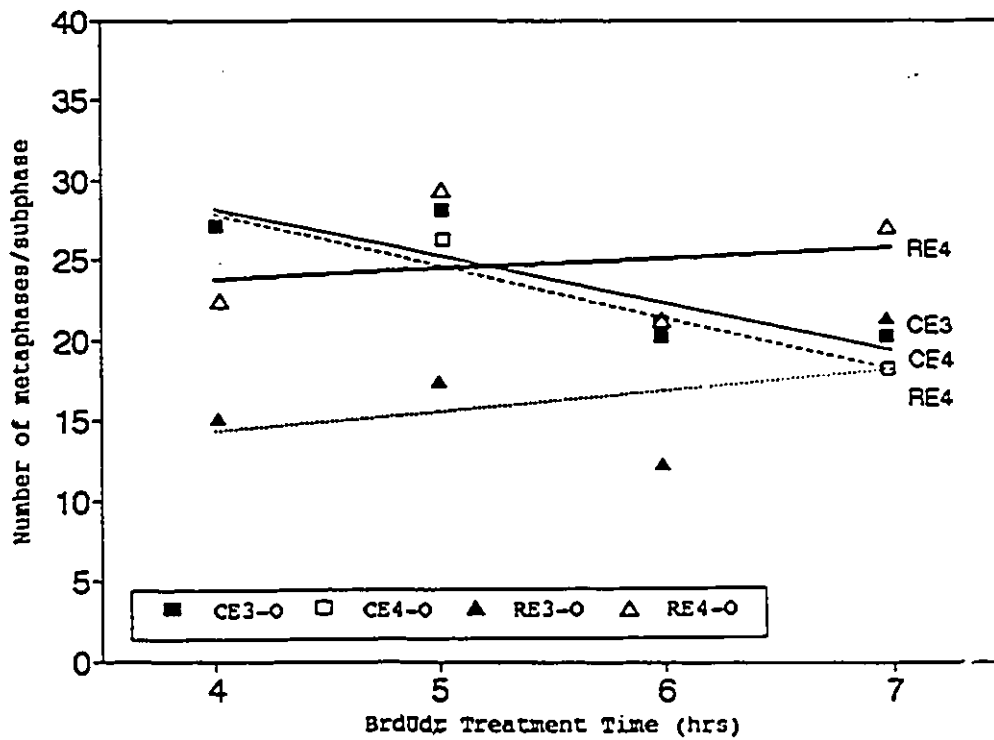
Figure 22. Comparison of the number of metaphases classified as SkIV from RS+ (R) and control (C) lymphoblastoid cell lines. The data were obtained from a Generalized Linear Model using a probit transformation. Modelled data are indicated by lines and observed values are indicated by symbols. A. RS+, LB1; C, JaKr. Experiment 1 (E1); Experiment 2 (E2). B. RS+, R20; C, DM. Experiment 3 (E3); Experiment 4 (E4). A straight line was not obtained with the data modelled from the control cell line, DM, in Experiment 3.

A

SkIV subphase distribution
Comparison of Experiments 1 and 2
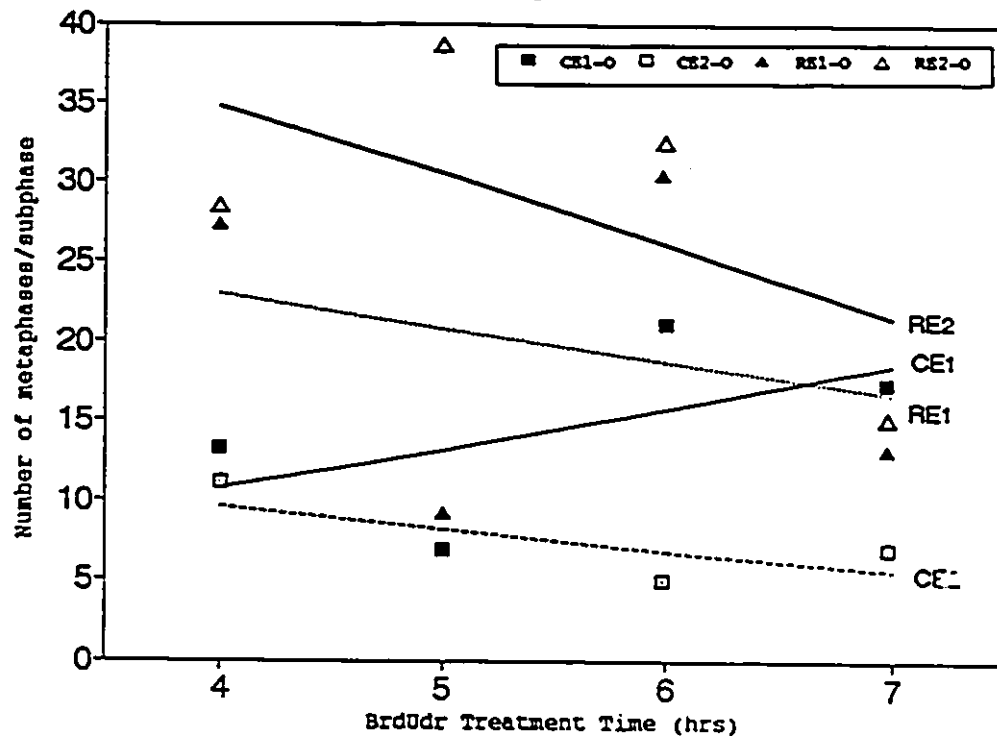
B

SkIV subphase distribution
Comparison of Experiments 3 and 4
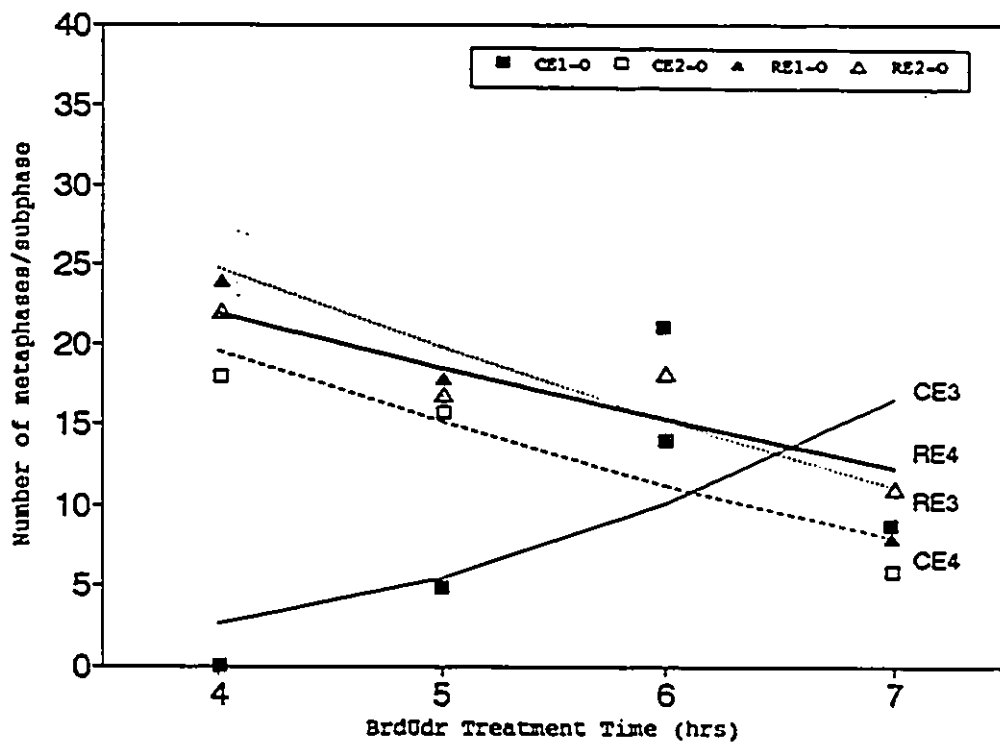
probit transformed linear predictor model, $y=t+r+rt$, plotted against the four BrdUrd treatment times, comparing each cell line and experiment.

The observed frequency of cells classified within the subphases SkII, SkIII or SkIV proved to be somewhat variable between cell lines and experiments. The predicted linear equations obtained for each subphase for control (JaKr and DM) and RS+ (LB1 and R20) cell lines were compared between experiments for differences in their slopes. For both cell lines, significant differences in slopes were observed when the predicted subphase frequencies between experiments and between cell lines were compared (Table 15).

The observed subphase distribution of the RS+ lymphoblastoid cell lines was less variable within a cell line than between cell lines. The SkIII subphase frequency distribution of LB1 was found to be significantly different between experiments (Table 16). However, significant differences in the subphase frequency with respect to BrdUrd treatment times were observed between the RS+ cells compared in Experiment 2 and 4. For this reason, the subphase frequency distribution of RS+ and control cell lines were analysed and compared for each experiment.

The comparison of the female RS+ cell line, LB1, with the control, JaKr, revealed certain differences during the early subphases that were observed in both Experiments 1 and

2 (Figure 20A). The frequency of cells in SkII was observed to be higher in controls and the frequency of cells in SkIV was higher in RS+ cell lines. A temporal response to BrdUrd treatment was also observed. With the early subphase, a similar increase in the frequency of SkII cells was observed with increasing BrdUrd treatment time for both cell lines. Differences in this subphase distribution, determined by a comparison of the slopes of the lines, were not statistically significant (Table 17).

A comparison of the subphase distribution of the male RS+ cell line, R20, with the control, DM, also revealed significant differences between the early and late subphases, although the response was more variable than for the female cell lines (early subphase shown in Figure 20B). Significant differences in the SkII subphase distribution were observed between R20 and DM for Experiment 3 (p<0.05) but not for Experiment 4 (p>0.05) (Table 18). With R20, an increase in the frequency of SkII cells was observed with increasing BrdUrd treatment time for both experiments. However, the response of DM was variable between experiments for this subphase, as a lower frequency of SkII cells was observed with the shorter BrdUrd treatment time for Experiment 4. The subphase distribution observed for Experiment 4 was similar for both cell lines with the frequency of SkII cells increasing with longer BrdUrd treatment times.

A comparison of the predicted frequency of SkIII cells observed with increasing BrdUrd treatment time for LB1 (RS+) and JaKr (C) resulted in significant differences between slopes for both experiments. With the control cell line, the frequency of SkIII cells decreased with BrdUrd treatment time (Experiment 1) or remained relatively constant (Experiment 2, Figure 21). This would be expected as the shorter BrdUrd treatment time would result in the labelling of cells in the last half of S phase, namely SkIII and SkIV cells. With longer BrdUrd treatment times, more cells would be detected in early S phase resulting in a shift in the number of cells classified within later subphases to earlier subphases. With LB1, an increase in the frequency of SkIII cells was observed with each BrdUrd treatment time. This increase was more pronounced for Experiment 2 than for 1. This would suggest that there was a difference in the duration of S phase in general or that SkIII is longer in LB1 cells than in controls but the difference was not significant.

Similar SkIII subphase distributions were observed between experiments for both R20 and DM (Figure 21B). The frequency of SkIII cells observed for DM decreased with increasing BrdUrd treatment time. This response can be expected if one considers that more cells in the latter half of S phase (SkIII or SkIV) would be labelled with shorter BrdUrd treatment times. With longer BrdUrd treatment time,

more cells would be classified in the early half of S phase. The RS+ cell line, on the other hand, consistently demonstrated a slight but not statistically significant increase in the frequency of SkIII observed with increasing BrdUrd treatment time for each experiment.

The SkIV subphase distribution was statistically different for LB1 and JaKr with Experiment 1. An increase in the frequency of SkIV cells was observed with increasing BrdUrd treatment time for the control while a slight decrease in frequency was observed for LB1 (Figure 22A). This would be expected if the duration of S phase were longer in RS+ cells than in controls. However, the difference was not statistically significant in Experiment 2 (Table 17).

A comparison of the SkIV frequency distribution of R20 and DM cells did not result in consistent differences between experiments. The response of DM was slightly more variable between experiments as an increase in the frequency of SkIV cells with increasing BrdUrd treatment time was observed in Experiment 3. This distribution was found to be significantly different from R20 as the slope and intercept of both cell lines were significantly different. With Experiment 4, a decrease in the frequency of SkIV cells was observed for DM. This distribution was not significantly different from that of R20. A decrease in the frequency of SkIV cells with increasing BrdUrd treatment time was observed

with R20 for both Experiment 3 and 4 (Figure 22B). This frequency distribution was consistent for both experiments.

Because the response was variable between experiments, it was difficult to draw any firm conclusions from the results presented so far. For this reason, the estimated slopes of the RS+ and control cell line were compared for each subphase using a Student's t-test, with replicate experiments used as repeated measures. It was predicted that if the subphase distributions of RS+ and control cells were significantly different, this would be represented by significant differences in slopes. There were no significant differences in the estimated slopes of LB1 and JaKr (Experiments 1 and 2) or R20 and DM (Experiments 3 and 4) for any of the subphases ($\alpha=0.05$) (Table A-29, Appendix 2).

3.2.3. CHARACTERIZATION OF CONSTITUTIVE HETEROCHROMATIN REPLICATION IN ROBERTS SYNDROME

The replication programme of the constitutive heterochromatin regions was characterized by analysing the proportion of cells within each subphase, defined in the previous four experiments, that incorporated BrdUrd within the constitutive heterochromatin regions of chromosomes 1, 9, 16 and Y (referred to as 1qh, 9qh, 16qh and Yqh). Figures 23 and 24 are examples of partial metaphases that were classified as SkIV using the subclassification system of Key 4. Those constitutive heterochromatin regions of chromosomes

Figure 23. BrdUrd labelling pattern of the constitutive heterochromatin regions of chromosomes 1, 9, 16 and Yqh obtained from two cells classified as having replicated in SkIV of S phase. The chromosomes were harvested from the male control lymphoblast cell line, DM, and the male RS+ cell line, R20. Those regions of the chromosome that have incorporated BrdUrd are represented by pale staining regions indicated by (◄). The puffing of the constitutive heterochromatin regions of the RS+ chromosomes is quite prominent.

Control   RS+

1qh

9qh

16qh

Yqh
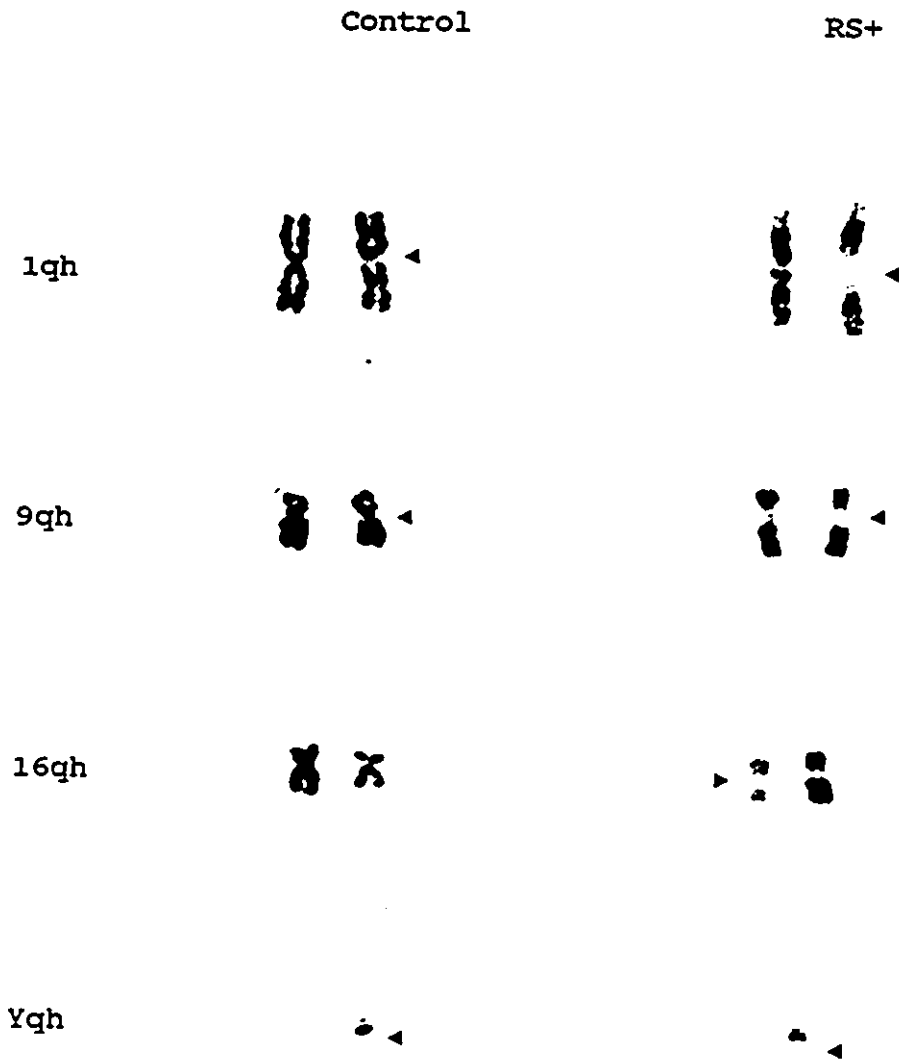
Figure 24.   BrdUrd labelling pattern of the constitutive heterochromatin regions of chromosomes 1, 9 and 16 obtained from two cells classified as having replicated in SkIV of S phase.   The late replicating X chrcmosome is an example of facultative heterochromatin.   The chromosomes were harvested from the female control lymphoblast cell line, JaKr, and the female RS+ cell line, LB1.   Those regions of the chromosome that have incorporated BrdUrd are represented by, pale staining regions indicated by (◄).   There is some puffing of the   constitutive   heterochromatin   regions   of   the   RS+ chromosomes and LB1 has additional X chromosomes.

Control   RS+

1qh

9qh

16qh

X
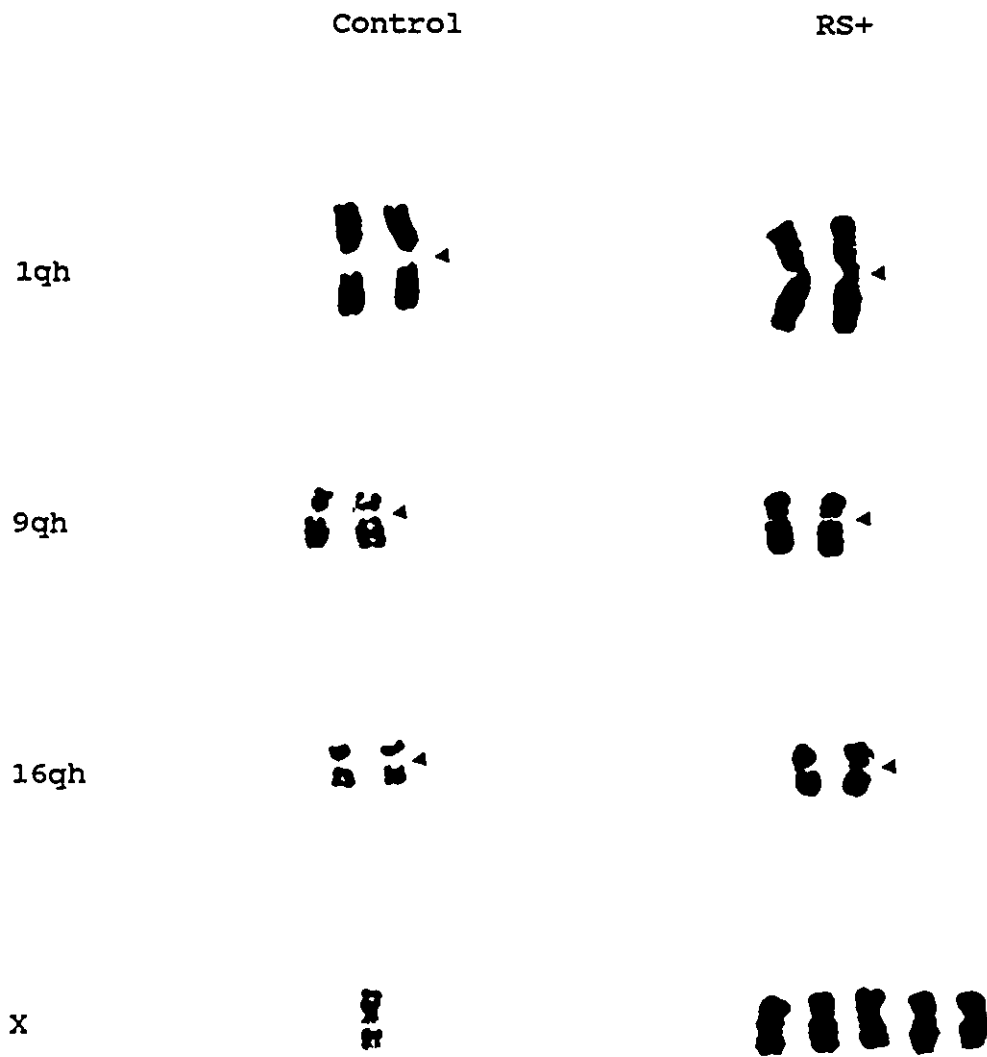
1, 9, 16 and in the males, Y, having incorporated BrdUrd during replication late in S phase (SkIV) are shown to be pale staining.

The chromosome replication pattern of the X chromosome was also assessed in female RS+ and control lymphoblastoid cell lines. The late replicating X chromosome was identified by its light and dark banding pattern. The early replicating X chromosome could not be identified in SkIV metaphases as it is solid stained and could not be distinguished from other C group chromosomes. The data obtained for the four constitutive heterochromatin regions and the X chromosome are summarized in Tables 19-26. Comparison of the replication pattern of the constitutive heterochromatin regions and facultative heterochromatin of RS+ and control chromosomes was made.

3.2.3.1. STATISTICAL ANALYSIS OF CONSTITUTIVE AND FACULTATIVE HETEROCHROMATIN REPLICATION USING GENERALIZED LINEAR MODELLING

The data presented in Tables 19-26 were analysed using GLIM and probit transformation using GLIM 3.77 (Royal Statistical Society, 1985). The methodology used to define the appropriate model to fit the observed results was similar to that described for the S subphase distributions except that the linear predictor formula was defined to be y=r+t, using the same abbreviations described in the previous

Table 19. Comparison of labelling percentage of specific heterochromatin regions of metaphases chromosomes from a control lymphoblastoid cell line, JaKr, subjected to various BrdUrd treatment times and classified into four substages of S phase (Experiment 1).

S Subphase	BrdUrd Treatment	N	Percentage of chromosome regions that have replicated during S phase substages			
			1q1-2	9q1-2	16q1	X (n-1)
SkII	4	16	100	94	88	13
	5	24	96	92	88	58
	6	21	100	81	90	43
	7	25	100	80	60	84
	m	86	98.8	86.3	80.3	53.5
	(s)		(1.8)	(6.3)	(13.1)	(24.9)
SkIII	4	20	100	90	80	13
	5	18	83	94	67	9
	6	8	100	75	75	8
	7	6	100	67	50	13
	m	52	98.8	86.3	80.3	10.8
	(s)		(1.8)	(6.3)	(13.1)	(2.2)
SkIV	4	13	82	73	45	15
	5	7	100	71	57	14
	6	21	86	48	52	38
	7	17	71	53	35	47
	m	58	82.4	57.8	46.1	32.5
	(s)		(9.0)	(10.8)	(8.0)	(13.6)

N-number of cells classified in each S subphase
n-number of pale staining X chromosomes
m-weighted mean percentage of replicated chromosome regions
s - standard deviation of weighted mean

Table 20. Comparison of labelling percentage of specific heterochromatin regions of metaphases chromosomes from a control lymphoblastoid cell line, JaKr, subjected to various BrdUrd treatment times and classified into four substages of S phase (Experiment 2).

S Subphase	BrdUrd Treatment	N	Percentage of chromosome regions that have replicated during S phase substages			
			1q1-2	9q1-2	16q1	X (n-1)
SkII	4	8	100	100	100	13
	5	9	100	100	100	22
	6	12	100	100	100	75
	7	13	100	100	100	69
	m	42	100	100	100	64.4
	(s)		(0)	(0)	(0)	(19.3)
SkIII	4	31	94	97	94	0
	5	34	94	94	94	75
	6	33	100	100	91	48
	7	30	97	97	73	67
	m	128	97.0	97.0	89.0	51.4
	(s)		(2.6)	(2.2)	(8.0)	(15.0)
SkIV	4	11	82	100	64	0
	5	7	86	100	57	0
	6	5	100	100	80	0
	7	7	100	100	71	20
	m	30	91.0	100	67.4	5.0
	(s)		(8.5)	(0)	(8.1)	(10.0)

N-number of cells classified in each S subphase.
n-number of pale staining X chromosomes.
m-weighted mean percentage of replicated chromosome regions.
s - standard deviation of weighted mean.

Table 21. Comparison of labelling percentage of specific heterochromatin regions of metaphases chromosomes from an RS+ lymphoblastoid cell line, LB1, subjected to various BrdUrd treatment times and classified into four substages of S phase (Experiment 1).

S Subphase	BrdUrd Treatment	N	Percentage of chromosome regions that have replicated during S phase substages			
			1q1-2	9q1-2	16q1	X^*
SkII	4	8	75	88	75	63
	5	8	75	100	63	63
	6	7	86	100	100	86
	7	13	100	77	46	92
	m	36	86.1	89.0	66.7	77.9
	(s)		(11.3)	(10.2)	(20.0)	(13.7)
SkIII	4	15	80	73	53	33
	5	33	85	85	61	45
	6	13	92	77	77	54
	7	24	100	71	71	66
	m	85	89.4	77.7	64.9	50.2
	(s)		(7.5)	(6.1)	(8.0)	(11.7)
SkIV	4	27	44	70	41	0
	5	9	67	67	78	22
	6	30	80	57	73	33
	7	13	92	54	62	38
	m	79	68.2	62.1	60.8	21.3
	(s)		(18.7)	(6.7)	(15.1)	(16.0)

N-number of cells classified in each S subphase
n-number of pale staining X chromosomes
m-weighted mean percentage of replicated chromosome regions
s - standard deviation of weighted mean
* number of X chromosomes n-1-6

Table 22. Comparison of labelling percentage of specific heterochromatin regions of metaphases chromosomes from an RS+ lymphoblastoid cell line. LB1, subjected to various BrdUrd treatment times and classified into four substages of S phase (Experiment 2).

S Subphase	BrdUrd Treatment	N	Percentage of chromosome regions that have replicated during S phase substages			
			1q1–2	9q1–2	16q1	X*
SkII	4	12	92	100	92	42
	5	4	75	100	100	50
	6	2	50	100	100	50
	7	10	100	100	100	33
	m	28	91.3	100	96.6	41.6
	(s)		(11.7)	(0)	(4.2)	(6.5)
SkIII	4	10	80	100	90	0
	5	8	100	100	100	13
	6	16	94	100	100	47
	7	25	84	100	100	44
	m	59	88.7	100	98.4	28.3
	(s)		(7.0)	(0)	(3.7)	(21.8)
SkIV	4	28	61	93	64	11
	5	38	66	95	87	16
	6	32	66	94	91	25
	7	15	93	100	100	60
	m	113	69.8	95.0	86.0	33.4
	(s)		(11.2)	(2.2)	(11.5)	(20.2)

N–number of cells classified in each S subphase.
n–number of pale staining X chromosomes.
m–weighted mean percentage of replicated chromosome regions.
s – standard deviation of weighted mean.
* number of X chromosomes n–1–6

Table 23. Comparison of labelling percentage of specific heterochromatin regions of metaphases chromosomes from a control lymphoblastoid cell line, DM, subjected to various BrdUrd treatment times and classified into four substages of S phase (Experiment 3).

Subphase	BrdUrd Treatment	N	Percentage of chromosomes regions that have replicated during S phase substages			
			1q1–2	9q1–2	16q1	Y
SkII	4	23	87	74	52	91
	5	17	100	71	47	100
	6	9	100	78	44	100
	7	21	95	86	29	95
	m	70	94.9	77.4	43.0	96.1
	(s)		(5.5)	(5.7)	(9.0)	(3.8)
SkIII	4	27	96	93	52	89
	5	28	89	82	46	86
	6	20	85	55	60	100
	7	20	100	70	35	100
	m	95	91.2	73.1	50.4	94.0
	(s)		(5.8)	(15.1)	(8.9)	(6.4)
SkIV	4	0	—	—	—	—
	5	5	80	0	25	80
	6	21	86	52	14	86
	7	9	100	44	44	89
	m	35	87.7	39.1	19.8	85.9
	(s)		(5.7)	(11.2)	(11.1)	(2.2)

N—number of cells classified in each S subphase
n—number of pale staining X chromosomes
m—weighted mean percentage of replicated chromosome regions
s — standard deviation of weighted mean

Table 24. Comparison of labelling percentage of specific heterochromatin regions of metaphases chromosomes from a control lymphoblastoid cell line, DM, subjected to various BrdUrd treatment times and classified into four substages of S phase (Experiment 4).

| Subphase | BrdUrd Treatment | N | Percentage of chromosome regions that have replicated during S phase substages | | | |
			1q1–2	9q1–2	16q1	Y
SkII	4	5	100	100	100	100
	5	8	100	100	88	100
	6	15	100	100	100	93
	7	26	96	96	100	100
	m	54	98.0	98.0	98.3	98.2
	(s)		(2.0)	(2.0)	(4.3)	(3.1)
SkIII	4	27	89	96	78	74
	5	26	92	100	77	100
	6	21	95	100	81	95
	7	18	100	100	83	100
	m	92	93.5	99.0	79.5	92.6
	(s)		(4.0)	(1.8)	(2.4)	(10.7)
SkIV	4	18	94	100	65	72
	5	16	94	88	31	100
	6	14	79	71	43	93
	7	6	100	67	83	100
	m	54	91.2	87.1	51.2	90.5
	(s).		(7.2)	(12.6)	(18.4)	(11.8)

N=number of cells classified in each S subphase.
n=number of pale staining X chromosomes.
m=weighted mean percentage of replicated chromosome regions.
s = standard deviation of weighted mean.

Table 25. Comparison of labelling percentage of specific heterochromatin regions of metaphases chromosomes from an RS+ lymphoblastoid cell line, R20, subjected to various BrdUrd treatment times and classified into four substages of S phase (Experiment 3).

| Subphase | BrdUrd Treatment | N | Percentage of chromosome regions that have replicated during S phase substages | | | |
			1q1-2	9q1-2	16q1	Y
SkII	4	11	100	91	55	82
	5	15	93	93	73	93
	6	17	94	100	88	88
	7	21	100	100	81	86
	m	64	96.8	96.8	76.5	87.5
	(s)		(3.3)	(3.9)	(11.2)	(3.6)
SkIII	4	15	73	100	80	73
	5	17	82	88	65	76
	6	12	92	75	100	92
	7	21	100	86	90	94[a]
	m	65	87.6	87.7	83.0	84.1[b]
	(s)		(10.6)	(8.2)	(12.6)	(9.5)
SkIV	4	24	75	96	58	58
	5	18	56	76	67	67
	6	21	86	76	90	80[c]
	7	8	88	100	100	88
	m	71	74.9	85.3	74.5	70.2[d]
	(s)		(12.2)	(11.5)	(15.9)	(10.9)

N-number of cells classified in each S subphase.
n-number of pale staining X chromosomes.
m-weighted mean percentage of replicated chromosome regions.
s-standard deviation of weighted mean.
a: N-18; b: N-62; c: N-20; d:n-70.

Table 26. Comparison of labelling percentage of specific heterochromatin regions of metaphases chromosomes from an RS+ lymphoblastoid cell line, R20, subjected to various BrdUrd treatment times and classified into four substages of S phase (Experiment 4).

Subphase	BrdUrd Treatment	N	Percentage of chromosomes regions that have replicated during S phase substages			
			1q1–2	9q1–2	16q1	Y
SkII	4	6	83	100	100	100
	5	4	100	100	75	100
	6	11	100	91	100	100
	7	12	100	100	92	100
	m	33	97.0	97.0	95.0	100.0
	(s)		(6.3)	(4.2)	(7.6)	(0.0)
SkIII	4	22	95	91	77	91
	5	29	97	97	66	100
	6	21	100	100	95	100
	7	27	100	96	85	100
	m	99	98.0	96.0	81.0	98.0
	(s)		(2.1)	(3.0)	(10.6)	(3.7)
SkIV	4	22	91	95	91	73
	5	17	88	87	93	93
	6	18	94	78	89	89
	7	11	100	91	91	100
	m	68	93.0	88.0	91.0	88.0
	(s).		(4.0)	(6.7)	(1.4)	(10.0)

N=number of cells classified in each S subphase.
n=number of pale staining X chromosomes.
m=weighted mean percentage of replicated chromosome regions.
s = standard deviation of weighted mean.

section. The predicted equations for each constitutive heterochromatin region are summarized in Tables A30-33 (Appendix 2). The predicted values were calculated from the linear predictor equation, y=r+t. With this statistical approach, differences in constitutive heterochromatin replication were determined for subphases SkII, III and IV by estimating the slopes of the line obtained by plotting the predicted values (defined as the ratio of y=predicted value/n) against BrdUrd treatment time. GLIM analysis of the frequency of metaphases with labelled constitutive heterochromatin with various BrdUrd treatment times allowed one to determine if differences existed between RS+ and control lymphoblastoid cell lines by comparing the slope of the predicted linear equation.

With this analysis, very few differences were detected between RS+ and controls. The results also suggested that there was little effect of the duration of BrdUrd treatment time as the slopes were often approaching zero. One could predict that once a cell has been classified at a certain substage of S phase, there would be very little effect of BrdUrd treatment time on the frequency of constitutive heterochromatin labelling as the cells were selected on the basis of when in S phase the BrdUrd was incorporated. Because there was no significant effect of BrdUrd treatment time, the cells in each subphase were pooled over all BrdUrd

treatment times for an analysis of variance of the frequency of labelling of different chromosomes among subphases and cell type (see Section 3.2.3.2).

An example of the 1qh replication patterns observed for the RS+ (LB1) and control (JaKr) lymphoblastoid cell lines in SkII, SkIII and SkIV is shown in Figure 25. For each subphase, the frequency of the predicted values tended to increase slightly with increasing BrdUrd treatment time for both RS+ and control cell lines. However the slopes of the lines were not significantly different ($\alpha=0.05$, Table A-27, Appendix 1). Small differences in frequencies of the predicted values between subphases SkII and SkIII were observed. The fourth subphase, SkIV, showed the lowest frequency of metaphases with BrdUrd-labelled 1qh regions and the greatest difference between LB1 and JaKr. Figure 26 shows the results of GLIM for the 1qh labelling of SkIV only from two replicate experiments, Experiments 1 and 2 with LB1 and JaKr. The 1qh replication frequencies for both the control cell line, DM, and the RS+ cell line, R20, for all subphases, including SkIV were similar (data not shown).

Similar results were obtained for the other constitutive heterochromatin regions of chromosomes 9, 16 and Y and all cell lines studied. The labelling frequencies of all constitutive heterochromatin regions were lower in SkIV than in SkII or SkIII, for all cell lines. This could be

Figure 25. Comparison of 1qh labelling frequencies of control, JaKr, (A) and RS+, LB1, (B) lymphoblastoid cell lines for all substages of S phase obtained from Experiment 1. The proportions (F) were derived by dividing the predicted value by the number of observations from the Generalized Linear Model with a probit transformation. Observed proportions (O) indicated by symbols. A straight line was not obtained with the SkIII data modelled from the RS+ cell line, LB1.

Experiment 1: JaKr (C)
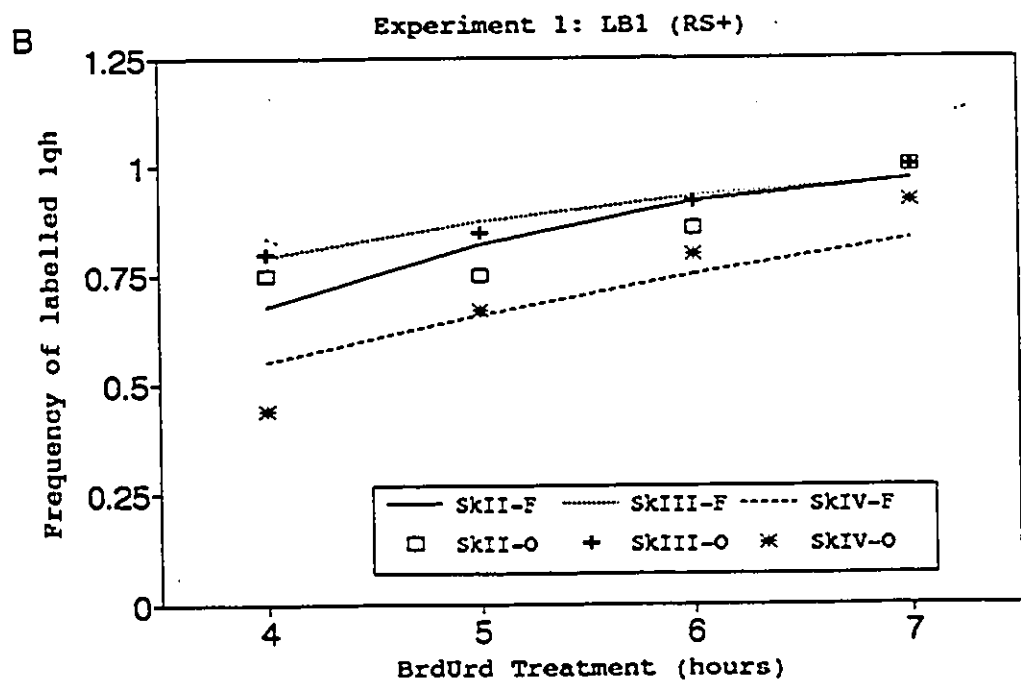
Experiment 1: LB1 (RS+)

Figure 26. Comparison of modelled 1qh labelling frequencies
(F) of RS+ (LB1) and control (JaKr) lymphoblastoid cell lines
during SkIV obtained from Experiment 1 (A) and Experiment 2
(B). Observed proportions (O) indicated by symbols.

A

Experiment 1: JaKr (C) and LB1 (RS+)
Subphase SkIV

B

Experiment 2: JaKr (C) and LB1 (RS+)
Subphase SkIV
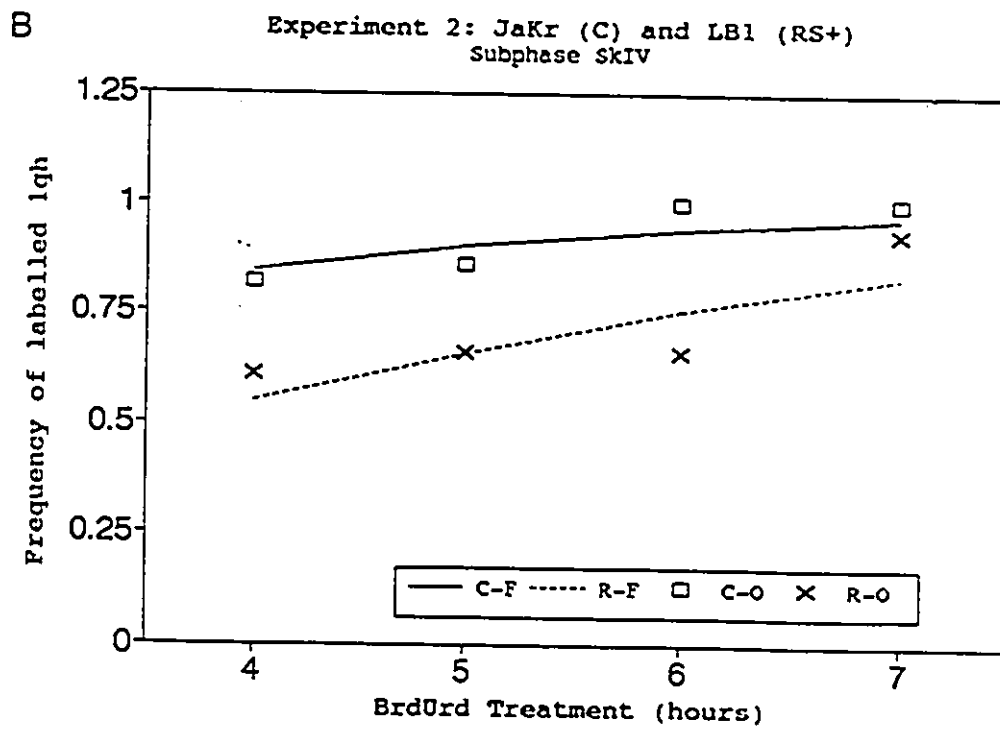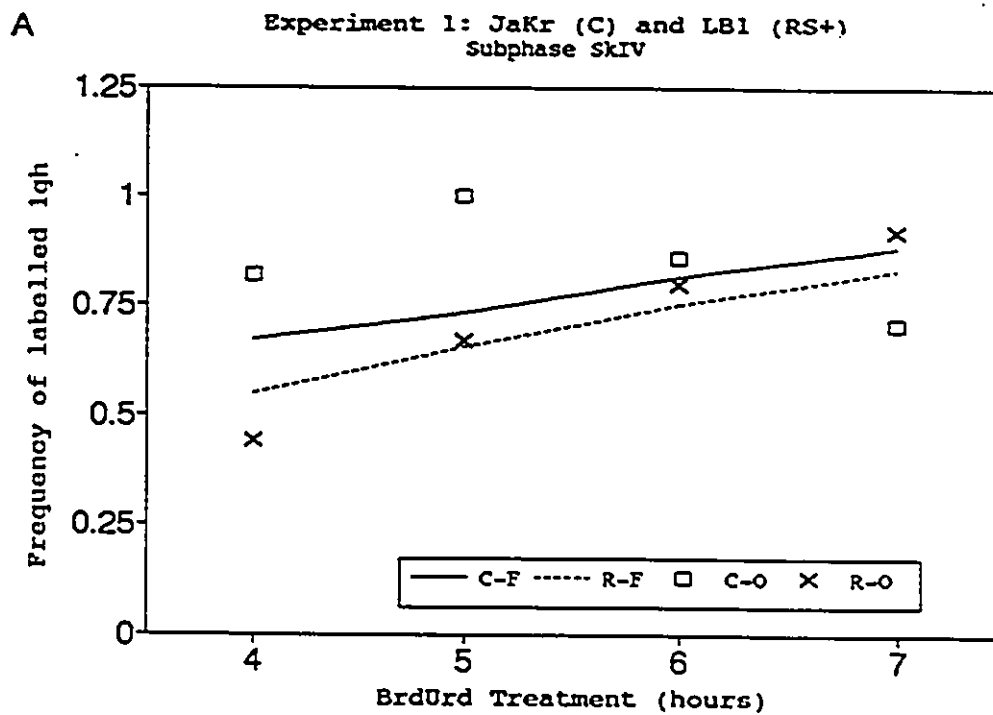
expected as constitutive heterochromatin replicates late in S phase and would most likely replicate sometime during SkIV. Thus, as the cell progresses through S phase, less replication would take place in SkIV than in the earlier subphases. As expected, no significant differences were observed in the slopes of the lines of RS+ and control cell lines for all constitutive heterochromatin regions (Tables A30-33, Appendix 2).

However differences were observed in the labelling frequency among the constitutive heterochromatin regions and cell lines. The labelling frequency of 9qh was similar for all subphases, including SkIV and less difference was observed between RS+ and control cell lines (Figures 27 and 28). The 9qh labelling frequency was also more variable between control cell lines and RS+ cell lines as well as between experiments. The labelling frequencies of 16qh differed slightly from 1qh as they were observed to be slightly higher in SkII and SkIII cells for both RS+ and control cell lines (Figure 29). In SkIV cells, the 16qh labelling frequency was observed to be higher in RS+ cell lines, suggesting that there may be a delay in 16qh replication in RS+ cell lines (Figure 30). The labelling pattern of Yqh was similar to 1qh except that lower frequencies observed for SkIV cells was less marked (Figures 31 and 32). For this reason the constitutive heterochromatin

Figure 27.   Comparison of 9qh labelling frequencies of control, JaKr, (A) and RS+, LB1, (B) lymphoblastoid cell lines for all substages of S phase obtained from Experiment 1.   The proportions (F) were derived by dividing the predicted value by the number of observations from the Generalized Linear Model with a probit transformation.

A

Experiment 1: JaKr (C)

B

Experiment 1: LB1 (RS+)
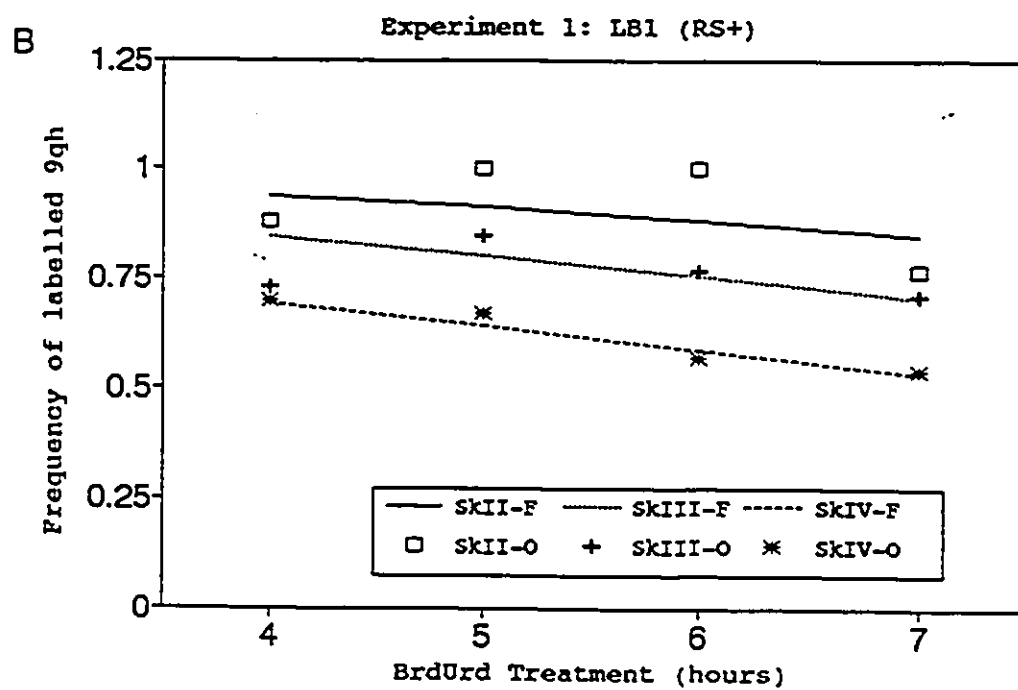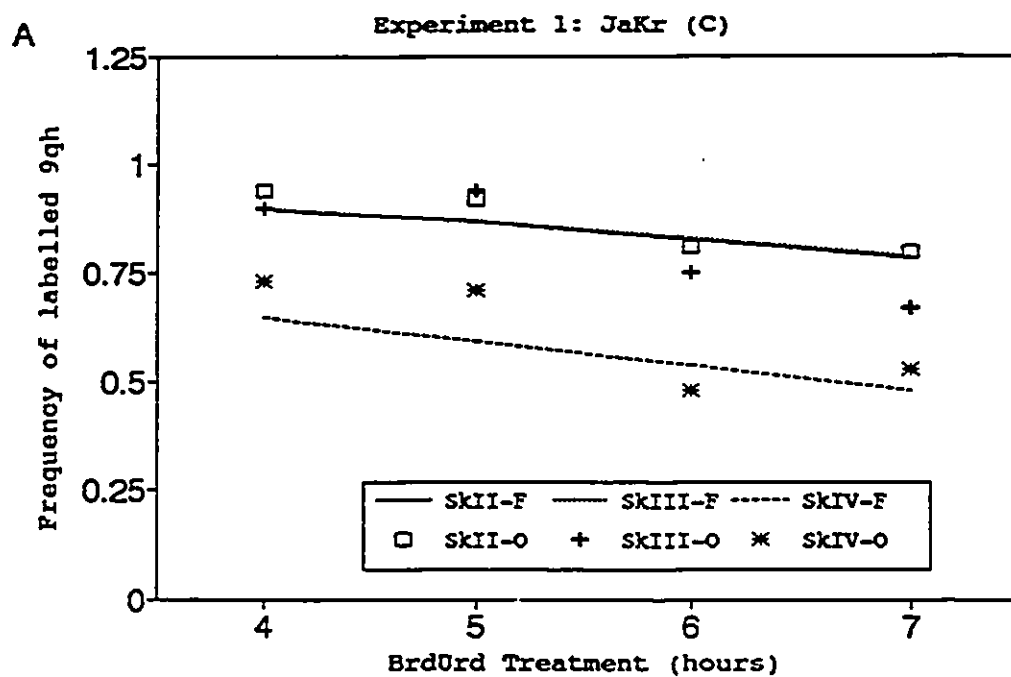
Figure 28.   Comparison of 9qh labelling frequencies of control, DM, (A) and RS+, R20, (B) lymphoblastoid cell lines for all substages of S phase obtained from Experiment 4. The proportions (F) were derived by dividing the predicted value by the number of observations from the Generalized Linear Model with a probit transformation. Observed proportions (O) indicated by symbols.

A

Experiment 4: DM (C)

1.25

Frequency of labelled 9qh

1

0.75

0.5

0.25

0

	SkII-F	SkIII-F	SkIV-F
□ SkII-O	+ SkIII-O	✳ SkIV-O	

4   5   6   7

BrdUrd Treatment (hours)

B

Experiment 4: R20 (RS+)

1.25

Frequency of labelled 9qh

1

0.75

0.5

0.25

0

	SkII-F	SkIII-F	SkIV-F
□ SkII-O	+ SkIII-O	✳ SkIV-O	

4   5   6   7

BrdUrd Treatment (hours)
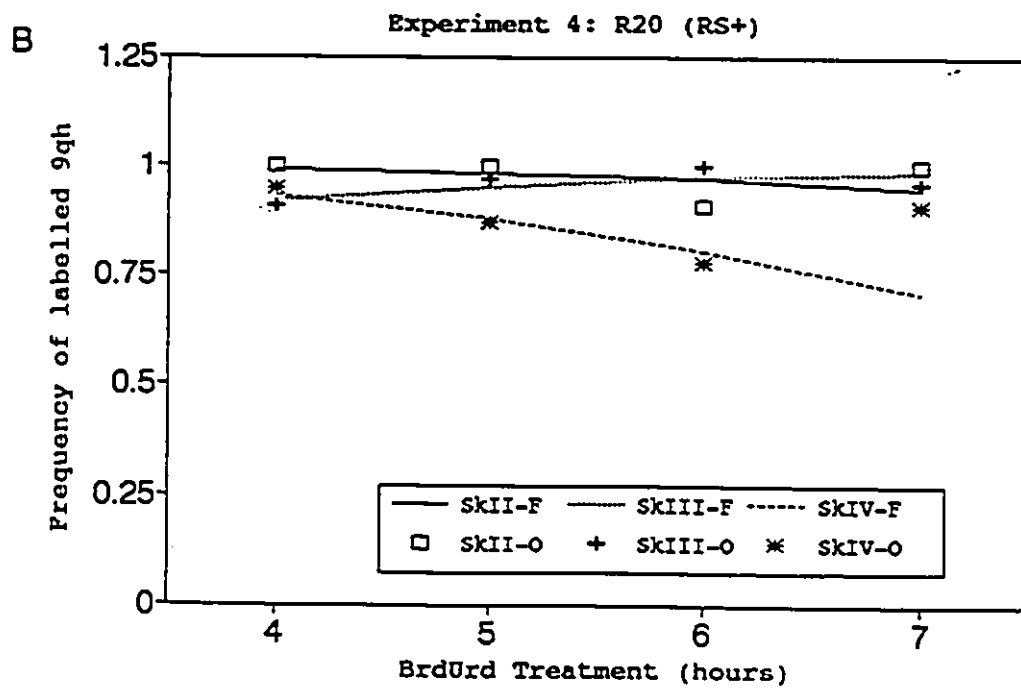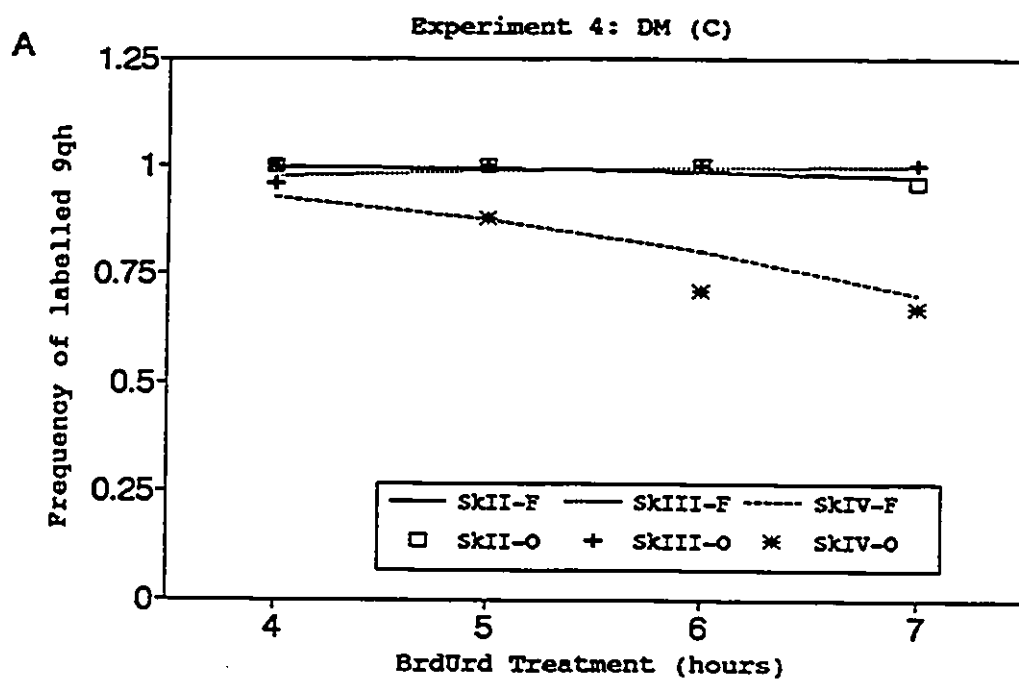
Figure 29.   Comparison of 16qh labelling frequencies of control, JaKr, (A) and RS+, LB1, (B) lymphoblastoid cell lines for all substages of S phase obtained from Experiment 2.   The proportions (F) were derived by dividing the predicted value by the number of observations from the Generalized Linear Model with o probit transformation. Observed proportions (O) indicated by symbols.   A straight line was not obtained with the SkIII data modelled from the RS+ cell line, LB1.

A

Experiment 2: JaKr (C)

B
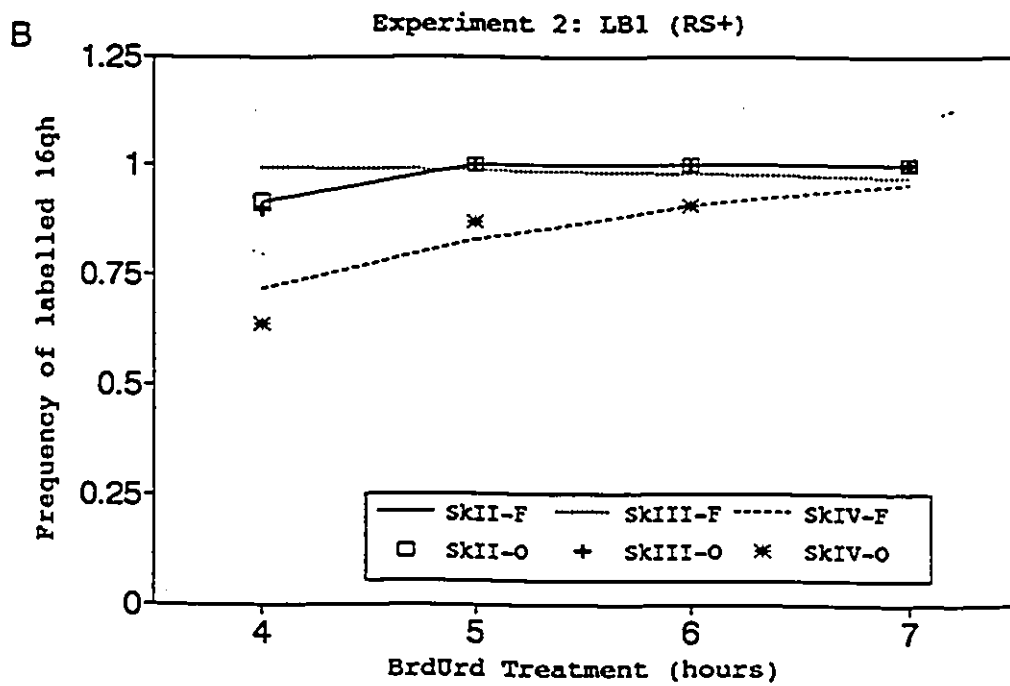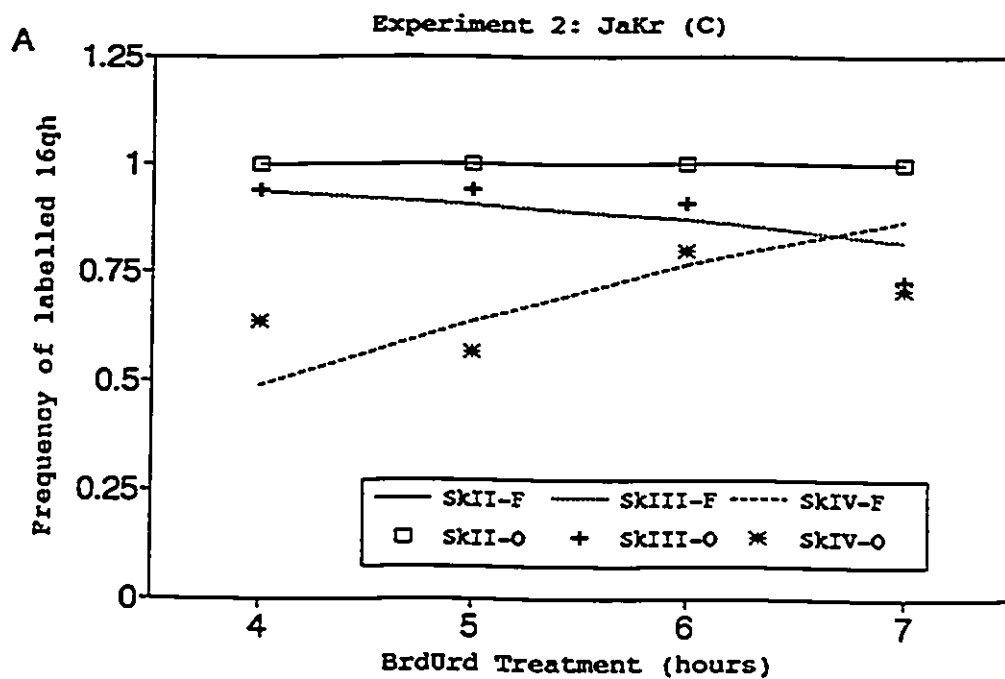
Experiment 2: LB1 (RS+)

Figure 30. Comparison of modelled 16qh labelling frequencies
(F) of RS+ (LB1) and control (JaKr) lymphoblastoid cell lines
during SkIV obtained from Experiment 1 (A) and Experiment 2
(B). Observed proportions (O) indicated by symbols.

A

Experiment 1: JaKr (C) and LB1 (RS+)
Subphase SkIV

B

Experiment 2: JaKr (C) and LB1 (RS+)
Subphase SkIV
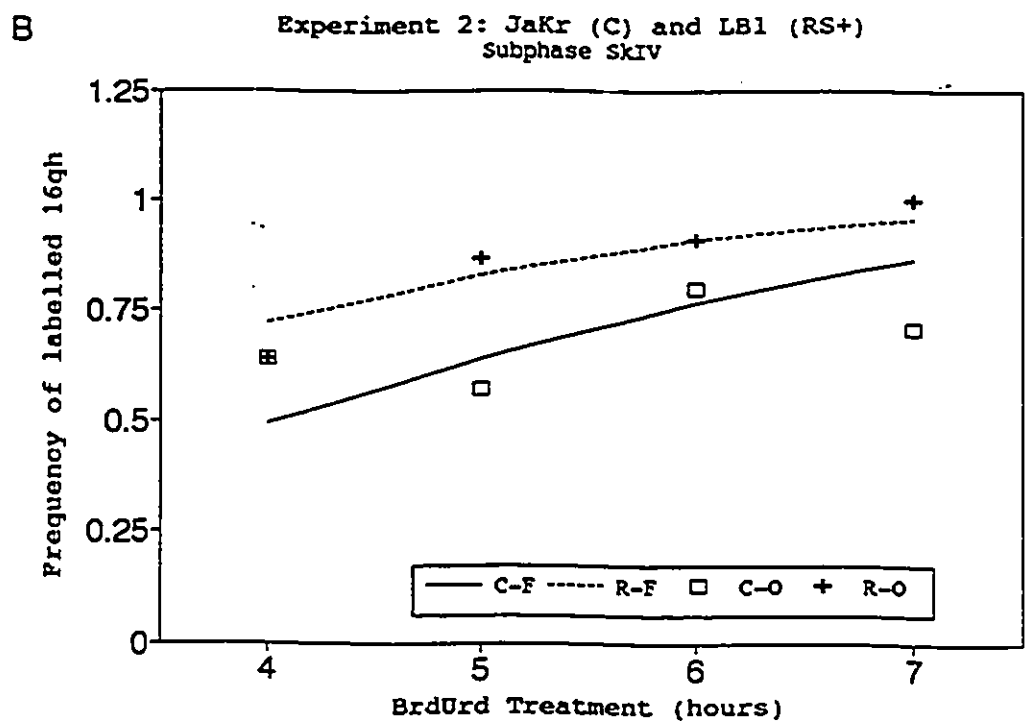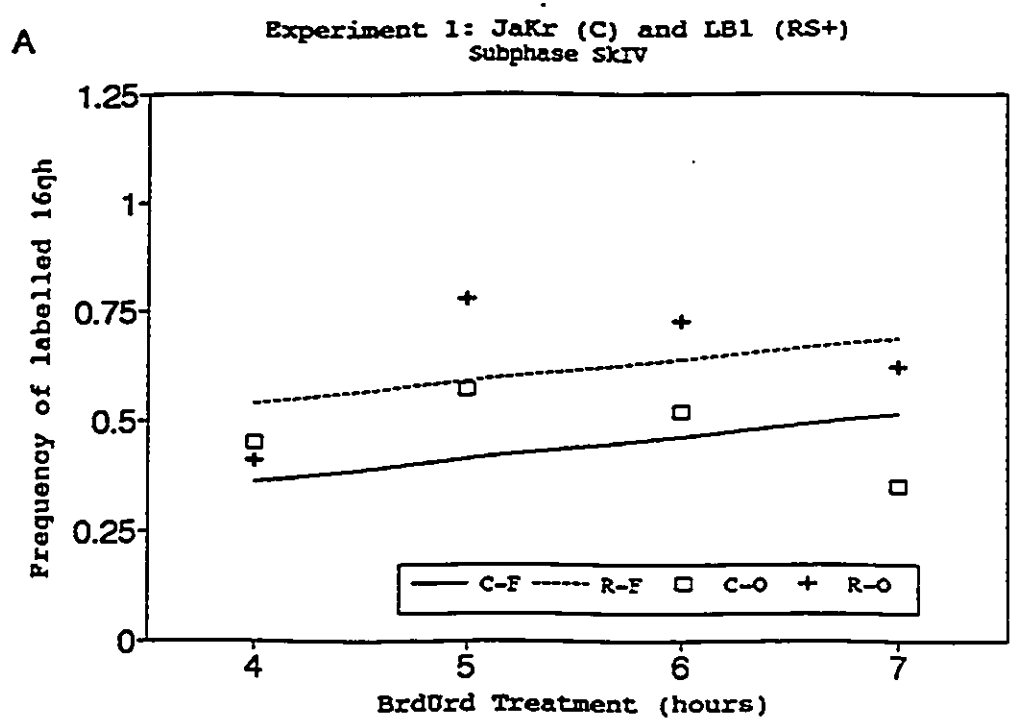
Figure 31.   Comparison of Yqh labelling frequencies of control (DM, A) and RS+ (R20, B) lymphoblastoid cell lines for all substages of S phase obtained from Experiment 4. The proportions (F) were derived by dividing the predicted value by the number of observations from the Generalized Linear Model with a probit transformation. Observed proportions (O) indicated by symbols.

Experiment 4: DM (C)
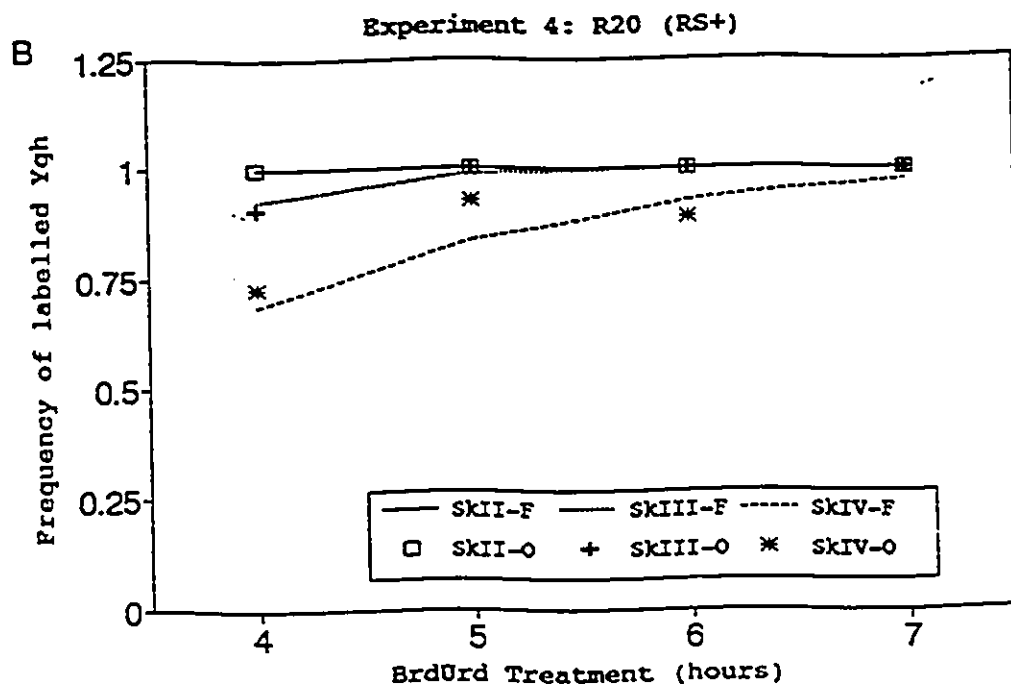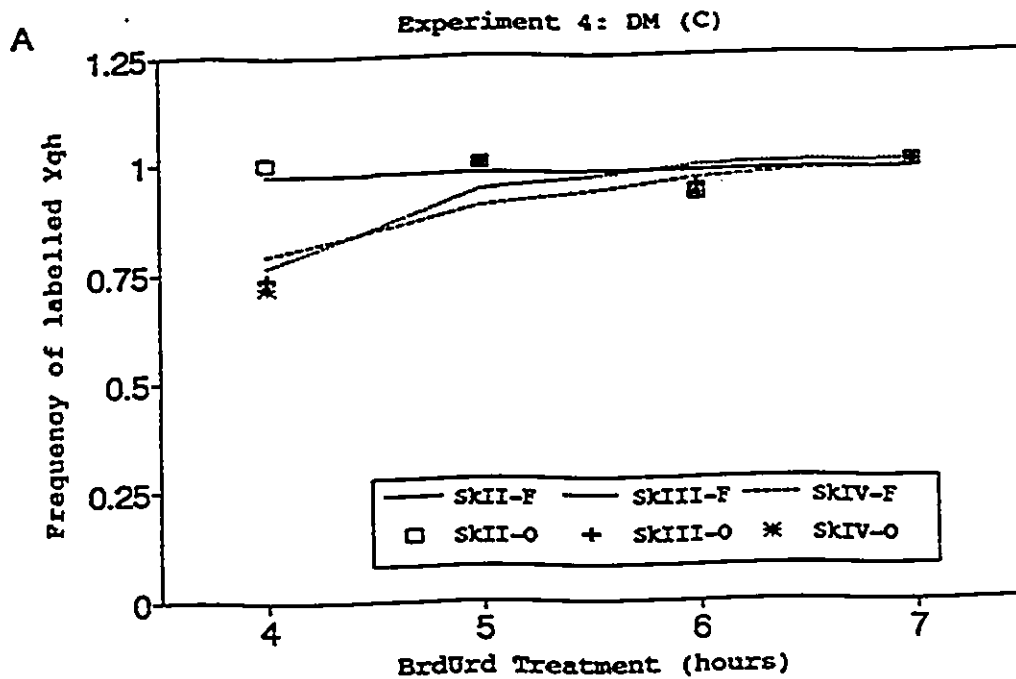
Experiment 4: R20 (RS+)

Figure 32. Comparison of modelled Yqh labelling frequencies (F) of RS+ (R20) and control (DM) lymphoblastoid cell lines during SkIV obtained from Experiment 3 (A) and Experiment 4 (B). Observed proportions (O) indicated by symbols. There were no SkIV cells observed with the 4 hour BrdUrd treatment time for the control cell line, DM.

A

Experiment 3: DM (C) and R20 (RS+)
Subphase SkIV
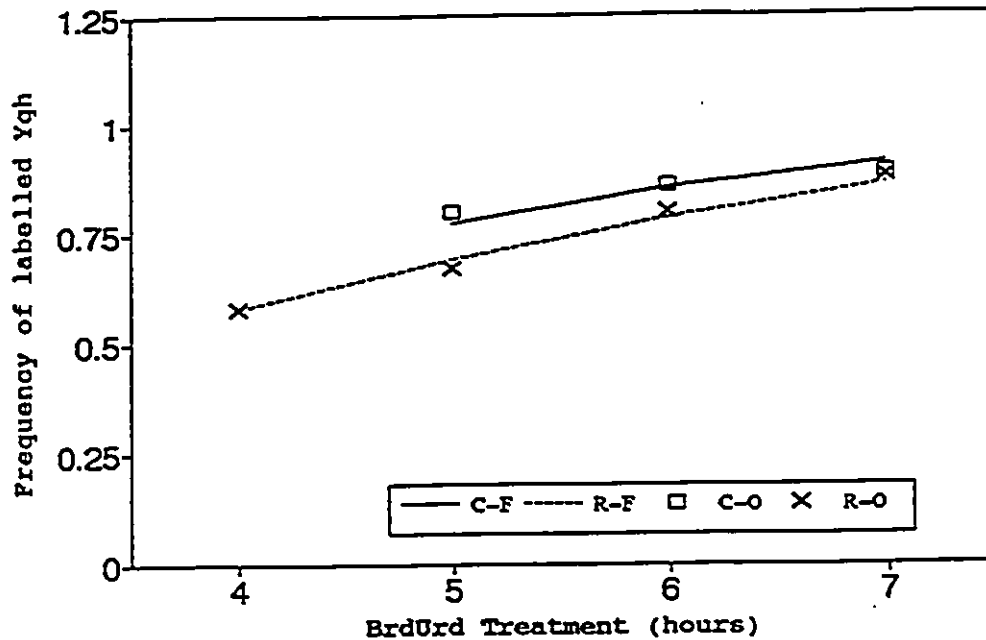
B

Experiment 4: DM (C) and R20 (RS+)
Subphase SkIV
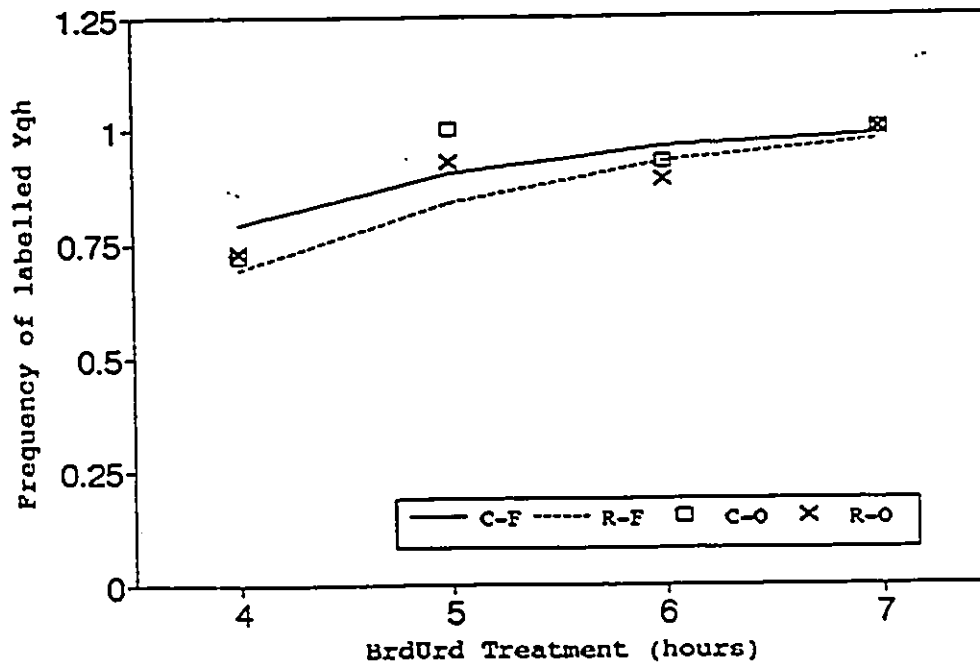
labelling frequency data were subjected to further statistical analysis (see Section 3.2.3.2).

The analysis of X chromosome replication in two female cell lines, JaKr and LB1, provided an example of facultative heterochromatin replication. Based upon the findings reported in the literature, it was assumed that the early replicating X chromosome would replicate during SkII and the late replicating X in late SkIII or in SkIV. It was observed that the frequency of labelled X chromosomes increased with increasing BrdUrd treatment time (Figure 33). However differences were observed in the frequencies observed for each subphase. The frequency of labelling of the late replicating X was generally lower than for constitutive heterochromatin with the highest labelling frequencies observed for SkII, followed by SkIII and SkIV. This suggests that the late replicating X replicates earlier than constitutive heterochromatin.

There was some variability in the frequencies observed for RS+ and control between experiments. For Experiment 1, higher frequencies were observed in SkII and SkIII for the RS+ cell line, LB1, but not in SkIV. This was not the case with Experiment 2, as similar SkII and SkIII frequencies were observed for both LB1 and JaKr. With the latter experiment, higher replication frequencies were observed for LB1 in SkIV (Figure 34) and the slopes of the lines estimated for SkIV

Figure 33. Comparison of X chromosome labelling frequencies of control, JaKr, (A) and RS+, LB1, (B) lymphoblastoid cell lines for all substages of S phase obtained from Experiment 2. The proportions (F) were derived by dividing the predicted value by the number of observations from the Generalized Linear Model with a probit transformation. Observed proportions (O) indicated by symbols.

Experiment 2: JaKr (C)
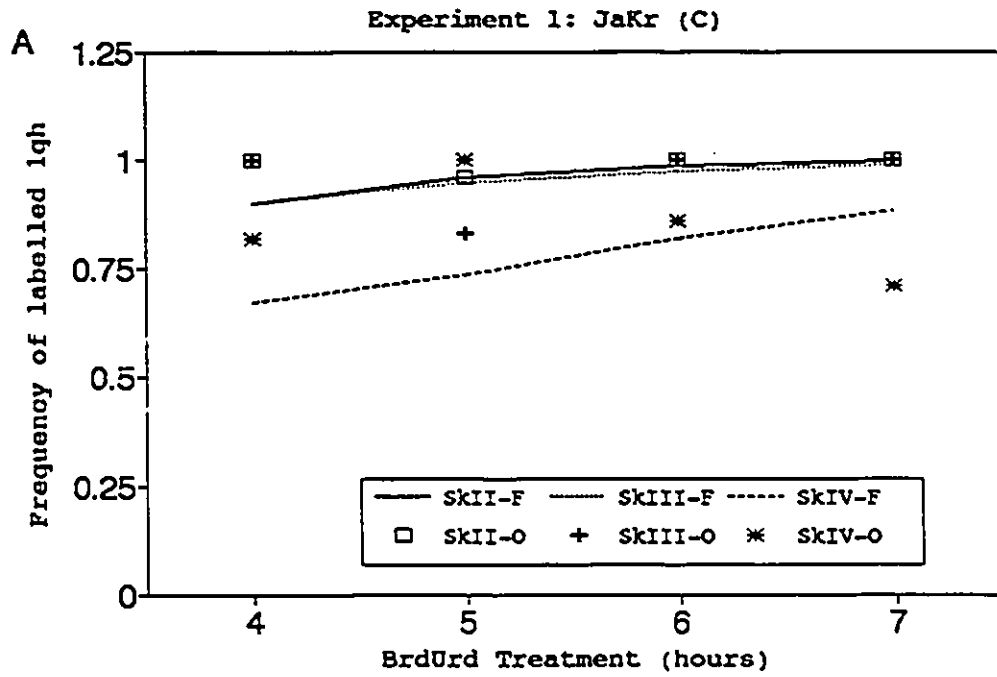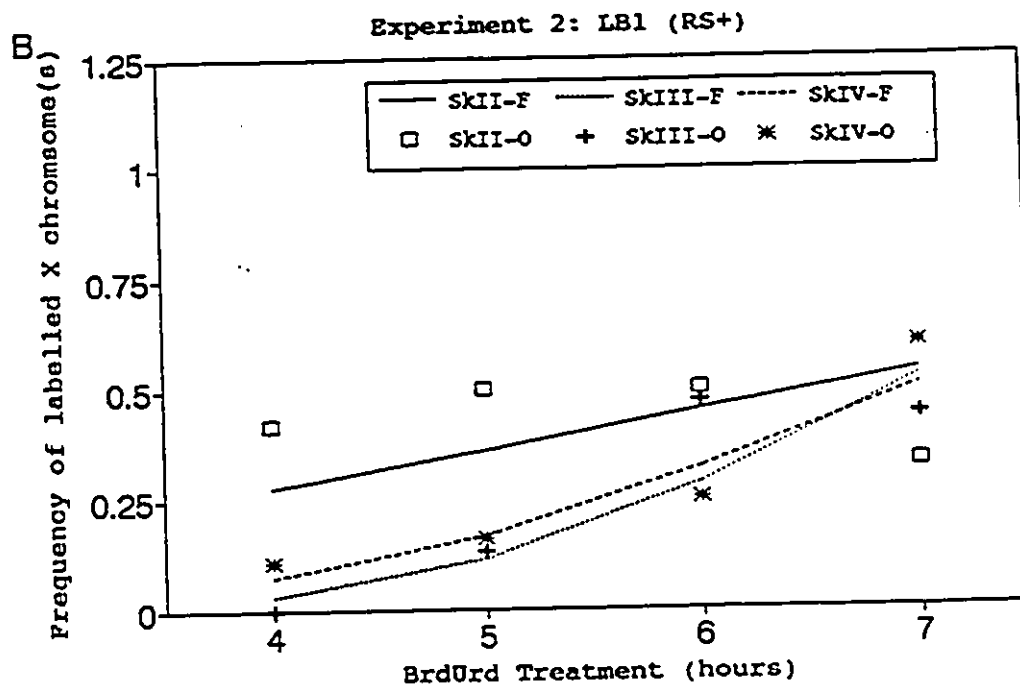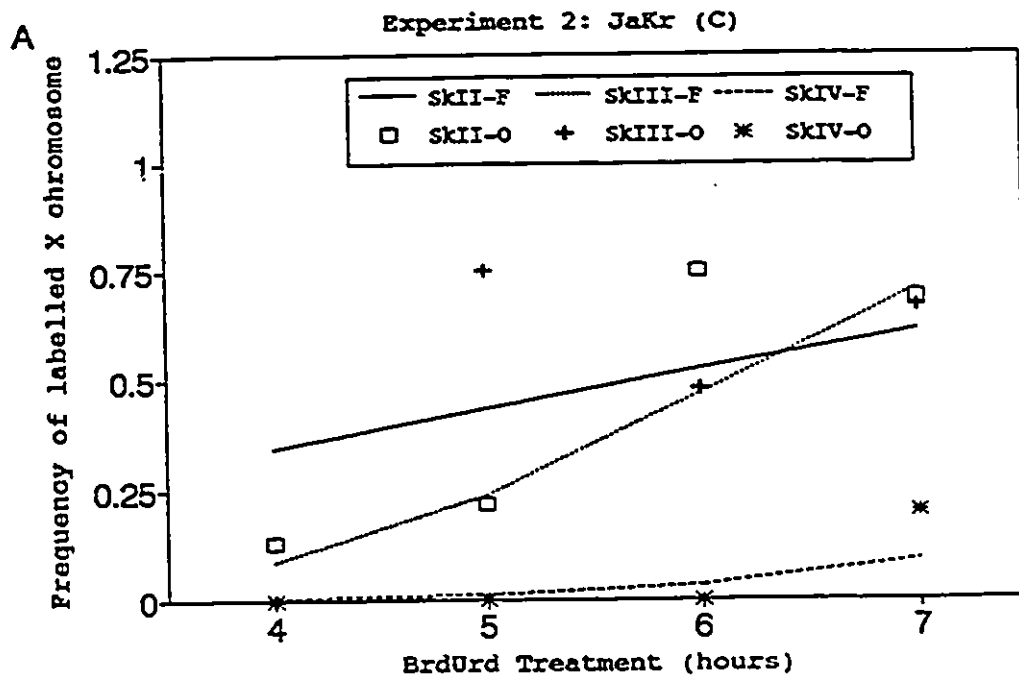
Experiment 2: LB1 (RS+)

Figure 34. Comparison of modelled X chromosome labelling frequencie> (F) of RS+ (LB1) and control (JaKr) lymphoblastoid cell lines during SkIV obtained from Experiment 1 (A) and Experiment 2 (B). Observed proportions (O) indicated by symbols.

A

Experiment 1: JaKr (C) and LB1 (RS+)
Subphase SkIV

B
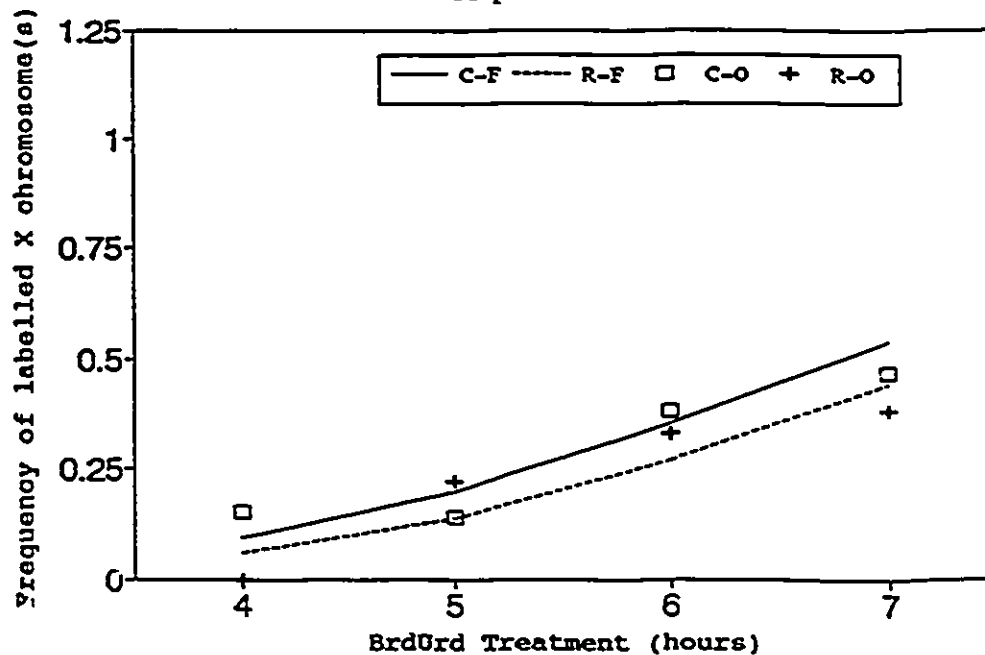
Experiment 2: JaKr (C) and LB1 (RS+)
Subphase SkIV
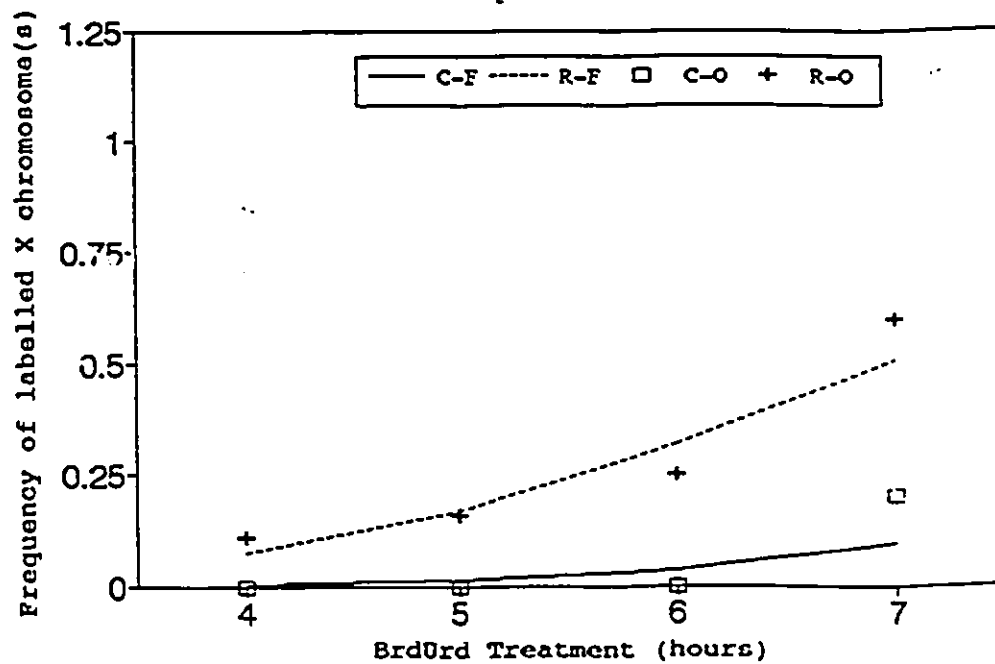
were found to be significantly different in Experiment 2. Altogether this suggests that the rate of X chromosome replication was significantly earlier in the control (Table A-34, Appendix 2). However, these results were not observed for both experiments. The results suggest that facultative heterochromatin replication is not affected in the RS+ cell line.

The temporal replication pattern of the constitutive heterochromatin regions of chromosomes 1, 9, 16, and Y and of facultative heterochromatin were also analysed by comparing the graphs represented by the linear predictor equations obtained for cells in SkIV for each cell line. With reference to the control cell lines, JaKr and DM, a general chronological order of replication was consistently observed between experiments (Figures 35 and 36). The low SkIV replication frequencies of the 16qh indicate that this region may replicate the earliest of all constitutive heterochromatin regions. The higher labelling frequencies of 9qh suggested that this region replicated later than 16qh and in Experiments 1, 3 and 4, appeared to replicate slightly earlier than 1qh and Yqh. The constitutive heterochromatin regions of chromosomes 1 and Y were interpreted as being the last to replicate, as shown by their higher labelling frequencies. The replication pattern of the X chromosomes, representative of facultative heterochromatin, showed the

Figure 35. Chronological order of replication for constitutive heterochromatin regions of chromosomes 1, 9, 16 and facultative heterochromatin, X chromosome, during SkIV for the female control cell line, JaKr. (A) Experiment 1, (B) Experiment 2. Modelled proportions indicated by lines and observed proportions indicated by symbols.

A

Experiment 1: JaKr (C)
Subphase SkIV

B
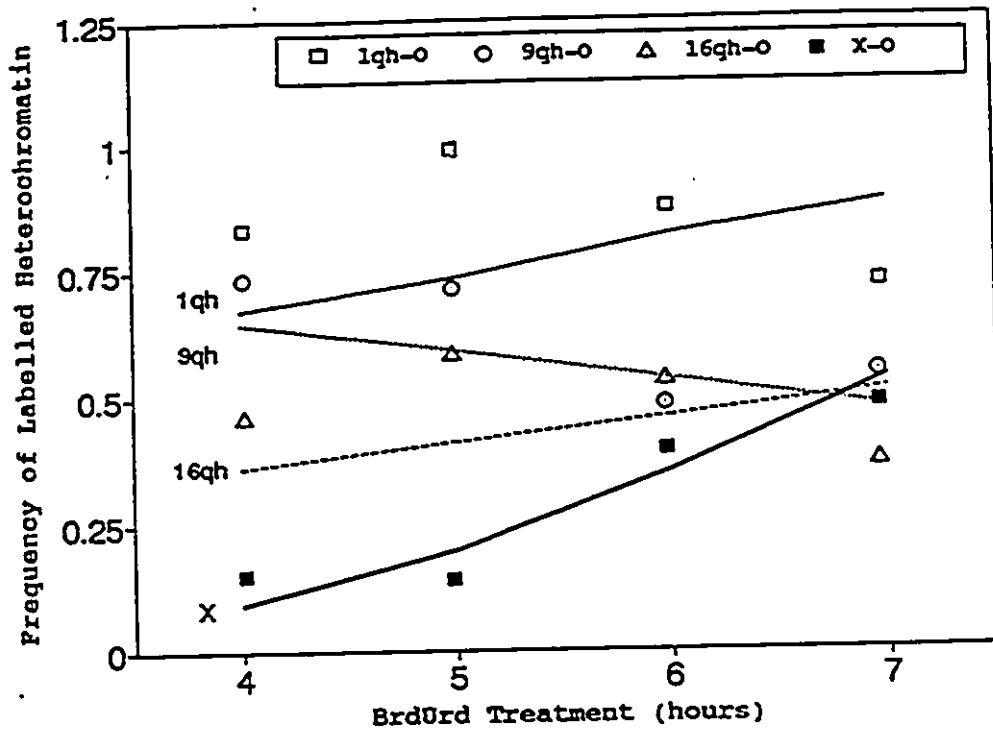
Experiment 2: JaKr (C)
Subphase SkIV
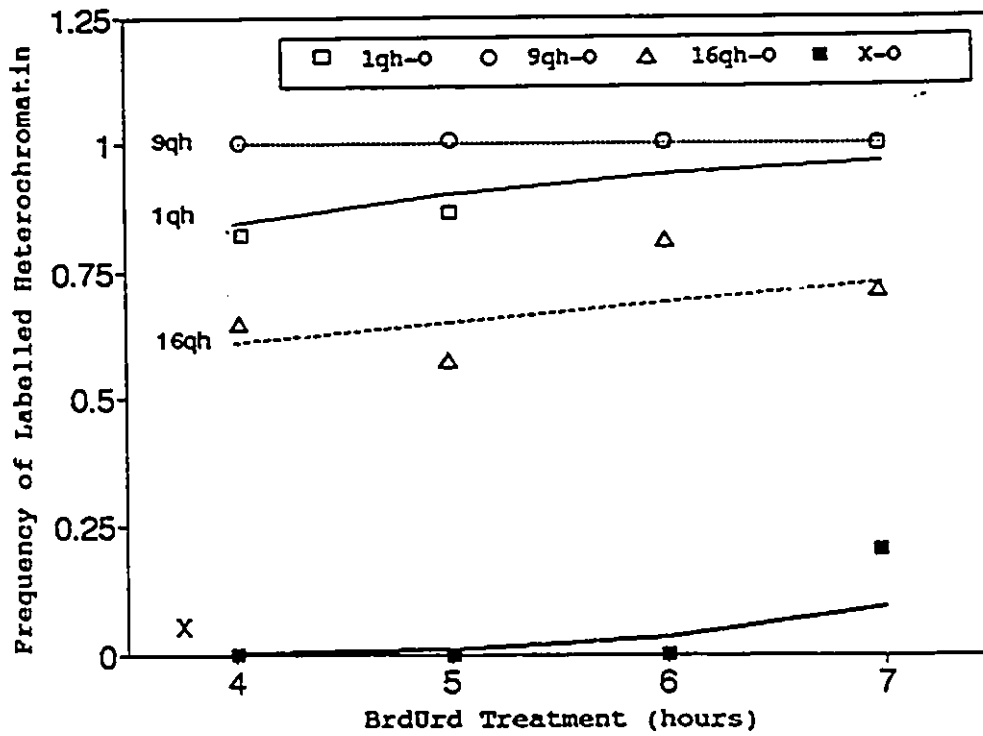
Figure 36. Chronological order of replication for constitutive heterochromatin regions of chromosomes 1, 9, 16 and Y during SkIV for the male control cell line, DM. (A) Experiment 3, no cells in SkIV at 4 hour (B) Experiment 4. Modelled proportions indicated by lines and observed proportions indicated by symbols.

A

Experiment 3: DM (C)
Subphase SkIV

B

Experiment 4: DM (C)
Subphase SkIV
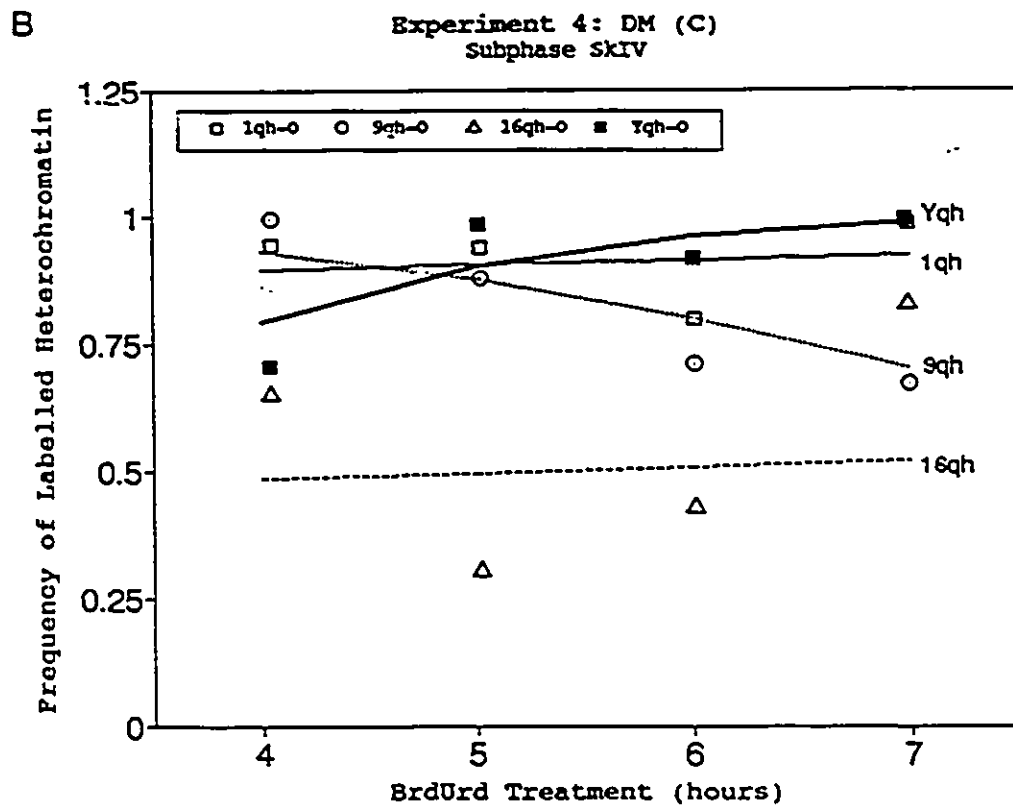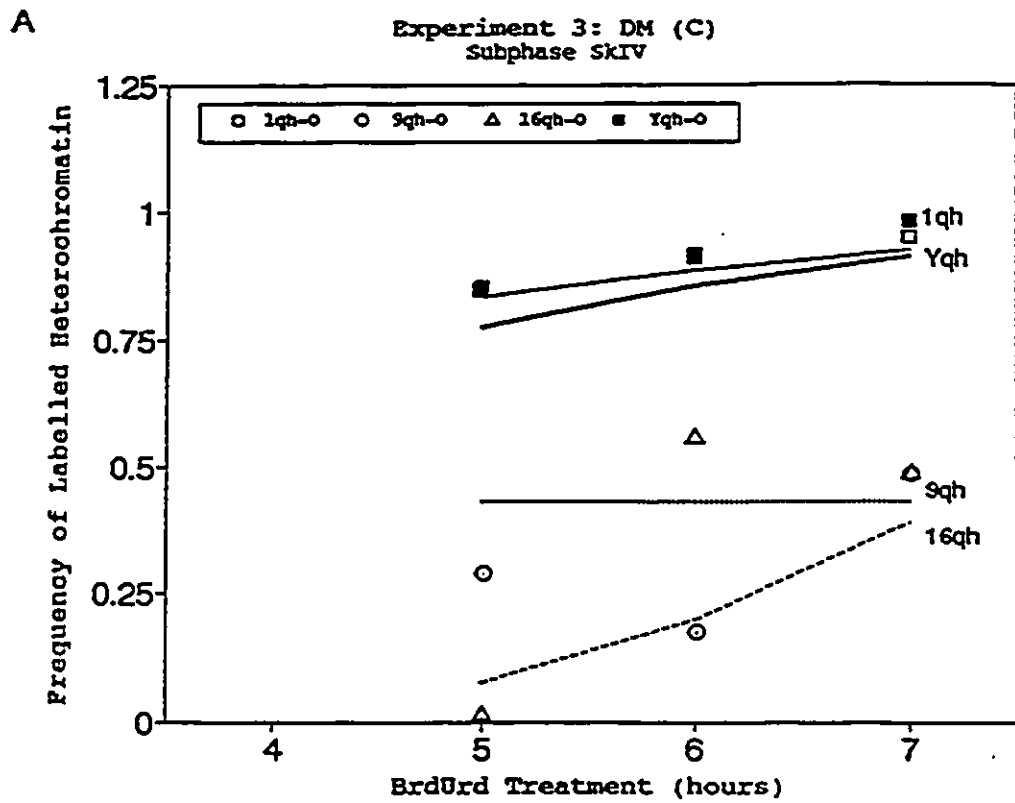
lowest labelling frequencies for SkIV. This would imply that replication of the inactive (late-replicating) X chromosome had been initiated or completed before constitutive heterochromatin replication.

The order of constitutive heterochromatin replication was not as well defined for the RS+ cell lines, LB1 and R20, as shown in Figures 37 and 38. The temporal order was much more variable, as all four constitutive heterochromatin regions appeared to replicate with similar frequencies. Looking specifically at Experiment 1 (Figure 37A), the order of c-heterochromatin replication, from earliest to latest, appeared to be defined as 9qh, 16qh and 1qh, although all three regions were variable between experiments. This order was defined as 1qh, 16qh and 9qh for Experiment 2 (Figure 37B). The results of the male RS+ cell line also revealed a variable order of replication for Experiments 3 and 4 (Figure 38). The chronological order of constitutive heterochromatin replication was defined to be 9qh, 1qh, 16qh and Yqh for Experiment 3 and 9qh, 16qh, 1qh and Yqh for Experiment 4. The results of the all four experiments suggest that the temporal order of replication was not as well defined for the RS+ cell lines and may be due to a delay in constitutive heterochromatin replication when compared with the controls. This was particularly apparent for 16qh, as the replication frequencies suggest this to be one of the earliest

Figure 37.   Chronological   order   of   replication   for
constitutive heterochromatin regions of chromosomes 1, 9, 16
and facultative heterochromatin, X chromosome, during SkIV
for the female RS+ cell line, LB1.   (A) Experiment 1, (B)
Experiment 2.   Modelled proportions indicated by lines and
observed proportions indicated by symbols.

A

Experiment 1: LB1 (RS+)
Subphase SkIV

B

Experiment 2: LB1 (RS+)
Subphase SkIV

238
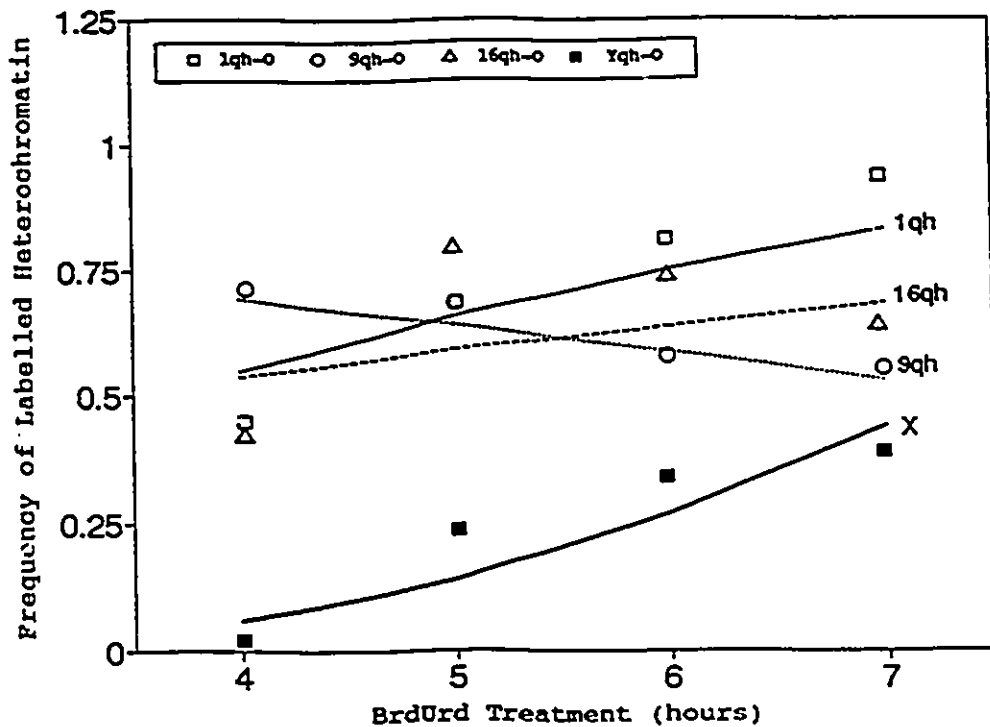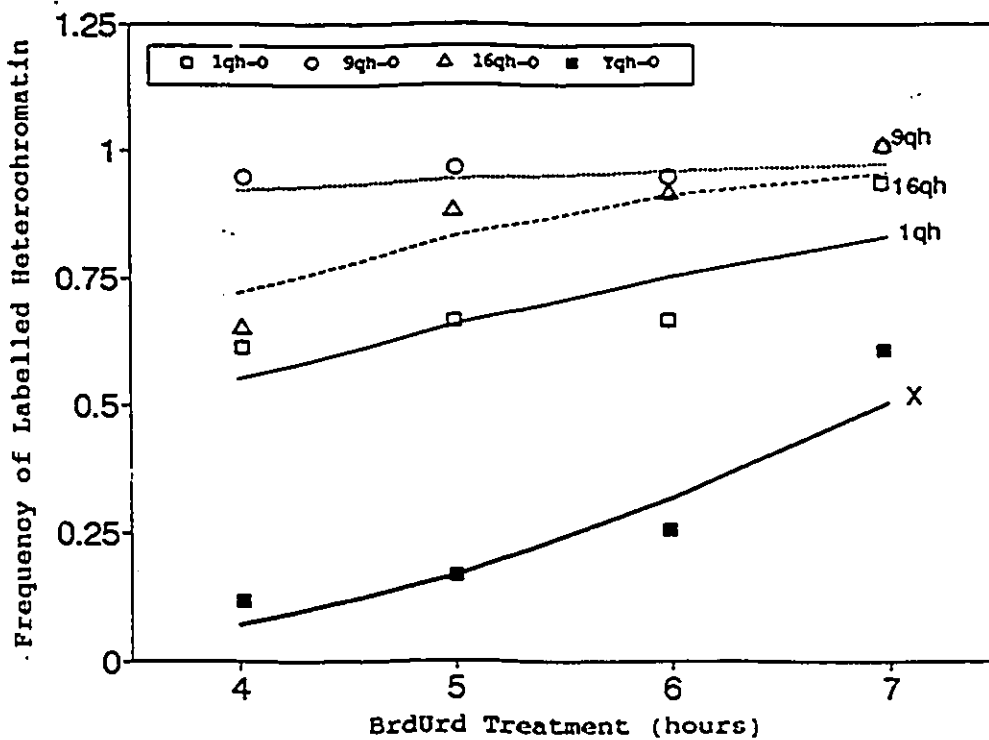
Figure 38. Chronological order of replication for constitutive heterochromatin regions of chromosomes 1, 9, 16 and Y during SkIV for the male RS+ cell line, R20. (A) Experiment 3, (B) Experiment 4. Modelled proportions indicated by lines and observed proportions indicated by symbols.

A

Experiment 3: R20 (RS+)
Subphase SkIV
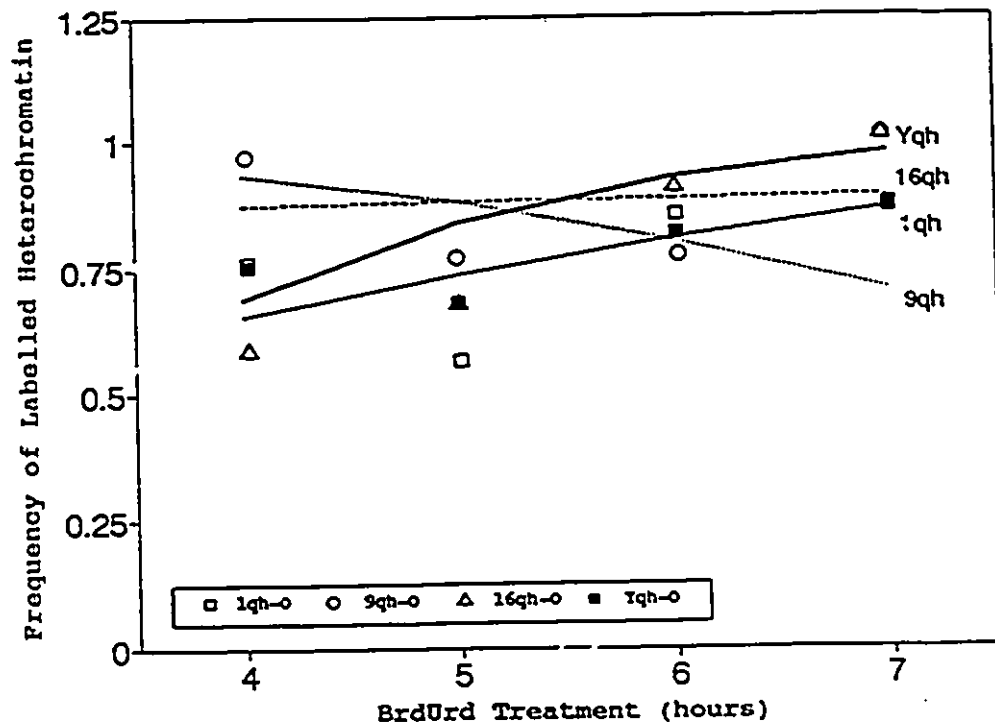
B

Experiment 4: R20 (C)
Subphase SkIV
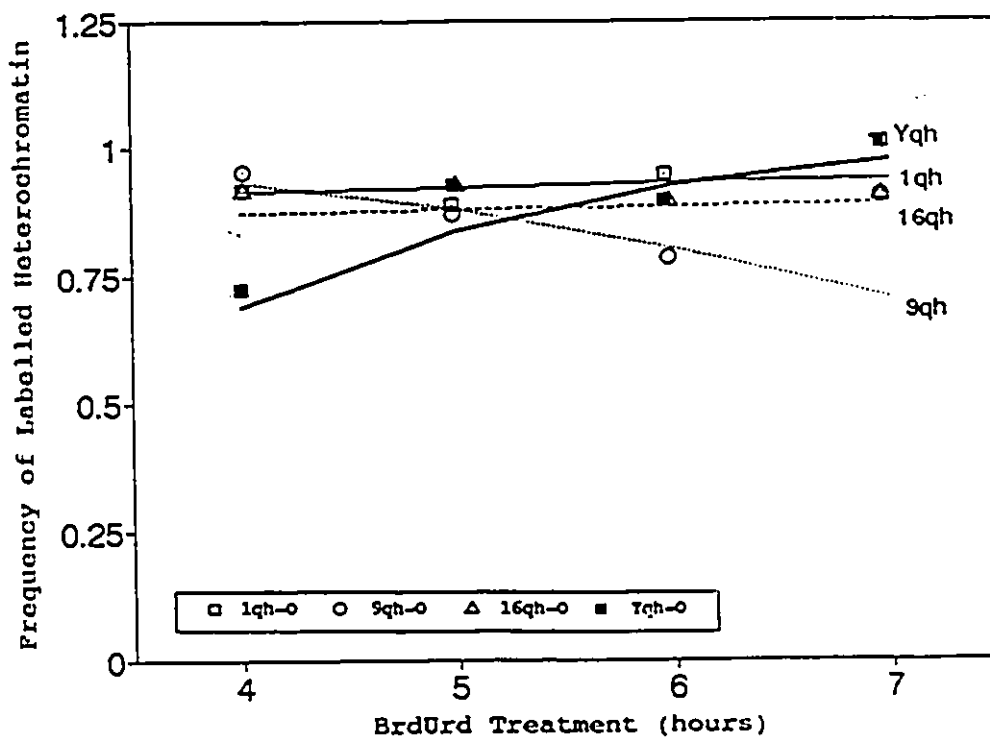
replicating constitutive heterochromatin regions for the control cell lines but not for RS+ cell lines. The chronological order of X chromosome replication during SkIV did not appear to be altered in the female RS+ cell line, suggesting that facultative heterochromatin replication is most likely unaffected.

3.2.3.2. ANALYSIS OF VARIANCE OF CONSTITUTIVE HETEROCHROMATIN REPLICATION FREQUENCIES

Because there appeared to be differences in frequency of labelling for constitutive heterochromatin between RS+ and control lymphoblastoid cell lines additional comparisons were also made using ANOVA. For this statistical analysis, the mean frequency of labelled constitutive heterochromatin was taken over BrdUrd treatment times. The weighted mean number of metaphase cells with labelled constitutive heterochromatin regions observed for each subphase of RS+ and control cell lines were compared (Table A-27-28, Appendix 1). The data obtained from Experiments 1-4 were modelled using factors representing the effect of subphase (s, 3 levels), chromosome (c, 4 levels) and cell type (r, 2 levels) as well as the effect of interaction between subphase and chromosome, and cell type and chromosome. Two models were used for the ANOVA because the order of the factors of each model affected the sum of square associated with each factor. The models were defined as $y=s+c+r+s*c+r*s$ and $y=c+s+r+s*c+r*s+r$. The

ANOVA's were constructed to represent a 2X3X4 design, with the number of levels of each factor previously indicated in parentheses and with replicate data as repeated measures.

The ANOVA for the mean number of metaphase cells with labelled constitutive heterochromatin regions observed for each substage of S phase obtained for the RS+ lymphoblastoid cell line, R20, and the control cell line, DM, is shown in Tables 27 and 28. With the model, $y=c+s+r+s*c+r*s+r*c$, highly significant differences between subphases, constitutive heterochromatin regions and cell type were observed ($p<0.001$). There was no significant effect of interaction between subphase and chromosome ($s*c$) or subphase and cell type ($r*s$). A significant effect of interaction between cell type and chromosome ($r*c$) was observed ($p=0.004$).

The ANOVA for the second model, $y=s+c+r+s*c+r*s+r*c$, shown in Table 28, resulted in a slightly higher sum of squares for the factor 'c' model and a slightly lower sum of squares for the factor 's'. With this model, highly significant differences between subphases, constitutive heterochromatin regions and cell type were also observed ($p<0.001$). The effect of interaction was the same as for the first model described.

The ANOVA for the mean number of metaphase cells with labelled constitutive and facultative heterochromatin

Table 27. ANOVA for model y=c+s+r+s*c+r*s+r*c representing the mean number of metaphase cells with labelled constitutive heterochromatin regions observed for each substage of S phase obtained for the RS+ lymphoblastoid cell line, R20, and the control cell line, DM (Experiments 3 and 4).

Model	df	SS	MS	F	P
Within groups					
chromosome (c)	3	159.00	53.00	53.00	0.004
subphase (s)	2	53.94	26.97	26.97	0.021
C vs. RS+ (r)	1	33.40	33.40	33.40	0.001
Between groups					
s * c	6	11.51	1.92	1.92	0.097
r * s	2	0.12	0.06	0.06	0.942
r * c	3	48.63	16.21	16.21	0.004
Total	47	521.78			

Table 28. ANOVA for model y=s+c+r+s*c+r*s representing the
mean number of metaphase cells with labelled constitutive
heterochromatin regions observed for each substage of S phase
obtained for the RS+ lymphoblastoid cell line, R20, and the
control cell line, DM (Experiments 2 and 4).

Model	df	SS	MS	F	P
Within groups					
subphase (s)	2	50.86	25.43	25.43	<0.001
chromosome (c)	3	162.10	54.03	54.03	<0.001
C vs. RS+ (r)	1	33.40	33.40	33.40	<0.001
Between groups					
s * c	6	11.51	1.92	1.92	0.097
r * s	2	0.12	0.06	0.06	0.942
r * c	3	48.63	16.21	16.21	0.004
Total	47	521.78			

observed for each substage of S phase of the RS+ cell line, LB1, and control cell line, JaKr, are summarized in Tables 29 and 30. With the model y=c+s+r+s*c+r*s+r*c, the effect of subphase and chromosome were highly significant (p<0.001). The comparison of cell type (Control vs. RS+) was also significant with p<0.05. The effect of interaction between subphase and chromosome (s*c) was not significant but the effect of interaction between subphase and cell type (r*s, p<0.020) and chromosome and cell type (r*c, p<0.001) were.

With the model y=s+c+r+s*c+r*s+r*c, a lower sum of square value for factor 's' was obtained and a higher sum of square value was obtained for factor 'c'. The F values associated with factors 's' and 'c' were highly significant (p<0.001) and cell type, 'r', was just significant (p<0.05). The effect due to interaction was the same as for the first model.

The order of the factors in the model affected the sum of square values of factors 'c' and 'r' but this did not affect the level of significance. The ANOVA of the two models resulted in similar F-ratios and P values for each factor for all comparisons made for all cell lines. The results of all ANOVA indicated that there were significant differences in the mean observed frequency of cells with

Table 29. ANOVA for model y=c+s+r+s*c+r*s+r*c representing the mean number of metaphase cells with labelled constitutive heterochromatin regions observed for each substage of S phase obtained for the RS+ lymphoblastoid cell line, LB1, and the control cell line, JaKr (Experiments 1 and 2).

Model	df	SS	MS	F	P
Within groups					
chromosome (c)	2	28.41	14.21	14.21	<0.001
subphase (s)	2	89.11	44.56	44.56	<0.001
C vs. RS+ (r)	1	5.28	5.28	5.28	0.028
Between groups					
s * c	4	7.39	1.84	1.84	0.143
r * s	2	16.02	8.01	8.01	0.028
r * c	2	33.71	16.85	16.85	<0.001
Total	35	374.96			

Table 30. ANOVA for model y=s+c+r+s*c+r*s+r*c representing the mean number of metaphase cells with labelled constitutive heterochromatin regions observed for each substage of S phase obtained for the RS+ lymphoblastoid cell line, LB1, and the control cell line, JaKr (Experiments 1 and 2).

Model	df	SS	MS	F	P
Within groups					
subphase (s)	2	87.94	43.97	43.97	<0.001
chromosome (c)	2	29.58	14.79	14.79	<0.001
C vs. RS+ (r)	1	5.28	5.28	5.28	0.028
Between groups					
s * c	4	7.39	1.84	1.84	0.143
r * s	2	16.02	8.01	8.01	0.028
r * c	2	33.71	16.85	16.85	<0.001
Total	35	374.96			

labelled constitutive heterochromatin regions between RS+ and
control lymphoblastoid cell lines.

4. DISCUSSION

4.1. ANALYSIS OF METHYLATION LEVELS OF CONSTITUTIVE HETEROCHROMATIN DNA IN ROBERTS SYNDROME

The original question addressed in this study was whether altered levels of DNA methylation were associated with the abnormal constitutive heterochromatin structure of RS+ chromosomes. Levels of constitutive heterochromatin DNA methylation levels were assessed in RS and control fibroblast cell strains using MspI and HpaII isoschizomer restriction enzyme analysis and Southern blot hybridization with a moderately repetitive probe, D15Z1. The level of D15Z1 DNA methylation was quantified and mathematically represented by the ratio of the area OD of the MspI 3.5 kb band to the area OD of the HpaII 3.5 kb band, for each cell strain. Statistical analysis of these results involved the use of GLM and ANOVA, allowing one to compare D15Z1 DNA methylation levels of RS+, RS- and control fibroblast cell strains. The models were designed so that the mean area OD ratio (A/B) of the three cell strain groups could be compared while minimizing the effect of experimental variability and passage.

Four GLM models were used to fit the mean area OD ratio values obtained for control RS+, RS- and controls. Two of the models, comparing RS+ and RS- with controls

simultaneously [Models i) and ii)], did not demonstrate any significant differences in the area OD ratios among the three groups using ANOVA. They also showed no significant effect of passage on D15Z1 DNA methylation levels. The third model separately compared the RS fibroblast cell strains, RS+ and RS-, with controls. There were no significant differences in the mean area OD ratios between RS+ and controls or RS- and controls.

Power of a statistical test has been defined as "the probability that it will yield statistically significant results" (Cohen, 1988). It depends upon three main factors; the significance criterion, the reliability of the sample results and the "effect size" (reviewed by Cohen, 1988). A small significance criterion results in a lower power level. Even though a small significance criterion is generally desirable as it increases the probability that the result observed is not due to chance, it also diminishes the power of the statistical test. The reliability of the sample result is estimated by the standard error of the mean. Therefore variability has an important effect on power. The "effect size" is defined as the "degree to which the phenomenon exists," (cited from Cohen, 1988). Thus the "effect size" would be defined as an expected measurable difference in the mean area OD ratio of RS+ and controls. It was difficult to define the effect size for Models i)-iii) as

there is no known biological measure for the differences expected in D15Z1 DNA methylation levels.

The power of Models i)-iii) was calculated as described for a one-way ANOVA with unequal sample size by Cohen (1988). An example calculation is given in Appendix 2. The effect size was defined as the difference observed in the mean area OD ratios of RS+ cell strains compared with RS- and control cell strains from Model iv). The power for Models i)-iii) was estimated to be only 10-15% which is well below the conventionally accepted level of 80% (Cohen, 1988). To obtain a power level of 80% for Models i)-iii) a sample size of 200 would be required. This number could never have been achieved with the number of RS patients or fibroblast cell strains available for study.

The fourth model compared the mean area OD of RS+ cell strains to cell strains which have normal constitutive heterochromatin (RS- and controls). This model allowed one to test the original hypothesis of whether altered levels of DNA methylation were associated with abnormal RS+ constitutive heterochromatin structure. With this comparison, statistically significant differences in the mean area OD ratios were observed between the two groups. This suggests that there are statistically significant differences in the level of D15Z1 DNA methylation, as represented by the 3.5 kb band area OD ratio, between RS+ fibroblast cell

strains and cell strains with normal constitutive heterochromatin. This model also indicated that there was a statistically significant effect of passage on the area OD ratios of the other two groups, suggesting that there were statistically significant differences in D15Z1 DNA methylation levels between early and late passage, for all cell strains.

The lack of evidence for statistically significant differences in the levels of D15Z1 DNA methylation with models i)-iii) needs to be interpreted in the context of the strengths and weaknesses of each model. The three way comparison of the mean OD ratio for RS+, RS- and control fibroblast cell strains made in Models i) and ii) maximized the sample size used for the GLM and ANOVA. However, this comparison did not test the original hypothesis of whether altered levels of D15Z1 DNA methylation were associated with abnormal constitutive heterochromatin structure of RS+ chromosomes. The comparison of RS+ with controls, defined by Model iii), did address this question and a p-value of 0.062 was obtained. This could reflect a trend for decreased D15Z1 DNA methylation levels for RS+ fibroblast cell strains.

There are several reasons why statistically significant differences were detected with the fourth model but perhaps not with the third. The nearly significant p value obtained for the comparison of RS+ and controls with

Model iii) suggested that undermethylation may be associated with the RS effect but was most likely affected by the smaller sample size and the low power of the statistical test. The comparison of the mean OD ratio of RS+ with RS- and controls with Model iv) resulted in an increase in sample size of the two groups so that the difference between the two groups could be easier to detect.

Analysis of DNA methylation levels using single MspI and HpaII digestion indicated that a specific subset of D15Z1 heterochromatin sequences, represented by the 3.5 kb band, is undermethylated in RS+ fibroblast cell strains. Genomic DNA of RS+, RS- and control fibroblast cell strains was digested with MspI/EcoRI or HpaII/EcoRI to determine if additional D15Z1 methylation sensitive restriction fragments could be identified. Two such fragments were identified and were estimated to be 0.5 and 2.5 kb in size. Although the use of double restriction enzyme analysis resulted in a greater number of fragments recognized by D15Z1, the results were more difficult to interpret, for several reasons. There was a great deal of restriction fragment length polymorphism between cell strains and of all of the bands identified, only two bands showed differential digestion by MspI and HpaII. The large number of bands also made quantification by video densitometry more difficult because of the increased background signal observed in the regions of the higher

molecular weight fragments. The area OD of the bands were extremely sensitive to unequal amounts of DNA present in each of the autoradiograph. To control for this problem, the 1.6 kb band was used to calculated the "adjusted area O.D" ratio of the 2.5 kb band.

Analysis of D15Z1 DNA methylation levels in RS+, RS- and control genomic DNA samples, represented by the 2.5 kb, resulted in adjusted area OD ratios (C/D) that were greater than 1. This indicated that these sequences were methylated in all fibroblast cell strains. If RS+ D15Z1 DNA were less methylated, one would predict that the adjusted area OD ratio would be less for RS+ cell strains compared to RS- or controls. The adjusted area OD ratio could not be determined for all digested DNA samples as the intensity of HpaII/EcoRI 2.5 kb band could not always be quantified by video densitometry. For this reason, a quantitative comparison of the D15Z1 DNA methylation levels of RS+, RS- or control fibroblast cell strains using MspI/EcoRI and HpaII/EcoRI restriction enzyme analysis could not be made.

One of the limitations of using methylation dependent restriction enzyme analysis to assess levels of DNA methylation is that restriction enzyme digestion with MspI and HpaII recognizes only a small percentage of methylated CpG sequences in the genome, those at a 5'-CCGG-3' site. This problem was encountered in a study by Howlett et al.

(1989) investigating the in vivo methylation status of mouse major and minor satellite DNA sequences to determine age-related changes in DNA methylation. Changes in DNA methylation were assessed using HPLC analysis and MspI and HpaII restriction enzyme analysis. HPLC analysis indicated a decrease in methylated cytosine content of satellite DNA sequences while MspI and HpaII Southern blot hybridization indicated that the sequences remained fully methylated with increasing age. The results presented by Howlett et al. (ibid) suggest that several experimental approaches may be useful in analysing levels of DNA methylation.

4.1.1. POSSIBLE ORGANIZATION OF D15Z1 DNA SEQUENCES

Restriction enzyme digestion of genomic DNA with MspI, EcoRI, HpaII, MspI/EcoRI and HpaII/EcoRI indicated that D15Z1 sequences may be organized as several domains. Several models outlining the possible organization of D15Z1 sequences have been considered. The simplest model defines the D15Z1 1.8 kb monomer to be organized as imperfect tandem repeats. Digestion of genomic DNA with the restriction enzyme, EcoRI, resulted in the recognition of restriction fragments that were multiples of the 1.8 kb monomer as well as a 1.6 kb fragment. This arrangement of imperfect tandem repeats is well documented for D15Z1 (Higgins et al. 1985).

Hybridization of MspI digested fibroblast genomic DNA

with D15Z1 resulted in the recognition of a 3.5 kb fragment that was methylation sensitive. Subsequent digestion with EcoRI resulted in the loss of this fragment, and in the appearance of two new methylation sensitive fragments, 2.5 and 0.5 kb. One could predict that the two smaller MspI/EcoRI fragments could have been derived from the MspI 3.5 kb fragment. To test this hypothesis, two models are presented in Figure 39, outlining the possible fragments that could be expected with single restriction enzyme digestion with MspI, HpaII and EcoRI as well as double digestion with MspI/EcoRI and HpaII/EcoRI. The arrangement of restriction enzyme recognition sites presented in Models A and B do not support the hypothesis that the MspI/EcoRI 2.5 and 0.5 kb fragments are derived from the MspI 3.5 kb fragment as the corresponding 3.0 and 0.5 kb bands that should result from EcoRI digestion alone were never observed. This suggests that there may be other domains where D15Z1 sequences are located. Therefore, the MspI 3.5 kb band was lost with subsequent EcoRI digestion, as EcoRI recognition sequences are present within this fragment. Therefore, one cannot definitely state that the MspI/EcoRI 2.5 and 0.5 kb bands were not derived from the MspI 3.5 kb band. To determine where the EcoRI sites are within the MspI 3.5 kb band, one would have to excise the band from an agarose gel and digest it with EcoRI to determine the size of the MspI/EcoRI

Figure 39. Models illustrating the organization of D15Z1 sequences based upon observed MspI/EcoRI and HpaII/EcoRI restriction fragments. Model A. EcoRI (E) recognition sites are clustered within the MspI derived 3.5 kb fragment. All fragments that would be produced by MspI, HpaII, MspI/EcoRI were observed but the fragments that would be produced by EcoRI were never observed. Model B. Two EcoRI restriction sites are localized within the MspI derived 3.5 kb fragment. All fragments that would be produced by MspI, HpaII, MspI/EcoRI were observed but the fragments that would be produced by EcoRI were never observed. M* denotes methylated 5'-CCGG-'3 sequences.

A

H   no fragments if 5'-CCGG-3' methylated

M

3.5 kb   3.5 kb

Hx   E   Hx   E   Hx

M/E

2.5 kb   0.5 kb   2.5 kb   0.5 kb

E

3.0 kb

B

H   no fragments if 5'-CCGG-3' methylated

M

3.5 kb   3.5 kb

Hx   E   Hx   E   Hx

M/E

2.5 kb   0.5 kb   2.5 kb   0.5 kb

E

0.5 kb   3.0 kb   0.5 kb
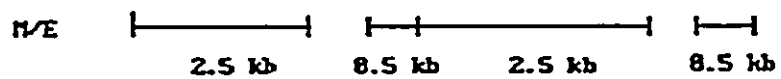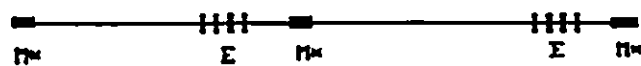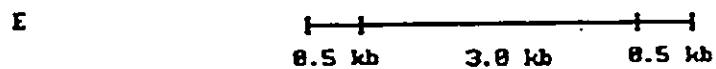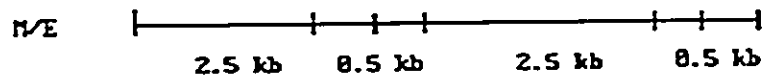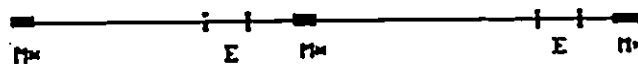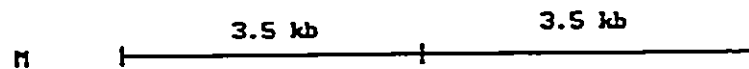
restriction products.

The D15Z1 sequences may possibly be localized to a third domain. There were approximately three restriction enzyme fragments produced with HpaII/EcoRI digestion that were not observed with MspI/EcoRI digestion. These fragments were estimated to range in size from 1.8 kb to 2.2 kb and were referred to as a 1.8+ kb band. The second model, outlined in Figure 40, shows the possible organization of the D15Z1 sequences with respect to EcoRI, MspI and HpaII recognition sites, resulting HpaII/EcoRI fragments that vary approximately from 1.8-2.2 kb in size. This model requires the presence of a cluster of 5'-CCGG-3' recognition sequences, approximately 0.2 kb apart, with variable methylation at each site to produce the HpaII/EcoRI restriction fragments observed. This would give a domain consisting of a 1.8 kb tandem repeat flanked by multiple MspI recognition sequences. One model could assume that the 1.8+ kb fragments were derived from the MspI 3.5 kb band but does not produce an EcoRI restriction fragment of the correct size. All fragments that would be produced by MspI, HpaII, MspI/EcoRI, HpaII/EcoRI were observed but the fragment that would be produced by EcoRI was never observed.

The use of MspI/EcoRI and HpaII/EcoRI restriction enzyme analysis did not provide a useful alternative method of analysing D15Z1 DNA methylation levels in RS as

Figure 40. Model illustrating the organization of D15Z1
sequences flanked by a cluster of MspI and HpaII sites. All
fragments that would be produced by MspI, HpaII, MspI/EcoRI
and HpaII/EcoRI were observed but the 4.0 kb fragment that
would be produced by EcoRI was never observed. MspI (M),
HpaII (H) and EcoRI (E) recognition sites.

H   no fragments if 5'-CCGG-3' methylated

3.5 kb   3.5 kb

M

  M M H   E   M H M   E   M M H

M/E

1.8 kb   1.8 kb   1.8 kb   1.8 kb

H/E

1.8 kb   2.8 kb   1.8 kb   2.2 kb

E

4.8 kb
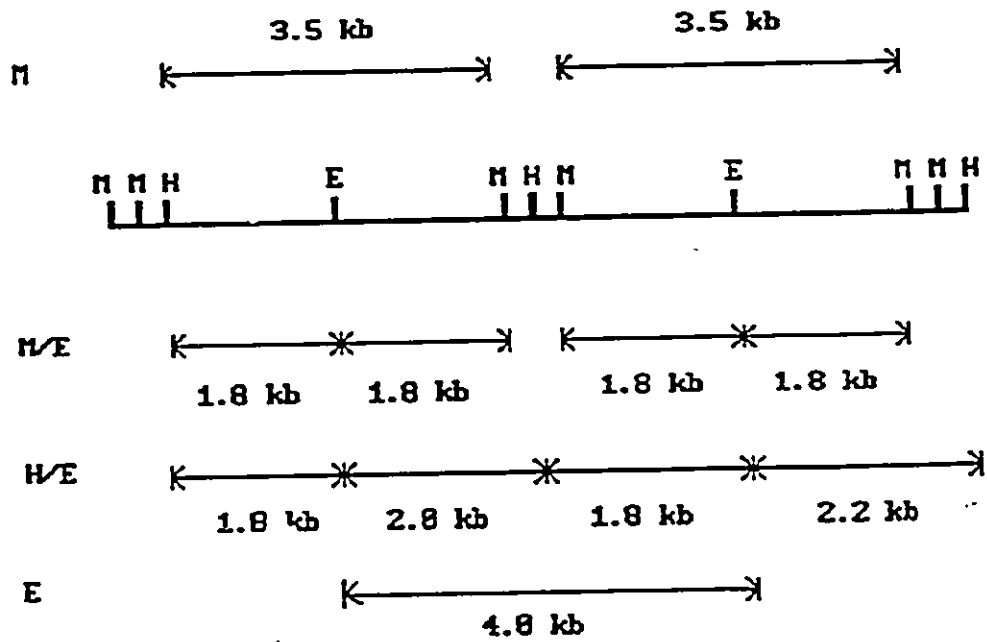
quantification of the methylation sensitive MspI/EcoRI 2.5 kb fragment by video densitometry was limited. Restriction enzyme analysis with more than one enzyme did provide some insight as to the possible organization of D15Z1 sequences within constitutive heterochromatin. There was some indication that D15Z1 sequences may be localized to more than one domain, suggesting a defined organization of a subset of constitutive heterochromatin sequences.

4.1.2. DNA METHYLATION AND ITS EFFECT ON CHROMATIN STRUCTURE

The results of this study suggest that altered DNA methylation levels of specific subset of sequences recognized by D15Z1 are associated with a cytogenetic abnormality of the constitutive heterochromatin in RS+ fibroblast cell strains. Changes in DNA methylation have been largely associated with differentiation and development (Sanford et al. 1984; Chapman et al. 1984), chromatin structure (Kautiainen and Jones, 1985; Keshet et al. 1986; Davis et al. 1986) and aging (Shmookler-Reis and Goldstein, 1982a,b; Howlett et al. 1989). Changes in methylation pattern have been shown to be due to defective DNA methyltransferases, demethylation by enzymes that remove or replace m^5cyt or by excision DNA repair (reviewed by Cooney and Bradbury, 1990).

The changes in DNA methylation known to be associated with changes in chromatin structure have been derived from

studies involving euchromatin. It is not known if similar alterations in DNA methylation would be associated with similar structural changes in constitutive heterochromatin. For this reason, it should be pointed out that the hypotheses presented in the remainder of this text have been derived from what is known about euchromatin.

Constitutive heterochromatin sequences are highly methylated with many of the m^5cyt residues localized to the nucleosomes containing histone H1 protein. This nucleosome configuration is generally found in inactive chromatin fractions (Ball et al. 1983). Davis et al. (1986) reported that DNA of chromatin fractions resistant to micrococcal nuclease digestion (or inactive chromatin fractions) are enriched with newly synthesized m^5cyt and are preferentially methylated compared to nuclease-sensitive chromatin. This suggests that DNA methylation is influenced by or may influence specific DNA-protein interactions, as nucleosomes without histone H1 are less methylated and generally associated with active, less condensed chromatin fractions (Gottesfeld et al. 1974).

The decondensed appearance of the constitutive heterochromatin of RS+ chromosomes suggests that the chromatin structure of these regions may be altered. One could hypothesize that an alteration in chromatin structure could result in abnormal DNA methylation. Methylation of

newly synthesized DNA has been reported to occur shortly after DNA replication. This may take place as soon as 1-2 minutes after replication or even several hours later in G_2 (Cooney and Bradbury, 1990). Histone association with newly replicated DNA to form nucleosomes also occurs shortly after DNA replication (cited in Kautiainen and Jones (1985)). Kautiainen and Jones (ibid) postulated that a heritable loss of DNA methylation could occur if histone proteins bound to the newly synthesized DNA before methylation by endogenous methyltransferases took place. One could predict that an alteration in RS+ constitutive heterochromatin structure could result in undermethylation of these sequences.

One could alternatively hypothesize that DNA methylation influences chromatin structure. This could be achieved by influencing the interaction of the methylated sequences with structural nuclear proteins Methylation would therefore play an important role in the organization of a specific chromatin state within a defined region. Changes in DNA methylation could be caused by defective methyltransferase activity or other by other enzymatic processes known to remove or replace m^5cyt. One of the limitations of this hypothesis is that it would require DNA methylation to be the primary regulator of chromatin structure and the correlation of undermethylation of gene sequences, active chromatin configurations and gene activity

to be absolute. This model would also predict that global demethylation of genomic DNA associated with aging would result in the dedifferentiation of normal aging tissue, a phenomenon that has not generally been observed except in cancers. This suggests that other regulatory processes in addition to DNA methylation are involved in the formation of chromatin structure.

4.1.3. DNA METHYLATION AND AGING

Many of the reported changes of DNA methylation have been associated with aging. Generally, decreases in total DNA methylation and variations in methylation patterns of specific genes have been observed *in vitro* in aging diploid human and rodent fibroblast cultures (Shmookler-Reis and Goldstein, 1982a,b; Wilson and Jones, 1983). The results of Shmookler-Reis and Goldstein (1982a) indicated that three classes of highly repetitive DNA isolated from human fibroblast cell strains remained consistently methylated with *in vitro* aging. Although there was variability between cell strains, it was estimated that 70-80% of the cytosine residues remained methylated. Howlett *et al*. (1989), on the other hand, reported *in vivo* age-related demethylation of mouse satellite repetitive DNA that paralleled that seen for total DNA.

The results presented in this thesis indicated that

there was a statistically significant effect of passage on D15Z1 DNA methylation levels, as represented by the 3.5 kb band. This was observed for all cell fibroblast cell strains, indicating that in vitro aging had an effect on the methylation levels of repetitive DNA sequences localized within constitutive heterochromatin regions.

4.1.4. FUTURE DIRECTIONS: FURTHER CHARACTERIZATION OF RS+ CONSTITUTIVE HETEROCHROMATIN DNA METHYLATION LEVELS

The major focus of this project has been to use MspI and HpaII isoschizomer restriction enzyme digestion and Southern blot hybridization with D15Z1, a repetitive DNA probe, to assess levels of heterochromatin repetitive DNA methylation in RS fibroblast cell strains. The results of this study suggest that altered DNA methylation levels of a specific subset of sequences recognized by D15Z1 are associated with a cytogenetic abnormality of the constitutive heterochromatin in RS+ fibroblast cell strains. D15Z1 is a member of the KpnI family of middle repetitive sequences and is thought to belong to a subset of satellite III or IV sequences (Frommer et al. 1982). The results of Fowler et al. (1987, 1988) indicate that D15Z1 belongs to the satellite III-related "K domains", localized to chromosomes 15 and Y. Heterochromatin DNA is made up of many simple and complex repeats of satellite DNA sequences as well as other repetitive sequences that may or may not be related to

satellite DNA. It would be of interest to assess the methylation levels of other heterochromatin DNA sequences, particularly those localized to the major constitutive heterochromatin regions of chromosomes 1, 9, 16 and Y. DNA probes are available for all four constitutive heterochromatin regions. The use of an alphoid human DNA sequence, p82H, that hybridizes to the centromeric regions of all human chromosomes, may also provide additional information about DNA methylation levels of centromeric DNA sequences in RS (Mitchell et al. 1985).

Alternative experimental approaches could also be used to follow up the findings that RS+ D15Z1 DNA sequences are undermethylated. Treatment of human cells with 5-azaC, a potent inhibitor or DNA methyltransferase activity, results in the subsequent hypomethylation of newly replicated DNA. This also affects chromosome structure, resulting in the decondensation of the constitutive heterochromatin regions of human chromosomes (Viegas-Pequignot and Dutrillaux, 1976), although the appearance of the heterochromatic regions was not similar to the RS effect (Gunby, 1986).

The treatment of control fibroblast cell strains with 5-azaC and its effect on DNA methylation could be analysed using MspI and HpaII isoschizomer restriction analysis and Southern blot hybridization with D15Z1. One would predict that 5-azaC treatment of control fibroblast cell strains

would result in demethylation of D15Z1 DNA sequences. This experimental approach could provide some information about the degree of undermethylation that could be expected with altered chromatin structure as there is really no biological measure of the differences expected in levels of DNA methylation associated with altered chromatin structure. The degree of undermethylation observed in 5-azaC treated control cell strains could then be compared to that observed for 5-azaC treated and untreated RS+ cell strains. The methylation status of other constitutive heterochromatin sequences using additional DNA probes could also be investigated.

One of the limitations of restriction enzyme analysis of DNA methylation levels is that this method detects only 5-15% of the CpG sites and does not distinguish hemimethylated and fully methylated DNA (Weissbach et al. 1989). Several alternative methods of assessing levels of DNA methylation have been reported (reviewed by Cooney and Bradbury, 1990). In vitro methylation systems have been used to determine the methylation status of active and inactive chromatin fractions (Kautiainen and Jones, 1985; Davis et al. 1986) and specific gene sequences (Ward et al. 1987) as well as the heritability of methylation patterns (Keshet et al. 1986). The heritability of DNA methylation patterns of specific sequences can be tested using in vitro methylated sequences transfected into recipient cells followed by subsequent

rounds of replication _in_ _vivo_.

Decreased levels of D15Z1 DNA methylation could be caused by an unstable heritable methylation pattern in RS+ fibroblast cell strains. One could test this by introducing _in_ _vitro_ methylated sequences into RS+ fibroblast cell strains and examine their methylation status after several rounds of replication. This would provide information about endogenous methyltransferase enzyme activity.

4.2. CHROMOSOME REPLICATION STUDIES OF ROBERTS SYNDROME

4.2.1. CHARACTERIZATION OF S SUBPHASE DISTRIBUTIONS IN ROBERTS SYNDROME

The original question proposed for this study asked whether the timing of DNA replication of constitutive heterochromatin relative to the rest of the genome was altered in RS+ cells with abnormal heterochromatin structure. There is some indication that the timing of DNA synthesis in RS+ cells is impaired (Gani _et_ _al_. 1984).

The replication patterns of chromosomes was investigated in RS+ and control lymphoblastoid cells by terminally labelling cells in S phase with BrdUrd. Classification involved the use of an artificial key that placed a cell within one of four successive substages of S phase, SkI-SkIV. It was predicted that alterations in the subphase distributions between RS+ and control cell lines could be due to differences in rate or timing of replication.

Savage and Papworth (1988) studied the replication program of various lymphocyte and fibroblast cell strains using a probit transformation of the chromosome replication-band frequencies obtained with the subclassification system. The chromosome replication band frequencies were plotted against BrdUrd treatment time to give a family of cumulative Normal Frequency Curves. If the family of curves was sampled twice, the two observed frequencies for each curve would be considered to be related. If the frequencies were transformed to probits, then it would be predicted that their probits would lie on a straight line. The replication program of two cell strains were compared by plotting the probits of one cell strain against the probits of the other. If this plot resulted in a straight line with a 45° slope, then the replication program of the cell strains being compared were said to be similar. However, if the replication program of the two cell strains were different, then the probit-probit plot did not give a straight line with a slope of 45°.

The replication program of RS+ and control lymphoblastoid cell lines were analysed using a modification of the method of Savage and Papworth. With the use of the statistical program, GLIM v3.77 (Royal Statistical Society, 1985), the observed frequencies of cells in each subphase of RS+ and control lymphoblastoid cell lines were subjected to

a probit transformation and modelled using a defined GLIM predictor equation. This program took the observed frequencies, transformed them into probits which where then modelled using GLIM. The modelled probit values were then converted back to frequencies, to plot the fitted values against the various BrdUrd treatment times for each cell line. The replication program of cell lines were then compared using the estimates of the slope of each line. This analysis, although not exactly the same as that used by Savage and Papworth (ibid), is a similar approach.

Differences were observed in the frequency of cells in each subphase for different BrdUrd treatment times, but they were variable between experiments. Comparisons of the slopes of RS+ and its matched control for each subphase were not shown to be significantly different using a Student's t-test. It was concluded that there were no significant differences in the subphase distribution of RS+ and control lymphoblastoid cell lines.

The replication programs of RS+ and control lymphoblastoid cell lines were compared using a classification system that allowed one to place a cell within a certain substage of S phase using an "artificial key". This classification system was initially based upon the concept that structural chromosome bands replicate in a regulated and reproducible manner. However, the frequency of

cells classified within a certain substage can be influenced by a number of factors, thereby producing sample variation. The original experimental setup of Savage and Papworth (ibid) required a narrow sampling time, with short Colcemid[R] treatments of 1 hour being ideal. The use of a 2 hour Colcemid[R] treatment, which was necessary for lymphoblast cultures to obtain a mitotic index that would result in a sufficient number of metaphases for analysis, could have resulted in increased variability. A longer Colcemid[R] treatment time could introduce imprecision to the S phase classification system by affecting the standard deviation of the Band Appearance Distribution curve. In addition to this, variability may have been caused by differences in the rate of DNA synthesis in early and late S phase, which does not proceed at a constant rate (Schmidt, 1980). Variation was more evident later in S phase (Savage and Papworth, 1988). Because the experiments were set up so that cells replicating in the latter half of S phase were labelled with BrdUrd, a greater variation in subphase distribution could be expected. The cell type used for analysis may also result in variability. This classification system was initially developed using untransformed, fresh fibroblast explants and lymphocyte cultures. Cell cycle times may not be as consistent for transformed lymphoblastoid cells.

Additional sources of variation in subphase

distribution between experiments could also be caused by culture synchrony rather than asynchrony. The seeding density and culture conditions used for lymphoblast cells generally result in the cells being at the logarithmic phase of growth at the time of BrdUrd treatment and chromosome harvesting. If the stock culture from which the experimental cultures were set up was not at logarithmic phase of growth, this could have resulted in a higher degree of synchrony than expected. Because it is unlikely that the stage in which the cells are at would be the same for each experiment, such synchronization due to culture initiation could conceivably influence the subphase distributions observed.

The results of this study showed that there were no significant differences in the subphase distribution of RS+ and control lymphoblastoid cell lines. This suggests that there are no significant differences in the replication program of RS+ and control cell lines as determined by the S phase classification system used.

4.2.2. CHARACTERIZATION OF CONSTITUTIVE HETEROCHROMATIN REPLICATION IN ROBERTS SYNDROME

The original hypothesis of this study proposed that the timing of constitutive heterochromatin DNA replication may be altered in RS+ cells, due to its altered structure. The consequences of such an alteration may be important as it is well established that different regions of each chromosome

replicate in a reproducible order during S phase and that the timing of replication patterns are specific. The replication programme of the constitutive heterochromatin regions was characterized by analysing the proportion of cells within each subphase, defined in the previous four experiments, that incorporated BrdUrd within the constitutive heterochromatin regions of chromosomes 1, 9, 16 and Y (referred to as 1qh, 9qh, 16qh and Yqh). The chromosome replication pattern of the X chromosome was also assessed in female RS+ and control lymphoblastoid cell lines. The statistical analysis was similar to that described in the previous section, comparing the subphase distributions of RS+ and control cell lines.

The labelling frequencies of the constitutive heterochromatin regions of RS+ and control lymphoblastoid cells were very similar in SkII and SkIII. This result would be expected as these cells would have progressed through the rest of S phase. One would also expect that all or almost all SkII and SkIII cells would have labelled constitutive heterochromatin regions. A small number of SkII and SkIII cells did not have pale staining constitutive heterochromatin regions. This finding could be due to aberrant scoring of pale staining constitutive heterochromatin regions. The constitutive heterochromatin regions of the male control cell line were very small and in some cells, it was difficult to distinguish these regions from the centromere. This problem

could have been avoided using a reverse labelling protocol whereby cells are labelled with BrdUrd early in S phase followed by thymidine labelling late in S phase. With this labelling protocol, late replicating regions of chromosomes would have been darkly stained by fluorescence-plus-Giemsa technique, resulting in their easier identification.

The greatest differences in labelling frequencies of RS+ and control cells were observed in the last subphase of S phase, SkIV. This result would be expected if one takes into consideration that the constitutive heterochromatin regions replicate very late in S phase. One could predict that a difference in the labelling frequencies of RS+ and control cells would be detected in SkIV if there was an alteration in the timing of constitutive heterochromatin replication.

Although it is well documented that constitutive heterochromatin replicates later in S phase, a review of a number of studies showed that it has been very difficult to establish a consistent chronological pattern of replication for the large regions found on chromosomes 1, 9, 16 and Y (Epplen et al. 1975, Grzeschek et al. 1975 and Camargo and Cervenka, 1982). Preliminary analysis of the labelling frequencies of the constitutive heterochromatin regions of chromosomes 1, 9, 16 and Y in the last substage of S phase using the subclassification system, indicated that a temporal

order could be established for these regions in control cells. The constitutive heterochromatin region of chromosome 16 appeared to replicate earliest, followed by the replication of 9qh, 1qh and Yqh. The labelling frequencies of the last three constitutive heterochromatin regions were very similar and showed some variability, suggesting that all three regions replicated at a similar time very late in S phase. The labelling pattern of chromosome 9qh appeared to be the most variable. This could simply be due to variable replication of this constitutive heterochromatin region or it could be due to scoring difficulties.

Statistical analysis using Generalized Linear Modelling and comparison of slopes indicated that there were no significant differences in the replication frequencies of c-heterochromatin with respect to BrdUrd treatment time of RS+ and control lymphoblastoid cell lines. This result would be expected using an S phase subclassification system to compare the constitutive heterochromatin replication patterns of cells within a particular substage. Cells classified within a particular subphase would be considered to be at a similar stage of DNA synthesis and the constitutive heterochromatin replication frequencies would not be significantly influenced by BrdUrd treatment time. Thus the frequency of labelled c-heterochromatin could be summarized over BrdUrd treatment time. This allowed one to ask if

differences existed in the frequency of c-heterochromatin replication relative to subphase distribution between RS+ and controls. Generalized Linear Modelling and ANOVA indicated that there were significant differences in the replication frequencies with respect to subphase, c-heterochromatin region and cell type.

The differences observed in the c-heterochromatin frequencies of RS+ and control lymphoblastoid cell lines could be explained if a delay in RS+ constitutive heterochromatin replication exists. This appeared to be particularly evident for the 16qh region as it did not replicate as early as in the control cell lines. All constitutive heterochromatin regions of chromosomes 1, 9, 16 and Y appeared to replicate at a similar time in RS+ cell, somewhat later in S phase, suggesting that the alteration in constitutive heterochromatin structure may be associated with an alteration in the timing of its DNA replication relative to the rest of the DNA in RS+ lymphoblastoid cells.

4.2.3. MODEL FOR CONSTITUTIVE HETEROCHROMATIN REPLICATION

It is well documented that constitutive heterochromatin replicates late in S phase. A model is presented in Figure 41 to illustrate the timing of normal constitutive heterochromatin replication late in S phase. The model presented represents an idealized cell cycle

Figure 41. Figure illustrating a hypothetical model for the normal replication of constitutive heterochromatin late in SkIV of S phase. The timing of each constitutive heterochromatin region within the "replication window" is indicated. S phase is 8 hours in length with each subphase being 2 hours in length. G_2 and mitosis (not shown) are defined to be 3 hours in length.
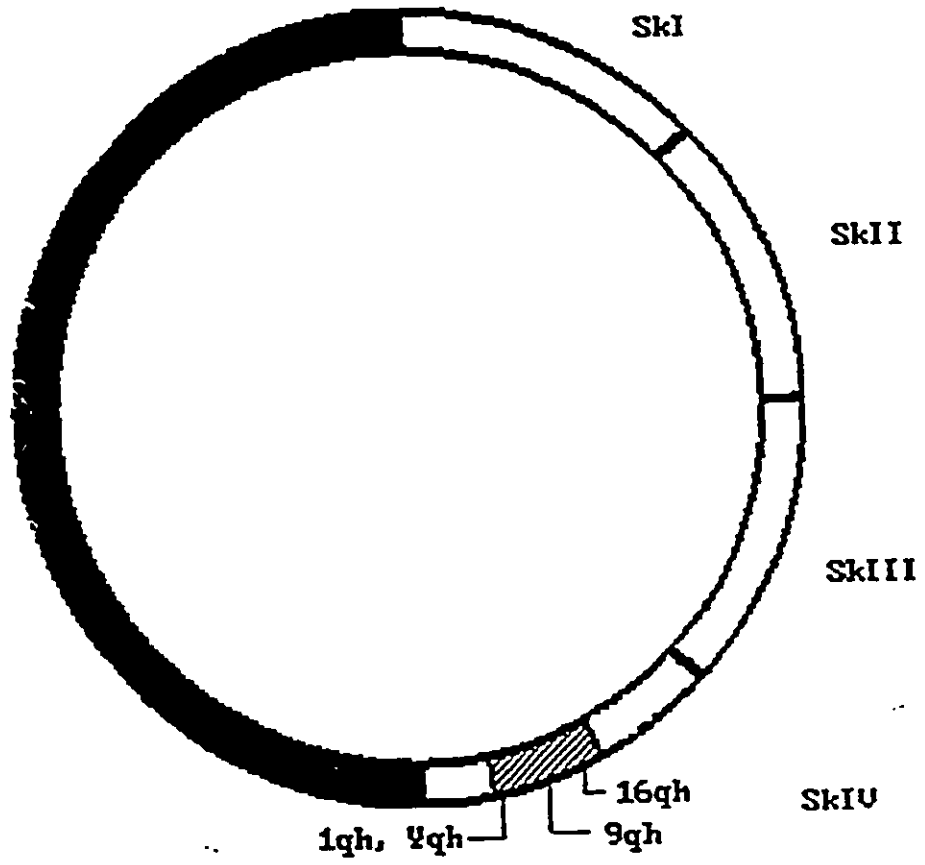
whereby S phase is arbitrarily defined to be 8 hours in length and G_2 and mitosis are 3 hours in length. Each subphase duration of S phase is arbitrarily defined to be 2 hours long. The mean observed labelling percentages for the constitutive heterochromatin regions of chromosomes 1 (88%, s=3.6), 9 (71.0%, s=26.8), 16 (45.8%, s=19.3) and Y (87.3%, s=2.2) of SkIV cells, calculated for the control cell lines from all experiments, were used to model constitutive heterochromatin replication in SkIV. A "replication window" within SkIV representing when each constitutive heterochromatin region replicates has been shown.

The model presented in Figure 42 is an idealized representation of the timing of RS+ constitutive heterochromatin relative to control. The length of S phase and its subphase durations are the same as that outlined for Figure 41. The timing of RS+ constitutive heterochromatin was based upon the mean labelling percentages of all four constitutive heterochromatin regions of RS+ from all experiments. The mean labelling percentages for the RS+ cell lines were calculated to be 75.9% (s=11.5) for 1qh, 81.6% (s=13.9) for 9qh, 76.9% (s=12.2) for 16qh and 77.1% (s=9.5) for Yqh. The higher mean labelling percentages suggest that the constitutive heterochromatin regions of RS+ cell lines replicate later in SkIV than the control cell lines. The similar mean labelling percentages of all RS+ constitutive

Figure 42.   Figure illustrating a hypothetical model comparing the timing of constitutive heterochromatin replication of control and RS+ lymphoblastoid cells in late SkIV of S phase.   The duration of S phase is 8 hours in length, with each subphase defined as 2 hours in length.
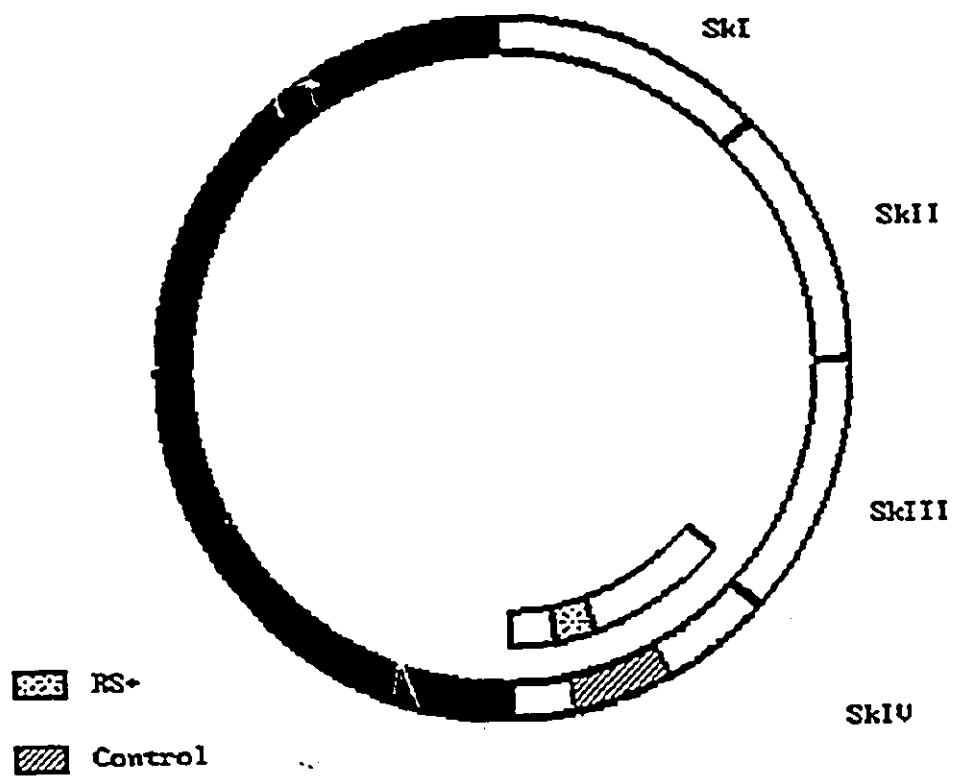
heterochromatin regions suggest they replicate at a similar time in SkIV, thereby resulting in a narrower "replication window". Because the labelling percentages of 1qh, 9qh and Yqh were similar for both RS+ and control cell lines, the replication window of each cell type is shown to overlap to some extent.

4.2.4. DNA REPLICATION AND CHROMATIN STRUCTURE

Nucleosome assembly occurs shortly after DNA replication and normal protein synthesis is required for proper chromatin assembly to occur. The synthesis of histones and non-histones proteins is linked with DNA replication, generally occurring during S phase although synthesis of certain proteins also occurs during G_1. In vitro nucleosome studies have shown that in the absence of protein synthesis, approximately half of the newly synthesized DNA is not assembled (reviewed by Annunziato, 1990).

The decondensed appearance of the constitutive heterochromatin regions of RS+ chromosomes suggest an alteration in chromatin structure. One could hypothesize that a delay in constitutive heterochromatin replication may conceivably affect proper chromatin assembly. The alternative hypothesis is that abnormal constitutive heterochromatin structure affects the timing of its

replication.

4.2.5. FUTURE DIRECTIONS: FURTHER CHARACTERIZATION OF CONSTITUTIVE HETEROCHROMATIN REPLICATION IN ROBERTS SYNDROME

The replication program of RS+ and control lymphoblastoid cell lines were compared using a subclassification system that allowed one to place a cell within a certain substage of S phase using an "artificial key" that depended upon the replication of key bands found on chromosomes 3 and 4. However, the classification system used did not appear to entirely correct the variability of the replication programme of individual cells from an asynchronous population. This was particularly evident when the labelling percentages of cell lines from replicate experiments were compared. Izumikawa et al. (1991) recently reported the use of a classification system that was based upon the pattern of R-bands that appeared in the late-replicating X chromosome that allowed one to stage replication in mid S phase. Such a classification system that uses late replicating bands may prove to be more suitable for analysing replication events that occur in the latter half of S phase.

The use of in vitro replication systems may provide additional insight into the possible causes of delayed DNA replication in RS+ cells. Gani et al. (1984) demonstrated, using BrdUrd incorporation into newly synthesized DNA, that

the rate of DNA synthesis in RS+ cells is significantly slower than controls. It was concluded that DNA synthesis was defective in RS+ cells. Cell free systems that replicate DNA _in vitro_ have aided in the identification of the proteins involved in DNA synthesis (Laskey _et_ _al_. 1989). Investigation of these proteins in RS+ cells may provide insight into the possible defect(s) involved in DNA synthesis.

The timing of replication of certain genes can also be investigated using BrdUrd pulse labelling and hybridization with probes for specific genes (reviewed by Laskey _et_ _al_. 1989). DNA extracted from cells that were labelled with BrdUrd at different stages of S phase can be fractionated using a cesium chloride gradient. The BrdUrd-incorporated DNA is denser than DNA that is not labelled with the thymidine analogue. The DNA fractions are then hybridized with specific DNA probes to determine the time of DNA replication during S phase. This approach could be used to determine the replication timing of D15Z1 DNA sequences or any other probes of interest that are specific for the constitutive heterochromatin regions affected in RS+ cells.

4.3. DNA METHYLATION, REPLICATION AND CHROMATIN STRUCTURE

DNA sequences that replicate early in S phase are

generally undermethylated and are located in active chromatin fractions. This phenomenon can be reproduced _in vitro_ by treating cells with 5-azaC, resulting in hypomethylation of DNA sequences, decondensation of chromatin structure and a shift in the timing of replication from late to early S phase (Viegas-Pequignot and Dutrillaux, 1976; Shafer and Priest, 1984).

The decondensed appearance of the constitutive heterochromatin of RS+ cells could lead one to hypothesize that the timing of its replication is altered. The results of this thesis have shown that there is a delay in the constitutive heterochromatin replication of RS+ lymphoblastoid cells and that altered levels of DNA methylation are associated with the cytogenetic abnormality. One could speculate that the replication of constitutive heterochromatin regions of RS+ cells is delayed or incomplete for several reasons.

One model predicts that the altered chromatin structure of the constitutive heterochromatin regions of RS+ cells could influence the methylation pattern of the DNA sequences, resulting in decreased methylation levels. The delay in the timing of replication could be explained by the fact that the decondensed appearance of the RS effect is not of the same chromatin configuration as that of early replicating euchromatin. This would suggest that the delay

in constitutive heterochromatin replication is due to some other related but yet undefined defect in DNA metabolism.

To test this hypotheses, RS+ and control cells could be treated with 5-azaC in late S phase so that the constitutive heterochromatin DNA sequences become undermethylated and the chromatin configuration is decondensed. The methylation status of the constitutive heterochromatin sequences could be assessed using MspI and HpaII restriction enzyme analysis and Southern blot hybridization with D15Z1. The timing of the constitutive heterochromatin replication in S phase could be analysed using an S phase subclassification system.

Treatment of control cells would provide information about the effect of 5-azaC on the methylation status of D15Z1 sequences and its effect on the timing of replication. It is not known if 5-azaC treatment would result in an alteration in the timing of constitutive heterochromatin replication. Shafer and Priest (1984) showed that 5-azaC treatment induced normally late replicating X chromosome sequences to replicate earlier in S phase. It would be of interest to see if and how 5-azaC treatment of control cells affects the timing of constitutive heterochromatin replication. This could then be compared to what has been observed for RS+ cells.

5. CONCLUSIONS

The characterization of constitutive heterochromatin DNA conformation and replication programme of RS+ cells has provided greater insight into the nature of the RS defect. The abnormal appearance of the constitutive heterochromatin of RS+ chromosomes has prompted one to ask whether this alteration is associated with altered processes affecting normal structure and function. The results suggest that the cytogenetic abnormality of the constitutive heterochromatin of RS+ cells is associated with alterations in DNA modification and metabolism, although they cannot be considered the underlying cause of the heterochromatin abnormality.

Molecular analysis using MspI and HpaII isoschizomer restriction enzyme analysis and Southern blot hybridization with a constitutive heterochromatin-specific DNA probe has shown that DNA methylation levels are undermethylated in RS+ fibroblast cell strains compared to cell strains with normal constitutive heterochromatin structure (RS- and control). Although altered levels of D15Z1 DNA methylation are significantly associated with the constitutive heterochromatin abnormality of RS+ chromosomes, it is clear that these altered levels of DNA methylation are not directly responsible for the alteration in constitutive heterochromatin structure. At this time, DNA methylation is

thought to influence chromatin structure but is not considered to be a primary regulator of specific chromatin configurations. Analysis of DNA methylation levels in fibroblast cell strains of all three groups indicated that D15Z1 DNA methylation levels were significantly lower in late passage as compared with early, suggesting an in vitro aging effect. This result supports the observation that decreases in total DNA methylation and variations in methylation patterns of specific genes occur in aging diploid human and rodent fibroblast cultures.

The DNA replication pattern of constitutive regions of chromosomes was investigated in RS+ and control lymphoblast cell lines using terminal BrdUrd labelling and a S phase classification system. The timing of constitutive heterochromatin replication in RS+ lymphoblastoid cells was shown to be significantly delayed compared to controls. This delay appeared to be specifically associated with the RS effect as facultative heterochromatin did not appear to be affected. The characterization of constitutive heterochromatin replication in RS+ lymphoblastoid cell lines support the finding that the timing of its DNA synthesis, relative to the rest of the genome, is impaired.

REFERENCES

Allan, J., Cowling, G.J., Harborne, N., Gattini, P., Craigie, R., and Gould, H. 1981. Regulation of the higher-order structure of chromatin by histones H1 and H5. J. Cell Biol. 90: 279-288.

Allingham, D.J. and Tomkins, D.J. 1990. Correction of both the cytogenetic abnormality and the mutagen hypersensitivity in Roberts syndrome lymphoblasts by hybridization with normal lymphoblasts. Environ. Mol. Mutagen. 15(17):5A.

Annunziato, A.T. 1990. Chromatin replication and nucleosome assembly. In: The Eukaryotic Nucleus: Molecular Biochemistry and Macromolecular Assemblies. Volume 2. Strauss, P.R. and Wilson, S.H. eds. Telford Press Inc. West Caldwell, NJ, U.S.A. pp 687-712.

Appelt, H., Gerken, H. and Lenz, W. 1966. Tetraphokomelie mit lippen-kiefer-gaumenspalte und clitorishypertrophie-Ein syndrome. Paediat. Paedol. 2: 119-124.

Arrighi, F.E. and Hsu, T.C. 1971. Localization of heterochromatin in human chromosomes. Cytogenet. 10: 81-86.

Ausubel, F.M., Brent, R., Kingston, R.E., Moore, D.D., Smith, J.A., Seidman, J.G., Struhl, K., eds. 1987. Current Protocols of Molecular Biology. Volumes 1 and 2. Greene Publishing Associates and Wiley-Interscience. New York, NY, U.S.A.

Babu, A. and Verma, R.S. 1988. Chromosome structure: Euchromatin and heterochromatin. Int. Rev. Cytol. 108: 1-60.

Ball, D.J., Gross, D.S., and Garrard, W.T. 1983. 5-Methylcytosine is localized in nucleosomes that contain histone H1. Proc. Natl. Acad. Sci. USA. 80: 5490-5494.

Bianchi, N.O., Morgan, W.F. and Cleaver, J.E. 1985. Relationship of ultraviolet light-induced DNA-protien cross-linkage to chromatin structure. Exp. Cell Res. 156: 405-418.

Bird, A.P. and Southern, E.M. 1978. Use of restriction enzymes to study eukaryotic DNA methylation: I. The methylation pattern in ribosomal DNA from _Xenopus laevis_. J. Mol. Biol. 118: 27-47.

Bourgeois, C.A., Lacquerriere, F., Hemon, D., Hubert, J. and Bouteille, M. 1985. New data on the _in situ_ position of the inactive X chromosome in the interphase nucleus of human fibroblasts. Hum. Genet. 69: 122-129.

Burk, R.D., Szabo, P., O'Brien, S., Nash, W.G., Lohchung, Y. and Smith, K.D. 1985. Organization and chromosomal specificity of autosomal homologs of human Y chromosome repeated DNA. Chromosoma 92: 225-233.

Burkholder, G.D. and Weaver, M.G. 1977. DNA-protein interactions and chromosome banding. Exp. Cell Res. 110: 251-262.

Burns, M.A. and Tomkins, D.J. 1989. Hypersensitivity to mitomycin C cell-killing in Roberts syndrome fibroblasts with, but not without, the heterochromatin abnormality. Mutation Research 216: 243-249.

Buys, C.H.C.M. and Stienstra, S. 1980. Involvement of sulfhydryl groups of chromosomal proteins in sister chromatid differentiation. Chromosoma 77: 325-332.

Calderon, D. and Schnedl, W. 1973. A comparison between quinacrine fluorescence banding and ^{3}H-thymidine incorporation patterns in human chromosomes. Humangenetik 18:63-70.

Camargo, M. and Cervenka, J. 1980. Pattern of chromosomal replication in synchronized lymphocytes. Hum. Genet. 54: 47-53.

Camargo, M and Cervenka, J. 1982. Patterns of DNA replication of human chromosomes. II. Replication map and replication model. Am. J. Hum. Genet. 34: 757-780.

Chapman, V., Forrester, L., Sanford, J., Hastie, N. and Rossant, J. 1984. Cell lineage-specific undermethylation of mouse repetitive DNA. Nature 307: 284-286.

Cihak, A., Weiss, J. and Pitot, H. 1974. Characterization of polyribosomes and maturation of ribosomal RNA in hepatoma cells treated with 5-azacytidine. Cancer Res. 34: 3003-3009.

Cohen, J. 1988. Statistical Power Analysis for the Behavioral Sciences (2nd Edition). L. Erlbaum Associates, Publisher. Hillsdale, NJ, U.S.A.

Cooke, H.J. and Hindley, J. 1979. Cloning of human satellite III DNA: different components are on different chromosomes. Nucl. Acids Res. 6: 3177-3197.

Cooney, C.A. and Bradbury, E.M. 1990. DNA methylation and chromosome organization in eukaryotes. In: The Eukaryotic Nucleus: Molecular Biochemistry and Macromolecular Assemblies. Volume 2. Strauss, P.R. and Wilson, S.H. eds. Telford Press Inc. West Caldwell, N J, U.S.A. pp. 813-843.

Corneo, G., Ginelli, E., and Polli, E. 1968. Isolation of the complementary strands of a human satellite DNA. J. Mol. Biol. 33: 331-335.

Corneo, G., Ginelli, E., and Polli, E. 1970. Repeated sequences in human DNA. J. Mol. Biol. 48: 319-327.

Corneo, G., Ginelli, E., and Polli, E. 1971. Renaturation properties and localization in heterochromatin of human satellite DNA's. Biochim. Biophys. Acta. 247: 528-534.

Corneo, G., Zardi, L. and Polli, E. 1972. Elution of human satellite DNAs on a methylated albumin kieselguhr chromatographic column: isolation of satellite DNA IV. Biochim. Biophys. Acta 269: 201-204.

Davis, T., Rinaldi, A., Clark, L. and Adams, R.L.P. 1986. Methylation of chromatin in vitro. Biochim. Biophys. Acta 866: 233-241.

Dev, V.G. and Wertelecki, W. 1984. Elimination of abnormal centromere-chromatid apposition (ACCA) in selected human-mouse cell hybrids. Am. J. Hum. Genet. 36: 90S.

Drouin, R., Messier, P.-E. and Richer, C.-L . 1989. DNA denaturation for ultrastructural banding and the mechanism underlying the fluorochrome-photolysis-Giemsa technique studied with anti-5-bromodeoxyuridine antibodies. Chromosoma 98: 174-180.

DuPraw, E.J. 1965. Macromolecular organization of nuclei and chromosomes: a folded fiber model based on whole mount electron microscopy. Nature 206: 338-343.

Egan, P.A. and Levy-Wilson, B. 1981. Structure of transcriptionally active and inactive nucleosomes from butyrate-treated and control HeLa cells. Biochem. 20: 36-95.

Epplen, J.T., Siebers, J.-W. and Vogel, W. 1975. DNA replication patterns of human chromosomes from fibroblasts and amniotic fluid cells revealed by a Giemsa staining technique. Cytogen. Cell Genet. 15: 177-185.

Evans, J.S. and Mengel, G.D. 1964. The reversal of cytosine arabinoside activity in vivo by deoxycytidine. Biochem. Pharmacia 13: 989-994.

Finney, D.J. 1971. In: Probit analysis. Third edition. Cambridge University Press. Great Britain.

Fowler, J.C., Drinkwater, R.D., Burgoyne, L.A. and Skinner, J.D. 1987. Hypervariable lengths of human DNA associated with a human satellite III sequence found in the 3.4 kb Y-specific fragment. Nucl. Acids Res. 15: 3929.

Fowler, J.C., Drinkwater, R.D., Burgoyne, L.A. and Skinner, J.D. 1988. Human satellite III DNA: an example of a "macrosatellite" polymorphism. Hum. Genet. 79: 265-272.

Freeman, M.V.R., Williams, D.W., Schimke, R.N., Tetamy, S.A., Vachier, E. and German, J. 1974. The Roberts syndrome. Clin. Genet. 5: 1-16.

Frommer, M., Prosser, J., Tkachuk, D., Reisner, A.H., Vincent, P.C. 1982. Single repeated sequences in human satellite DNA. Nucl. Acids Res. 10: 547-561.

Fryns, H., Goddeeris, P., Moerman, F., Herman, F. and van den Burghe, H. 1980. The tetraphocomelia-cleft palate syndrome in identical twins. Hum. Genet. 53: 279-281.

Gama-Sosa, M.A., Slagel, V.A., Trewyn, R.W., Oxenhandler, R., Kuo, K.C., Gehrke, C.W. and Ehrlich, M. 1983. The 5-methylcytosine content of highly repeated sequences in human DNA. Nucl. Acids Res. 11: 3087-3095.

Gani, R., Sisken, J.E. and Tomkins, D.J. 1984. Evidence for an abnormality in DNA synthesis in Roberts syndrome. Am. J. Hum. Genet. 37S: A9.

Ganner E. and Evans, H.J. 1971. The relationship between patterns of DNA replication and of quinacrine fluorescence in the human chromosome complement. Chromosoma 35: 326-341.

Gatti, M., Smith, D.A. and Baker, B.S. 1983. A gene controlling condensation of heterochromatin in Drosophila melanogaster. Science 221: 83-85.

Gentner, N.E., Tomkins, D.J. and Paterson, M.C. 1985. Roberts syndrome fibroblast with heterochromatin abnormality show hypersensitivity to carcinogen-induced cytotoxicity. Am. J. Hum. Genet. 37 suppl.: A231.

Gentner, N.E., Smith, B.P., Norton, G.M., Courchesne, L., Moeck, L. and Tomkins, D.J. 1986. Carcinogen hypersensitivity in cultured fibroblast strains from Roberts syndrome patients. Proc. Can. Fed. Biol. Sci. 29:144.

German, J. 1979. Roberts' syndrome. I. Cytological evidence for a disturbance in chromatid pairing. Clin. Genet. 16: 441-447.

Gosden, J.R., Buckland, R.A., Clayton, R.P. and Evans, H.J. 1975a. Chromosomal localisation of DNA sequences in condensed and dispersed human chromatin. Exp. Cell Res. 92: 138-147.

Gosden, J.R., Mitchell, A.R., Buckland, R.A., Clayton, R.P. and Evans, H.J. 1975b. The location of four human satellite DNAs on human chromosomes. Exp. Cell Res. 92:148-158.

Gottesfeld, J.M., Garrard, W.T., Wilson, R.F. and Bonner, J. 1974. Partial purification of the template-active fraction of chromatin: a preliminary report. Proc. Natl. Acad. Sci. USA. 71: 2193-2197.

Grosse, F.R., Pandel, C. and Wiedemann, H.R. 1975. The tetraphocomelia-cleft palate syndrome. Humangenetik 28: 353-356.

Grzeschik, K.-H., Kim, M.A. and Johannsmann, R. 1975. Late replicating bands if human chromosomes demonstrated by fluorochrome and Giemsa staining. Humangenetik 29: 41-59.

Gunby, J.L. 1986. Manipulations of Roberts syndrome cells. M.Sc. thesis. McMaster University.

Gunby, J.L., Tomkins, D.J. and Chang, P.L. 1987. Somatic cell hybridization of Roberts syndrome and normal fibroblasts transfected with plasmids carrying dominant selection markers. Som. Cell Mol. Genet. 13: 245-252.

Hancock, R. and Boulikas, T. 1982. Functional organization in the nucleus. Int. Rev. Cyt. 79: 165-214.

Harbers, K., Harbers, B., and Spencer, J.H. 1975. Nucleotide clusters in deoxyribonucleic acids. XII. The distribution of 5-methylcytosine in pyrimidine oligonucleotides of mouse L-cell satellite DNA and main band DNA. Biochim. Biophys. Acta 66: 738-746.

Heitz, E. 1928. Das Heterochromatin der Moose. I. Jahrb. Wissensch. Bot. 69: 762-818 (cited in John, 1988).

Herrmann, J., Feingold, M., Tuffli, G.A. and Opitz, J.M. 1969. A familial dysmorphogenetic syndrome of limb deformities, characteristic facial appearance and associated anomalies: The "pseudothalidomide" or "SC-syndrome". Birth Defects 5(3): 81-89.

Herrmann, J. and Opitz, J.M. 1977. The SC phocomelia and the Roberts syndrome: nosologic aspects. Eur. J. Pediatr. 125: 117-134.

Higgins, M.J., Wang, H., Shtromas, I., Haliotis, T., Roder, J.C., Holden, J. and White, B.N. 1985. Organization of a repetitive human 1.8 kb KpnI sequence localized in the heterochromatin of chromosome 15. Chromosoma 93: 77-86.

Hilliker, A.J. and Appels, R. 1980. The genetic analysis of D. melanogaster heterochromatin. Cell 21: 607-619.

Holmquist, G. 1987. Role of replication time in the control of tissue-specific gene expression. Am. J. Hum. Genet. 40: 151-173.

Holmquist, G., Gray, M., Porter, T. and Jordan, J. 1982. Characterization of Giemsa dark and light band DNA. Cell 31: 121-129.

Howlett, D., Dalrymple, S. and Mays-Hoopes, L.L. 1989. Age-related demethylation of mouse satellite DNA is easily detectable by HPLC but not by restriction endonucleases. Mut. Res. 219: 101-106.

Igo-Kemenes, T., Horz, W. and Zachau, H.G. 1982. Chromatin. Ann. Rev. Biochem. 51: 89-121.

Izumikawa, Y., Naritomi, K. and Hirayama, K. 1991. Replication asynchrony between homologs 15q11.2: cytogenetic evidence for genomic imprinting. Hum. Genet. 87: 1-5.

John, B. 1988. The biology of heterochromatin. In: Heterochromatin: molecular and structural aspects. R.S. Verma, ed. Cambridge University Press, New York, U.S.A. pp.1-147.

Jones, P.A. and Taylor, S.M. 1980. Cellular differentiation, cytidine analogs and DNA methylation. Cell 20: 85-93.

Judge, C. 1973. A sibship with the pseudothalidomide syndrome and an association with Rh incompatibility. Med. J. Aust. 2:280-281.

Kautiainen, T.L. and Jones, P.A. 1985. Effects of DNA binding proteins on DNA methylation in vitro. Biochem. 24: 1193-1196.

Keshet, I., Lieman-Hurwitz, J. and Cedar, H. 1986. DNA methylation affects the formation of active chromatin. Cell 44: 535-543.

Knight, L.A. and Luzzatti, L. 1973. Replication pattern of the X and Y chromosomes in partially synchronized human lymphocyte cultures. Chromosoma 40: 153-166.

Knoll, J.H. and Ray, M. 1986. Roberts syndrome: Correction of chromosomal abnormality by somatic cell fusion. G.S.C. Bull. 17:70A.

Kondra, P.M. and Ray, M. 1978. Analysis of DNA replication patterns of human fibroblast chromosomes the replication map. Hum. Genet. 43: 139-149.

Krassikoff, N.E., Cowan, J.M., Parry, D.M. and Francke, U. 1986. Chromatid repulsion associated with Roberts/SC phocomelia syndrome is reduced in malignant cells and not expressed in interspecies somatic-cell hybrids. Am. J. Hum. Genet. 39: 618-630.

Laskey, R.A., Fairman, M.P. and Blow, J.J. 1989. S phase of the cell cycle. Science 246: 609-614.

Latt, S.A. 1973. Microfluorometric detection of deoxyribonucleic acid replication in human metaphase chromosomes. Proc. Natl. Acad. Sci. USA. 70: 3395-3399.

Lawler, S.D., Roberts, P.D. and Hoffbrand, A.V. 1971. Chromosome studies in megaloblastic anaemia before and after treatment. Scand. J. Haemat. 8: 309-320.

Lewis, C.D. and Laemmli, U.K. 1982. Higher order metaphase chromosome structure: evidence for metalloprotein interactions. Cell 29: 171-181.

Louie, E. and German, J. 1981. Robert's syndrome. II. Aberrant Y chromosome behavior. Clin. Genet. 19: 71-74.

Lubit, B.W., Pham, T.D., Miller, O.J. and Erlanger, B.F. 1976. Localization of 5-methylcytosine in human metaphase chromosomes by immunoelectron microscopy. Cell 9: 503-509.

Macgregor, H.C. and Kezer, J. 1971. The chromosomal localization of a heavy satellite DNA in the testis of Plethodon cinereus cinereus. Chromosoma 33: 167-182. (cited in John, 1988)

Maniatis, T., Fritsch, E.F. and Sambrook, J. 1982. Molecular cloning (a laboratory manual). Cold Spring Harbor Laboratory. Cold Spring Harbor, NY, U.S.A.

Manuelidis, L. 1978a. Complex and simple sequences in human repeated DNAs. Chromosoma 66: 1-21.

Manuelidis, L 1978b. Chromosomal localization of complex and simple repeated human DNAs. Chromosoma 66: 23-32.

Manuelidis, L. 1985. Individual interphase chromosome domains revealed by in situ hybridization. Hum. Genet. 71: 288-293.

Mathis, D., Oudet, P. and Chambon, P. 1980. Structure of transcribing chromatin. Prog. Nucl. Acids. Res. Mol. Biol. 24: 1-24.

Mays-Hoopes, L.L. 1989. Age-related changes in DNA methylation: Do they represent continued developmental changes? Int. Rev. Cytol. 114: 181-220.

McGhee, J.D and Ginder, G.D. 1979. Specific DNA methylation sites in the vicinity of the chicken β-globin genes. Nature 280: 419-420.

McGhee, J.D. and Felsenfeld, G. 1980. Nucleosome structure. Annu. Rev. Biochem. 49: 1115-1156.

Mezzanotte, R., Peretti, D., Orru, S., Rossine, R., Ennas, M.G., Gosalvex, J. 1989. DNA alteration induced by ultraviolet light in human metaphase chromosomes substituted with 5'-bromodeoxyuridine: monitoring by monoclonal antibodies to double-stranded and single stranded DNA. Chromosoma 97: 356-362.

Miller, O.J., Schnedl, W., Allen, J. and Erlanger, B.F. 1974. 5-Methylcytosine localised in mammalian constitutive heterochromatin. Nature 251: 636-637.

Mitchell, A.R., Beauchamp, R.S., and Bostock, C.J. 1979. Study of sequence homologies in four satellite DNAs of man. J. Mol. Biol. 135: 127-149.

Mitchell, A.R., Gosden, J.R. and Miller, D.A. 1985. A cloned sequence, p82H, of the alphoid repeated DNA family found at the centromeres of all human chromosomes. Chromosoma 92: 369-377.

Morgan, A.R., Lee, J.S., Pulleybank, D.F., Murray, N.L., and Evans, D.H. 1979. Review: Ethidium fluorescence assays. Part I. Physiochemical studies. Nucl. Acids Res. 7: 547-569.

Moyzis, R.K., Albright, K.L., Bartholdi, M.F., Cram, L.S., Deaven, L.L., Hildebrand, C.E., Joste, N.E., Longmire, J.L., Meyne, J., and Schwarzacher-Robinson, T. 1987. Human chromosome-specific repetitive DNA sequences: novel markers for genetic analysis. Chromosoma 95: 375-386.

Neitzel, H. 1986. A routine method for the establishment of permanent growing lymphoblastoid cell lines. Hum. Genet. 73: 320-326.

Olins, A.L. and Olins, D.E. 1979. Stereo electron microscopy of the 25 nm chromatin fibers in isolated nuclei. J. Cell Biol. 81: 260-265.

Paulson, C., Mann, E., Rabin, A., Marion, R. Nitowsky, H. and Schmidt, R. 1989. Premature centromeric separation in an obligate heterozygote for Roberts-SC phocomelia syndrome. Am. J. Hum. Genet. 45(4): A87.

Prosser, J., Frommer, M., Paul, C. and Vincent, P.C. 1986. Sequence relationships of three human satellite DNAs. J. Mol. Biol. 187: 145-155.

Rappold, G.A., Cremer, T., Hager, H.D., Davies, K.E., Muller, C.R. and Yang, T. 1984. Sex chromosome position in human interphase nuclei as studies by in situ hybridization with chromosome specific DNA probes. Hum. Genet. 67: 317-325.

Rattner, J.B. and Lin, C-C. 1988. The organization of the centromere and centromeric heterochromatin. In: Heterochromatin: molecular and structural aspects. R.S. Verma, ed. Cambridge University Press, New York, U.S.A. pp.203-227.

Razin, A. and Riggs, A.D. 1980. DNA methylation and gene function. Science 210: 604-610.

Razin, A., Feldmesser, B., Kafris, T. and Szyf, M. 1985. In: Biochemistry and Biology of DNA Methylation. Cantoni, G. and Razin, A., eds. Wiley Publishers. New York, NY. U.S.A. pp. 239-254.

Reeves, R. 1984. Transcriptionally active chromatin. Biochim. Biophys. Acta 782: 343-393.

Ris, H. and Korenberg, J. 1979. Chromosome structure and levels of organization. In: Cell Biology, Vol. 2. D.M. Prescott and L. Goldstein, eds. Academic Press, New York, U.S.A. pp. 268-361.

Roberts, J.B. 1919. A child with double cleft lip and palate, protrusion of the intermaxillary portion of the upper jaw and an imperfect development of the bones of the four extremities. Ann. Surg. 70: 252-253.

Saksela, E. and Moorhead, P.S. 1962. Enhancement of secondary constrictions and the heterochromatic X in human cells. Cytogenetics 1: 225-244.

Sanford, J., Forrester, L., Chapman, V., Chandley, A. and Hastie, N. 1984. Methylation patterns of repetitive DNA sequences in germ cells of Mus musculus. Nucl. Acids Res. 12: 2823-2836.

Sasaki, M.S. and Makino, S. 1963. The demonstration of secondary constrictions in human chromosomes by means of a new technique. Am. J. Hum. Genet. 15: 24-33.

Savage, J.R.K. and Papworth, D.G. 1988. A method for comparing DNA replication programmes at the level of the chromosome bands. J. Theor. Biol. 134: 365-377.

Savage, J.R.K., Prasad, R. and Papworth, D.G. 1984. Subdivision of S-phase and its use for comparative purposes in cultured human cells. J. Theor. Biol. 111: 355-367.

Schemp, W., Sigwarth, I. and Vogel, W. 1978. Demonstration of replication patterns corresponding to G- and R-type banding of chromosomes after partial synchronization of cell cultures with BrdU or dT surplus. Hum. Genet. 45: 199-202.

Schmid, M, Haaf, T. and Grunert, D. 1984. 5-Azacytidine-induced undercondensation in human chromosomes. Hum. Genet. 67:257-263.

Schmid, W. 1963. DNA replication patterns of human chromosomes. Cytogenetics 2: 175-193.

Schmid, W. and Leppert, M.F. 1969. Rates of DNA synthesis in heterochromatic and euchromatic segments of the chromosome complements of two rodents. Cytogenetics 8: 125-135.

Schmidt, M. 1980. Two phases of DNA replication in human cells. Chromosoma 76: 101-110.

Shafer, D.A. and Priest, J.H. 1984. Reversal of DNA methylation with 5-azacytidine alters chromosome replication patterns in human lymphocyte and fibroblast cultures. Am. J. Med. Genet. 36: 534-545.

Shmookler-Reis, R. and Goldstein, S. 1980. Loss of reiterated DNA sequences during serial passage of human diploid fibroblasts. Cell 21:739-749.

Shmookler-Reis, R. and Goldstein, S. 1982a. Variability of DNA methylation patterns during serial passage of human diploid fibroblasts. Proc. Natl. Acad. Sci. USA. 79: 3949-3953.

Shmookler-Reis, R. and Goldstein, S. 1982b. Interclonal variation in methylation patterns for expressed and non-expressed genes. Nucl. Acids. 10:4293-4304.

Simmons, M.C., Maxwell, J., Hallotis, T., Higgins, M.J., Roder, J.C., White, B.N. and Holden, J.J.A. 1984. Amplified KpnI repetitive DNA sequences in homogenously staining regions of a human melanoma cell line. J.N.C.I. 72: 801-808.

Singer, M.F. 1982. Highly repeated sequences in mammalian genomes. Int. Rev. Cytol. 76: 67-76.

Singer, J., Stellwagan, R.H., Roberts-Ems, J. and Riggs, A. 1977. 5-Methylcytosine content of rat hepatoma DNA substituted with bromodeoxyuridine. J. Biol. Chem. 252: 5509-5513.

Solage, A. and Cedar, H. 1978. Organization of 5-methylcytosine in chromosomal DNA. Biochemistry 17:2934-2938.

Stubblefield, E. 1975. Replication pattern of Chinese hamster chromosomes. Chromosoma 53: 209-221.

Sumner, A.T. 1972. A simple technique for demonstrating centromeric heterochromatin. Exp. Cell. Res. 75: 304-306.

Taylor, J.H., Woods, P.S. and Hughes, W.L. 1957. The organization and duplication of chromosomes as revealed by autoradiographic studies using tritium labelled thymidine. Proc. Natl. Acad. Sci. USA. 43: 122-128.

Tomkins, D.J. 1978. Cytogenetic findings in Roberts-SC phocomelia syndrome. Am. J. Hum. Genet. 30:95A.

Tomkins, D.J., Hunter, A. and Roberts, M. 1979. Cytogenetic findings in Roberts-SC phocomelia syndrome(s). Am. J. Med. Genet. 4:17-26.

Tomkins, D.J. and Siskens, J.E. 1984. Abnormalities in the cell-division cycle in Roberts syndrome fibroblasts: A cellular basis for the phenotypic characteristics? Am. J. Hum. Genet. 36: 1332-1340.

Tyers, M, D. 1988. Molecular aspects of differentiation in the HL-60 promyelocytic leukemia cell line. Ph.D thesis. McMaster University.

Verma, R.S., Jacob, J.P. and Babu, A. 1986. Heterochromatin organization in the nucleus of the Indian muntjac (Muntiacus muntjac). Can. J. Gen. Cyt. 28: 628-630.

Verma, R.S. and Babu, A. 1989. Human chromosomes: manual of basic techniques. Pergammon Press Inc. New York, U.S.A

Viegas-Pequignot, E. and Dutrillaux, B. 1976. Segmentation of human chromosomes induced by 5-ACR (5-azacytidine). Hum. Genet. 34: 247-254.

Vig, B.K. 1981. Sequence of centromere separation: Analysis of mitotic chromosomes in man. Hum. Genet. 57: 247-252.

Vogel, W., Boldin, S., Reisacher, A. and Speit, G. 1985. Characterization of chromosome replication during S-phase with bromodeoxyuridine labelling in Chinese hamster ovary and HeLa cells. Chromosoma 92: 363-368.

Waalwijk, C. and Flavell, R.A. 1978. DNA methylation at a CCGG sequence in the large intron of the rabbit β-globin gene: tissue-specific variations. Nucl. Acids Res. 12: 4631-4641.

Ward, C., Bolden, A., Nalin, C.M. and Weissbach, A. 1987. In vitro methylation of the 5'-flanking regions of the mouse β-globin gene. J. Biol. Chem. 262: 11057-11063.

Weintraub, H. and Groudine, M. 1976. Chromosomal subunits in active genes have altered conformation. Science 193: 848-856.

Weisbrod, S. 1982. Active chromatin. Nature 297: 289-295.

Weissbach, A., Ward, C. and Bolden, A. 1989. Eukaryotic DNA methylation and gene expression. Current Topics in Cellular Regulation 30:1-21.

Wigler, M.H. 1981. The inheritance of methylation patterns in vertebrates. Cell 24: 285-286.

Wilson, V.L. and Jones, P.A. 1983. DNA methylation decreases in aging but not immortal cells. Science 220: 1055-1057.

Wolf, S. and Perry, P. 1974. Differential Giemsa staining of sister chromatids and the study of sister chromatid exchanges without autoradiography. Chromosoma 48: 341-353.

Yamamoto, M. 1977. Cytological studies of heterochromatin function in the Drosophila melanogaster male: autosomal meiotic pairing. Chromosoma 72: 293-328 (cited in John, 1988).

Yamato, M. and Miklos, G.L.G. 1977. Genetic dissection of heterochromatin in Drosophila: the role of basal X chromosome heterochromatin in meiotic sex chromosome behavior. Chromosoma 60: 71-98 (cited in John, 1988).

Yunis, J.J. and Yasmineh, W.G. 1971. Heterochromatin, satellite DNA and cell function. Science 174: 1200-1209.

Zakharov, A.F., Baranovskaya, L.T., Ibraimov, A.I. Benjusch, V.A., Demintseva, V.S. and Oblapenko, N.G. 1974. Differential spiralization along mammalian mitotic chromosomes. II. Bromodeoxyuridine and 5-Bromodeoxycytidine-revealed differentiation in human chromosomes. Chromosoma 44: 343-359.

Zakharov, A.F. and Egolina, N.A. 1972. Differential
 spiralization along mammalian mitotic chromosomes. I.
 5-Bromodeoxyuridine and 5-Bromodeoxycytidine-revealed
 differentiation in human chromosomes. Chromosoma 38:
 341-365.

Zergollen, L. and Hitrec, V. 1982. Four siblings with
 Robert's syndrome. Clin. Genet. 21: 1-6.

Appendix 1 - Data

Table A-1: Quantitative comparison of the linear binding of
D15Z1 to increasing amounts of MspI and HpaII digested control
genomic DNA isolated from a fibroblast cell strain, GM0969B
P23, using densitometry scanning. (Experiment 1)

Band (kb)	Area OD (A)	Band (kb)	Area OD (B)	Ratio A/B
LANE 1: 1.5 ug DNA MspI		**LANE 2: 1.5 ug DNA HpaII**		
6.0	-*	6.0	-	A>B
4.0	0.214	4.0	-	A>B
3.5	1.013	3.5	-	A>B
LANE 3: 2.5 ug DNA MspI		**LANE 4: 2.5 ug DNA HpaII**		
6.0	0.042	6.0	-	A>B
4.0	0.166	4.0	-	A>B
3.5	3.332	3.5	-	A>B
LANE 5: 3.5 ug DNA MspI		**LANE 6: 3.5 ug DNA HpaII**		
6.0	0.489	6.0	-*	A>B
4.0	0.433	4.0	-*	A>B
3.5	5.262	3.5	0.192	27.406
LANE 7: 5.0 ug DNA MspI		**LANE 8: 5.0 ug DNA HpaII**		
6.0	0.490	6.0	-*	A>B
4.0	0.486	4.0	0.184	2.641
3.5	5.854	3.5	0.093	62.946

* Band visible on autoradiograph but could not be
distinguished by densitometry scanning.

Table A-2: Quantitative comparison of the linear binding of D15Z1 to increasing amounts of MspI and HpaII digested control genomic DNA isolated from a fibroblast cell strain, GM0969B P23, using densitometry scanning. (Experiment 2)

Band (kb)	Area OD (A)	Band (kb)	Area OD (B)	Ratio A/B
LANE 1: 1.5 ug DNA MspI		LANE 2: 1.5 ug DNA HpaII		
6.0	0.912	6.0	0.104	8.769
4.0	1.748	4.0	0.082	21.317
3.5	6.907	3.5	0.506	13.650
LANE 3: 2.5 ug DNA MspI		LANE 4: 2.5 ug DNA HpaII		
6.0	0.327	6.0	0.243	1.345
4.0	0.153	4.0	0.245	0.624
3.5	8.240	3.5	0.911	9.045
LANE 5: 3.5 ug DNA MspI		LANE 6: 3.5 ug DNA HpaII		
6.0	0.738	6.0	-*	A>B
4.0	1.332	4.0	0.096	13.875
3.5	8.644	3.5	0.351	24.626
LANE 7: 5.0 ug DNA MspI		LANE 8: 5.0 ug DNA HpaII		
6.0	0.893	6.0	0.085	10.505
4.0	1.220	4.0	0.143	8.531
3.5	7.653	3.5	0.779	9.824

* Band visible on autoradiograph but could not be distinguished by densitometry scanning.

Table A-3: Quantitative comparison of the linear binding of D15Z1 to increasing amounts of MspI and HpaII digested control genomic DNA isolated from a fibroblast cell strain, GM3349 P36, using densitometry scanning. (Experiment 3)

Band (kb)	Area OD (A)	Band (kb)	Area OD Ratio (B)	A/B
LANE 1: 1.5 ug DNA MspI		LANE 2: 1.5 ug DNA HpaII		
6.0	–	6.0	–	–
4.0	–	4.0	–	–
3.5	1.090	3.5	–	A>B
LANE 3: 2.5 ug DNA MspI		LANE 4: 2.5 ug DNA HpaII		
6.0	–	6.0	–	–
4.0	–	4.0	–	–
3.5	4.010	3.5	–	A>B
LANE 5: 3.5 ug DNA MspI		LANE 6: 3.5 ug DNA HpaII		
6.0	0.060	6.0	–	A>B
4.0	0.143	4.0	–	A>B
3.5	5.272	3.5	0.186	28.344
LANE 7: 5.0 ug DNA MspI		LANE 8: 5.0 ug DNA HpaII		
6.0	–*	6.0	–	A>B
4.0	–*	4.0	–	A>B
3.5	2.602	3.5	–	A>B

* Band visible on autoradiograph but could not be distinguished by densitometry scanning.

Table A-4: Quantitative comparison of the linear binding of
D15Z1 to increasing amounts of MspI and HpaII digested control
genomic DNA isolated from a fibroblast cell strain, GM3349
P36, using densitometry scanning. (Experiment 4)

Band (kb)	Area OD Band (A)	(kb)	Area OD (B)	Ratio A/B
LANE 1: 1.5 ug DNA MspI		LANE 2: 1.5 ug DNA HpaII		
6.0	0.267	6.0	-	A>B
4.0	-	4.0	-	-
3.5	1.374	3.5	0.153	8.980
LANE 3: 2.5 ug DNA MspI		LANE 4: 2.5 ug DNA HpaII		
6.0	0.395	6.0	0.212	1.863
4.0	-*	4.0	0.399	A=B
3.5	1.220	3.5	0.272	4.485
LANE 5: 3.5 ug DNA MspI		LANE 6: 3.5 ug DNA HpaII		
6.0	0.997	6.0	0.972	1.025
4.0	-*	4.0	-	A>B
3.5	2.707	3.5	2.345	1.154
LANE 7: 5.0 ug DNA MspI		LANE 8: 5.0 ug DNA HpaII		
6.0	0.986	6.0	-*	A>B
4.0	-*	4.0	-*	A>B
3.5	3.631	3.5	0.823	4.411

* Band visible on autoradiograph but could not be
distinguished by densitometry scanning.

Table A-5: Quantitative comparison of the linear binding of D15Z1 to increasing amounts of MspI and HpaII digested control genomic DNA isolated from a fibroblast cell strain, GM3349 P30, using densitometry scanning. (Experiment 5)

Band (kb)	Area OD (A)	Band (kb)	Area OD (B)	Ratio A/B
LANE 1: 1.5 ug DNA MspI		LANE 2: 1.5 ug DNA HpaII		
6.0	0.201	6.0	0.118	1.703
4.0	−	4.0	−	−
3.5	0.366	3.5	−	A>B
LANE 3: 2.5 ug DNA MspI		LANE 4: 2.5 ug DNA HpaII		
6.0	0.219	6.0	−*	A>B
4.0	−*	4.0	−*	A>B
3.5	1.054	3.5	−	A>B
LANE 5: 3.5 ug DNA MspI		LANE 6: 3.5 ug DNA HpaII		
6.0	0.322	6.0	−*	A>B
4.0	−*	4.0	0.139	A<B
3.5	2.199	3.5	0.232	9.478
LANE 7: 5.0 ug DNA MspI		LANE 8: 5.0 ug DNA HpaII		
6.0	0.949	6.0	0.245	3.873
4.0	0.088	4.0	−	A>B
3.5	3.088	3.5	0.226	13.663

* Band visible on autoradiograph but could not be distinguished by densitometry scanning.

Table A-6: Quantitative comparison of the linear binding of D15Z1 to increasing amounts of MspI and HpaII digested control genomic DNA isolated from a fibroblast cell strain, S6007 P15, using densitometry scanning. (Experiment 6)

Band (kb)	Area OD (A)	Band (kb)	Area OD (B)	Ratio A/B
LANE 1: 3.0 ug DNA MspI		LANE 2: 3.0 ug DNA HpaII		
6.0	3.026	6.0	–	A>B
4.0	1.032	4.0	–	A>B
3.5	6.794	3.5	–	A>B
LANE 3: 2.0 ug DNA MspI		LANE 4: 2.0 ug DNA HpaII		
6.0	0.754	6.0	–	A>B
4.0	1.068	4.0	–.	A>B
3.5	5.635	3.5	–	A>B
LANE 5: 1.0 ug DNA MspI		LANE 6: 1.0 ug DNA HpaII		
6.0	0.427	6.0	–	A>B
4.0	0.111	4.0	–	A>B
3.5	0.787	3.5	–	A>B
LANE 7: 0.5 ug DNA MspI		LANE 8: 0.5 ug DNA HpaII		
6.0	0.243	6.0	–	A>B
4.0	–	4.0	–	–
3.5	0.827	3.5	–	A>B

Table A-7:   Comparison of D15Z1 DNA methylation levels of genomic DNA isolated from RS+ fibroblast cell strains, S6012 and R22, and control cell strains, GM0969B and GM3349, at early and late passages using MspI and HpaII restriction analysis (Experiment 7).

| Cell Strain | Area OD (mm) | | |
	MspI 3.5 kb band (A)	HpaII 3.5 kb band (B)	Ratio (A/B)
S6012 P10	2.589	0.088	29.420
GM0969B P23	3.902	0.088*	44.340
R22 P26	2.316	0.159	14.566
GM3349 P32	1.995	0.088*	22.670

* Area OD (mm) of HpaII 3.5 kb band obtained from S6012 HpaII 3.5 kb band

Table A-8. Comparison of D15Z1 DNA methylation levels of genomic DNA isolated from an RS+ fibroblast cell strain, S6012, and a control cell strain, GM0969B, at early and late passages using MspI and HpaII restriction analysis (Experiment 8).

Cell Strain	Area OD (mm)		
	MspI 3.5 kb band (A)	HpaII 3.5 kb band (B)	Ratio (A/B)
S6102 P12	3.098	0.281	11.024
S6012 P32	1.781	0.479	3.718
GM0969B P23	4.631	0.385	12.029
GM0969B P35	3.905	0.249	15.683

Table A-9. Comparison of D15Z1 DNA methylation levels of genomic DNA isolated from an RS+ fibroblast cell strain, S6012, and a control cell strain, GM0969B, at early and late passages using MspI and HpaII restriction analysis (Experiment 9).

| Cell Strain | Area OD (mm) | | |
	MspI 3.5 kb band (A)	HpaII 3.5 kb band (B)	Ratio (A/B)
S6012 P12	3.426	1.358	2.522
S6012 P36	2.990	0.604	4.950
GM0969B P19	2.833	−*	−
GM0969B P23	3.592	0.412	8.718

* Area OD value for 3.5 kb band excluded from statistical analysis due to autoradiograph whiteout

Table A-10. Comparison of D15Z1 DNA methylation levels of genomic DNA isolated from an RS+ fibroblast cell strain, R22, and a control cell strain, GM3349, at early and late passages using MspI and HpaII restriction analysis (Experiment 10).

Cell Strain	Area OD (mm)		
	MspI 3.5 kb band (A)	HpaII 3.5 kb band (B)	Ratio (A/B)
R22 P16	6.864	1.692	4.057
R22 P27	2.316	1.284	1.804
GM3349 P18	5.327	0.474	11.238
GM3349 P30	6.517a	0.417*	15.628*

* Area OD value for 3.5 kb band excluded from statistical analysis due to autoradiograph whiteout

Table A-11. Comparison of D15Z1 DNA methylation levels of genomic DNA isolated from an RS+ fibroblast cell strain, R22, RS- cell strain, S6006 and control cell strains, GM3349, at early and late passages using MspI and HpaII restriction analysis (Experiment 11).

Cell Strain	Area OD (mm)		
	MspI 3.5 kb band (A)	HpaII 3.5 kb band (B)	Ratio (A/B)
R22 P12	5.409	0.110*	49.173*
GM3349	5.362	0.131	40.931
S6006 P20	5.357	0.110*	48.700*
GM0969B P23	6.370	0.110	57.909

* Area OD (mm) of HpaII 3.5 kb band obtained from GM0969B HpaII 3.5 kb band

Table A-12. Comparison of D15Z1 DNA methylation levels of genomic DNA isolated from an RS- fibroblast cell strain, S6006, and a control cell strain, GM0969B, at early and late passages using MspI and HpaII restriction analysis (Experiment 12).

Cell Strain	Area OD (mm)		
	MspI 3.5 kb band (A)	HpaII 3.5 kb band (B)	Ratio (A/B)
S6006 P20	1.717	0.855	2.008
S6006 P30	2.820	0.710	3.972
GM0969B P19	4.693	1.149	4.084
GM0969B P23	6.613	0.485	13.635

Table A-13. Comparison of D15Z1 DNA methylation levels of genomic DNA isolated from an RS- fibroblast cell strain, S6008, and a control cell strain, S6007, at early and late passages using MspI and HpaII restriction analysis (Experiment 13).

Cell Strain	Area OD (mm)		
	MspI 3.5 kb band (A)	HpaII 3.5 kb band (B)	Ratio (A/B)
S6008 P15	5.558	0.311*	17.871*
S6008 P28	5.233	0.311*	16.826*
S6007 P15	5.213	0.311	16.762
S6007 P31	6.114	0.428	14.285

* Area OD (mm) of HpaII 3.5 kb band obtained from S6007 P15 HpaII 3.5 kb band

Table A-14. Comparison of D15Z1 DNA methylation levels of genomic DNA isolated from an RS- fibroblast cell strain, S6008, and a control cell strain, S6007, at early and late passages using MspI and HpaII restriction analysis (Experiment 14).

| Cell Strain | Area OD (mm) | | |
	MspI 3.5 kb band (A)	HpaII 3.5 kb band (B)	Ratio (A/B)
S6008 P15	2.972	0.218*	13.633*
S6008 P15	1.504	0.218	6.899
S6007 P15	1.075	0.218*	4.931*
S6007 P34	1.363	0.504	2.704

* Area OD (mm) of HpaII 3.5 kb band obtained from S6008 P15 HpaII 3.5 kb band

Table A-15. Area OD of autoradiograph of MspI/EcoRI and HpaII/EcoRI digested RS+ (S6102) fibroblast genomic DNA (Experiment 16)

Lane 1 Band (kb)	S6102 P10 M/E Area OD (A)	Area OD/Ref (C)	Lane 2 S6012 P10 H/E Area OD (B)	Area OD/Ref (D)	Ratio (C/D)
0.5	0.180	0.076	—	—	C>D
1.6[R]	2.378	1.000	1.784	1.000	1.000
1.8	0.310	0.130	0.457	0.256	0.507
1.8+	0.115	0.048	0.434	0.243	0.198
2.5	0.629	0.265	0.154	0.086	3.070
3.0	0.047	0.020	0.096	0.054	0.370
3.6	2.262	0.951	1.406	0.788	1.206
4.0	0.371	0.156	0.119	0.066	2.363
4.3	0.312	0.131	0.119	0.067	1.955
5.0	1.006	0.423	0.998	0.559	0.423
6.4	0.240	0.100	0.564	0.316	0.757
12.0	0.476	0.200	0.953	0.534	0.374
+23	6.984	2.936	9.619	5.391	0.544

R   Reference band Area OD used to calculate C=Area OD band/Area OD Reference band

Table A-16. Area OD of autoradiograph of MspI/EcoRI and HpaII/EcoRI digested RS+ (S6102) fibroblast genomic DNA (Experiment 16)

Lane 3 Band (kb)	S6102 P28 Area OD (A)	M/E Area OD/Ref (C)	Lane 4 Area OD (B)	S6012 P28 Area OD/Ref (D)	H/E Ratio (C/D)
0.5	0.522	0.543	–	–	C>D
1.6[R]	0.961	1.000	2.700	1.000	1.000
1.8	0.326	0.339	0.207	0.076	4.460
1.8+	0.140	0.145	0.395	0.146	0.993
2.5	0.279	0.290	0.039	0.014	20.714
3.0	0.070	0.072	0.115	0.042	1.714
3.6	1.941	2.019	1.824	0.675	2.991
4.0	0.197	0.204	0.133	0.049	4.163
4.3	0.126	0.131	0.124	0.045	2.911
5.0	1.106	1.150	1.654	0.612	1.879
6.4	0.509	0.529	0.415	0.153	3.457
+23	19.801	20.604	16.368	6.062	3.398

R   Reference band Area OD used to calculate C=Area OD band/Area OD Reference band

Table A-17. Area OD of autoradiograph of MspI/EcoRI and HpaII/EcoRI digested control (GM0969B) fibroblast genomic DNA (Experiment 16)

Lane 5 Band (kb)	GM0969B P23 M/E Area OD (A)	Area OD/Ref (C)	Lane 6 GM0969B P23 H/E Area OD (B)	Area OD/Ref (D)	Ratio (C/D)
0.5	0.824	0.155	0.147	0.026	5.961
1.0	0.220	0.041	–	–	C>D
1.6^R	5.289	1.000	5.501	1.000	1.000
1.8	0.832	0.157	1.090	0.198	0.792
1.8+	0.436	0.082	0.618	0.112	0.732
2.5	1.644	0.310	–*	–	C>D
3.0	0.302	0.057	0.410	0.074	0.770
3.6	2.289	0.432	2.353	0.427	1.011
4.0	0.244	0.046	0.011	0.001	46.000
5.0	2.678	0.506	1.727	0.313	1.616
5.4	0.871	0.164	0.977	0.177	0.926
+23	18.153	3.423	10.322	1.876	1.825

* Band visible on autoradiograph but could not be distinguished by densitometry scanning.
R Reference band Area OD used to calculate C=Area OD band/Area OD Reference band

Table A-18.   Area OD of autoradiograph of MspI/EcoRI and HpaII/EcoRI digested control (GM0969B) fibroblast genomic DNA (Experiment 16)

Lane 7 Band (kb)	GM0969B Area OD (A)	P32 M/E Area OD/Ref (C)	Lane 8 Area OD (B)	GM0969B Area OD/Ref (D)	P32 H/E Ratio (C/D)
0.5	0.628	0.419	0.174	0.073	5.739
1.6^R	1.498	1.000	2.355	1.000	1.000
1.8	0.204	0.136	0.358	0.152	0.894
1.8+	0.308	0.205	0.724	0.307	0.667
2.5	0.261	0.174	0.097	0.041	4.243
3.0	0.203	0.135	0.195	0.082	1.646
3.6	0.923	0.616	1.304	0.553	1.113
4.0	0.045	0.030	0.060	0.025	1.200
5.0	0.912	0.608	0.704	0.298	2.040
6.4	0.963	0.642	0.763	0.323	1.987
+23	14.287	9.537	16.769	7.120	1.339

R   Reference band Area OD used to calculate C=Area OD band/Area OD Reference band

Table A-19.   Area OD of autoradiograph of <u>Msp</u>I/<u>Eco</u>RI and <u>Hpa</u>II/<u>Eco</u>RI digested RS+ (R22) fibroblast genomic DNA (Experiment 17)

Band (kb)	Lane 1 R22 P12 M/E Area OD (A)	Area OD/Ref (C)	Lane 2 R22 P12 H/E Area OD (B)	Area OD/Ref (D)	Ratio (C/D)
0.5	–	–	–	–	–
1.6[R]	1.146	1.000	2.675	1.000	1.000
1.8	1.841	1.606	3.759[a]	1.405	1.143
1.8+	–	–	0.119	0.044	C>D
2.5	1.538	1.342	–	–	C>D
3.3	–*	–	0.087	0.032	C=D
3.6	2.884	2.516	2.467	0.922	2.728
3.8	–*	–	0.057	0.021	C=D
4.3	0.378	0.329	–	–	C>D
5.0	3.245	2.831	2.527	0.944	2.998
+23	13.404	11.696	19.502	7.290	1.604

* Band is visible on autoradiograph but cannot be distinguished by video densitometry
a Area OD for both 1.8 and 1.8+ bands; values may be overestimated for 1.8 kb band and underestimated for 1.8+ kb band
R   Reference band Area OD used to calculate C=Area OD band/Area OD Reference band

Table A-20. Area OD of autoradiograph of MspI/EcoRI and HpaII/EcoRI digested RS+ (R22) fibroblast genomic DNA (Experiment 17)

Lane 3 R22 P26 M/E			Lane 4 R22 P26 H/E		
Band (kb)	Area OD (A)	Area OD/Ref (C)	Area OD (B)	Area OD/Ref (D)	Ratio (C/D)
0.5	0.652	0.348	1.220	0.550	0.632
0.8	–	–	0.249	0.112	C<D
1.1	–	–	0.105	0.047	C<D
1.6^R	1.869	1.000	2.216	1.000	1.000
1.8	1.919	1.026	5.330	2.405	0.426
1.8+	–	–	2.140	0.965	C<D
2.5	0.544	0.291	2.705	1.220	0.238
3.3	0.083	0.044	–	–	C>D
3.6	3.033	1.622	5.148	2.323	0.698
3.8	0.192	0.102	–	–	C>D
5.0	2.262	1.210	1.579	0.712	1.699
+23	27.086	14.492	11.465	5.173	2.801

R   Reference band Area OD used to calculate C=Area OD band/Area OD Reference band

Table A-21. Area OD of autoradiograph of MspI/EcoRI and HpaII/EcoRI digested control (GM3349) fibroblast genomic DNA (Experiment 17)

Lane 5 Band (kb)	GM3349 P17 Area OD (A)	M/E Area OD/Ref (C)	Lane 6 Area OD (B)	GM3349 P17 Area OD/Ref (D)	H/E Ratio (C/D)
0.5	0.394	0.274	–	–	C>D
1.6^R	1.433	1.000	2.787	1.000	1.000
1.8	0.066	0.046	0.277	0.099	0.465
1.8+	–	–	0.175	0.062	C<D
2.5	1.385	0.966	–	–	C>D
3.3	0.057	0.039	–*	–	C≥D
3.6	2.101	1.466	2.314	0.830	1.766
3.8	0.411	0.286	–*	–	C≥D
4.0	0.402	0.280	0.255	0.091	3.076
5.0	1.606	1.120	1.948	0.698	1.605
6.6	0.545	0.380	0.614	0.220	1.727
9.0	0.105	0.073	0.289	0.103	0.708
+23	8.633	6.024	5.387	1.932	3.118

* Band visible on autoradiograph but cannot be distinguished by video densitometry
R   Reference band Area OD used to calculate C=Area OD band/Area OD Reference band

Table A-22.   Area OD of autoradiograph of MspI/EcoRI and HpaII/EcoRI digested control (GM3349) fibroblast genomic DNA (Experiment 17)

Lane 7 Band (kb)	GM3349 P32 Area OD (A)	M/E Area OD/Ref (C)	Lane 8 Area OD (B)	GM3349 P32 Area OD/Ref (D)	H/E Ratio (C/D)
0.5	0.703	0.195	–	–	C>D
1.6[R]	3.599	1.000	4.695	1.000	1.000
1.8	0.408	0.113	1.954[a]	0.416	0.271
1.8+	–	–	a	a	a
2.5	1.937	0.538	–	–	C>D
3.3	–*	–	–*	–	C≥D
3.6	3.256	0.904	3.474	0.739	1.223
3.8	–*	–	–*	–	C≥D
4.0	1.185	0.329	0.240	0.051	6.450
5.0	2.523	0.701	2.324	0.494	1.419
+23	24.063	6.686	25.409	5.411	1.235

*   Band is visible on autoradiograph but cannot be distinguished by video densitometry
a   Area OD value is for both 1.8 and 1.8+ kb bands as they could be distinguished by video densitometry
R   Reference band Area OD used to calculate C=Area OD band/Area OD Reference band

Table A-23. Area OD of autoradiograph of MspI/EcoRI and HpaII/EcoRI digested RS- (S6008) fibroblast genomic DNA (Experiment 18)

Lane 1 Band (kb)	S6008 P15 M/E Area OD (A)	Area OD/Ref (C)	Lane 2 Area OD (B)	S6008 P15 H/E Area OD/Ref (D)	Ratio (C/D)
0.5	0.992	0.187	0.196	0.027	6.925
1.6[R]	5.303	1.000	7.133	1.000	1.000
1.8	1.969	0.371	3.581	0.502	0.739
1.8+	0.114	0.021	1.942	0.272	0.077
2.3	0.243	0.045	0.284	0.039	1.153
2.5	1.821	0.343	0.295	0.041	8.365
2.9	0.084	0.015	0.365	0.051	0.294
3.2	0.044	0.008	0.201	0.028	0.285
3.6	7.237	1.364	5.394	0.756	1.804
4.1	0.241	0.045	0.121	0.016	2.812
4.6	0.160	0.030	0.028	0.003	10.000
5.0	5.356	1.009	3.741	0.524	1.925
7.5	4.386	0.827	2.024	0.283	2.922
+23	33.616	6.339	27.529	3.859	1.642

R   Reference band Area OD used to calculate C=Area OD band/Area OD Reference band

Table A-24. Area OD of autoradiograph of MspI/EcoRI and HpaII/EcoRI digested RS- (S6008) and control (S6007) fibroblast genomic DNA (Experiment 18)

Lane 3 S6008 P28 M/E Band (kb)	Area OD (A)	Area OD/Ref (C)	Lane 4 S6008 P28 H/E Area OD (B)	Area OD/Ref (D)	Ratio (C/D)
0.5	1.326	0.311	—	—	C>D
1.6[R]	4.258	1.000	5.125	1.000	1.000
1.8	2.031	0.476	2.666	0.520	0.915
1.8+	—	—	1.310	0.254	C<D
2.3	0.121	0.028	0.172	0.033	0.848
2.5	0.596	0.139	0.277	0.053	2.622
2.9	0.220	0.051	0.143	0.027	1.888
3.2	0.164	0.038	—*	—	C≥D
3.6	6.998	1.643	3.653	0.713	2.304
4.1	0.136	0.031	0.102	0.019	1.631
4.6	0.142	0.033	0.078	0.015	2.200
5.0	6.060	1.423	3.655	0.713	1.996
7.5	1.927	0.452	5.858	1.143	0.395
+23	29.659	6.965	45.286	8.836	0.788

* Band visible on autoradiograph but could not be distinguished by densitometry scanning
R Reference band Area OD used to calculate C=Area OD band/Area OD Reference band

Table A-25. Area OD of autoradiograph of MspI/EcoRI and HpaII/EcoRI digested control (S6007) fibroblast genomic DNA (Experiment 18)

Lane 5 S6007 P15 M/E			Lane 6 S6007 P15 H/E		
Band (kb)	Area OD (A)	Area OD/Ref (C)	Area OD (B)	Area OD/Ref (D)	Ratio (C/D)
0.5	2.558	0.419	–	–	C>D
1.6[R]	6.104	1.000	6.945	1.000	1.000
1.8	0.923	0.151	1.516	0.218	0.692
1.8+	0.009	0.001	3.785	0.544	0.001
2.5	0.249	0.040	0.041	0.005	8.000
3.6	1.364	0.233	3.260	0.469	0.497
4.0	0.160	0.026	0.097	0.013	2.000
4.3	0.302	0.049	–	–	C>D
4.6	0.141	0.023	0.079	0.011	2.090
5.0	1.645	0.269	1.812	0.260	1.034
6.0	0.046	0.007	0.064	0.009	0.777
6.3	0.107	0.017	0.143	0.020	0.850
7.3	1.988	0.325	1.943	0.279	1.164
9.5	1.184	0.193	0.836	0.120	1.608
+23	13.847	2.268	23.503	3.384	0.670

R   Reference band Area OD used to calculate C=Area OD band/Area OD Reference band

Table A-26. Area OD ɔf autoradiograph of MspI/EcoRI and HpaII/EcoRI digested control (S6007) fibroblast genomic DNA (Experiment 18)

Lane 7 S6007 P31 M/E			Lane 8 S6007 P31 H/E		
Band (kb)	Area OD (A)	Area OD/Ref (C)	Area OD (B)	Area OD/Ref (D)	Ratio (C/D)
0.5	-	-	-	-	
1.6[R]	4.748	1.000	5.285	1.000	1.000
1.8	1.765	0.371	1.204	0.227	1.634
1.8+	-	-	1.263	0.238	C<D
2.5	0.431	0.090	0.041	0.007	12.857
3.6	2.652	0.558	1.607	0.304	1.835
4.0	0.098	0.020	0.180	0.034	0.588
4.3	0.237	0.049	0.144	0.027	1.814
4.6	0.077	0.016	0.059	0.011	1.454
5.0	1.904	0.401	1.225	0.231	1.735
6.0	0.191	0.040	-*	-	C≥D
6.3	1.612	0.339	0.138	0.026	13.038
7.3	1.017	0.214	1.241	0.234	0.914
+23	11.609	2.445	12.501	2.365	1.033

* Band is visible on autoradiograph but cannot be distinguished by video densitometry
R Reference band Area OD used to calculate C=Area OD band/Area OD Reference band

Table A-27. Summary of weighted mean number of metaphase cells with labelled constitutive heterochromatin regions obtained from the female RS+ lymphoblastoid cell line, LB1, and the control cell line, JaKr (Experiment 1, 2).

Subphase	Exp.	N	Mean number of cells with labelled chromosome regions			
			1q1-2	9q1-2	16q1	X
A. RS+ cell line						
SkII	1	36	31	32	24	32
	2	28	25	28	27	11
SkIII	1	85	76	66	55	69
	2	59	42	59	58	19
SkIV	1	79	54	49	48	37
	2	113	77	107	95	26
B. Control cell line						
SkII	1	86	85	74	69	66
	2	42	42	42	42	21
SkIII	1	52	49	45	37	27
	2	128	123	124	113	·48
SkIV	1	58	48	34	27	25
	2	30	2⁻	30	20	1

Exp. = Experiment
N = total number of cells

Table A-28. Summary of weighted mean number of metaphase cells with labelled constitutive heterochromatin regions obtained from the male RS+ lymphoblastoid cell line, R20, and the control cell line, DM (Experiment 3, 4).

Subphase	Exp.	N	Mean number of cells with labelled chromosome regions			
			1q1-2	9q1-2	16q1	Yq1
A. RS+ cell line						
SkII	3	64	62	62	49	56
	4	33	32	32	31	33
SkIII	3	65	57	57	54	52
	4	99	97	95	79	97
SkIV	3	71	53	60	53	50
	4	68	63	58	60	57
B. Control cell line						
SkII	3	70	67	54	30	67
	4	54	53	53	53	53
SkIII	3	95	86	69	48	89
	4	92	86	91	73	84
SkIV	3	35	31	14	7	30
	4	54	49	46	27	48

Exp. = Experiment
N = total number of cells

Appendix 2 – Statistical analyses

Table A-29.   Comparison of slopes of RS+ and control lymphoblastoid cell lines for each subphase of S phase using a two-sample t-test (Experiments 1-4)

Subphase	Exp.	Slope (b)		t	p
		RS+	Control		
SkII	1	0.1054	0.1172	-1.16	0.45
	2	-0.0672	0.1210		
	3	0.1816	-0.0742	-0.02	0.99
	4	0.2046	0.4695		
SKIII	1	0.0359	-0.3385	-2.59	0.23
	2	0.3145	-0.1627		
	3	0.0717	-0.1466	-10.41	0.06
	4	0.0351	-0.1627		
SKIV	1	-0.1099	0.1526	1.2ö	0.43
	2	-0.2298	-0.1183		
	3	-0.2505	0.3935	0.91	0.53
	4	-0.1776	-0.2394		

* Two-sample t-test with df=1

Table A-30.   Generalized linear model (GLM) equations of probit transformed frequency distributions of RS+ and control metaphases with replicated 1qh constitutive heterochromatin obtained with BrdUrd treatment times of 4, 5, 6 and 7 hours.

Subphase	Exp.	Predicted GLM Equation y=a+bx Control	RS+	Comparison of slopes p
SkII	1	y=-0.543+0.460t	y=-1.436+0.473t	0.975
	2	y= 4.155+0.029t	y= 0.556+0.132t	>0.05
	3	y= 0.433+0.223t	y= 1.280+0.104t	0.50
	4	y=16.580-2.116t	y=-8.917+2.471t[NC]	0.95
SkIII	1	y= 1.577-0.001t	y=-1.270+0.484t	0.25
	2	y= 0.757+0.190t	y= 1.321-0.023t	>0.05
	3	y= 1.292+0.030t	y=-1.672+0.547t	0.10
	4	y=-0.208+0.342t	y=-0.341+0.479t	0.95
SkIV	1	y= 0.900-0.014t	y=-2.151+0.504t	0.02
	2	y=-1.523+0.585t	y=-0.777+0.238t	>0.05
	3	y=-2.60+0.637t	y=-0.314+0.191t	0.50
	4	y= 2.08-0.144t	y=0.220+0.243t	0.50

Exp. = Experiment
Controls: Experiment 1,2 - JaKr; Experiment 3,4 - DM
RS+ : Experiment 1,2 - LB1; Experiment 3,4 - R20
NC = no convergence at 10 iterations

Table A-31. Generalized linear model (GLM) equations of probit transformed frequency distributions of RS+ and control metaphases with replicated 9qh constitutive heterochromatin obtained with BrdUrd treatment times of 4, 5, 6 and 7 hours.

Subphase	Exp.	Predicted GLM Equation $y=a+bx$		Comparison of Slopes p ($\alpha=0.05$)
		Control	RS+	
SkII	1	$y= 1.775-0.136t$	$y= 2.605-0.235t$	0.75
	2	$y= 4.155+0.0290t$	$y= 4.319-0.0146t$	>0.99
	3	$y=-0.022+0.144t$	$y=-1.247+0.608t$	0.25
	4	$y=16.580-2.116t$[NC]	$y= 2.194-0.053t$	0.50
SkIII	1	$y= 2.777-0.323t$	$y= 1.259-0.089t$	0.50
	2	$y= 1.393-0.087t$	$y= 4.034+0.060t$[NC]	>0.99
	3	$y= 2.608-0.341t$	$y= 2.719-0.268t$	0.90
	4	$y=-6.831+2.154t$[NC]	$y= 0.685+0.199t$	0.25
SkIV	1	$y= 0.778-0.113t$	$y= 1.179-0.162t$	0.90
	2	$y= 4.404-0.026t$	$y= 0.764+0.165t$[NC]	>0.99
	3	$y=-3.019+0.462t$	$y= 1.658-0.122t$	0.25
	4	$y= 4.382-0.610t$	$y= 1.787-0.138t$	0.25

Exp. = Experiment
Controls: Experiment 1,2 - JaKr; Experiment 3,4 - DM
RS+ : Experiment 1,2 - LB1; Experiment 3,4 - R20
NC = no convergence at 10 iterations

Table A-32. Generalized linear model (GLM) equations of probit transformed frequency distributions of RS+ and control metaphases with replicated 16qh constitutive heterochromatin obtained with BrdUrd treatment times of 4, 5, 6 and 7 hours.

Subphase	Exp.	Predicted GLM Equation $y=a+bx$ Control	RS+	Comparison of Slopes p $(\alpha=0.05)$
SkII	1	$y= 2.146-0.238t$	$y= 1.609-0.205t$	0.90
	2	$y= 4.155+0.029t$	$y=-6.957+2.085t^{NC}$	>0.99
	3	$y= 0.887-0.199t$	$y=-0.750+0.261t$	0.25
	4	$y=-0.594+0.478t$	$y= 1.867-0.053t$	0.50
SkIII	1	$y= 1.677-0.221t$	$y=-0.564+0.171t$	0.10
	2	$y= 3.086-0.332t$	$y=-7.997+2.320t^{NC}$	0.025
	3	$y= 0.425-0.087t$	$y=-0.490+0.267t$	0.90
	4	$y= 0.444+0.071t$	$y=-0.251+0.200t$	0.05
SkIV	1	$y= 0.038-0.294t$	$y=-1.052+0.249t$	0.25
	2	$y=-0.151+0.111t$	$y=-1.837+0.563t$	0.25
	3	$y=-3.852+0.503t$	$y=-2.201+0.576t$	0.25
	4	$y=-0.236+0.046t$	$y= 1.146+0.008t$	0.90

Exp. = Experiment
Controls: Experiment 1,2 - JaKr; Experiment 3,4 - DM
RS+ : Experiment 1,2 - LB1; Experiment 3,4 - R20
NC = no convergence at 10 iterations

Table A-33. Generalized linear model (GLM) equations of probit transformed frequency distributions of RS+ and control metaphases with replicated Yqh constitutive heterochromatin obtained with BrdUrd treatment times of 4, 5, 6 and 7 hours.

Subphase	Exp.	Predicted GLM Equation $y=a+bx$		Comparison of slopes p ($\alpha=0.05$)
		Control	RS+	
SkII	3	$y= 1.076+0.123t$	$y= 1.150-1.636X10^{-8}t$	0.75
	4	$y= 1.673+0.068t$	$y= 4.007+0.048t^{NC}$	>0.99
SkIII	3	$y=-0.818+0.456t$	$y= 0.217+0.113t$	0.25
	4	$y=-2.176+0.736t$	$y=-9.097+2.608t^{NC}$	0.90
SkIV	3	$y=-0.065+0.186t$	$y=-1.077+0.315t$	0.90
	4	$y=-1.730+0.615t$	$y=-1.138+0.423t$	0.75

Exp. = Experiment
Controls: Experiment 3,4 - DM
RS+: Experiment 3,4 - R20
NC = no convergence at 10 iterations

Table A-34. Generalized linear model (GLM) equations of probit transformed frequency distributions of RS+ and control metaphases with replicated X chromosome(s) labelled with BrdUrd treatment times of 4, 5, 6 and 7 hours.

Subphase	Exp.	Predicted GLM Equation y=a+bx		Comparison of Slopes (α=0.05)
		Control	RS+	
SkII	1	y= -3.062+0.557t	y=-1.422+0.399t	0.75
	2	y= -3.538+0.615t	y= 0.2655-0.101t	0.01
SkIII	1	y= -2.751+0.351t	y=-1.528+0.278t	0.90
	2	y= -4.070+0.666t	y=-3.800+.543t[NC]	0.75
SkIIV	1	y= -2.473+0.348t	y=-4.237+0.607t	0.50
	2	y=-21.450+2.911t	y=-3.299+0.469t[NC]	0.50

Exp. = Experiment
Controls: Experiment 1,2 - JaKr
RS+ : Experiment 1,2 - LB1
NC = no convergence at 10 iterations

Sample Calculation: Power of ANOVA Models i) and ii)
(method of Cohen, 1988)

1. Mean Area OD ratios and standard deviations (s) for Groups
with sample size (n).

Controls (E+L) mean OD = 19.279 (16.680) n=14
RS+ (E+L) mean OD = 13.470 (16.002) n=9
RS- (E+L) mean OD = 15.701 (15.820) n=7

Case: one way analysis of variance, k means, with unequal
sample size

pooled mean = m_p = [(14)(19.279)+(9)(13.470)+(7)(15.701)]/30
= 16.701

pooled standard deviation = 16.293

$$\sigma_m = \sqrt{[\Sigma n_i (m_i - m)^2]/N}$$

$$= \sqrt{[(14)(19.279-16.701)^2 + (9)(13.470-}$$

$$16.701)^2 + (7)(15.701-16.701)^2]/30$$

$$= \sqrt{[193.999/30]}$$

$$= 2.542$$

Effect size $f = \sigma_m$/pooled standard deviation = 0.156
Level of significance $\alpha = 0.05$
                       $\mu = k-1 = 3-1 = 2$
                       $n = 30/3 = 10$

∴   power = 10%